

**ATOMIC BONDING AND CRYSTAL TYPES****PRIMARY READING ASSIGNMENT**

"Atomic Bonding and Crystal Types", from *Fundamentals of Semiconductor Theory and Device Physics*, Shyh Wang

**SUPPLEMENTARY REFERENCE**

"Principles of Formation of the Atomic Structure of Crystals" from *Structure of Crystals*, Boris K. Vainshtein, Vladimir M. Fridkin, Vladimir L. Indenbom

"Atomic Structure", from *Fundamentals of Semiconductor Theory and Device Physics*, Shyh Wang

**LECTURE PROGRAM**

1. Interatomic Forces
  - a. Attractive and repulsive forces
  - b. System energy
  - c. Minimum energy law
  - d. Coulomb interaction and potential energy
  - e. Core repulsive energy
  - f. Kinetic energy
  - g. Electric dipole
  - h. van der Waals energy
  - i. Total system energy
2. Classification of Bond Types
  - a. Cohesive energy
  - b. Ionic
  - c. Covalent
  - d. Metallic
  - e. van der Waals
3. Ionic Crystals
4. Metallic Crystals
5. Hydrogen Molecule
6. Saturation and Directional Properties of Covalent Bonds
7. Covalent Crystals

# **Atomic Bonding and Crystal Types**

## **3.1 INTERATOMIC FORCES**

When substances are cooled down to sufficiently low temperatures, they all become solids. Obviously there must be bonding forces of some kind to keep atoms together to form a solid material. On the other hand, the atoms in a solid maintain a finite distance from each other. Therefore, there must be two opposite types of forces: an attractive force  $F_{\text{att}}$  and a repulsive force  $F_{\text{rep}}$ . Both forces are a function of the interatomic distance  $R$ . At large distances, the attractive force dominates; hence atoms are drawn toward each other. At small distances, the repulsive force becomes much larger than the attractive force, and atoms are held back from getting too close to each other. At equilibrium, the two opposing forces balance out, and we have

$$F_{\text{att}}(R) = F_{\text{rep}}(R) \quad (3.1.1)$$

Equation (3.1.1) determines the atomic spacing  $R$  in a crystal.

In dealing with the interactions between atoms, it is more convenient that the mathematical formulation is based on energies rather than forces. Realizing that the force is the derivative of energy, we can rewrite Eq. (3.1.1) in terms of two energies, one attractive and one repulsive, as

$$\frac{d}{dR} [\mathcal{E}_{\text{rep}}(R) - \mathcal{E}_{\text{att}}(R)] = 0 \quad (3.1.2)$$

As we shall see shortly, the attractive energy is negative and the repulsive energy is positive. The total energy  $\mathcal{E}_{\text{tot}}$  is thus equal to  $\mathcal{E}_{\text{rep}} - \mathcal{E}_{\text{att}}$ . In terms of the total energy, Eq. (3.1.2) becomes

$$\frac{d}{dR} \mathcal{E}_{\text{tot}} = 0 \quad (3.1.3)$$

Equation (3.1.3) says that at equilibrium the total energy of a system has a minimum value. This minimum-energy law is a fundamental law of nature.

As we shall see in discussions of subsequent sections, the nature of the attractive and repulsive energy is different in different types of crystals. In general, we consider an atom as consisting of an ion core (nucleus plus core electrons) and some valence electrons. The nature of the interaction between neighboring atoms depends on whether the orbits of neighboring core electrons overlap or not. For example, Na in metallic sodium has an ion core of charge  $+e$  and one valence electron of charge  $-e$ . This valence electron keeps the  $\text{Na}^+$  ion core from coming into contact with neighboring  $\text{Na}^+$  ion cores. However, the situation in NaCl is different. In NaCl crystal, a sodium atom loses its valence electron and becomes a  $\text{Na}^+$  ion. The  $\text{Na}^+$  ion core now makes direct contact with neighboring  $\text{Cl}^-$  ion cores, and thus overlapping of these two ion cores may occur.

In cases where there are valence electrons to keep the orbits of neighboring core electrons from overlapping, the principal interaction is of electrostatic nature. Consider the Coulomb interaction between two charged particles, one with charge  $q_1$  and the other with charge  $q_2$ , separated at a distance  $r_{12}$ . The potential energy  $\mathcal{E}_P$  is

$$\mathcal{E}_P = \frac{q_1 q_2}{4\pi\epsilon_0 r_{12}} \quad (3.1.4)$$

as can be derived from Coulomb's law. Between charges of like polarity, the force is repulsive. Since work must be done to bring the two charges together,  $\mathcal{E}_P$  is positive. Between charges of opposite polarities, the force is attractive and hence  $\mathcal{E}_P$  is negative.

If the orbits of core electrons of two neighboring atoms overlap, interaction of a different kind must also be considered. Since core electrons have closed-shell configurations, all quantum states in the shell (e.g., the  $2s2p$  shell in  $\text{Na}^+$  and Ne) are occupied, and hence no quantum state in the shell is available for an additional electron. When the orbits of core electrons begin to overlap, some of the core electrons must go to unoccupied shells of higher energy. The lifting of an electron from a lower-energy state to a higher-energy state raises the energy of the entire system. This increase in energy is known as the *core repulsive energy*  $\mathcal{E}_C$ . The cause of this energy can be understood only on the basis of quantum mechanics (the exclusion principle).

Besides  $\mathcal{E}_P$  and  $\mathcal{E}_C$ , there are two other kinds of energy that may be important in certain types of crystals. As we all know, metals conduct electric current with very little resistance. This high electrical conductivity is generally attributed to the fact that the valence electrons of metals move rather freely in a crystal. Associated with this freedom of movement, there is a kinetic energy  $\mathcal{E}_K$ . Since the kinetic energy tends to make the volume of a crystal expand, the term  $\mathcal{E}_K$  is repulsive in nature. The fourth interaction energy  $\mathcal{E}_W$  comes from electrostatic interaction between two charge pairs. The charge pair, known as an *electric dipole*, consists of two charges of opposite polarities kept apart at a small distance. The energy  $\mathcal{E}_W$ , known as the *van der Waals energy* (attractive), is discussed in more detail in Section 3.2.

Summarizing the discussion above, we may express the total energy  $\mathcal{E}_{\text{total}}$  of a system as

$$\mathcal{E}_{\text{total}} = \sum \mathcal{E}_K + \sum \mathcal{E}_C - \sum \mathcal{E}_P - \sum \mathcal{E}_W \quad (3.1.5)$$

In Eq. (3.1.5) it is assumed that the electrostatic interaction between charges of opposite polarities predominates and hence the sign of  $\mathcal{E}_P$  is chosen negative. As discussed in

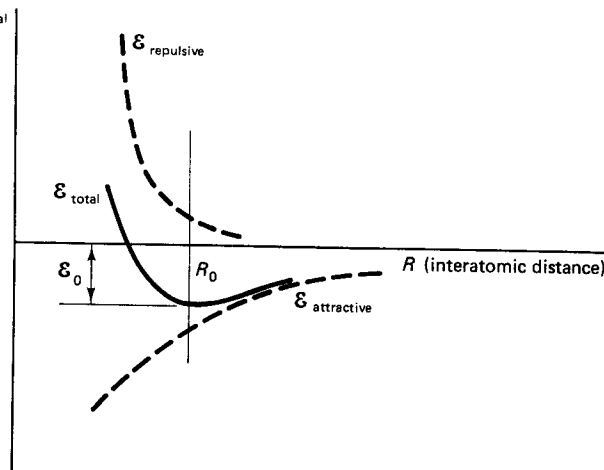


**Figure 3.1** Schematic diagram showing the total energy per atom as a function of the interatomic distance. The total energy is a sum of the repulsive and attractive energies. The position at which  $\mathcal{E}_{\text{tot}}$  is a minimum determines the interatomic spacing  $R_0$  in a crystal. The amount of energy  $\mathcal{E}_0$  lowered by forming a crystal is the bonding energy of the crystal.

Section 3.2, crystals can be classified into four general groups. For each crystal group, different terms in Eq. (3.1.5) are important. It is the purpose of our discussions in subsequent sections to show the important differences between different crystal types.

Figure 3.1 shows the general behavior of the attractive and repulsive energies as functions of the interatomic distance  $R$ . The equilibrium separation  $R_0$  in a crystal is determined by the condition  $d\mathcal{E}_{\text{tot}}/dR = 0$  or by the position of minimum  $\mathcal{E}_{\text{tot}}$ . In Fig. 3.1 we choose the energy of isolated atoms as the reference energy. The energy of a system is lowered by an amount  $\mathcal{E}_0$  if the atoms come to the proximity of one another. This lowering of energy constitutes the bonding between the atoms in a crystal.

## 3.2 CLASSIFICATION OF BOND TYPES

In Section 1.6 we discussed the periodic structure of chemical elements. One important observation is that elements having their shells completed are chemically inert. This means that a stable electron configuration is one which has its shells completed. The attractive forces differ in nature from one class of materials to another, and this difference can be understood on the basis of the shell structure of atoms. The general tendency is that atoms will give up electrons, receive electrons from other atoms, or share electrons with other atoms so that they may achieve individually or collectively a stable electron configuration. According to the different ways in which atoms achieve a stable electron configuration, the bonding between atoms in a crystal is commonly classified into four distinct types: the ionic bond, the covalent bond, the metallic bond, and the van der Waals bond.

The strength of a bond can be measured by the energy required to dissociate a solid into isolated neutral atoms or molecules. This energy is called the *cohesive energy* of a solid. Values for a selected number of materials representing each bond type are listed in Table 3.1. The bond strength in ionic, covalent, and metallic crystals is much stronger than that in molecular crystals. Hence the three strong bonds, ionic, covalent, and metallic, are termed *primary bonds*. In molecular crystals, the constituent atoms or molecules already have a stable electron configuration. The bond between such atoms

**TABLE 3.1** COHESIVE ENERGIES<sup>a</sup> (eV) OF DIFFERENT CRYSTAL TYPES

Ionic		Covalent		Metallic		Molecular	
Material	Energy	Material	Energy	Material	Energy	Material	Energy
LiCl	8.9	Diamond	7.4	Na	1.13	Ar	0.08
NaCl	8.0	Si	4.6	Au	3.78	Kr	0.11
KI	6.6	Ge	3.9	Mg	1.56	CH <sub>4</sub>	0.10

<sup>a</sup>Energy required to dissociate a solid into monatomic gas in the case of element solids and into molecular gas in the case of compound solids.

or molecules comes from a much weaker interaction. In the following discussion we describe the bonding mechanisms in crystals of the four distinct types: the ionic, the covalent, the metallic, and the molecular type.

### The Ionic Bond

Alkali metals such as sodium have a single valence electron outside closed shells, whereas halogens such as chlorine are one electron short of having a complete outer shell (Fig. 3.2). An electron transfer from the alkali metal X to the halogen Y results in closed-shell configurations in both X<sup>+</sup> and Y<sup>-</sup> ions. For example, Na<sup>+</sup> has an electron configuration 1s<sup>2</sup>2s<sup>2</sup>2p<sup>6</sup> (the numbers in the superscripts indicating the number of electrons), which is the same as that of neon, whereas Cl<sup>-</sup> has an electron configuration 1s<sup>2</sup>2s<sup>2</sup>2p<sup>6</sup>3s<sup>2</sup>3p<sup>6</sup>, which is the same as that of argon. The Coulomb attraction between X<sup>+</sup> and Y<sup>-</sup> ions keeps the ions together in an ionic XY molecule or crystal. Besides alkali halides, ionic bonds can also be formed between divalent and trivalent elements. Selected examples are CaO, MgCl<sub>2</sub>, Al<sub>2</sub>O<sub>3</sub>, and ZnO.

### The Covalent Bond

Besides electron transfer, an incomplete shell can be filled if atoms in a molecule or solid share their electrons. The bond thus formed between atoms is called the covalent bond. To illustrate the essential difference between an ionic and a covalent bond, we use a nitrogen molecule N<sub>2</sub> as an example. From Table 1.2 we find that the 2p level with only three electrons in nitrogen is incomplete. If one nitrogen atom transfers its three 2p electrons to the other nitrogen atom, we have complete 1s and 2s levels in the N<sup>3+</sup> ion, and complete 1s, 2s, and 2p levels in the N<sup>3-</sup> ion (Fig. 3.3a). This arrange-

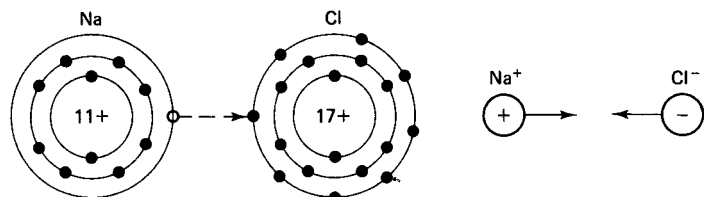


**Figure 3.2** Electron configuration in NaCl. An electron transfer from Na to Cl (indicated by a broken arrow) results in closed-shell configurations in both Na<sup>+</sup> and Cl<sup>-</sup> ions. The bonding in NaCl is due to Coulomb attraction between Na<sup>+</sup> and Cl<sup>-</sup> ions.

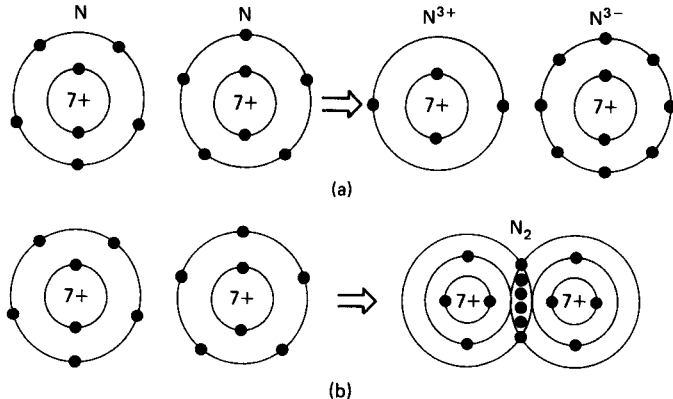


**Figure 3.3** Schematic diagram illustrating the difference between (a) ionic bonding and (b) covalent bonding in a nitrogen molecule. Electron transfer is needed in forming an ionic bond. A closed-shell configuration is formed in the covalent bond by sharing electrons, the  $2p$  electrons in the case of  $N_2$ , between two atoms. The actual bonding in  $N_2$  is covalent.

ment of electrons is similar to that in  $NaCl$  and hence results in an ionic bond. In the covalent bond, the six  $2p$  electrons do not really belong to a particular nitrogen atom but are shared equally between the two atoms. In other words, the charge cloud formed by the six  $2p$  electrons is orbiting around and hence surrounds both nitrogen atoms (Fig. 3.3b).

If the six  $2p$  electrons are shared equally by the two atoms, each atom does not lose or gain any electron, and hence both atoms should remain electrically neutral. On the basis of classical physics, it is quite impossible to understand why two neutral nitrogen atoms form a nitrogen molecule. The physical origin as well as the basic properties of a covalent bond can be understood only on the basis of quantum mechanics. The previous statement about electron sharing in a covalent bond is an oversimplified description of a quantum-mechanical phenomenon known as *electron-pair bond*. The six  $2p$  electrons in a nitrogen molecule are bound in pairs with spins aligned antiparallel in each pair (Fig. 3.4a). A similar bond is formed between the two  $1s$  electrons in a hydrogen molecule (Fig. 3.4b).

To describe the physical situation in the formation of an electron-pair bond, we may consider first the case of a singly ionized  $H_2^+$  molecule, in which the two protons are held together by one electron. This problem can be solved exactly by quantum mechanics. The result of quantum-mechanical calculation shows that the two lowest-energy states have spatially symmetric and antisymmetric wave functions. As illustrated

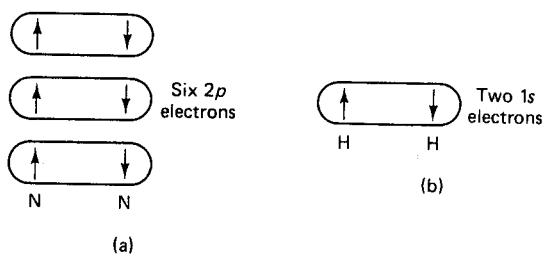


**Figure 3.4** Electron-pair bond in (a)  $N_2$  and (b)  $H_2$ . The bond is formed between a pair of electrons with antiparallel spins.

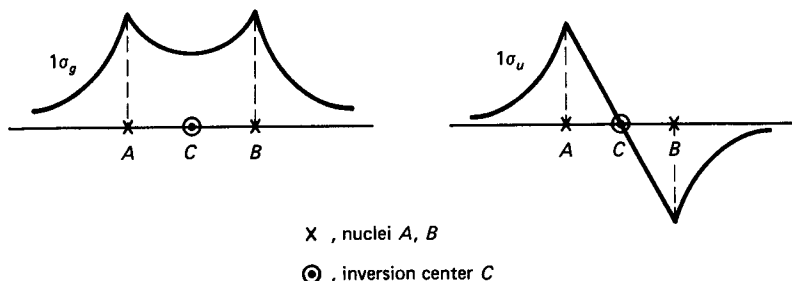


**Figure 3.5** (a) Symmetrical and (b) antisymmetric wave function of a hydrogen molecule-ion  $\text{H}_2^+$  along the line passing through the nuclei.

in Fig. 3.5, the symmetric (even) wave function, denoted by a subscript  $g$ , is unchanged and the antisymmetric (odd) wave function, denoted by a subscript  $u$ , merely changes sign when we perform an inversion operation with respect to the midpoint between the two nuclei. The wave function that describes the electron motion in a molecule is called the *molecular orbital*. It is customary to use Greek  $\sigma$ ,  $\pi$ ,  $\delta$  in reference to the various molecular orbitals.

The variation of the nuclear potential along the line joining the two nuclei is illustrated schematically in Fig. 3.6. Note that the Coulomb potential in the region  $AB$  between the two nuclei is depressed as compared to the potential in a single atom (represented by the dashed curves in Fig. 3.6). Using the expression of the electron density defined in Eq. (1.3.11), we can write the potential energy of a  $\text{H}_2^+$  molecule ion as

$$\mathcal{E}_p = - \frac{e}{4\pi\epsilon_0} \iiint_{-\infty}^{\infty} \left( \frac{e}{r_a} + \frac{e}{r_b} \right) |\Psi|^2 dx dy dz + \frac{e^2}{4\pi\epsilon_0 R} = -V_{en} + V_{nn} \quad (3.2.1)$$

where  $r_a$  and  $r_b$  are the electron distance from the two nuclei. In Eq. (3.2.1) the term  $V_{en}$  represents the electron–nucleus interaction energy and is attractive, whereas the term  $V_{nn}$  represents the nucleus–nucleus interaction energy and is repulsive. Evidently, the two states *gerade* and *ungerade* (German words for *even* and *odd*, respectively) will have different potential energies because they have different electron distributions (Fig. 3.5), especially in the region  $AB$  between the two nuclei.

In the gerade state, the electron density (i.e., the probability of finding the electron) has an appreciable value in the region  $AB$  of low potential energy. This means

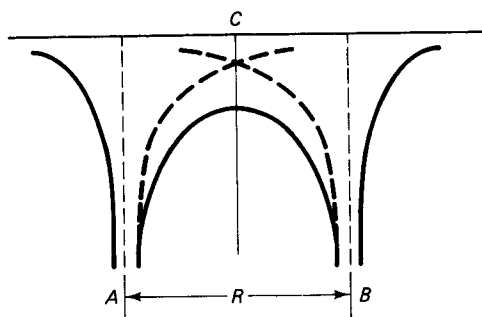


**Figure 3.6** Potential energy (solid curve) of an electron in the field of two hydrogen nuclei, along the line passing through the nuclei  $A$  and  $B$ . The dashed curve is the potential energy in the field of a single hydrogen nucleus.

that the term  $V_{en}$  in Eq. (3.2.1) is expected to be lowered by the accumulation of negative charge in the low-potential-energy region. This lowering of the potential energy produces attraction in a  $H_2^+$  molecule ion. The energy of a  $H_2^+$  molecule ion can be calculated through the use of quantum mechanics, and the result of such a calculation is shown in Fig. 3.7 as a function of the internuclear distance  $R$ . At large  $R$ , the term  $V_{en}$  in Eq. (3.2.1) dominates. As  $R$  decreases, not only is the Coulomb potential (Fig. 3.6) further depressed but the amplitude of  $|\psi|^2$  is increased in region  $AB$ . Therefore, the energy of the gerade state decreases with decreasing  $R$  until it reaches a minimum. For further decrease of  $R$ , the energy rises as the electrostatic interaction between the two nuclei (represented by the  $V_{nn}$  term) becomes the predominant term in Eq. (3.2.1). The situation for the ungerade state is entirely different. The electron cloud in the ungerade state is not concentrated in the region of low potential energy. As the two nuclei approach each other, the term  $V_{en}$  no longer decreases. Since there is nothing in Eq. (3.2.1) to compensate the nuclear repulsion, the energy increases continuously with decreasing  $R$ .

The discussion above can be extended to a neutral hydrogen molecule by considering the two electrons of  $H_2$  separately. Each of the two electrons moves in the field of the two nuclei and in an average field (averaged over the electron distribution) of the other electron. The average electron field, of course, compensates the nuclear field. However, the main features concluded from the quantum-mechanical treatment of a  $H_2^+$  molecule-ion can still be used to describe the situation in a neutral hydrogen molecule. The electron wave function will still be either symmetric (gerade) or antisymmetric (ungerade). Again it is the gerade state that shows a minimum in the total-energy curve. Therefore, the ground (lowest energy) state of a hydrogen molecule is the one in which both electrons have the symmetric wave function. Since the two electrons have the same orbital wave function, they must have different spin orientations.

Note that the electron in a  $H_2^+$  molecule-ion does not belong to a particular nucleus. Similarly, the two electrons in a  $H_2$  molecule are shared equally by the two nuclei. The bond formed between two atoms by sharing two electrons with antiparallel spins is known as the electron-pair bond. The two electrons have antiparallel spins not on account of any magnetic interaction between the spins but because of the Pauli exclusion principle.

In summary we have used the hydrogen molecule to illustrate how the potential energy can be lowered in a molecule. In atomic and molecular physics few simple problems have either exact solutions or simple enough, approximate solutions. Hydro-

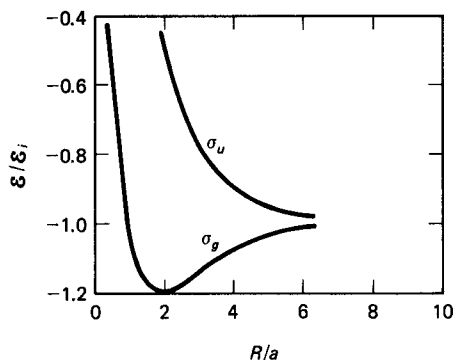


**Figure 3.7** Total energy  $\mathcal{E}_p$  of symmetric ( $\sigma_g$ ) and antisymmetric ( $\sigma_u$ ) states of the hydrogen molecule-ion as a function of the interatomic distance. The abscissa is expressed in units of the Bohr radius and the ordinate in units of the ionization energy of a hydrogen atom.

gen atom and hydrogen molecule are such problems. The principles that we learn from these examples are general and applicable to more complicated atoms and molecules. The principal features of a covalent bond, so far discussed, are electron sharing and spin antiparallel arrangement. Other important features are the directional and saturation properties. These properties are discussed in Section 3.6.

## The Metallic Bond

Metallic bonds differ from ionic and covalent bonds in many respects. First, a metallic bond exists only in the condensed state. In the gaseous state, metallic elements appear as monatomic vapors. Although molecules formed by metallic elements, for example  $\text{Li}_2$  and  $\text{Na}_2$ , have been observed, these molecules are not very stable. In our present discussion, we are not concerned with the formation of such molecules. Instead, we describe the bonding mechanism in a metallic crystal.

The outstanding characteristic of a metal is its high electrical conductivity. It can be inferred from this property that the valence electrons, such as the 2s electrons in Li and the 3s electrons in Na, must be free to move about. Because alkali metals have only a single valence electron outside closed shells, it is possible to find reasonably accurate solutions of the Schrödinger wave function. In the classical theory of metals, we think of valence electrons as forming an electron sea and the positive ions as being embedded in this sea. The positive ion is made of the nucleus and the core electrons in the closed-shell configuration. Later, quantum-mechanical calculations on alkali metals have generally supported this picture.

In Fig. 3.8 we compare the wave function of the valence electron in sodium crystals (solid curve) with the 3s wave function of a sodium atom (dashed curve). The wave function is not disturbed inside the ion-core region. However, in the outer region the crystal wave function is considerably flattened and squeezed in by neighboring valence electrons. It should be pointed out that the electron distribution in a volume element  $4\pi r^2 dr$  (in spherical coordinates) is, according to Eq. (1.3.11), given by  $|\psi|^2 4\pi r^2 dr$ . From the shape of  $\psi$  shown in Fig. 3.8, we can see that over 90% of the electron distribution is in the flat region. The potential energy of the electron is obviously lowered because the average electron distribution in a crystal is closer to the nucleus. The kinetic energy, being proportional to  $|\hbar \partial\psi/\partial r|^2$ , is also reduced because of a smaller  $\partial\psi/\partial r$  in the flattened region. This reduction in the total energy constitutes the bond in a metallic crystal.

## The van der Waals Bond

When inert gases are cooled down to sufficiently low temperatures, they also become solids. The bonding between inert-gas atoms in a crystal comes from interactions of

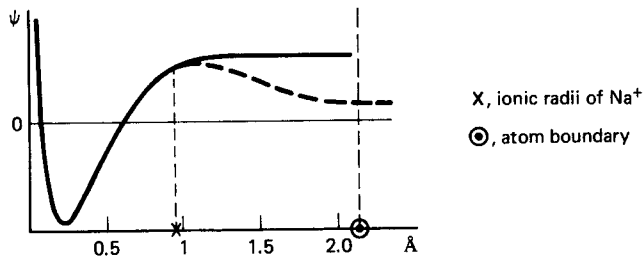


**Figure 3.8** Electron wave function in a sodium crystal (solid curve) as compared to that in an isolated sodium atom (dashed curve). One vertical line indicates the boundary between neighboring atoms in a sodium crystal, and the other indicates the region of the  $\text{Na}^+$  ion core.

electric dipoles. An electric dipole is made of two electric charges of opposite polarities placed at a small but finite distance  $2d$  apart (Fig. 3.9). The electric field  $E$  at point  $P$  situated at a distance  $R$  from the center of the charge distribution is

$$E = \frac{-e}{4\pi\epsilon_0(R + d)^2} + \frac{e}{4\pi\epsilon_0(R - d)^2} = \frac{2p}{4\pi\epsilon_0 R^3} \quad (3.2.2)$$

for  $R \gg d$ . Equation (3.2.2) is derived for the configuration of Fig. 3.9a. In Equation (3.2.2),  $p = 2ed$  is the *electric dipole moment*, which is defined as the product of the charge and the separation.

We all know that an insulator can become polarized in an electric field. A familiar example of polarizable material is a dielectric used in a capacitor. The origin of electric polarization lies in the fact that charges of opposite polarities are displaced in opposite directions in an electric field. This relative displacement of opposite charges produces an electric dipole. If an atom is placed at point  $P$  in Fig. 3.9, the atom will become polarized and will have an electric dipole moment  $p'$  induced by the field of Eq. (3.2.2). The induced dipole moment  $p'$  is related to  $E$  through

$$p' = \alpha E \quad (3.2.3)$$

where the proportionality constant  $\alpha$  is called the *polarizability*, and further, the potential energy of the induced dipole is given by

$$\mathcal{E}_w = -p'E = -\frac{2pp'}{4\pi\epsilon_0 R^3} = -\alpha \left( \frac{2p}{4\pi\epsilon_0 R^3} \right)^2 \quad (3.2.4)$$

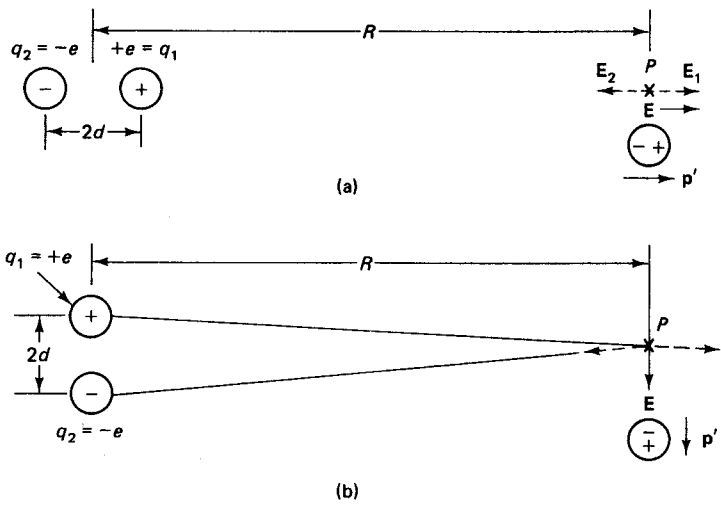


**Figure 3.9** Illustration showing the effect of an electric dipole, which consists of a pair of charges of opposite polarities separated at a distance  $2d$  apart. Two situations are considered: (a) The point  $P$  is along the line passing through the dipole and (b) the point  $P$  is along the line perpendicular to the dipole. If a molecule is placed at  $P$ , the dipole  $p'$  induced in the molecule will point in the same direction as the direction of  $E$  which is horizontal in (a) and vertical in (b).

It is clear from Fig. 3.9 that the two dipoles  $p$  and  $p'$  attract one another. This accounts for the negative sign in Eq. (3.2.4).

The interaction of the type described in Eq. (3.2.4) is known as the *van der Waals interaction* and is used for the attractive term in the gas equation of van der Waals. The van der Waals interaction is responsible for the cohesion not only in inert-gas crystals but also in other molecular crystals such as  $H_2$  and  $CH_4$ . The molecules  $H_2$  and  $CH_4$  are formed by covalent bonds. However, all the bonds in  $H_2$  and  $CH_4$  have been used up in forming the molecules  $H_2$  and  $CH_4$ ; thus no additional bond pairs can be formed with neighboring  $H_2$  or  $CH_4$  molecules. The attraction between molecules in solid  $H_2$  and  $CH_4$  comes from forces of the van der Waals type. We should point out that the van der Waals interaction is a relatively weak interaction. The molecules  $H_2$  and  $CH_4$  have already achieved a stable configuration through electron sharing, whereas the inert-gas elements have a closed-shell configuration to begin with. Hence the dipole electric field can only cause a slight distortion of the electron distribution. The fact that all molecular and inert-gas crystals have very low melting and boiling temperatures is a manifestation of the very weak bond.

The reader may ask what gives rise to a nonvanishing dipole moment  $p$  in Eq. (3.2.4) in the first place. The electron distribution associated with a closed-shell configuration is known to be spherically symmetrical with respect to the nucleus. From electrostatics, we know that we can replace a spherical charge distribution by an equivalent charge at the center of the sphere. Consequently, no electric dipole is expected. Here we must distinguish between time-average and instantaneous dipole moment. It is true that the average dipole moment of an inert-gas atom is zero, as obtained from the electron wave function. However, at a given instant, an atom may possess a nonvanishing dipole moment because of the motion of the electron around the nucleus.

To prove our point about instantaneous and time-average values, we consider a one-dimensional harmonic oscillator which consists of a stationary positive charge  $+e$  and a moving electron of charge  $-e$ . For harmonic motion, the instantaneous displacement  $x$  changes with time as

$$x = x_0 \sin(\omega_0 t + \phi) \quad (3.2.5)$$

Although the average value of  $x$  (over a period) is zero, both the instantaneous value and the mean-square value of  $x$  are nonzero. In Eq. (3.2.4) it is the average value of  $pp'$  that is to be evaluated. Since the motions of electrons in neighboring atoms (Fig. 3.9) are in harmony with one another, the time-average value of  $pp'$  is equal to the time-average value of  $p^2$  and hence is nonzero.

In summary, we have given in this section some general characterizations of the four distinct bond types. In ionic crystals, electron transfer from atoms of one kind to atoms of another kind is involved. In covalent crystals, the bond is formed between neighboring atoms by sharing a pair of electrons. In metallic crystals, the valence electrons are essentially free. The different arrangements in these crystals are designed such that the atoms or ions involved may achieve a closed-shell configuration. In molecular and inert-gas crystals, the constituent molecule or atom already has a stable configuration, and hence the bond is much weaker. The weak bond comes from attraction between electric dipoles. In some cases we may even have to consider attraction arising from electric quadrupoles (van der Waals interaction having a  $1/R^8$  dependence). In making the foregoing general characterization of the four bond types, we must emphasize that the transition between crystal types is not at all sharp. Many materials have

two bonding mechanisms operating simultaneously. For example, ZnS can be considered as having an admixture of ionic and covalent bonding, with the character of the former being stronger than that of the latter. The situation in SiC is just the opposite. Some metal alloys such as Mg<sub>3</sub>Sb<sub>2</sub> and Zn<sub>3</sub>As<sub>2</sub> can be considered partly metallic and partly ionic, and some element crystals such as S and P can be considered partly molecular and partly covalent.

### 3.3 IONIC CRYSTALS

In Section 3.2 we presented a general discussion concerning the bonding mechanisms in four principal crystal types: the ionic, the covalent, the metallic, and the molecular crystals. In discussing material properties, especially the conductive and dielectric properties, we must know how tightly electrons are bound to the parent atoms or ions in a crystal. More specifically, electrons are known to be free to move in metals, but not so in ionic crystals. The foundations of the classical theory of ionic and metallic crystals were laid before the quantum theory was advanced. The classical theory provides us with a physical model that is simple to understand and easy to work with. In this section and in Section 3.4, we explore the physical models for these crystals and see how accurate are the predictions based on the classical model.

The idealized model of an ionic crystal assumes that the constituent ions have closed-shell configurations. Hence it is expected that these ions have spherically symmetric charge distributions as inert-gas atoms. X-ray study of ionic crystals has indeed confirmed this picture of spherical electron distribution except near the region where neighboring ions come in contact. This spherical model makes the calculation of the cohesive energy of a crystal tractable.

According to the theory of electrostatics, the Coulomb energy between two non-overlapping spherical charge distributions is the same as that between two point charges. Thus the total electrostatic energy of an ionic crystal is given by

$$\mathcal{E}_P = \sum (\pm) \frac{e^2}{4\pi\epsilon_0 r_{ij}} \quad (3.3.1)$$

where  $r_{ij}$  is the distance between the two ions involved,  $\epsilon_0$  the dielectric constant of free space, and the positive and negative signs are for interactions between charges of like and opposite polarities, respectively. The summation in Eq. (3.3.1) extends over all ion pairs.

To illustrate how the summation can be evaluated, we use NaCl as an example, the structure of which is shown in Fig. 2.7a. First, we choose the center Cl ion as the reference ion. In other words, we let the index  $j$  in Eq. (3.3.1) be fixed. The contribution to Eq. (3.3.1) from the six nearest Na ions is  $6e^2/R$ ,  $R$  being the distance between the nearest neighbors. Next are the 12 nearest Cl ions, which are  $\sqrt{2} R$  apart from the center Cl ion. Then there are eight next to the nearest Na ions at a distance  $\sqrt{3} R$  apart and six next to the nearest Cl ions at a distance  $\sqrt{4} R$  apart. If there are  $2N$  ions or  $N$  pairs of NaCl ions in a crystal, summing Eq. (3.3.1) over the index  $j$  simply means repeating the same process of calculation  $N$  times. Thus Eq. (3.3.1) can be written as

$$\mathcal{E}_P = \frac{Ne^2}{4\pi\epsilon_0 R} \left( \frac{6}{1} - \frac{12}{\sqrt{2}} + \frac{8}{\sqrt{3}} - \frac{6}{\sqrt{4}} + \frac{24}{\sqrt{5}} - \dots \right) = \frac{ANe^2}{4\pi\epsilon_0 R} \quad (3.3.2)$$

In Eq. (3.3.2) the constant  $A$  is a numerical constant known as the *Madelung constant*. Since the series in parentheses converges very slowly, many terms are needed to make a fair estimate of  $A$ . For the NaCl structure the value of  $A$  is found to be 1.75, and for the CsCl structure,  $A = 1.76$ .

Equation (3.3.2) accounts for the attractive energy  $\mathcal{E}_{\text{att}}$  in Eq. (3.1.2). Let us now turn to the repulsive energy. Because the ions, the  $\text{Na}^+$  and  $\text{Cl}^-$  ions in NaCl for example, have closed-shell configurations, the repulsive energy is due to the ion-core repulsion energy  $\mathcal{E}_C$ , which increases very rapidly with decreasing interatomic distance  $R_0$ . The actual dependence of this repulsive energy can be calculated quantum mechanically as a function of  $R$ . However, we are interested only in the variation of this repulsive energy near  $R_0$ , the equilibrium value of  $R$  (Fig. 3.1). For this purpose, the repulsive energy can be approximated by

$$\mathcal{E}_C = \frac{BN}{R^n} \quad (3.3.3)$$

Since the two energies  $\mathcal{E}_P$  and  $\mathcal{E}_C$  are opposite in nature, the total energy of a NaCl crystal is given by  $\mathcal{E}_C - \mathcal{E}_P$ .

At the equilibrium separation  $R_0$ ,  $\mathcal{E}_C - \mathcal{E}_P$  is a minimum. Using Eq. (3.3.3) and setting  $R = R_0$ , we obtain

$$\frac{-nBN}{R_0^{n+1}} + \frac{ANe^2}{4\pi\epsilon_0 R_0^2} = 0 \quad \text{or} \quad R_0^{n-1} = \frac{4\pi\epsilon_0 B n}{A e^2} \quad (3.3.4)$$

Substituting  $R_0$  from Eq. (3.3.4) into Eqs. (3.3.2) and (3.3.3), we find the binding energy  $\mathcal{E}_0$  (Fig. 3.1) to be

$$\mathcal{E}_0 = (\mathcal{E}_C - \mathcal{E}_P)_{R=R_0} = - \frac{ANe^2}{4\pi\epsilon_0 R_0} \left( 1 - \frac{1}{n} \right) \quad (3.3.5)$$

To compare the theoretical and experimental values of  $\mathcal{E}_0$ , we need to know the value of  $n$  in Eq. (3.3.5). Such information can be obtained from the compressibility  $K$ . By definition,

$$K = \frac{-1}{V} \frac{dV}{dp} \quad (3.3.6)$$

where  $V$  is the volume of a crystal and  $p$  is the applied pressure. If we assume that each ion occupies a small cube of volume  $R^3$ , the volume of the crystal is given by  $V = 2NR^3$ . Noting that under constant  $p$ ,  $d\mathcal{E} = -p dV$ , we obtain from Eqs. (3.3.2) and (3.3.3),

$$\frac{1}{K} = V \frac{d^2\mathcal{E}}{dV^2} = \frac{(n-1)e^2 A}{72\pi\epsilon_0 R_0^4} \quad (3.3.7)$$

Take NaCl as an example of an ideal ionic crystal. The value of  $K$  is  $4.1 \times 10^{-12}$  cm<sup>2</sup>/dyn, and the value of  $R_0$  is 2.82 Å (Table 2.3). Using these values in Eq. (3.3.7) gives a value of  $n = 7.9$ . The binding energy of NaCl crystal (Table 3.1) is found experimentally to be 183 kcal/mol or 7.95 eV/molecule. Using  $A = 1.75$ ,  $R_0 = 2.82$  Å, and  $n = 7.9$  in Eq. (3.3.5), we find the value of  $\mathcal{E}_0/N = 7.85$  eV. The small discrepancy between the calculated and measured values is due to the fact that we have

neglected in our calculation a small contribution from van der Waals forces to the total energy. A good agreement between the two values is also found in other alkali-halide crystals. This general agreement confirms that the physical model of an ionic crystal as being made of  $X^+$  and  $Y^-$  ions is a correct one. We further note from Eq. (3.3.5) that the repulsive energy is smaller than the Coulomb energy by the factor  $1/n$ . Therefore, the cohesive energy of an ionic crystal is due mostly to Coulomb attraction between the ions.

### 3.4 METALLIC CRYSTALS

According to the classical description mentioned in Section 3.2, metallic crystals are generally considered as being composed of arrays of positive ions embedded in a uniform sea of conduction electrons. In the following discussion we use this classical model in the calculation of the cohesive energy of a metallic crystal. For the calculation, we take sodium as an example. As shown in Fig. 3.8, the distribution of valence electrons in sodium crystals is essentially uniform over 90% of the volume occupied by electrons. Therefore, in the calculation of the electrostatic interaction energy  $\mathcal{E}_P$ , it seems reasonable to treat a sodium atom as being made of a point charge of  $+e$  (which represents the nucleus plus core electrons) and an electron cloud of charge  $-e$  (which represents the valence electron) uniformly distributed over a sphere of volume  $V$ .

Referring to Fig. 3.10, we see that the charge  $dq$  carried by the electron cloud in a volume element  $4\pi r^2 dr$  is given by

$$dq = -e \frac{4\pi r^2 dr}{V} \quad (3.4.1)$$

This charge  $dq$  experiences a positive Coulomb potential  $e/4\pi\epsilon_0 r$  due to the positive point charge and a negative Coulomb potential  $-q/4\pi\epsilon_0 r$  due to the electron cloud, where  $q$  is the charge carried by the electron cloud. From electrostatics, we know that to evaluate the potential at a point  $r$  from the center of a spherical charge distribution, we count only the charge within a sphere of radius  $r$ . Thus  $q = e4\pi r^3/3V$ . The total Coulomb energy per atom is therefore given by

$$\mathcal{E}_P = \int_0^R \left( \frac{e}{4\pi\epsilon_0 r} - \frac{er^2}{3\epsilon_0 V} \right) \left( -e \frac{4\pi r^2 dr}{V} \right) = \frac{-9e^2}{40\pi\epsilon_0 R} \quad (3.4.2)$$

For alkali metals, the other important term in the calculation of cohesive energy is the kinetic energy  $\mathcal{E}_K$  in Eq. (3.1.5). To calculate this energy, we must know the energy distribution of electrons. Figure 3.11a is the X-ray emission spectrum of sodium caused by the  $3s \rightarrow 2p$  transition (Fig. 3.11b). As a result of the impact of high-energy electrons (Section 2.7), the  $2p$  electrons are liberated from certain sodium atoms. The

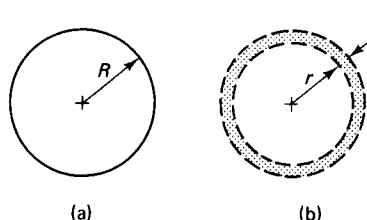
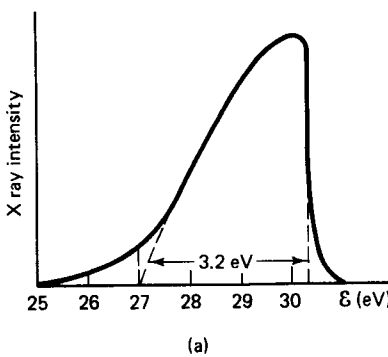
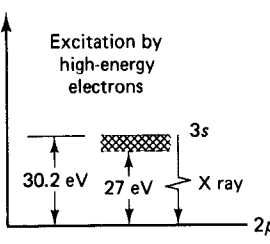


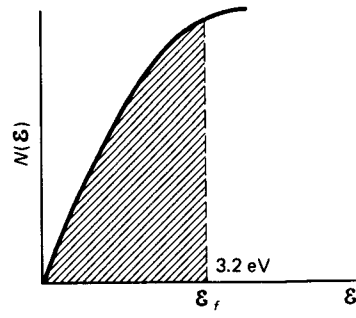
**Figure 3.10** Diagrams used for the calculation of electrostatic energy in a metallic crystal. Consider the electrostatic potential experienced by charge  $dq$  in a spherical shell (shaded area). The potential consists of two parts: (a) due to the positive ion core and (b) due to the electron cloud inside the spherical shell.



(a)



(b)



(c)

**Figure 3.11** Information used in the calculation of kinetic energy in a sodium crystal: (a) X-ray emission spectrum, (b) energy levels involved in the X-ray emission, and (c) energy distribution of the 3s electrons (valence electrons) as derived from the X-ray emission spectrum. Note the similarity between the curves in (a) and (c). In curve c, the abscissa represents the kinetic energy only.

2p levels thus vacated are ready for reoccupation by electrons from the 3s levels. The energy of the 3s electrons in a sodium crystal, unlike the 3s electron in a free sodium atom, is not discrete but forms a band. Therefore, the emission spectrum of the X ray ( $\mathcal{E}_{3s} - \mathcal{E}_{2p}$ ) covers a range from approximately 27 to 30.2 eV because the energy of the 3s electrons spreads over a range of 3.2 eV.

As discussed in Chapter 4, the energies of atomic states broaden in a crystal to form energy bands. Since the 3s (valence) electrons in Na are free to move, the spread in energy is due to different kinetic energies. We define a distribution function  $D(\mathcal{E})$  such that the density of electrons  $dN$  within an energy interval  $d\mathcal{E}$  is

$$dN = D(\mathcal{E}) d\mathcal{E} \quad \text{electrons/m}^3 \quad (3.4.3)$$

The intensity of the X ray shown in Figure 3.11a is proportional to  $D(\mathcal{E})$  of Eq. (3.4.3). It is shown in Chapter 4 that the function  $D(\mathcal{E})$  is given by

$$D(\mathcal{E}) = \frac{4\pi(2m)^{3/2}}{h^3} \mathcal{E}^{1/2} \quad (3.4.4)$$

The  $\mathcal{E}^{1/2}$  dependence is shown in Fig. 3.11c. Since  $\mathcal{E}_K = 0$  for the 3s electron having the lowest energy, we move the origin to  $\mathcal{E}_K = 0$  in Fig. 3.11c. Otherwise, Fig. 3.11c is a reproduction of Fig. 3.11a.

We define a quantity  $\mathcal{E}_f$ , generally called the *Fermi energy*, as the topmost kinetic energy. From Eqs. (3.4.3) and (3.4.4) we find the total number of 3s electrons to be

$$n = \int_0^{\mathcal{E}_f} D(\mathcal{E}) d\mathcal{E} = \frac{8\pi}{3} \frac{(2m)^{3/2}}{h^3} \mathcal{E}_f^{3/2} \quad \text{electrons/m}^3 \quad (3.4.5)$$

The total kinetic energy of all electrons is

$$\sum \mathcal{E}_K = \int_0^{\mathcal{E}_f} \mathcal{E} D(\mathcal{E}) d\mathcal{E} = \frac{8\pi}{5} \frac{(2m)^{3/2}}{h^3} \mathcal{E}_f^{5/2} \quad (3.4.6)$$

Thus the average kinetic energy  $\bar{\mathcal{E}}_K$  per atom (the same as per 3s electron in the case of sodium) is

$$\bar{\mathcal{E}}_K = \frac{\Sigma \mathcal{E}_K}{n} = \frac{3}{5} \mathcal{E}_f = \frac{3h^2}{10m} \left( \frac{3n}{8\pi} \right)^{2/3} \quad (3.4.7)$$

Referring to Fig. 3.10, we see that each Na atom occupies a volume  $4\pi R^3/3$ . Since there is one  $3s$  electron per atom, the density of electrons is equal to  $n = 3/(4\pi R^3)$ . Using this value of  $n$  in Eq. (3.4.7), we obtain

$$\bar{\mathcal{E}}_K = \frac{3h^2}{10m} \left( \frac{9}{32\pi^2} \right)^{2/3} \frac{1}{R^2} \quad (3.4.8)$$

To calculate the value of  $R$  from the lattice constant, we note the following fact. In a body-centered cubic structure, the eight corner atoms are shared by eight cubes; hence the cube is occupied by two atoms, one being the center atom and the other being contributed by the eight corner atoms of one-eighth each. If  $a$  is the lattice constant, the volume occupied by each Na atom is  $a^3/2$ , which should be set equal to  $4\pi R^3/3$ . For sodium,  $a = 4.28 \text{ \AA}$  (Table 2.3) which gives a value of  $R = 2.11 \text{ \AA}$ . Using this value of  $R$  in Eqs. (3.4.2) and (3.4.7), we find that  $\mathcal{E}_P = -6.13 \text{ eV}$  and  $\bar{\mathcal{E}}_K = 1.92 \text{ eV}$ .

Now we refer to Fig. 3.12 in calculating the cohesive energy. The energy  $\mathcal{E}_P$  is the potential energy required to remove the valence ( $3s$ ) electron from Na in the crystal state. However, the cohesive energy is the energy difference between crystalline sodium and atomic sodium. The energy difference between atomic sodium and sodium in the ionized state ( $\text{Na}^+ + \text{free electron}$ ) is just the ionization energy ( $\mathcal{E}_i = 5.18 \text{ eV}$ ) of the  $3s$  electron. From Fig. 3.12 we have

$$\mathcal{E}_0 = |\mathcal{E}_P - \bar{\mathcal{E}}_K - \mathcal{E}_i| \quad (3.4.9)$$

Before we substitute the values in Eq. (3.4.9), we note that if Eqs. (3.4.2) and (3.4.8) are used in Eq. (3.1.2), we obtain an equilibrium value of  $R = 1.3 \text{ \AA}$  quite different from the value of  $2.11 \text{ \AA}$ . Apparently, either Eq. (3.4.2) or (3.4.8) must be in error. We may find the clue from the ionization energy. For the  $3s$  electron, the principal and orbital quantum numbers are  $n = 3$  and  $l = 0$ . If the  $3s$  electron felt an effective nuclear charge of  $+e$  as our model assumes, Eq. (1.6.1) would predict an ionization energy of  $13.6/9 = 1.5 \text{ eV}$ . The fact that the measured value ( $5.18 \text{ eV}$ ) is considerably larger than this value indicates that the  $3s$  electron sees an effective nuclear charge (nucleus plus core electrons) appreciably larger than  $+e$ .

The classical model, on which Eq. (3.4.2) is based, treats electrons of closed shells as if they form a spherical core. The model further assumes that the valence electron moves completely outside this core. A quantum-mechanical calculation of the  $3s$  electron wave function (Fig. 3.8) shows that the  $3s$  electron wave function penetrates the ion core. When the  $3s$  electron is inside the core region, that is, for  $r < 0.9 \text{ \AA}$  in Fig. 3.8, the shielding effect of the core electrons is much reduced. Therefore, it is Eq. (3.4.2), which is in error.

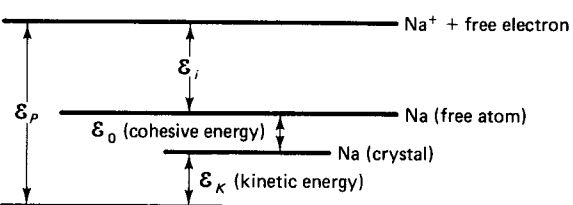


**Figure 3.12** Diagram used for the calculation of cohesive energy of sodium. The difference in energy between a crystalline sodium atom and an ionized sodium atom is  $\mathcal{E}_P - \bar{\mathcal{E}}_K$ . The energy difference between a free and ionized sodium atom is  $\mathcal{E}_i$ . The cohesive energy  $\mathcal{E}_0$  is, therefore, given by Eq. (3.4.9).

The correct value of  $\mathcal{E}_P$  is found quantum mechanically to be  $-8.40$  eV for  $R = 2.11$  Å. Using this value,  $\mathcal{E}_K = 1.98$  eV, and  $\mathcal{E}_i = 5.18$  eV in Eq. (3.4.9), we obtain a value of cohesive energy per atom  $\mathcal{E}_0 = 1.30$  eV, in reasonable agreement with the observed value of  $1.13$  eV (Table 3.1). The agreement is a confirmation of the validity of Eq. (3.4.7). As shown in Chapter 4, Eq. (3.4.4) is derived on the basis of the relation

$$\mathcal{E} = \frac{p^2}{2m} = \frac{\hbar^2 k^2}{2m} \quad (3.4.10)$$

between the energy  $\mathcal{E}$  and the wave number  $k$  of an electron. Equation (3.4.10), in turn, is based on the assumptions that valence electrons in a metal are essentially free and that the wave number  $k (= 2\pi/\lambda)$  is related to the momentum  $p$  of an electron by the de Broglie relation  $\lambda = h/p$ . The success that we have had with Eq. (3.4.4) in predicting the value of  $\mathcal{E}_K$  proves the correctness of these assumptions. As we shall see in Chapters 4 and 5, these assumptions lead to a great simplification of the treatments of the conductive properties of metals and semiconductors.

We should point out that the relative importance of  $\mathcal{E}_K$  and  $\mathcal{E}_P$  varies from metal to metal; therefore, sodium should not be taken as a typical example for other metals. If the size of the inner shell is large, ion-core repulsive energy  $\mathcal{E}_C$  may become significant. The wide variation of cohesive energy from  $0.8$  eV in Cs (alkali metal) to  $4.2$  eV in Fe (transition metal) is an indication that bonding forces of different physical origins may be involved. It is generally believed that covalent bonding plays a significant part in transition metals with incomplete  $3d$  shells. However, for alkali metals, the binding energies calculated from Eq. (3.4.9) are in good agreement with the measured values. Because the orbits of core electrons are relatively small compared with the interatomic distances, the simple model (Fig. 3.10) works well for these metals. For this reason alkali metals are considered the closest to being ideal metals.

### 3.5 THE HYDROGEN MOLECULE

In the study of atoms the hydrogen atom is generally used as a model in understanding the structure of other atoms. Similarly, a great deal can be learned from the hydrogen molecule. As discussed in Section 3.2, the bond between two hydrogen atoms is formed by sharing a pair of electrons with antiparallel spins. Many important properties of covalent bonds are illustrated in this simple case. We outline below the methods used in the study of hydrogen molecules. The material presented in this section supplements our discussion in Section 3.2.

The Schrödinger equation for a hydrogen molecule is

$$\frac{\hbar^2}{2m} (\nabla_1^2 \psi + \nabla_2^2 \psi) + \left[ \mathcal{E} + \frac{1}{4\pi\epsilon_0} \left( \frac{e^2}{r_{1a}} + \frac{e^2}{r_{1b}} + \frac{e^2}{r_{2a}} + \frac{e^2}{r_{2b}} - \frac{e^2}{r_{12}} - \frac{e^2}{r_{ab}} \right) \right] \psi = 0 \quad (3.5.1)$$

where the subscripts  $a$  and  $b$  refer to the two nuclei, the subscripts 1 and 2 refer to the two electrons, and  $r$  is the distance between them, as illustrated in Fig. 3.13. In Eq. (3.5.1),  $\nabla^2$  is the Laplacian operator. Because of the various mutual interaction terms, it is difficult to find the solution of Eq. (3.5.1). Therefore, we must resort to approxi-

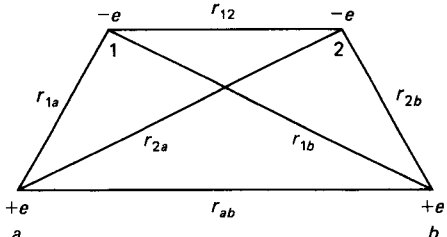


**Figure 3.13** Coordinates of electrons and nuclei in a hydrogen molecule. Points *a* and *b* represent the positions of the two hydrogen nuclei, whereas points 1 and 2 represent the positions of the two electrons.

mate methods. There are two approaches that are taken to find an approximate solution of Eq. (3.5.1): the method of molecular orbitals and the method of Heitler and London.

As pointed out in Section 3.2, the Schrödinger equation for the  $\text{H}_2^+$  molecule ion [Eq. (3.5.1) without electron 2, that is, without the  $r_{2a}$ ,  $r_{2b}$ , and  $r_{12}$  terms] can be exactly solved. The wave function obtained from such a solution is called the *molecular orbital*. The wave functions  $\sigma_g$  and  $\sigma_u$  used in the computation of the two curves in Fig. 3.7 are molecular orbitals. If we neglect the mutual interaction between the two electrons in  $\text{H}_2$ , we can treat the neutral  $\text{H}_2$  molecule as if the two electrons move independently in the Coulomb potential of  $\text{H}_2^+$  ion. For the lowest-energy state of a neutral  $\text{H}_2$  molecule, both electrons have the  $\sigma_g$  wave function. Since the orbital wave functions of the two electrons are the same, their spin wave functions must be different because of the exclusion principle. This treatment of a  $\text{H}_2$  molecular, known as the *method of molecular orbitals*, is used in Section 3.2 to explain the bonding property and spin antiparallel arrangement of an electron-pair bond.

The other approach to the  $\text{H}_2$  problem is the method of Heitler and London. As discussed in Section 1.4, the Schrödinger equation for a hydrogen atom can be solved exactly. If we neglect the mutual interaction terms  $r_{1b}$ ,  $r_{2a}$ ,  $r_{12}$ , and  $r_{ab}$  in Eq. (3.5.1), we can write Eq. (3.5.1) as

$$\frac{\hbar^2}{2m} (\nabla_1^2 \psi + \nabla_2^2 \psi) + \left[ \mathcal{E} + \frac{1}{4\pi\epsilon_0} \left( \frac{e^2}{r_{1a}} + \frac{e^2}{r_{2b}} \right) \right] \psi = 0 \quad (3.5.2)$$

Let  $\psi_{1a}$  and  $\psi_{2b}$  be two atomic wave functions of a hydrogen atom. In associating the subscript 1 with *a* and the subscript 2 with *b*, we assign electron 1 to nucleus *a* and electron 2 to nucleus *b*. Since electron 1 belongs to nucleus *a*, the wave function must satisfy the equation

$$\frac{\hbar^2}{2m} \nabla_1^2 \psi_{1a} + \left( \mathcal{E}_1 + \frac{e^2}{4\pi\epsilon_0 r_{1a}} \right) \psi_{1a} = 0 \quad (3.5.3)$$

Equation (3.5.3) is simply the Schrödinger equation for a hydrogen atom. A similar equation for electron 2 and nucleus *b* can be obtained from Eq. (3.5.3) by substituting the subscript 2 for 1 and the subscript *b* for *a*.

Using separation of variables, we can express the solution of Eq. (3.5.2) as

$$\Psi = \psi_{1a} \psi_{2b} \quad (3.5.4)$$

if we let  $\mathcal{E} = \mathcal{E}_1 + \mathcal{E}_2$ . Now let us return to Eq. (3.5.1). We see that Eq. (3.5.1) remains the same if the subscripts 1 and 2 are interchanged. Since  $|\Psi|^2$  is the joint probability function, there is no a priori reason why electron 1 should belong to nucleus *a* and electron 2 should belong to nucleus *b*. If the function  $\psi_{1a} \psi_{2b}$  is an approximate

solution to Eq. (3.5.1), the function  $\psi_{2a}\psi_{1b}$  with electron 1 belonging to nucleus *b* and electron 2 belonging to nucleus *a* is just as good an approximate solution. Both these functions must be considered in finding the approximate solution of Eq. (3.5.1).

Let  $\Psi(1, 2)$  be the joint wave function of the two electrons in a hydrogen molecule. The indistinguishability of electrons requires that the probability of finding electron 1 at  $r_{1a}$  and electron 2 at  $r_{2b}$  be the same if the labels of the two electrons are interchanged. In other words,

$$\Psi^*(1, 2)\Psi(1, 2) = \Psi^*(2, 1)\Psi(2, 1) \quad (3.5.5)$$

Equation (3.5.5) is satisfied if

$$\Psi(1, 2) = \Psi(2, 1) \quad (3.5.6)$$

or if

$$\Psi(1, 2) = -\Psi(2, 1) \quad (3.5.7)$$

The wave function that satisfies Eq. (3.5.6) is the symmetric wave function, whereas the wave function that satisfies Eq. (3.5.7) is the antisymmetric wave function. The functions

$$\Psi_{S-Or} = \psi_{1a}\psi_{2b} + \psi_{2a}\psi_{1b} \quad (3.5.8)$$

$$\Psi_{A-Or} = \psi_{1a}\psi_{2b} - \psi_{2a}\psi_{1b} \quad (3.5.9)$$

certainly satisfy the symmetric and antisymmetric requirement of Eqs. (3.5.6) and (3.5.7), respectively. The subscripts S-Or and A-Or are used to denote, respectively, symmetric and antisymmetric orbital wave functions.

In the treatment of a hydrogen molecule by Heitler and London, products of atomic wave functions expressed in symmetric and antisymmetric forms as in Eqs. (3.5.8) and (3.5.9) are used as the approximate solution to Eq. (3.5.1). The electron density for the symmetric wave function tends to be concentrated in the region of low potential energy between the two nuclei. Using the symmetric and antisymmetric wave functions of Eqs. (3.5.8) and (3.5.9), the energy of a hydrogen molecule can be calculated quantum mechanically. The results of such a calculation are shown in Fig. 3.14 as a function of the internuclear distance  $r_{ab}$ . As expected, the state represented by the symmetric wave function is the bonding state, whereas the state represented by the antisymmetric wave function is the antibonding state.

Besides the orbital wave function, we must consider the spin wave function. Like the orbital wave function, the spin wave function must also be either symmetric (denoted by  $\Psi_{S-Sp}$ ) or antisymmetric (denoted by  $\Psi_{A-Sp}$ ). The symmetric spin wave function can be expressed in either one of the following three combinations:

$$\Psi_{S-Sp} = \begin{cases} \alpha_1\alpha_2 \\ \beta_1\beta_2 \\ \alpha_1\beta_2 + \beta_1\alpha_2 \end{cases} \quad (3.5.10)$$

whereas the antisymmetric spin wave function is given by

$$\Psi_{A-Sp} = \alpha_1\beta_2 - \beta_1\alpha_2 \quad (3.5.11)$$

where  $\alpha$  and  $\beta$  denote the one-electron spin wave function having  $s_z = +\frac{1}{2}$  and  $s_z = -\frac{1}{2}$ , respectively.

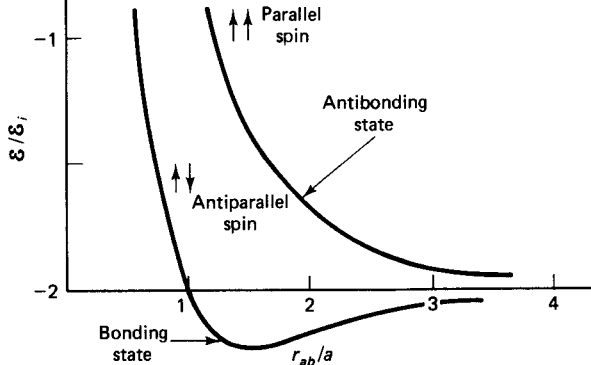


**Figure 3.14** Energy curves for the hydrogen molecule plotted as a function of the internuclear distance. The ordinate and abscissa are normalized with respect to the ionization energy and the Bohr radius of a hydrogen atom. The lower curve has an energy lower than the energy of two separate hydrogen atoms. Therefore, the state represented by the antisymmetric spin wave function is the bonding state.

The total wave function in a hydrogen molecule is a product of the orbit and spin wave functions, or

$$\Psi_{\text{total}} = \frac{\Psi_{S-\text{Or}}}{\Psi_{A-\text{Or}}} \times \begin{cases} \Psi_{A-\text{Sp}} \\ \Psi_{S-\text{Sp}} \end{cases} \quad (3.5.12)$$

The question as to which combinations in Eq. (3.5.12) occur in nature can only be answered by experiments. Analyses of the atomic and molecular spectra show that only the combinations of  $\Psi_{S-\text{Or}}\Psi_{A-\text{Sp}}$  and  $\Psi_{A-\text{Or}}\Psi_{S-\text{Sp}}$  are allowed. In other words, the total wave function  $\Psi_{\text{total}}$  must be antisymmetric. This condition is consistent with the Pauli exclusion principle. Let us take the case of  $\text{H}^-$ , that is, a hydrogen ion with two electrons. Since we have a single nucleus,  $a = b$  in Eqs. (3.5.8) and (3.5.9). The Pauli exclusion principle demands that the probability of finding two electrons in the same state must be zero. This means that if we change  $\alpha$  to  $\beta$  or  $\beta$  to  $\alpha$  in Eqs. (3.5.10) and (3.5.11),  $\Psi_{\text{total}}$  must be zero. The antisymmetric  $\Psi_{\text{total}}$  indeed satisfies this condition.

In Section 1.5, the exclusion principle is stated as follows. No two electrons can have the same set of four quantum numbers,  $n$ ,  $l$ ,  $m$ , and  $s_z$ . So that the principle can easily be applied to electrons in molecules, this principle has been changed to the following statement: If any two electrons are interchanged, the proper wave function must remain unchanged except for the factor  $-1$ . This antisymmetric requirement on the total wave function demands that the bonding state have antiparallel spins. It can be shown quantum mechanically that the resultant spin of the two electrons as represented by  $\Psi_{A-\text{Sp}}$  of Eq. (3.5.11) is zero and thus the spins must be antiparallel.

Although in the two methods (the method of molecular orbitals and the method of Heitler and London), different wave functions are used as the starting approximate solution of Eq. (3.5.1), the conclusions drawn from the two analyses are qualitatively the same. The energy of the bonding state is lowered by an accumulation of negative charges in the region of low potential energy between the two nuclei. The two electrons do not specifically belong to a particular nucleus, but are shared equally between the two nuclei. The spins of the two electrons must have an antiparallel arrangement because of the exclusion principle. These properties as derived from the analysis of a hydrogen molecule are the general properties of a covalent bond.

### 3.6 SATURATION AND DIRECTIONAL PROPERTIES OF COVALENT BONDS

In Sections 3.2 and 3.5 we described a covalent bond as an electron-pair bond which is formed between two atoms as a result of minimizing the energy by sharing a pair of electrons with antiparallel spins. On the other hand, the wave function of the antibonding state (Fig. 3.14) is represented by  $\Psi_{A-Or}\Psi_{S-Sp}$ , a product of antisymmetric orbital wave function and symmetric spin wave function. It can be shown quantum mechanically that the resultant spin of the two electrons as represented by  $\Psi_{S-Sp}$  of Eq. (3.5.10) is 1 ( $= \frac{1}{2} + \frac{1}{2}$ ), and thus the two spins are parallel. The property of an electron-pair bond can be stated in terms of spin orientations as follows. Sharing a pair of electrons with antiparallel spins results in an attraction of the two atoms (the bonding state), whereas sharing a pair of electrons with parallel spins results in a repulsion of the two atoms (the antibonding state).

The requirement on the spin orientation leads to an important property of a covalent bond, the saturation property. Consider the interaction of a hydrogen atom with a helium atom. As illustrated in Fig. 3.15, there are only two possible interactions: sharing a pair of electrons with antiparallel spins or sharing a pair of electrons with parallel spins. If the He atom and H atom share electrons with antiparallel spins, the other electron of the He atom will have the same spin orientation as the electron from the hydrogen atom (Fig. 3.15a). This situation clearly violates the Pauli exclusion principle unless either one of the two electrons is promoted to an unoccupied shell of higher energy. On the other hand, if the He atom and H atom share electrons with parallel spins, our previous discussion of a hydrogen molecule tells us that the state will be an antibonding state. In either case, the energy of the hypothetical H—He molecule would be higher than the combined energy of two separate atoms. In other words, a bond will not form between a H atom and a He atom.

The saturation property of a covalent bond, as illustrated by the foregoing example, can be stated as follows. An electron-pair bond can be formed only by those electrons of an atom that have unpaired spins. The spins of the two electrons in He are already paired (one with  $s_z = +\frac{1}{2}$  and the other with  $s_z = -\frac{1}{2}$ ), and hence no electron-pair bond will be formed between either one of the two electrons and a third electron from another atom.

To illustrate the saturation property of a covalent bond further, we examine the situation in  $H_2O$ ,  $NH_3$ , and  $CH_4$ . Referring to Table 1.2, we see that oxygen has an electron configuration  $1s^22s^22p^4$  and nitrogen has an electron configuration  $1s^22s^22p^3$ . The  $s$  electrons already have their spins paired (one up and the other down), so only the  $p$  electrons need to be considered. For  $l = 1$ , there are three possible values for  $m$ , the

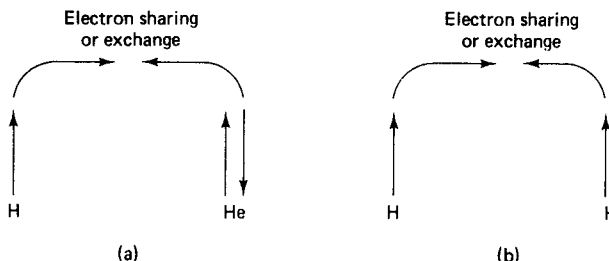


**Figure 3.15** Interaction between a hydrogen and a helium atom. The arrows indicate the direction of spin. There are two possible situations: (a) sharing electrons with antiparallel spins, and (b) sharing electrons with parallel spins.

magnetic quantum number. Therefore, there are altogether six possible arrangements for the  $p$  electrons:

$m$	1	0	-1	1	0	-1
Spin	Up	Up	Up	Down	Down	Down

For a nitrogen atom we can have a maximum of three electrons that have unpaired spins, whereas for an oxygen atom, at least two of the four electrons must have paired spins, leaving a maximum of two electrons having unpaired spins. Therefore, a nitrogen atom is capable of making three electron-pair bonds with three hydrogen atoms in  $\text{NH}_3$ , and an oxygen atom is capable of forming only two electron-pair bonds in  $\text{H}_2\text{O}$  even though it has four  $2p$  electrons. The situation is illustrated in Fig. 3.16.

Let us turn to  $\text{CH}_4$ . The ground state of carbon has the electron configuration  $1s^22s^22p^2$ . For the ground state, we would expect a maximum of two unpaired spins. As pointed out in Section 1.6, the energy of the  $2p$  state is not too far above the energy of the  $2s$  state. In  $\text{CH}_4$ , the carbon atom actually has an electron configuration  $1s^22s2p^3$ . In this configuration, the carbon atom can have a maximum of four unpaired spins. In  $\text{CH}_4$ , all four unpaired spins of the carbon atom become paired with spins of the four hydrogen atoms; therefore, the state of saturation is reached in forming four electron-pair bonds. Energy is gained in promoting one electron of the carbon atom from the  $2s$  level to the  $2p$  level, but at the same time, energy is reduced by forming electron-pair bonds. The  $\text{CH}_4$  molecule is a stable one because the reduction in energy is bigger than the gain in energy.

Typical examples of crystals having purely covalent bonds are diamond, silicon, and germanium. All these elements crystallize in the diamond structure. As discussed in Section 2.3, each atom in this structure (Figs. 2.11 and 2.12) has four nearest neighbors. Again, one electron must be promoted from the  $s$  to the  $p$  level ( $2s$  to  $2p$  in diamond,  $3s$  to  $3p$  in silicon, and  $4s$  to  $4p$  in germanium) in order that a maximum of four bonds can be achieved. Thus the four outmost electrons have the following configurations:  $2s2p^3$  in diamond,  $3s3p^3$  in silicon, and  $4s4p^3$  in germanium. These four electrons are said to form  $sp^3$  hybrid orbitals.

The reader may wonder why  $\text{CH}_4$  does not crystallize in the diamond structure. The difference in the bond properties of  $\text{CH}_4$  and Ge, for example, can be understood on the basis of the saturation property of the covalent bond. Figure 3.17a is a schematic representation of the bond pairs of Ge in a diamond structure. Note that germanium

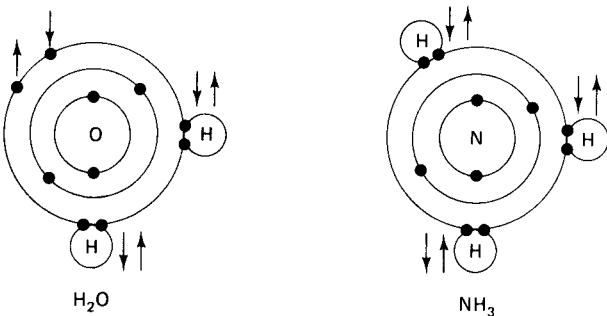


**Figure 3.16** Electron-pair bonds in (a)  $\text{H}_2\text{O}$  and (b)  $\text{NH}_3$ . Oxygen has two free (unpaired) spins and nitrogen three free spins. The number of free spins determines the maximum number of hydrogen bonds which an atom can make.

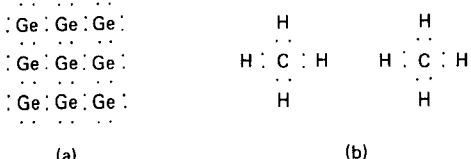


**Figure 3.17** Electron-pair bonds in (a) Ge and (b)  $\text{CH}_4$ . The bond is indicated by two dots.

atoms can always be added to the existing structure because there exist unpaired bonds at the boundary of the structure. Therefore, covalent bonding is all that is needed for Ge atoms to form a Ge crystal. This is not the case with  $\text{CH}_4$ . The bonds in  $\text{CH}_4$  are all used up (Fig. 3.17b); thus no additional bonds can be formed with neighboring  $\text{CH}_4$  molecules. In Table 3.1 the  $\text{CH}_4$  crystal is classified as a molecular crystal. It is true that the bonding between atoms in a  $\text{CH}_4$  molecule is of the covalent type. However, the bonding between two  $\text{CH}_4$  molecules in a  $\text{CH}_4$  crystal is of the van der Waals type. Because  $\text{CH}_4$  forms a stable molecule, they stay together as a molecule in the crystal. In other words, each lattice point in a molecular crystal (e.g., the lattice point in Fig. 2.1) actually represents a whole molecule. The same situation applies to other covalent-bond molecules, such as  $\text{H}_2$ .

Now let us discuss the directional property of a covalent bond. It is known from experiments that the  $\text{H}_2\text{O}$  molecule forms a triangle and the  $\text{NH}_3$  molecule is in the form of a pyramid (Fig. 3.18). We also know that the angle  $\theta$  between O—H bonds in  $\text{H}_2\text{O}$  and between any pair of the N—H bonds in  $\text{NH}_3$  is close to and slightly larger than  $90^\circ$ . As discussed in Sections 3.2 and 3.5, the lowering of energy is achieved in a covalent-bonding molecule by an accumulation of negative charges in the region between the two nuclei. In the language of quantum mechanics, the accumulation of negative charges is the result of the overlapping of two atomic wave functions. A strong bond is formed if there is a maximum of overlapping. Therefore, to understand the directional property of a covalent bond, we must examine the directional property of the atomic wave functions that take part in forming the bond.

Referring to the discussion in Section 1.4, we find that the wave function  $\psi_s$  for  $s$  electrons ( $l = 0$ ) is spherically symmetrical; that is, it has no  $\theta$  and  $\phi$  dependence. Thus we can write  $\psi_s$  as

$$\psi_s = g(r) \quad (3.6.1)$$

For the  $p$  electrons ( $l = 1$ ), there are three wave functions whose angular dependences are of the following form:  $\Theta(\theta)\Phi(\phi) \sim \sin \theta \exp(i\phi)$ ,  $\sin \theta \exp(-i\phi)$ ,  $\cos \theta$ . Since the Schrödinger equation is a linear differential equation, any linear combination of the solutions is also a solution to the differential equation. Combining the exponential functions to form  $\sin \phi$  and  $\cos \phi$ , we have  $\Theta(\theta)\Phi(\phi) \sim \sin \theta \cos \phi$ ,  $\sin \theta \sin \phi$ ,  $\cos \theta$ .

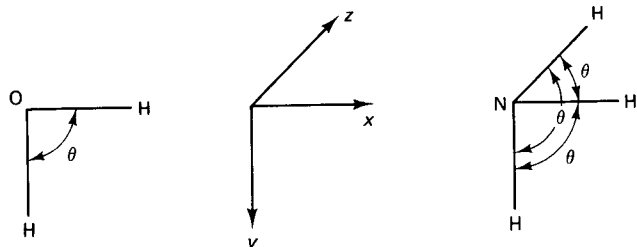


**Figure 3.18** Examples used to illustrate the directional property of a covalent bond.  
 (a) The  $\text{H}_2\text{O}$  molecule is in the form of a triangle and (b) the  $\text{NH}_3$  molecule is in the form of a pyramid. The angle between any pair of bonds is close to  $90^\circ$ . The characteristic is a result of the directional property of the  $p$  orbitals (Fig. 3.19).

Realizing that

$$x = r \sin \theta \cos \phi, \quad y = r \sin \theta \sin \phi, \quad \text{and} \quad z = r \cos \theta \quad (3.6.2)$$

and letting  $R(r) = rf(r)$ , we can express the three  $p$  wave functions as

$$\psi_{px} = xf(r), \quad \psi_{py} = yf(r), \quad \text{and} \quad \psi_{pz} = zf(r) \quad (3.6.3)$$

The electron distributions as represented by the  $s$  wave function of Eq. (3.6.1) and the  $p$  wave functions of Eq. (3.6.3) are shown in Fig. 3.19. We see that each of the three  $p$  orbitals extends along a certain coordinate axis, for example, the  $x$  axis for the  $\psi_{px}$  orbital. It is expected, therefore, that the covalent bond will be formed along one of these axes to achieve a bond of maximum strength. As stated earlier, a stable bond is formed if there is a maximum overlapping of electron distribution.

In the  $H_2O$  molecule, the two electrons of the oxygen atom whose spins are unpaired must have different orbital wave functions because of the Pauli exclusion principle. Let us say that the two electrons have  $\psi_{px}$  and  $\psi_{py}$ . The condition for maximum bond strength requires that the two hydrogen atoms be located along the  $x$  and  $y$  axes. Thus we have a  $H_2O$  molecule with an angle of  $90^\circ$  between the bonds. The actual bond angle  $\theta$  (Fig. 3.18a) in  $H_2O$  is  $109^\circ$ . Since the two hydrogen atoms have already used up their two electrons in forming bonds with the oxygen atom, they will not form an electron-pair bond between themselves. However, the repulsive force is still there, and the repulsion between the two hydrogen atoms increases the bond angle from  $90^\circ$  to  $109^\circ$ . The situation in  $NH_3$  is quite similar. The three electrons of the nitrogen atom

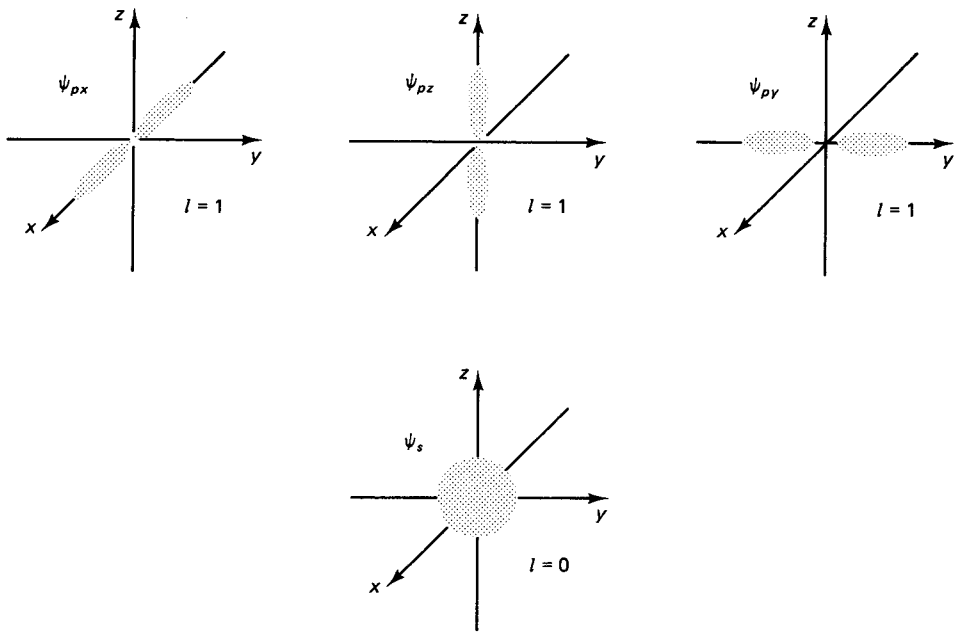


**Figure 3.19** Schematic illustration showing the electron distributions for the  $s$  and  $p$  atomic wave functions. The  $s$  wave function is spherically symmetrical, whereas each of the three  $p$  wave functions extends along a specific axis,  $\psi_{px}$  along the  $x$  axis,  $\psi_{py}$  along the  $y$  axis, and  $\psi_{pz}$  along the  $z$  axis.

take three different  $p$  wave functions and form bonds with the three hydrogen atoms located separately along the  $x$ ,  $y$ , and  $z$  axes. The bond angle  $\theta$  (Fig. 3.18b) between them is slightly greater than  $90^\circ$  because of the mutual repulsion between the three hydrogen atoms.

Let us discuss the situation in  $\text{CH}_4$ . The four electrons of the carbon atom have wave functions which are an admixture of the  $s$  and  $p$  wave functions called the  $sp^3$  hybrid orbitals. We learn from the theory of linear differential equations that the number of independent solutions is not altered by any linear combination of the independent solutions. Referring to the  $p$  state, we have three independent solutions irrespective of whether the solutions are expressed in terms of  $\sin \phi$  and  $\cos \phi$  or in terms of  $\exp(-i\phi)$  and  $\exp(i\phi)$ . For the carbon atom, we have one  $s$  orbital and three  $p$  orbitals to begin with. The total number is four. Therefore, we expect to have four different  $sp^3$  orbitals.

The four  $sp^3$  orbitals can be expressed in terms of the  $s$  orbital of Eq. (3.6.1) and the  $p$  orbitals of Eq. (3.6.3) as

$$\psi_{111} = \frac{1}{2} [g(r) + xf(r) + yf(r) + zf(r)] \quad (3.6.4)$$

$$\psi_{1\bar{1}\bar{1}} = \frac{1}{2} [g(r) + xf(r) - yf(r) - zf(r)] \quad (3.6.5)$$

$$\psi_{\bar{1}1\bar{1}} = \frac{1}{2} [g(r) - xf(r) + yf(r) - zf(r)] \quad (3.6.6)$$

$$\psi_{\bar{1}\bar{1}1} = \frac{1}{2} [g(r) - xf(r) - yf(r) + zf(r)] \quad (3.6.7)$$

The factor  $\frac{1}{2}$  in front of the brackets is to make the hybrid orbitals normalized. Each hybrid orbital represents an electron distribution which extends along one of the four body diagonals  $[111]$ ,  $[1\bar{1}\bar{1}]$ ,  $[\bar{1}1\bar{1}]$ , and  $[\bar{1}\bar{1}1]$  of a cube as illustrated in Fig. 3.20. This fact can easily be recognized by a rotation of  $120^\circ$  about one of the body diagonals. As

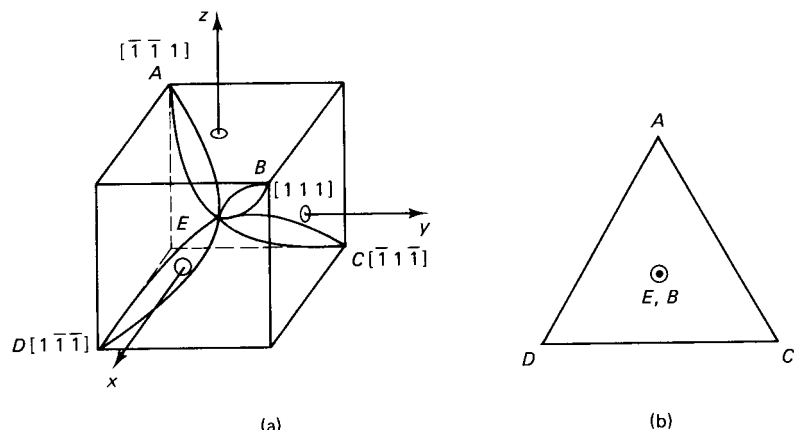


**Figure 3.20** (a) The four  $sp^3$  hybrid orbitals of carbon in  $\text{CH}_4$ , each having an electron distribution directed toward one of the four alternate corners of a cube. The center of the cube is chosen as the origin of the coordinates. (b) The tetrahedron formed by the  $\text{CH}_4$  molecule with the four hydrogen atoms,  $A$ ,  $B$ ,  $C$ , and  $D$ , occupying the four corners and the carbon atom  $E$  occupying the center of the tetrahedron. The view is taken along the direction  $BE$ .

discussed in Section 2.9, a counterclockwise rotation of  $2\pi/3$  about the [111] diagonal brings  $x \rightarrow y$ ,  $y \rightarrow z$ , and  $z \rightarrow x$ . Making these changes in Eqs. (3.6.4) to (3.6.7) results in the following transformations:

$$\psi_{111} \rightarrow \psi_{111}, \quad \psi_{1\bar{1}\bar{1}} \rightarrow \psi_{\bar{1}\bar{1}\bar{1}}, \quad \psi_{\bar{1}\bar{1}\bar{1}} \rightarrow \psi_{\bar{1}\bar{1}1}, \quad \psi_{\bar{1}11} \rightarrow \psi_{1\bar{1}\bar{1}} \quad (3.6.8)$$

In Fig. 3.20a, the electron distribution associated with each hybrid orbital is represented by a lobe extending along the four body diagonals. In  $\text{CH}_4$ , the carbon atom occupies the center of the cube, whereas the four hydrogen atoms occupy the alternate corners of the cube. As illustrated in Fig. 3.20b, a counterclockwise rotation of  $120^\circ$  about an axis joining atoms  $E$  and  $B$  brings atom  $B \rightarrow B$ ,  $D \rightarrow C$ ,  $C \rightarrow A$ , and  $A \rightarrow D$ . This is exactly what Eq. (3.6.8) says. We can apply similar rotations about other body diagonals. For example, a rotation of  $120^\circ$  about the  $[\bar{1}\bar{1}1]$  diagonal interchanges atoms  $B$ ,  $C$ , and  $D$ , or hybrid orbitals  $\psi_{1\bar{1}\bar{1}}$ ,  $\psi_{\bar{1}\bar{1}\bar{1}}$  and  $\psi_{111}$ . Note that a regular tetrahedron is formed by joining the four hydrogen atoms  $A$ ,  $B$ ,  $C$ , and  $D$  with the carbon atom sitting at the center of the tetrahedron. The C—H bonds are thus directed from the center toward each corner of the tetrahedron.

In summary, we have described two important properties of a covalent bond, the saturation and the directional property. First, an electron-pair bond can be formed only between electrons having unpaired spins. An oxygen atom has four  $p$  electrons. However, only two of the four electrons can have unpaired spins because of the Pauli exclusion principle. In carbon, one of the two  $s$  electrons must be promoted to become a  $p$  electron, so that carbon may have a maximum of four unpaired spins and thus form a maximum of four bonds. Once an atom has used up all its electrons having unpaired spins, no additional bond can be formed. The state of saturation is said to have been reached. Second, the strength of a bond depends on the overlapping of the electron wave function. Since each atomic orbital represents a specific charge distribution in space, maximum overlapping of the charge distributions is possible only if atoms are oriented with respect to one another in specific directions. The arrangements of atoms in covalent-bond molecules such as  $\text{H}_2\text{O}$ ,  $\text{NH}_3$ , and  $\text{CH}_4$  are such as to achieve maximum bond strength (or minimum energy) in these molecules.

### 3.7 COVALENT CRYSTALS

The elements in the periodic table (Table 1.1) can be grouped into several categories. The group VIIIb elements from He to Xe all have closed-shell configurations. Upon solidification, they form crystals of the molecular type in which bonding is due to the van der Waals force. The group I, II, and III elements are all metals. The alkali metals (from Li to Cs) and group Ib metals (Cu, Ag, and Au) are univalent. The alkali-earth metals (from Be to Ba) and the group IIB metals (Zn, Cd, and Hg) are divalent. The group IIIB metals (from Al to Tl) are trivalent. (Boron is a special case. It has been reported that the crystal may be of the covalent type.) The transition-metal group consists of elements having the incomplete  $3d$  shell (elements of the iron group from Sc to Ni), elements having the incomplete  $4d$  shell (from Y to Pd), elements having the incomplete  $4f$  shell (elements of the rare-earth group from La to Lu), and elements having the incomplete  $5d$  shell (from Hf to Pt). Almost all metals crystallize in either one of the three structures: the hcp, the fcc or the bcc structure.

If we remove the aforementioned elements from the periodic table, we are left with the group IVb–VIIb elements. These elements form covalent crystals. In the fol-

lowing discussion, we describe the structure and the bonding typical of each group. Let us start with the group IVb elements. Diamond, silicon, germanium, and gray tin all crystallize in the diamond structure. The bond between atoms is formed by the  $sp^3$  hybrid orbitals. As discussed in Section 3.6, there are four  $sp^3$  orbitals. Therefore, each atom needs four nearest neighbors to complete the covalent bond. It is not surprising to find that the basic unit in a diamond structure (Fig. 2.12) has a structure similar to that of  $\text{CH}_4$  (Fig. 3.20). In the tetrahedral unit of Figs. 2.12 and 3.20, the center atom is surrounded symmetrically by four atoms, and hence the atom arrangement satisfies the bonding requirement of the  $sp^3$  orbitals. We should mention that not all group IVb elements have structures in which all the bonds are covalent. Lead, which is metallic, has a fcc structure. Metallic white tin, which is stable at room temperature, takes the body-centered tetragonal structure having two atoms to each lattice point. Graphite, which is the other crystalline form of carbon, has a strong covalent bonding between atoms in the plane of a hexagon but a weak metallic bonding between the planes.

The atoms of the group Vb elements (P, As, Sb, and Bi), like the nitrogen atom, have three unpaired electrons, and the bond between the atoms is formed by the  $p^3$  orbitals. The structure suitable for the  $p^3$  orbitals must have a coordination number of 3. Although the four aforementioned elements crystallize in a trigonal structure, the characteristic feature of the structure is best seen in planes perpendicular to the trigonal axis. Figure 3.21 shows the double atomic layer structure of an arsenic crystal, with the atoms in the top layer drawn as dots and the atoms in the bottom layer drawn as circles. The basic unit in the structure consists of four atoms 1, 2, 3, and 4 in the form of a pyramid. From our discussion of the  $\text{NH}_3$  molecule in Section 3.6, we expect that the angle between two As—As bonds should be close to  $90^\circ$ . Table 3.2 lists some experimentally measured bond angles in materials whose atoms are held together by  $p^3$  and  $p^2$  bonds. As can be seen, the measured angles are indeed close to  $90^\circ$ .

Whereas the atoms of P, As, Sb, and Bi crystallize in puckered sheets to satisfy the  $p^3$  bond requirement, the atoms of Se and Te form spiral chains (Fig. 3.22) so that each atom has two close neighbors in fulfilling the  $p^2$  bond requirement. Since the two  $p$  electrons must have different  $p$  orbitals (e.g., one has  $\psi_{px}$  and the other has  $\psi_{py}$ ), the bond angle is again close to  $90^\circ$ . One arrangement of atoms to have a coordination number of two is a square ring. However, this arrangement requires a bond angle of exactly  $90^\circ$ . Furthermore, the ring is a closed structure and hence does not allow any extension of the structure. On the other hand, atoms can always be added to the open ends of the spiral chain so that the chain structure can be repeated while it propagates.

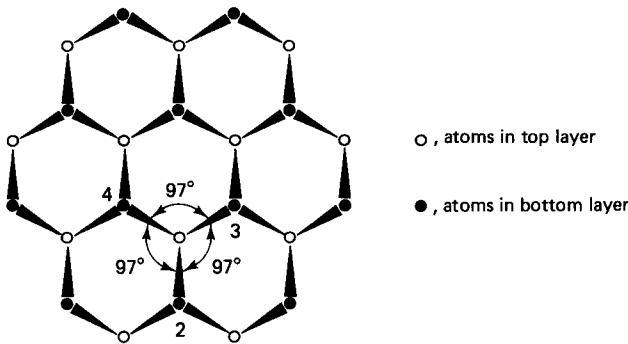


**Figure 3.21** The layer structure of arsenic crystals as viewed in a direction perpendicular to the plane of the layer structure. There are two layers in the diagram. Atoms in the top layer are shown as dots, whereas atoms in the bottom layer are shown as open circles. The two layers of atoms should be considered as forming a puckered sheet because the  $p^3$  bond requirement is satisfied by atoms in the sheet. Bond between atoms in the same sheet is strong, whereas bond between atoms in two adjacent sheets is weak.

**TABLE 3.2 BONDING ORBITAL AND BOND ANGLE IN A SELECTED NUMBER OF COVALENT SUBSTANCES**

Substance	Bonding orbital	Bond angle
P	$p^3$	99°
As	$p^3$	97°
Sb	$p^3$	96°
Bi	$p^3$	94°
NH <sub>3</sub>	$p^3$	107°
S	$p^2$	106°
Se	$p^2$	105°
Te	$p^2$	102°
H <sub>2</sub> O	$p^2$	109°

In both the trigonal structure of P, As, Sb, and Bi and the hexagonal structure of Se and Te, there is a weak secondary bond either of the van der Waals or metallic type. Adjacent sheets and adjacent chains in the two structures are loosely bound together by this weak force.

The group VIIb atoms Cl, Br, and I possess seven electrons (two *s* and five *p* electrons). Since these atoms have one unpaired spin, they need only another atom to complete the covalent bond. In the crystalline state, each lattice point thus represents a molecule Cl<sub>2</sub>, Br<sub>2</sub>, or I<sub>2</sub>, and the bond between the molecules is due to the van der Waals forces. Figure 3.23 shows the orthorhombic structure that the elements Cl, Br, and I take.

In summary, we have described the crystal structures of group IVb–VIIb elements. The number of unpaired spins in these elements is equal to  $8 - N$ , where *N* is the number of the group. Therefore, to fulfill the covalent-bond requirement, each atom

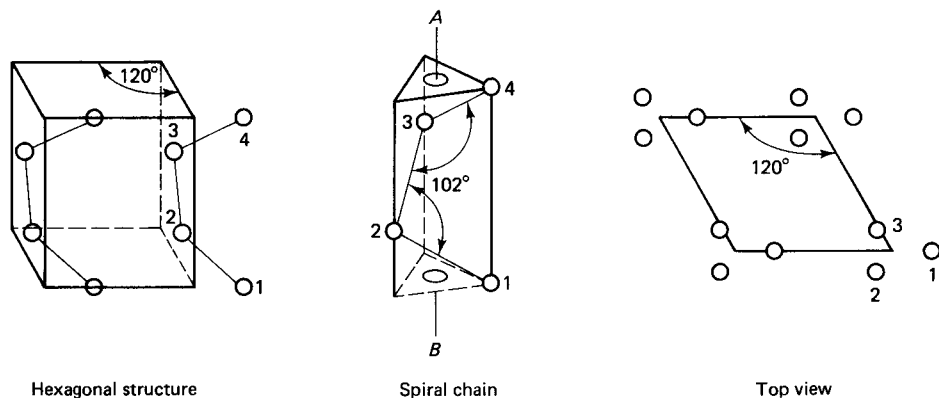
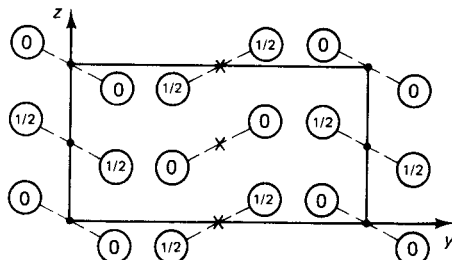
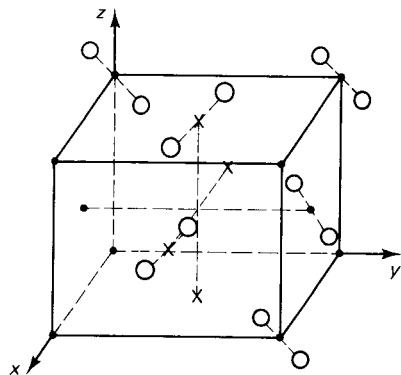


**Figure 3.22** The spiral chain structure of selenium and tellurium crystals. Although both crystals have the hexagonal structure, the basic structure that satisfies the  $p^2$  bond requirement is the spiral chain (formed by atoms 1, 2, 3, and 4, for example). Bonding among atoms in the same chain is strong, whereas bonding among atoms in two adjacent chains is weak.



Front view

**Figure 3.23** The face-centered orthorhombic structure of chlorine, bromine, and iodine. Each lattice point is occupied by a molecule. The numbers appearing inside circles are the  $x$  coordinates of the atoms, expressed in units of the lattice constant  $a$ .

must have  $8 - N$  close neighbors. The characteristic feature of a covalent-crystal structure is such that both this  $8 - N$  rule and the directional requirement of the bond can be satisfied. To meet the two conditions, covalent-bond crystals generally have fairly complicated structures. In contrast, metallic- and ionic-crystal structures are comparatively simple. We also see that only for the group IVb elements do the covalent bonds bind the whole structure. For the group Vb, VIb, and VIIb elements, the crystal structures involve both the primary covalent bond and a secondary weak bond. If the secondary bond is metallic, the crystal is partly covalent and partly metallic. If the secondary bond is of the van der Waals type, the crystal is partly covalent and partly molecular.

The reader may ask why covalent bonding starts with crystals of group IVb elements and not with crystals of group IIIb elements. One way to explain the difference is to say that metals have partially filled energy bands, whereas covalent crystals have fully occupied valence bands. The explanation based on the energy band is discussed further in Chapter 4. Here we give a more straightforward explanation based on the total ionization energy of an atom. In metals, the valence electrons are free from the attraction of the nucleus to form an electron sea. To free the valence electron (e.g.,  $3s$  electron in Na,  $3s^2$  electrons in Mg, and  $3s^23p$  electrons in Al) from the nucleus requires energy. Referring to Fig. 3.12, we see that a large part of the total energy is spent in raising a Na atom to the ionized state ( $\text{Na}^+ + \text{free electron}$ ). As the number of the valence electrons increases, the total ionization energy (e.g., the energy required to make  $\text{Al} \rightarrow \text{Al}^{3+} + 3$  free electrons) increases accordingly. If this energy becomes too large, valence electrons will not form an electron sea but instead, will form electron-bond pairs.

Table 3.3 lists the total ionization energies and the crystal structures of the group Ib–VIIb elements except for Li and Na, which belong to group Ia, and Be and Mg, which belong to group IIa. The boundary line between metallic and covalent bonding seems to be around 40 eV for the value of the total ionization energy. The atoms having the total ionization energy below this value tend to crystallize in close-packed or nearly close-packed structures. Boron, tin, and lead seem to be borderline cases. Boron has

**TABLE 3.3 CRYSTAL STRUCTURES AND TOTAL IONIZATION ENERGIES (IN eV) OF THE GROUP Ib–VIIb ELEMENTS<sup>a</sup>**

Li	Be	B	C	N	O	F
bcc 5.4	hcp 18.1	Tetrahedral 37.7	D 64.2	— 97.4	— 137	— 184
Na	Mg	Al	Si	P	S	Cl
bcc 5.2	hcp 15.0	fcc 28.3	D 44.9	8 – N 64.7	8 – N 87.6	8 – N —
Cu	Zn	Ga	Ge	As	Se	Br
fcc 7.7	hcp 18.0	Orthorhombic 30.6	D 45.5	8 – N 62.5	8 – N —	8 – N —
Ag	Cd	In	Sn	Sb	Te	I
fcc 7.5	hcp 16.8	fcc 27.9	D (gray) 39.4	8 – N 55.5	8 – N (72)	8 – N —
Au	Hg	Tl	Pb	Bi		
fcc 9.2	Trigonal 18.6	hcp 29.7	fcc 42.1	8 – N 55.7		

<sup>a</sup>Covalent bonding is favored over metallic bonding in elements with ionization energy exceeding 40 eV to the right of the heavy line.

been reported to be partly covalent, whereas lead is known to be metallic. Tin can exist in two forms, with gray tin being covalent and white tin being metallic.

## PROBLEMS

- 3.1. Discuss the essential differences between ionic and covalent bonding. Use KCl and H<sub>2</sub> to illustrate the differences.
- 3.2. The bonding in NH<sub>3</sub> and O<sub>2</sub> is known to be covalent. Use illustrations similar to Figs. 3.3b and 3.4 to explain how electron-pair bonds are formed in them.
- 3.3. Based on our discussion of the hydrogen (H<sup>+</sup>) molecule-ion, explain the bonding mechanism in a hydrogen molecule H<sub>2</sub>.
- 3.4. Find the interaction energy between a pair of collinear electric dipoles located at a distance *R* apart. Show that the energy is attractive. Explain the difference, if there is any, between your result and Eq. (3.2.4).
- 3.5. Consider a two-dimensional square lattice with alternate positive and negative ions. Choose any ion as the reference ion. Find the distances between this reference ion and its neighbors from the nearest neighbors up to the ninth nearest neighbors. Calculate the Modelung constant with terms up to the ninth nearest neighbors.
- 3.6. Verify Eq. (3.3.7). Explain why it is incorrect to use  $\mathcal{E}_0$  of Eq. (3.3.5) as  $\mathcal{E}$  in Eq. (3.3.7).
- 3.7. Find the values of *n* (the repulsive-energy parameter) and  $\mathcal{E}_0/N$  (the cohesive energy) in a KCl crystal, given  $K = 5.1 \times 10^{-12} \text{ cm}^2/\text{dyn}$  and  $R_0 = 3.14 \text{ \AA}$ . It is also known that the KCl crystal has an NaCl structure.

# 1

# Atomic Structure

## 1.1 THE RUTHERFORD ATOM

This book is concerned primarily with the physical principles of modern electronic devices that utilize the conductive, dielectric, and optical properties of materials. For a systematic and coherent discussion of these properties, a clear understanding of the structure of atoms and the chemical bonding between them is always helpful and often essential. To provide this requisite background, the first two chapters are devoted to a general review of the elements of modern physics and the fundamentals of crystals.

Since the turn of the century, a number of experiments, notably the scattering experiments of Lenard and Rutherford, have yielded definite information about the structure of atoms. (A thorough discussion of the subject can be found in textbooks on atomic physics. See, for example, M. Born, *Atomic Physics*, Hafner Publishing Company, New York, 1957, p. 60; R. L. Sproull, *Modern Physics*, John Wiley & Sons, Inc., New York, 1963, Chap. 3.) According to Rutherford, the constitution of an atom can be described as follows. In the center of the atom, there is the *nucleus*, which is composed of  $z$  protons and  $n$  neutrons. The *protons* contribute to both the charge (positive) and the mass of the nucleus, whereas the *neutrons* contribute only to the mass of the nucleus. To keep the atom electrically neutral, there are  $z$  electrons moving around the nucleus. (If atoms were not electrically neutral, an enormous electric field would be exhibited by objects of a finite physical dimension. This is contrary to facts.)

Insofar as the material properties (mentioned above) are concerned, the significant number is the number of electrons  $z$ , not the number of protons and neutrons,  $z + n$ . It is the electrons that determine the chemical behavior of an element. The number of electrons that an atom has can be determined from a scattering experiment. A beam of charged particles (say, protons carrying a charge  $+e$ ) is incident on a foil of a chosen target material (Fig. 1.1a). We note that the diameter of an atom is on the order  $10^{-10}$  m, whereas the nuclear dimension is on the order of  $10^{-14}$  m. Since the electron distribution in an atom is well dispersed compared to the nuclear charge distribution, its effect on the incident particle can be ignored. Therefore, the scattering problem is re-

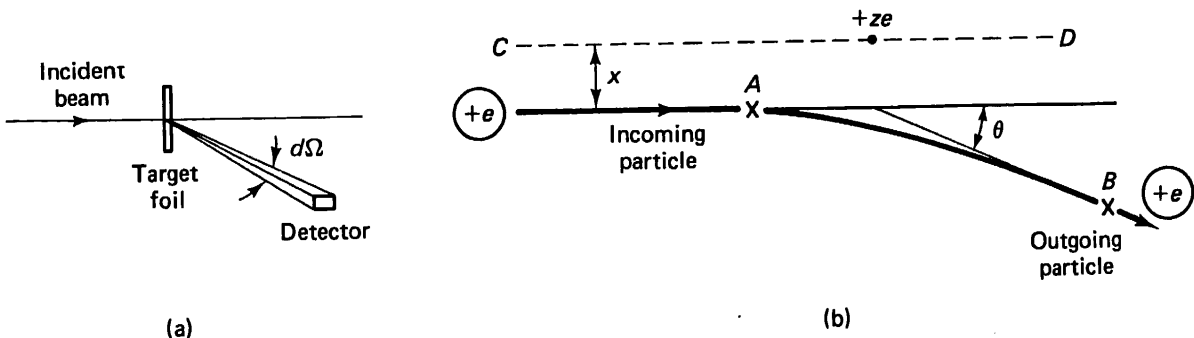


**Figure 1.1** Schematic diagram showing the Rutherford scattering experiment: (a) the experimental arrangement and (b) the trajectory of a moving proton in the field of a stationary nucleus having  $z$  protons.

duced to a simple electrostatic interaction between a moving charged particle of charge  $+e$  and a stationary charged particle of charge  $+ze$  (Fig. 1.1b).

The trajectory of the moving particle can be obtained from classical particle mechanics. At large distances from the nucleus, the motion of the particle is little affected by the nucleus; hence the trajectory approaches asymptotically two straight lines at the two ends away from the nucleus. The angle  $\theta$  formed by these two lines (Fig. 1.1b) defines the angle of scattering (i.e., the angle of deflection of the direction of the charged particle). The relation between  $\theta$  and  $x$  (the distance of the nuclear charge from the asymptotic straight line) is found to be

$$\tan \frac{\theta}{2} = \frac{ze^2}{8\pi\epsilon_0 Kx} \quad (1.1.1)^{\dagger}$$

where  $\epsilon_0$  is the dielectric constant of free space and  $K = Mv^2/2$  is the kinetic energy of the moving particle. (The relation can be derived from ordinary mechanics. See, for example, M. Born, *Atomic Physics*, Hafner Publishing Company, New York, 1956, Appendix IX; R. M. Eisberg, *Fundamentals of Modern Physics*, John Wiley & Sons, New York, 1961, pp. 100–106.) The dependences of  $\theta$  on  $K$  and  $x$  can be understood qualitatively from the following observations. Most of the deflection occurs in a portion  $AB$  of the trajectory when the particle is nearest to the nucleus. The smaller the distance  $x$ , the closer the portion  $AB$  is to the nucleus and hence the stronger is the electrostatic repulsion. The time during which a particle travels the distance  $AB$  depends on the velocity of the particle. A particle having a lower kinetic energy spends more time in the region  $AB$ , and hence the overall effect of the nuclear potential on the particle motion is greater.

In the actual scattering experiment, the significant quantity is the ratio of the number of particles collected at a fixed angle  $\theta$  by the detector to the incident particles. Let  $d\Omega$  be the solid angle extended to the detector surface from the target and  $S(\theta)$  be the number of particles collected per solid angle. Note that the problem at hand is symmetrical about the axis  $CD$ . Particles whose incoming path is inside a circular ring

<sup>†</sup>An alternate terminology for  $\epsilon$  is permittivity. In this text, dielectric constant and permittivity are used interchangeably.

about the axis  $CD$  have the same deflection angle  $\theta$ . If  $dA$  is the area of this ring and  $\rho$  is the density of incident particles per unit area, the total number of particles within this ring is  $\rho dA$ . Since these particles are all scattered into the same angle  $\theta$ ,

$$\rho dA = S(\theta) d\Omega \quad (1.1.2)$$

Realizing that in polar coordinates

$$dA = 2\pi x dx \quad \text{and} \quad d\Omega = 2\pi \sin \theta d\theta \quad (1.1.3)$$

we find the ratio of  $S(\theta)/\rho$ , called the *differential cross section of scattering*  $\sigma(\theta)$ , to be

$$\sigma(\theta) = \frac{S(\theta)}{\rho} = \frac{2\pi x}{2\pi \sin \theta} \frac{dx}{d\theta} = \left( \frac{ze^2}{16\pi\epsilon_0 K} \right)^2 \csc^4 \frac{\theta}{2} \quad (1.1.4)$$

[In the original experiment of Rutherford,  $\alpha$  particles ( $\text{He}^{2+}$  ions) were used. In that case, 16 should be replaced by 8.] Equation (1.1.4) is known as the *Rutherford scattering law*.

Now let us apply Eq. (1.1.4) to the scattering experiment. If  $N$  is the number of nuclei per square meter of the cross-sectional area of the target foil, each nucleus occupies an effective cross-sectional area of  $N^{-1} \text{ m}^2$ . Consider an incident beam of  $n_0$  particles having a cross-sectional area  $A_0$ . Imagine that the beam is divided into many minute beams, each having a cross-sectional area  $N^{-1} \text{ m}^2$  and each interacting with a different nucleus. The particle density in each minute beam is equal to  $n_0/A_0$ . However, there are all together  $A_0 N$  such minute beams. Summing the effects of all these minute beams as if the beams were on top of each other, we obtain an effective particle density

$$\rho = \frac{n_0}{A_0} \frac{A_0}{N^{-1}} = n_0 N \quad (1.1.5)$$

Substituting Eq. (1.1.5) into Eq. (1.1.4), we obtain

$$S(\theta) = n_0 N \sigma(\theta) \quad (1.1.6)$$

If a detector having an exposure area  $A_1$  normal to the deflected beam is placed at a distance  $R$  from the target, we have  $A_1 = R^2 d\Omega$ . Therefore, the number  $n_1$  of particles collected at the detector is given by

$$n_1 = S(\theta) d\Omega = \frac{n_0 N A_1}{R^2} \left( \frac{ze^2}{16\pi\epsilon_0 K} \right)^2 \csc^4 \frac{\theta}{2} \quad (1.1.7)$$

Knowing  $N$ ,  $K$ ,  $A_1$ , and  $R$ , we can determine the value of  $z$  from the plot of  $n_1/n_0$  as a function of  $\theta$ .

Long before the modern theory of atomic structure was firmly established, it was found that if chemical elements are arranged in a periodic table as shown in Table 1.1, those elements occupying similar places have similar chemical properties. The arrangement of elements in the table was first in the order of increasing atomic weight; however, it was later discovered that elements should be arranged according to the number of electrons that an element possesses. The number  $z$  is now called the *atomic number*, as it determines the position that an element occupies in the periodic table. For example, carbon has an atomic number  $z = 6$ , meaning that carbon has six electrons and occupies the sixth place in the periodic table. Different elements have different atomic numbers.

**TABLE 1.1 PERIODIC TABLE OF THE ELEMENTS<sup>a</sup>**

		Group VIII																							
		Group VII						Group VI						Group V						Group IV					
		a		b		a		b		a		b		a		b		a		b		a		b	
4	Period	Group I a b	Group II a b	Group III a b	Group IV a b	Group V a b	Group VI a b	Group VII a b	Group VII a b	Group VI a b	Group V a b	Group IV a b	Group III a b	Group II a b	Group I a b										
I	1 H 1.0079																			2. He 4.003					
II	3 Li 6.94	4 Be 9.02		5 B 10.82	6 C 12.01		7 N 14.01		8 O 16.00		9 F 19.00									10 Ne 20.18					
III	11 Na 22.99	12 Mg 24.32		13 Al 26.97	14 Si 28.06		15 P 30.98		16 S 32.06		17 Cl 35.45									18 Ar 39.94					
IV	19 K 39.09	20 Ca 40.08	21 Sc 44.96	22 Ti 47.90	23 V 50.95		24 Cr 52.01		25 Mn 54.93		26 Fe 55.85		27 Co 58.94		28 Ni 58.69					36 Kr 83.7					
V	37 Rb 85.48	38 Sr 87.63	39 Y 88.92	40 Zr 91.22	41 Nb 92.91		42 Mo 95.95		43 Tc 99		44 Ru 101.7		45 Rh 102.91		46 Pd 106.4					54 Xe 131.3					
VI	55 Cs 132.91	56 Ba 137.36	48 Cd 112.41	49 In 114.76	50 Sn 118.70		51 Sb 121.76		52 Te 127.61		53 I 126.92									76 Os 190.2	77 Ir 193.1	78 Pt 195.2		86 Rn 222	
VII	79 Au 197.2	80 Hg 200.61	81 Tl 204.39	82 Pb 207.21	83 Bi 209.00		84 Po 210		85 At 211																
	87 Fr 223	88 Ra 226.05	89 Ac 227	90 Th 232.12	91 Pa 231		92 U 238.07	93 Np 237	94 Pu 239	95 Am 241	96 Cm 242	97 Bk 246	98 Cf 249	99 Es 254	100 Fm 256	101 Md 256	102 Lr 256	103 Lu 256							
	<i>Rare Earths</i>																								
VI	57 La 138.92	58 Ce 140.13	59 Pr 140.92	60 Nd 144.27	61 Pm 147	62 Sm 150.43	63 Eu 152.0	64 Gd 156.9	65 Tb 159.2	66 Dy 162.46	67 Ho 164.90	68 Er 167.2	69 Tm 169.4	70 Yb 173.04	71 Lu 174.99										

<sup>a</sup>The numbers in front of the symbols of the elements denote the atomic numbers; the numbers underneath are the atomic weights.

Although more accurate methods of determining the atomic number were developed later, the Rutherford scattering experiment is of historical importance because it led to the discovery by Rutherford of the constitution of the atom.

## 1.2 THE BOHR POSTULATES AND THE WILSON-SOMMERFELD RULE

In Section 1.1 we discussed the constitution of an atom as conceived by Rutherford. The Rutherford atom is composed of a small, heavy, positively charged nucleus and one or more extranuclear electrons. This model of an atom has been verified by experiments. Our next task is to see how the classical theories can be applied to analyze the motion of electrons in an atom. For this purpose we use the hydrogen atom as an example. Hydrogen with atomic number  $z = 1$  has a nucleus of charge  $+e = 1.6 \times 10^{-19}$  C and of mass  $M = 1.67 \times 10^{-24}$  g. Since the mass of the electron  $m = 9.11 \times 10^{-28}$  g is much smaller than  $M$ , the nucleus can be considered as stationary in space. According to the classical theory, the electron that is attracted toward the nucleus by the Coulomb force would describe either an elliptical or a circular orbit about the nucleus, similar to the orbit of the earth about the sun.

For simplicity, we treat only the circular orbit (Fig. 1.2) in the following discussion. A balance of the centrifugal force and the Coulomb force gives the following equation:

$$\frac{mv^2}{r} = \frac{e^2}{4\pi\epsilon_0 r^2} \quad (1.2.1)$$

where  $r$  is the radius of the circular orbit and  $\epsilon_0$  is the dielectric constant of free space. However, consideration of the balance of mechanical forces alone is not enough. According to the classical electromagnetic theory, the acceleration of a charged particle would lead to the emission of light (electromagnetic radiation). Such a radiation would have a frequency  $\nu$  equal to the frequency of the electron motion, that is,  $\nu = v/2\pi r$ .

The total energy  $\mathcal{E}$  of the electron is equal to the sum of its kinetic and potential energy, or

$$\mathcal{E} = \frac{mv^2}{2} - \frac{e^2}{4\pi\epsilon_0 r} = -\frac{e^2}{8\pi\epsilon_0 r} \quad (1.2.2)$$

The negative sign in Eq. (1.2.2) accounts for the fact that the electron in the hydrogen atom is in the bound state. The last step in Eq. (1.2.2) is performed through the use of Eq. (1.2.1) in eliminating  $v$ . With the loss of energy through radiation, the electron would become more tightly bound to the nucleus. From Eqs. (1.2.2) and (1.2.1) we see that a more negative  $\mathcal{E}$  would require a smaller  $r$ , which in turn would result in a higher angular frequency  $\omega$ . Therefore, according to the classical theory, the emitted radiation should show a wide (continuous) range of frequencies. This prediction, however, is not borne out by experiments.

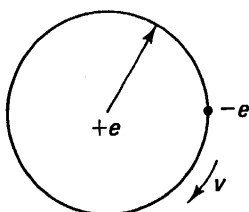


**Figure 1.2** Classical model of a hydrogen atom. An electron moves in a circular orbit around a proton.

The spectrum of the radiation emitted by hydrogen consists of sharply defined (discrete) frequencies. It is clear that classical theories alone cannot explain the electron motion in an atom. The first attempt to resolve this difficulty is to seek further restrictions that must be imposed on the electron motion. One of the most important steps toward an explanation of the discrete nature of the radiation spectrum was taken by Bohr, who postulated the existence of stationary states and the Bohr frequency rule. The two Bohr postulates can be stated as follows. An atom can exist only in certain stationary states, each state having a definite energy. An atom can change from a lower-energy state (with energy  $\mathcal{E}_1$ ) to a higher one (with energy  $\mathcal{E}_2$ ) by absorbing a photon of energy  $h\nu$  such that

$$h\nu = \mathcal{E}_2 - \mathcal{E}_1 \quad (1.2.3)$$

Similarly, emission of a photon of the same energy results if the atom returns from the higher ( $\mathcal{E}_2$ ) to the lower ( $\mathcal{E}_1$ ) energy state.

In Eq. (1.2.3),  $\nu$  is the frequency of the absorbed (or emitted) radiation and  $h$  is Planck's constant. In his theoretical analysis of the distribution law for blackbody radiation (which is discussed in detail in Chapter 12), Planck showed that the experimentally observed distribution can be accounted for by postulating that matter (in this case, the blackbody) absorbs or emits energy in units of  $h\nu$ . The proportionality constant  $h$ , which is of dimension energy-time, has a value  $6.625 \times 10^{-34}$  J-s. It is fitting to say that the quantum theory was born with the introduction of Planck's constant  $h$  in 1900.

Soon after the successful formulation by Bohr of the two postulates in 1913, Wilson and Sommerfeld independently discovered in 1915 a powerful method of finding the stationary states. They defined stationary states as those for which the following conditions are satisfied:

$$\int p \, dq = nh \quad (1.2.4)$$

where  $p$  is the linear momentum,  $q$  the space coordinate of the electron, and  $n$  an integer. The condition stated in Eq. (1.2.4) is known as the *Wilson-Sommerfeld rule of quantization*. The validity of Eq. (1.2.4) was tested by Sommerfeld in his analysis of the emission spectra of hydrogen and ionized helium.

Let us now apply Eq. (1.2.4) to the electron motion in a hydrogen atom (Fig. 1.2). The linear momentum  $p$  is equal to

$$p = mv \quad (1.2.5)$$

and the elementary path  $dq$  of the electron orbit is given by

$$dq = r \, d\phi \quad (1.2.6)$$

Substituting Eqs. (1.2.5) and (1.2.6) into Eq. (1.2.4) and integrating the resultant expression over  $d\phi$  from 0 to  $2\pi$ , we find that

$$mvr = \frac{nh}{2\pi} = n\hbar \quad (1.2.7)$$

The quantity  $\hbar = h/2\pi$  is called "h-bar" and is used as often as  $h$  in modern physics. Elimination of  $v$  from Eqs. (1.2.1) and (1.2.7) yields

$$r = n^2 a \quad (1.2.8)$$

where  $a$  is an atomic unit for distance known as the *Bohr radius* and has the value

$$a = \frac{4\pi\epsilon_0\hbar^2}{me^2} = 0.529 \text{ \AA} = 5.29 \times 10^{-11} \text{ m} \quad (1.2.9)$$

Using the value of  $r$  from Eq. (1.2.8) in Eq. (1.2.2), we obtain

$$\mathcal{E} = -\frac{me^4}{2(4\pi\epsilon_0\hbar)^2} \frac{1}{n^2} \quad (1.2.10)$$

Thus for transitions between any two states  $n_1$  and  $n_2$ , the energy of the emitted (or absorbed) radiation is given by

$$h\nu = \mathcal{E}_{n_1} - \mathcal{E}_{n_2} = \frac{me^4}{2(4\pi\epsilon_0\hbar)^2} \left( \frac{1}{n_1^2} - \frac{1}{n_2^2} \right) \quad (1.2.11)$$

with  $n_2 > n_1$ . The many emission lines of hydrogen can indeed be identified by assigning different integers for  $n_1$  and  $n_2$  in Eq. (1.2.11). One simple check of Eq. (1.2.11) is to calculate the ionization energy of a hydrogen atom. For the ground state,  $n_1 = 1$ . For the ionized state,  $n_2 = \infty$ . Using these values in Eq. (1.2.11), we find a value of  $h\nu = 13.6$  electron volts (eV), which agrees well with the experimentally determined value.

### 1.3 THE SCHRÖDINGER WAVE EQUATION

In Section 1.2 we discussed inadequacy of classical theories in dealing with the electron motion in an atom. The old quantum theory, which is based on the Bohr postulates and the Wilson–Sommerfeld quantization rule, helped greatly to overcome some of the difficulties with classical theories; however, many difficulties remained. For example, although the frequency of the emitted radiation can be predicted from Eq. (1.2.11), the intensity of the radiation cannot be calculated from the old quantum theory. The next giant step in the development of modern physics is the introduction of quantum mechanics.

As classical mechanics furnishes the description of the behavior of large objects, quantum mechanics provides the description of the behavior of matter on an atomic scale. Because all our direct experience and hence our intuition apply only to large objects, it is not surprising that we find quantum mechanics more difficult to understand than classical mechanics. For example, we cannot learn the Wilson–Sommerfeld rule of quantization by association with our direct experience as we learn Newton's law of motion. For this reason, the rule would appear to us to be merely an abstract concept. The correctness of such an abstract concept can be proved only by observing the consequences that result from the imposition of the concept. In the same way, we have to learn quantum-mechanical principles as abstract concepts. These concepts are accepted as valid principles because they give a consistent and correct description of the behavior of matter on an atomic scale. It is in this spirit that we introduce the Schrödinger wave equation in the following discussion.

Quantum mechanics differs from classical mechanics at its outset in the fundamental premises underlying them. Classical mechanics assumes that given the equation of motion, we can have a precise knowledge of the state of a particle in question. For example, we learn in kinetics that we can predict the trajectory of a falling body

provided that its initial conditions (regarding its position and velocity) and the force acting on it are known. Quantum mechanics, on the other hand, does not presuppose a complete and precise knowledge of the particle. As a matter of fact, quantum mechanics is built on the premise that it is not possible to predict exactly what will happen in a definite circumstance. Instead of specifying the state of a particle in motion by its position and velocity as we did in Eq. (1.2.1), we define a wave function  $\psi(x, y, z)$  such that the probability  $dW$  of finding a particle in a volume element  $d\tau = dx dy dz$  is equal to

$$dW = |\psi|^2 d\tau \quad (1.3.1)$$

The equation from which information concerning  $\psi$  can be derived is the *Schrödinger wave equation*:

$$\left( -\frac{\hbar^2}{2m} \nabla^2 + V \right) \psi = E\psi \quad (1.3.2)$$

where the Laplacian operator  $\nabla^2$  stands for

$$\nabla^2 = \frac{\partial^2}{\partial x^2} + \frac{\partial^2}{\partial y^2} + \frac{\partial^2}{\partial z^2} \quad (1.3.3)$$

We consider the Schrödinger wave equation [Eq. (1.3.2)] and the probabilistic interpretation of wave function [Eq. (1.3.1)] as fundamental postulates, similar to the Bohr postulates and the Wilson–Sommerfeld rule of quantization. As postulates, these two equations need no derivation from other principles to justify their existence. As stated earlier, the justification of their existence can only be supported by experiments, which are the sole test of the validity of these postulates. The following observation, however, may be useful to see the physical origin of the terms in Eq. (1.3.2). In the classical expression for energy,

$$E = K + V = \frac{1}{2m} \left( p_x^2 + p_y^2 + p_z^2 \right) + V \quad (1.3.4)$$

the term  $K$  is the kinetic energy and the term  $V$  is the potential energy of a particle. If we replace the classical momentum by a quantum-mechanical operator such that

$$p_x \rightarrow \frac{\hbar}{i} \frac{\partial}{\partial x}, \quad p_y \rightarrow \frac{\hbar}{i} \frac{\partial}{\partial y}, \quad p_z \rightarrow \frac{\hbar}{i} \frac{\partial}{\partial z} \quad (1.3.5)$$

with  $i = \sqrt{-1}$ , and if we let these operators operate on  $\psi$ , we obtain

$$E\psi = (K + V)\psi = \left( -\frac{\hbar^2}{2m} \nabla^2 + V \right) \psi \quad (1.3.6)$$

which is identical to Eq. (1.3.2).

Let us now recapitulate the quantum-mechanical treatment in contrast to the classical method. It is obvious from Eq. (1.3.2) that the wave function  $\psi$  is, in general, a function of the coordinates  $(x, y, z)$ . If the particle under consideration is an electron (e.g., the same electron as in Fig. 1.2), the electron motion can no longer be defined as precisely as in Eqs. (1.2.1) and (1.2.8), and thus the probability of finding the elec-

tron outside the prescribed orbit is zero. The wave function  $\psi$ , on the other hand, spreads over a finite region, and hence the probability of finding an electron is nonzero even in regions outside the classically allowed orbit. This smearing of electron orbit is a direct consequence of the notion that the electron orbit cannot be predicted in exact detail. The acceptance of the quantum-mechanical treatment, that is, the two postulates stated in Eqs. (1.3.1) and (1.3.2), necessitates our renunciation of the hope of exact prediction.

At first, the wave function  $\psi$  seems to be a rather poor substitute for knowing exactly where the electron is. However, there are many phenomena in nature, about which only the average properties are known and of interest to us. The thermionic emission from a vacuum tube is one example. The current density  $J$  resulting from thermionic emission is given by the *Dushman equation*:

$$J = \frac{4\pi me}{h^3} (kT)^2 \exp\left(-\frac{\mathcal{E}_w}{kT}\right) \quad (1.3.7)$$

where  $k = 1.38 \times 10^{-23}$  J/K is the Boltzmann constant,  $T$  the temperature (in Kelvin) of the cathode,  $\mathcal{E}_w$  the work function (or barrier potential) of cathode surface, and  $m$  the electron mass. The fact that we cannot predict exactly when the emission of an electron takes place does not prevent us from deriving Eq. (1.3.7), which is based on the average rate of emission. A similar situation applies to the quantum-mechanical treatment of the atomic system. Even though we do not know in exact details the behavior of the system, we can derive useful and definite information about the average properties of the system.

To illustrate how the average value of a physical quantity is found from a given probability distribution, we use the familiar example of computing the class average in an examination. The average score is computed from the data sheet of Fig. 1.3 as follows:

$$\frac{1}{5 + 6 + 7 + 8 + 10} (6 \times 45 + 8 \times 55 + 10 \times 65 + 7 \times 75 + 5 \times 85) = 64 \quad (1.3.8)$$

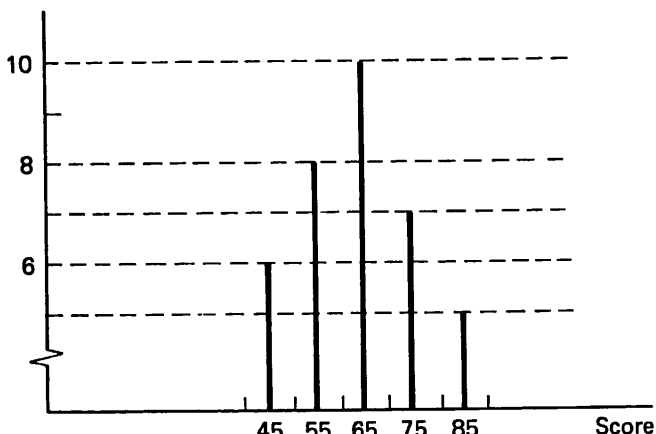


**Figure 1.3** Score sheet in an examination. There are five students having a score of 85, and so on.

Note that the probability of finding a student having a score of 65 is  $10/(5 + 6 + 7 + 8 + 10)$ . Thus if  $W_i$  is the probability of finding a student having a score  $f_i$ , the average score  $\langle f \rangle$  of the class is simply equal to

$$\langle f \rangle = \sum_i f_i W_i \quad (1.3.9)$$

Equation (1.3.9) applies only to a discrete distribution. (This means that  $f_i$  takes discrete values of 45, 55, and so on.) For a continuous distribution, Eq. (1.3.9) must be replaced by

$$\langle f \rangle = \int f dW \quad (1.3.10)$$

The quantity  $\langle f \rangle$  is generally known as the *expectation value* of  $f$ .

Let us now illustrate the use of Eq. (1.3.10) in the description of an atomic system. First, we can define an electron density function

$$\rho(x, y, z) = e|\psi(x, y, z)|^2 \quad (1.3.11)$$

If only a single electron is involved, the expectation value of the charge must be  $e$ . In other words,

$$\iiint_{-\infty}^{\infty} \rho(x, y, z) dx dy dz = e \quad \text{or} \quad \iiint_{-\infty}^{\infty} |\psi(x, y, z)|^2 dx dy dz = 1 \quad (1.3.12)$$

Another quantity of interest is the position of an electron. Although we do not know exactly where an electron is in an atom, we still can find the average distance  $\langle r \rangle$  away from the nucleus as follows:

$$\langle r \rangle = \iiint_{-\infty}^{\infty} r |\psi(x, y, z)|^2 dx dy dz \quad (1.3.13)$$

We should point out that the average value of  $f^{-1}$  is, in general, not equal to  $\langle f \rangle^{-1}$ . Thus the average value of the potential energy of an electron in a nuclear potential of  $e^2/4\pi\epsilon_0 r$  is

$$\langle V \rangle = \iiint_{-\infty}^{\infty} \frac{e^2}{4\pi\epsilon_0 r} |\psi(x, y, z)|^2 dx dy dz \quad (1.3.14)$$

and not  $e^2/4\pi\epsilon_0 \langle r \rangle$ . To find the expectation values of the momentum and the kinetic energy of an electron is much more involved, because as indicated in Eq. (1.3.5), both quantities are represented by differential operators. We postpone the discussion of how the values of  $\langle p \rangle$  and  $\langle K \rangle$  can be found until we have had chances of getting a little more acquainted with the Schrödinger wave equation and its solution.

## 1.4 THE HYDROGEN ATOM

In this section we analyze the electron motion in a hydrogen atom based on the Schrödinger wave equation. The analysis is a necessary step toward understanding the structure of atoms. Let us refer to Eq. (1.3.2). Because the potential-energy term  $V (= -e^2/$

$4\pi\epsilon_0 r$ ) has a  $1/r$  dependence, it is desirable to express Eq. (1.3.2) in spherical coordinates  $r$ ,  $\theta$ , and  $\phi$  (Fig. 1.4) as follows:

$$\frac{\hbar^2}{2m} \left[ \frac{1}{r^2} \frac{\partial}{\partial r} \left( r^2 \frac{\partial}{\partial r} \right) + \frac{1}{r^2 \sin \theta} \frac{\partial}{\partial \theta} \left( \sin \theta \frac{\partial}{\partial \theta} \right) + \frac{1}{r^2 \sin^2 \theta} \frac{\partial^2}{\partial \phi^2} \right] \psi + \left( \mathcal{E} + \frac{e^2}{4\pi\epsilon_0 r} \right) \psi = 0 \quad (1.4.1)$$

Equation (1.4.1) is a partial differential equation with  $\psi$  as the dependent variable and  $r$ ,  $\theta$ , and  $\phi$  as the independent variables. For those who have not been exposed to partial differential equations, Eq. (1.4.1) may look formidable indeed. Fortunately, Eq. (1.4.1) belongs to a class of partial differential equations that occur very frequently in physics and engineering problems and of which the solutions have been worked out by mathematicians.

The standard way of finding the solution of Eq. (1.4.1) is by the method of separation of variables. We propose a solution of the following form:

$$\psi(r, \theta, \phi) = R(r)\Theta(\theta)\Phi(\phi) \quad (1.4.2)$$

which is a product of three separate functions, each of which depends only on one independent variable. Substituting Eq. (1.4.2) into Eq. (1.4.1), we obtain

$$\begin{aligned} \frac{\Theta\Phi}{r^2} \frac{\partial}{\partial r} \left( r^2 \frac{\partial R}{\partial r} \right) + \frac{R\Phi}{r^2 \sin \theta} \frac{\partial}{\partial \theta} \left( \sin \theta \frac{\partial \Theta}{\partial \theta} \right) + \frac{R\Theta}{r^2 \sin^2 \theta} \frac{\partial^2 \Phi}{\partial \phi^2} \\ + \frac{2m}{\hbar^2} \left( \mathcal{E} + \frac{e^2}{4\pi\epsilon_0 r} \right) R\Theta\Phi = 0 \end{aligned} \quad (1.4.3)$$

In Eq. (1.4.3) we take outside the differentiation the part of  $\psi$  that does not depend on the independent variable with respect to which the differentiation is taken.

Dividing Eq. (1.4.3) by  $R\Theta\Phi$ , multiplying Eq. (1.4.3) by  $r^2 \sin \theta$ , and rearranging terms, we have

$$\begin{aligned} \frac{\sin^2 \theta}{R} \frac{d}{dr} \left( r^2 \frac{dR}{dr} \right) + \frac{\sin \theta}{\Theta} \frac{d}{d\theta} \left( \sin \theta \frac{d\Theta}{d\theta} \right) + \frac{2m}{\hbar^2} r^2 \sin^2 \theta \left( \mathcal{E} + \frac{e^2}{4\pi\epsilon_0 r} \right) \\ = - \frac{1}{\Phi} \frac{d^2 \Phi}{d\phi^2} \end{aligned} \quad (1.4.4)$$

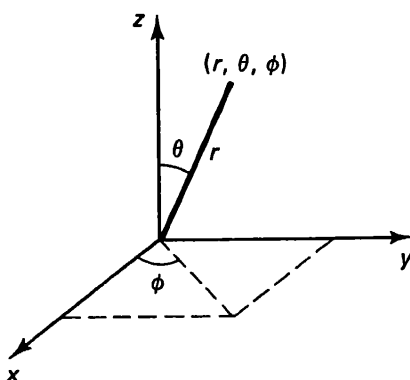


Figure 1.4 Spherical coordinates. The variable  $\phi$  takes values from 0 to  $2\pi$ , the variable  $\theta$  from 0 to  $\pi$  (not from 0 to  $2\pi$ ), and the variable  $r$  from 0 to  $\infty$  (not from  $-\infty$  to  $\infty$ ).

By virtue of the assumption that  $\Phi(\phi)$  is a function of  $\phi$  only, the right-hand side of Eq. (1.4.4) depends on  $\phi$  only. Applying similar reasoning to the left-hand side, we find that it must depend on  $r$  and  $\theta$  only. The only way that both conditions can be satisfied is to set both sides equal to a constant. Letting this constant be  $m^2$ , we have

$$\frac{d^2\Phi}{d\phi^2} = -m^2\Phi \quad (1.4.5)$$

$$\begin{aligned} \frac{1}{R} \frac{d}{dr} \left( r^2 \frac{dR}{dr} \right) + \frac{2m}{\hbar^2} r^2 \left( E + \frac{e^2}{4\pi\epsilon_0 r} \right) \\ = -\frac{1}{\Theta \sin \theta} \frac{d}{d\theta} \left( \sin \theta \frac{d\Theta}{d\theta} \right) + \frac{m^2}{\sin^2 \theta} \end{aligned} \quad (1.4.6)$$

Note that the left-hand side of Eq. (1.4.6) depends only on  $r$ , whereas the right-hand side of Eq. (1.4.6) depends only on  $\theta$ . Therefore, we must set both sides equal to a constant. Letting this new constant be  $l(l + 1)$ , we obtain

$$\frac{1}{\sin \theta} \frac{d}{d\theta} \left( \sin \theta \frac{d\Theta}{d\theta} \right) - \frac{m^2}{\sin^2 \theta} \Theta = -l(l + 1)\Theta \quad (1.4.7)$$

$$\frac{1}{r^2} \frac{d}{dr} \left( r^2 \frac{dR}{dr} \right) + \frac{2m}{\hbar^2} \left( E + \frac{e^2}{4\pi\epsilon_0 r} \right) R = \frac{l(l + 1)}{r^2} R \quad (1.4.8)$$

Equations (1.4.5), (1.4.7), and (1.4.8) are three ordinary differential equations from which the solutions are to be found. It may seem mysterious that out of the infinite possible values for the constants in Eqs. (1.4.4) and (1.4.6), we choose  $m^2$  and  $l(l + 1)$ . Equations (1.4.5), (1.4.7), and (1.4.8) would have different solutions if these constants were set in different forms. Only a certain type of solution yields a wave function  $\psi$  that is physically meaningful. The choice of  $m^2$  and  $l(l + 1)$  is to ensure a physically reasonable solution. We explain what we mean by *reasonable solution* in the following discussion.

Let us refer to Eq. (1.3.1) for the physical interpretation of the wave function. If  $|\psi|^2 d\tau$  indeed represents the probability of finding an electron in a volume element  $d\tau$ , the integral  $\int |\psi|^2 d\tau$  over the whole volume must be equal to the number of electrons involved and hence must be finite. Furthermore, a probability by its very definition can take one and only one value for the occurrence of a specific event. Thus the wave function  $\psi$  must be single valued. These two conditions on  $\psi$  are auxiliary postulates that must be taken into account together with the two fundamental postulates of quantum mechanics stated in Eqs. (1.3.1) and (1.3.2). These two auxiliary postulates, in essence, replace the Wilson-Sommerfeld rule of quantization in the old quantum theory.

The two auxiliary postulates stated above limit our selection of the two constants in separating the two sides of Eqs. (1.4.4) and (1.4.6). Let us now examine the  $\phi$  dependence of the wave function. The solution of Eq. (1.4.5) is

$$\Phi = A \exp (\pm im\phi) \quad (1.4.9)$$

where  $A$  is a proportionality constant to be fixed later. To examine whether the function  $\Phi$  satisfies the auxiliary postulates or not, we use Eq. (1.4.2) and examine each part separately. Realizing that in spherical coordinates (Fig. 1.4) the volume elements  $d\tau$  are given by

$$d\tau = r^2 dr \sin \theta d\theta d\phi \quad (1.4.10)$$

we can write

$$\int |\psi|^2 d\tau = \int_0^\infty |R(r)|^2 r^2 dr \int_0^\pi |\Theta(\theta)|^2 \sin \theta d\theta \int_0^{2\pi} |\Phi(\phi)|^2 d\phi \quad (1.4.11)$$

Using Eq. (1.4.9) in Eq. (1.4.11), we can easily show that  $\int |\Phi|^2 d\phi$  is finite. For the function  $\Phi(\phi)$  to be single valued at  $\phi = 0$  (which is identical to  $\phi = 2\pi$ ), that is,  $\Phi(0) \equiv \Phi(2\pi)$ , the parameter  $m$  must be an integer. Had we changed  $-m^2$  to  $m^2$  in Eq. (1.4.5), the solution would not be a periodic function and hence would not satisfy the condition of single valuedness.

Equation (1.4.7) is known in mathematics as the *associated Legendre equation*. The solution of Eq. (1.4.7) can be expressed in terms of an infinite series that diverges at  $\theta = 0$  and  $\pi$  if  $l$  is a noninteger. This type of solution is, of course, not acceptable. However, the infinite series terminates and thus becomes a polynomial if  $l$  is an integer such that

$$l = |m|, |m| + 1, |m| + 2, \dots \quad (1.4.12)$$

The polynomial is known as the *associated Legendre polynomial*, which is designated as  $P_l^{|m|}(\cos \theta)$ . Thus we write

$$\Theta(\theta) = P_l^{|m|}(\cos \theta) \quad (1.4.13)$$

The superscript  $|m|$  and the subscript  $l$  specify the two integers in Eq. (1.4.7). Only for integral  $l$  and  $m$  such that  $l \geq |m|$ , the solution of Eq. (1.4.7) behaves properly at  $\theta = 0$  and  $\theta = \pi$ . Therefore, Eq. (1.4.13) is the only acceptable solution of Eq. (1.4.7).

Similarly, the radial function of Eq. (1.4.8) has an acceptable solution only under certain conditions. First, the energy  $E$  can only take certain discrete values:

$$E = -\frac{me^4}{2(4\pi\epsilon_0\hbar)^2 n^2} \quad (1.4.14)$$

where  $n$  is a positive integer. Second, the integer  $n$  must be either equal to or greater than  $l + 1$ . If these conditions are met, the solution of Eq. (1.4.8) can be written as

$$R(r) = \left(\frac{r}{na}\right)^l \exp\left(-\frac{r}{na}\right) L_{n-l}^{2l+1}\left(\frac{2r}{na}\right) \quad (1.4.15)$$

where  $a$  is the Bohr radius. The function  $L_{n-l}^{2l+1}(2r/na)$  is the *associated Laguerre polynomial* of order  $2l + 1$  and of degree  $n - l - 1$ . In some books, the notation  $L_{n-l-1}^{2l+1}$  instead of  $L_{n-l}^{2l+1}$  is used so that the subscript  $n - l - 1$  denotes directly the degree of the polynomial. Here we follow the notation used by Pauling and Wilson and by Condon and Shortley. (L. Pauling and E. B. Wilson, *Introduction to Quantum Mechanics*, McGraw-Hill Book Company, New York, 1935; E. U. Condon and G. H. Shortley, *The Theory of Atomic Spectra*, Cambridge University Press, Cambridge, 1959). In their notation, the degree of the polynomial is equal to the difference between the subscript  $(n + l)$  and the superscript  $(2l + 1)$ .

Let us summarize the essential points in the discussion above. The wave function  $\psi(r, \theta, \phi)$  and hence the electron motion in a hydrogen atom are specified by three numbers,  $n$ ,  $l$ , and  $m$ . Symbolically, we write

$$\psi_{n,l,m} = R_{n,l}(r)\Theta_{l,m}(\theta)\Phi_m(\phi) \quad (1.4.16)$$

Since  $|\psi|^2$  represents a probability distribution function, the wave function  $\psi$  must be single valued and bounded. These two requirements limit the numbers,  $n$ ,  $l$ , and  $m$  to integers. Furthermore, for a fixed integer  $n$ , the allowed values of  $l$  are

$$l = 0, 1, 2, \dots, (n - 1) \quad (1.4.17)$$

Both  $n$  and  $l$  are positive integers. For a fixed value of  $l$ , the allowed values of  $m$  are

$$m = -l, -(l - 1), \dots, 0, \dots, (l - 1), l \quad (1.4.18)$$

The positive and negative values of  $m$  account for the  $\pm$  signs in Eq. (1.4.9).

The integer  $n$  is known as the *principal quantum number*; the integer  $l$ , the *azimuthal quantum number*; and the integer  $m$ , the *magnetic quantum number*. The following letter code is generally used by spectroscopists for the values of  $l$ :

$$\begin{aligned} l &= 0, 1, 2, 3, 4, 5, 6, 7 \\ &s, p, d, f, g, h, i, k \end{aligned} \quad (1.4.19)$$

Further, the number that precedes the letter is the value of  $n$ . Thus, if we refer to a  $3d$  electron, we mean an electron that is in the state with  $n = 3$  and  $l = 2$ .

The reader who has not been exposed to the associated Legendre and Laguerre polynomials may be anxious to know what they look like. We list here a selected number of these polynomials:

$$\begin{aligned} \Theta_{0,0} &= 1 \\ \Theta_{1,0} &= \cos \theta, & \Theta_{1,\pm 1} &= \sin \theta \\ \Theta_{2,0} &= 3 \cos^2 \theta - 1, & \Theta_{2,\pm 1} &= \sin \theta \cos \theta, & \Theta_{2,\pm 2} &= \sin^2 \theta \end{aligned} \quad (1.4.20)$$

$$\begin{aligned} R_{1,0} &= \exp \left( -\frac{r}{a} \right) \\ R_{2,0} &= \left( 2 - \frac{r}{a} \right) \exp \left( -\frac{r}{2a} \right), & R_{2,1} &= \frac{r}{a} \exp \left( -\frac{r}{2a} \right) \\ R_{3,0} &= \left( 27 - \frac{18r}{a} + 2 \frac{r^2}{a^2} \right) \exp \left( -\frac{r}{3a} \right) \\ R_{3,1} &= \frac{r}{a} \left( 6 - \frac{r}{a} \right) \exp \left( -\frac{r}{3a} \right), & R_{3,2} &= \left( \frac{r}{a} \right)^2 \exp \left( -\frac{r}{3a} \right) \end{aligned} \quad (1.4.21)$$

For a tabulation of these polynomials with indices  $n$ ,  $l$ , and  $m$  other than those given above, the reader is referred to the book by Pauling and Wilson. The reader can readily verify that the polynomials of Eq. (1.4.20) and those of Eq. (1.4.21) indeed satisfy, respectively, Eqs. (1.4.7) and (1.4.8). Furthermore, these polynomials do not have any singularities, and thus their values are finite.

Let us now illustrate how we obtain the wave function for a specific atomic state. For the  $1s$  state,  $n = 1$ ,  $l = 0$ , and thus  $m$  must be zero as required by Eq. (1.4.18). Combining  $\Phi_0$  of Eq. (1.4.9),  $\Theta_{0,0}$  of Eq. (1.4.20), and  $R_{1,0}$  of Eq. (1.4.21) gives

$$\psi_{1,0,0} = \frac{1}{\sqrt{\pi a^3}} \exp \left( -\frac{r}{a} \right) \quad (1.4.22)$$

which is the only wave function for the  $1s$  state. The reason for choosing  $A = (\pi a^3)^{-1/2}$  in Eq. (1.4.22) will be explained shortly. For the  $2p$  state, there exist three wave functions:

$$\begin{aligned}\psi_{2,1,1} &= \frac{-1}{\sqrt{64\pi a^3}} \frac{r}{a} \exp\left(-\frac{r}{2a}\right) (\sin \theta) \exp(i\phi) \\ \psi_{2,1,0} &= \frac{1}{\sqrt{32\pi a^3}} \frac{r}{a} \exp\left(-\frac{r}{2a}\right) (\cos \theta) \\ \psi_{2,1,-1} &= \frac{1}{\sqrt{64\pi a^3}} \frac{r}{a} \exp\left(-\frac{r}{2a}\right) (\sin \theta) \exp(-i\phi)\end{aligned}\quad (1.4.23)$$

because of three possible choices (1, 0, or  $-1$ ) for the value of  $m$ . Note that since  $l = 1$ , the  $p$  state must start with  $n = 2$  according to Eq. (1.4.17). This means that we have  $2p$ ,  $3p$ , . . . states but no  $1p$  state. Similarly, the  $d$  state must start with  $n = 3$ . The  $d$  state, irrespective of whether the state is  $3d$ ,  $4d$ , or  $5d$ , has five different wave functions because of five possible choices (2, 1, 0,  $-1$ , or  $-2$ ) for the value of  $m$ .

Other important properties of the wave function are that they are normalized and orthogonal to each other. According to Eq. (1.3.1), the total probability of finding an electron in a given state is equal to

$$W = \int_0^\infty \int_0^\pi \int_0^{2\pi} \psi_{n,l,m}^* \psi_{n,l,m} r^2 dr \sin \theta d\theta d\phi \quad (1.4.24)$$

where the asterisk indicates the complex conjugate. Note that the wave function is in general complex, and thus  $|\psi|^2 = \psi^* \psi$ . As required by one of the Bohr postulates, an electron can occupy only one of the quantum states. Once the electron is in that state, the total probability of finding the electron over all space coordinates of that state must be unity. In other words,

$$\int_0^\infty \int_0^\pi \int_0^{2\pi} |\psi|^2 r^2 dr \sin \theta d\theta d\phi = 1 \quad (1.4.25)$$

A wave function that satisfies Eq. (1.4.25) is said to be *normalized*. The constants in Eqs. (1.4.22) and (1.4.23) are chosen so as to make the wave functions normalized. By the same Bohr postulate, an electron is forbidden to change back and forth freely between any two atomic states without the absorption or emission of radiation. Therefore, it seems reasonable to expect that

$$\int_0^\infty \int_0^\pi \int_0^{2\pi} \psi_{n,l,m}^* \psi_{n',l',m'} r^2 dr \sin \theta d\theta d\phi = 0 \quad (1.4.26)$$

unless  $n' = n$ ,  $l' = l$ , and  $m' = m$ . The two wave functions that satisfy Eq. (1.4.26) are said to be *orthogonal* to each other. The solutions of Eq. (1.4.1) and hence all the atomic wave functions have this property.

Finally, let us compare the results based on quantum mechanics with those derived from old quantum theory. First, we see that the energy expression [Eqs. (1.2.10) and

(1.4.14)] are identical. Next we compute the probability distribution of the electron. Within a spherical shell of volume  $4\pi r^2 dr$ , the probability of finding the electron is

$$dW = \int_0^\pi \int_0^{2\pi} |\psi|^2 r^2 dr \sin \theta d\theta d\phi \quad (1.4.27)$$

For simplicity, we choose the ground state, that is, the lowest-energy state with  $n = 1$ ,  $l = 0$ , and  $m = 0$ . Substituting Eq. (1.4.22) into Eq. (1.4.27) and defining a density function  $D(r) = dW/dr$ , we find that

$$D(r) = 4\pi r^2 |\psi_{1,0,0}|^2 = \frac{4r^2}{a^3} \exp\left(-\frac{2r}{a}\right) \quad (1.4.28)$$

It is obvious that  $D(r) dr$  is the probability that the electron lies within the spherical shell of volume  $4\pi r^2 dr$ .

The top figure of Fig. 1.5 is a plot of Eq. (1.4.28) as a function of  $r/na$  with  $n = 1$ . The other two curves are the corresponding plots for the  $2s$  and  $3s$  states. The vertical dashed lines represent the radii of the various orbits as calculated from Eq. (1.2.8). By comparison, the solid lines are the average distances of the electron from the nucleus for these states as calculated from Eq. (1.3.13), or

$$\langle r_{n,0,0} \rangle = \int_0^\infty \int_0^\pi \int_0^{2\pi} r |\psi_{n,0,0}|^2 r^2 dr \sin \theta d\theta d\phi \quad (1.4.29)$$

It is to be noted that at distances far from the nucleus, the electron distribution drops exponentially with distance. Thus, from Fig. 1.5, we see that quantum mechanics predicts an atom size of the order of  $10^{-10}$  m, a result not far from the semiclassical result. The significant difference is that the quantum-mechanical electron distribution spreads diffusely in space instead of being confined to a certain orbit.

As stated earlier, one of the mysteries challenging the classical theory is what prevents the electron from falling on top of the nucleus. This question is answered in quantum mechanics by another postulate, known as the *uncertainty principle*, which says that the position and the momentum of a particle cannot be determined simultaneously. More precisely, the uncertainty  $\Delta x$  in the value of the position and the uncer-

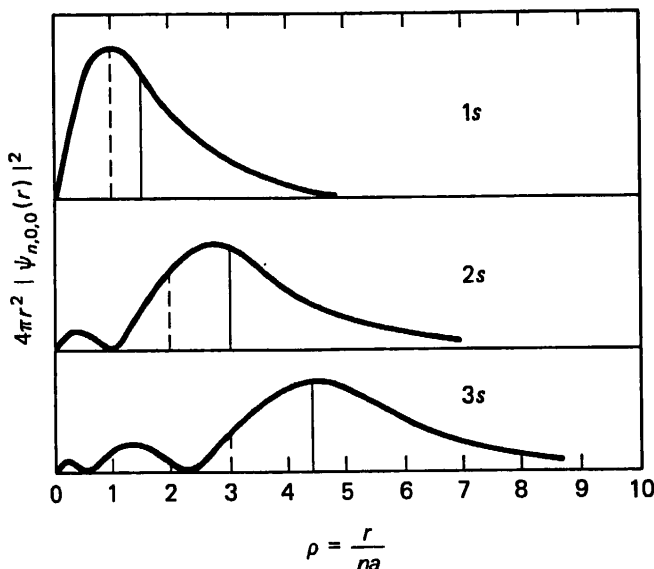


**Figure 1.5** Electron distribution functions  $D(r) = 4\pi r^2 |\psi_{n,0,0}|^2$  for a hydrogen atom. The abscissa is  $\rho = r/na$ , where  $a$  is the Bohr radius and  $n$  is the principal quantum number. The three curves are for  $n = 1$ ,  $n = 2$ , and  $n = 3$ . The dashed lines represent the orbital radii based on the old quantum theory, and the solid lines represent the expectation values  $\langle r \rangle$  based on quantum mechanics.

tainty  $\Delta p$  in the value of the corresponding momentum are such that the value of their product has a lower bound  $\hbar/2$ , which means that

$$\Delta p \Delta x \geq \frac{\hbar}{2} \quad (1.4.30)$$

If an electron fell into the nucleus, the position of the electron would be of nuclear dimension (of the order of  $10^{-14}$  m, in contrast to the atomic dimension of  $10^{-10}$  m). In other words,  $\Delta x$  would become so small as to require a tremendously large  $\Delta p$  in Eq. (1.4.30). This large value of  $p$  then would make the electron to have sufficient kinetic energy to break away from the nucleus. The spreading of the electron distribution in Fig. 1.5 can be understood on the same basis. Based on Eq. (1.4.30), an electron cannot be confined to a certain orbit with precisely defined position and momentum.

## 1.5 SPIN AND EXCLUSION PRINCIPLE

In Section 1.4 we discussed the motion of the electron in a hydrogen atom. However, experimental evidences indicate that the quantum description of an electron state based on three quantum numbers  $n$ ,  $l$ , and  $m$  is still incomplete. For example, in the Stern-Gerlach experiment, a beam of neutral hydrogen atom is sent into an inhomogeneous magnetic field  $B_z$ . If an atom possesses a magnetic dipole of moment  $u$ , the magnetic energy of the dipole is

$$\mathcal{E} = -\mathbf{B} \cdot \mathbf{u} = -B_z u_z \quad (1.5.1)$$

In the presence of an inhomogeneous field, the atom experiences a force

$$F_z = -\frac{\partial \mathcal{E}}{\partial z} = u_z \frac{dB_z}{dz} \quad (1.5.2)$$

The magnetic dipole moment  $u$  is related to the angular momentum  $L$  of an electron. Thus, to understand the physical significance of the experiment, we must know how the angular momentum of an electron can be found.

Classically, the angular momentum vector  $\mathbf{L}$  is defined as

$$\mathbf{L} = \mathbf{r} \times \mathbf{p} \quad (1.5.3)$$

Thus the  $z$  component of the angular momentum is equal to

$$L_z = x p_y - y p_x \quad (1.5.4)$$

According to our discussion in Section 1.3, the quantum-mechanical counterpart of  $L_z$  is

$$\langle L_z \rangle = \iiint_{-\infty}^{\infty} \psi^* \frac{\hbar}{i} \left( x \frac{\partial}{\partial y} - y \frac{\partial}{\partial x} \right) \psi dx dy dz \quad (1.5.5)$$

In obtaining Eq. (1.5.5), the classical momenta  $p_y$  and  $p_x$  of Eq. (1.5.4) are replaced by the corresponding momentum operator. Similar expressions are also obtained for  $L_x$  and  $L_y$ . Evaluation of Eq. (1.5.5) and similar expressions yields the following results:

$$\langle L_z \rangle = m\hbar \quad (1.5.6)$$

$$\langle L^2 \rangle = \langle L_x^2 + L_y^2 + L_z^2 \rangle = \hbar^2 l(l+1) \quad (1.5.7)$$

For hydrogen atoms in the ground state,  $l = 0$  and  $m = 0$ . If the angular momentum of the electron were totally accounted for by the orbital motion (i.e., the motion around the nucleus), we would have  $u_z = 0$  in Eq. (1.5.2), and hence no deflection of the beam would be expected. This is contrary to the experimental finding.

Actually, the original beam is split into two separate beams in an inhomogeneous magnetic field. The answer to this puzzling result was given by Uhlenbeck and Goudsmit, who postulated the following hypothesis. In addition to its motion around the nucleus, an electron also possesses rotational freedom about an axis through its charged body. Such an additional property of an electron is called the *spin*. From the deflection of the beam, the magnetic moment  $u_z$  and in turn the amount of angular momentum associated with the spinning motion can be determined.

The angular momentum associated with the spinning motion of an electron can be expressed, in a manner similar to Eqs. (1.5.6) and (1.5.7), in terms of two quantum numbers  $s$  and  $s_z$  as follows:

$$\langle L^2 \rangle = \hbar^2 s(s + 1) \quad (1.5.8)$$

$$\langle L_z \rangle = s_z \hbar \quad (1.5.9)$$

The value of  $s$  is found experimentally to be  $\frac{1}{2}$ . The relation between  $s_z$  and  $s$  is also similar to that between  $m$  and  $l$ . For a given  $l$ , the maximum and minimum values of  $m$  are  $\pm l$ , and the changes between successive  $m$ 's are  $\pm 1$ . Applying the same principle to  $s_z$ , we find that the only possible values for  $s_z$  are  $s_z = +\frac{1}{2}$  and  $s_z = -\frac{1}{2}$ . It is the existence of two possible values of  $s_z$  that gives rise to two different values of  $u_z$  in Eq. (1.5.2) and thus accounts for the splitting of the hydrogen beam.

In summary, the motion of an electron in an atom consists of two parts: the orbital motion around the nucleus and the spinning motion. It has been shown by Dirac that the electron spin is a purely relativistic property of an electron. For our present discussion of atomic theory, however, the classical concept of an electron having a spinning charge distribution can still be retained without special inquiry into the origin of spin. In other words, an electron can be visualized as a small solid body rather than a point, carrying out a rotation about its own axis similar to that of a spinning top. The angular momentum of the spinning motion is specified by the quantum number  $s_z$  ( $= \pm \frac{1}{2}$ ). Since the value of  $s$  is always  $\frac{1}{2}$ , it need not be specifically stated. Therefore, the total motion of an electron is specified by four quantum numbers  $n$ ,  $l$ ,  $m$ , and  $s$ .

Now we have four quantum numbers; our next task is the assignment of these numbers to each electron in an atom. The law that regulates the assignment is known as the *Pauli exclusion principle*, which states that no two electrons can have the same set of four quantum numbers. As we discuss in Section 1.6, the shell structure of atoms can be understood only in the light of this principle.

For our present discussion, let us apply the exclusion principle to a helium atom, which is next to hydrogen in the periodic table (Table 1.1). In the ground state (the lowest-energy state), the two electrons of helium belong to the  $1s$  configuration. Since these two electrons have the same orbital quantum numbers  $n = 1$ ,  $l = 0$ , and  $m = 0$ , their spin quantum numbers must be different, that is, one having  $s_z = -\frac{1}{2}$  and the other having  $s_z = +\frac{1}{2}$ . Note that the two combinations

$$n = 1, \quad l = 0, \quad m = 0, \quad s_z = +\frac{1}{2}$$

$$n = 1, \quad l = 0, \quad m = 0, \quad s_z = -\frac{1}{2}$$

are the only possible combinations of the four quantum numbers. Therefore, the maximum number of electrons that can be assigned to the  $1s$  level is two. The same applies to other  $ns$  levels. When this maximum occupancy is achieved in an  $s$  level, no more electrons can be assigned to that level.

The discussion above can be extended to other atomic states, such as  $p$  and  $d$  states. For  $p$  states,  $l = 1$ . Out of three possible choices (1, 0, or  $-1$ ) for  $m$  and two possible choices ( $+\frac{1}{2}$  or  $-\frac{1}{2}$ ) for  $s_z$ , there are, all together, six combinations. Therefore, the maximum number of electrons that can be accommodated in a  $p$  level is 6. In general, for a given  $l$ , there are  $(2l + 1)$  values of  $m$ . Counting the two possible spin orientations, there are all together  $2(2l + 1)$  different modes of electron motion in an atom. On the basis of the exclusion principle, only one electron can be assigned to a particular mode. The state of maximum occupancy is reached if all the  $2(2l + 1)$  different modes have been assigned to 2( $2l + 1$ ) electrons. Therefore, for the  $nd$  level, which starts with  $n = 3$ , the maximum number of electrons is 10.

## 1.6 THE PERIODIC SYSTEM

The periodic table of chemical elements (Table 1.1) has long been useful in studying material properties. Elements occupying similar places, to a large extent, have similar chemical properties. Notable examples of these elements are the alkali metals, the halogens, and the inert gases. The periodic table has also aided in the search for new materials by the semiconductor industry. Since the early development of semiconductor diodes and transistors, Si, GaAs, InSb, and many other compounds have joined Ge to appear on the list of useful semiconductor materials. Referring to Table 1.1, we see that Ge and Si both belong to the group IVb of elements, whereas GaAs and InSb are compounds of group IIIb and group Vb elements. As discussed later, all these materials have similar electrical properties. To explain this fact as well as to understand the origin of the periodic arrangement of elements, we must study the periodic table in conjunction with the electronic structure of atoms given in Table 1.2.

As discussed in Section 1.1, the Rutherford atom consists of a nucleus carrying a charge of  $+ze$  and a revolving electron cloud carrying a charge of  $-ze$  where  $z$  is the atomic number. If we neglect the electrostatic (Coulomb) interaction between the electrons, each electron can be considered as moving independently in a nuclear potential of  $ze/4\pi\epsilon_0 r$ . In other words, the result of our analysis in Section 1.4 for a hydrogen atom is also applicable to other atoms provided that we replace  $e^2$  by  $ze^2$  in the potential-energy  $V$  term in Eq. (1.4.1).

Many physics as well as engineering problems defy an exact solution simply because the problems are too complicated. Also, if we attempt to solve such problems exactly, we find ourselves deeply involved in mathematics and thus often lose physical insight. The general approach for treating problems of this kind is known as *successive approximation*. The important terms in an equation are treated first. In the present case, since the electron-electron interaction is much weaker than the electron-nucleus interaction, the terms representing the former are ignored in the Schrödinger equation. The solution thus obtained is the first-order approximate solution. Improvement of the results can be made later, when necessary, by taking into account the electron-electron interaction. Such a refinement, however, is not needed in our present discussion of the periodic system.

**TABLE 1.2 ATOMIC STRUCTURE OF THE ELEMENTS**

z	Element	$E_i$ (eV)	Electron Configuration			Atomic radius (Å)	Electro-negativity (Pauling)
			Inner shells	1s	Outer shells		
1	Hydrogen (H)	13.59		1			2.20
2	Helium (He)	24.56		2			—
						0.79 0.49	
							—
3	Lithium (Li)	5.40		1			2.05
4	Beryllium (Be)	9.32		2			0.98 1.40
5	Boron (B)	8.28		2			1.57 1.17
6	Carbon (C)	11.27		2			2.04 0.91
7	Nitrogen (N)	14.55		2			2.55 0.75
8	Oxygen (O)	13.62		3			3.04 0.65
9	Fluorine (F)	17.43		4			3.44 0.57
10	Neon (Ne)	21.56		2			3.98 0.51
				2			—
				6			
11	Sodium (Na)	5.14		1			2.23
12	Magnesium (Mg)	7.64		2			0.93 1.73
13	Aluminum (Al)	5.97		2			1.31 1.82
14	Silicon (Si)	8.15		2			1.61 1.46
15	Phosphorus (P)	10.49		2			1.90 1.23
16	Sulfur (S)	10.36		3			2.19 1.09
17	Chlorine (Cl)	12.90		4			2.58 0.97
18	Argon (Ar)	15.76		2			3.16 0.88
				6			—

			3d	4s		
19 Potassium	(K)	4.34	↑	1	2.77	0.82
20 Calcium	(Ca)	6.11	—	2	2.23	1.00
21 Scandium	(Sc)	6.54	1	2	2.09	1.36
22 Titanium	(Ti)	6.84	2	2	2.00	1.54
23 Vanadium	(V)	6.71	3	2	1.92	1.63
24 Chromium	(Cr)	6.74	5	1	1.85	1.66
25 Manganese	(Mn)	7.43	5	2	1.79	1.55
26 Iron	(Fe)	7.83	6	2	1.72	1.83
27 Cobalt	(Co)	7.84	7	2	1.67	1.88
28 Nickel	(Ni)	7.63	8	2	1.62	1.91
			3d	4s	4p	
29 Copper	(Cu)	7.72	10	1	—	1.57
30 Zinc	(Zn)	9.39	10	2	—	1.53
31 Gallium	(Ga)	5.97	10	2	1	1.65
32 Germanium	(Ge)	7.90	10	2	1	1.81
33 Arsenic	(As)	9.81	10	2	2	2.01
34 Selenium	(Se)	9.73	10	2	3	2.18
35 Bromine	(Br)	11.81	10	2	4	2.55
36 Krypton	(Kr)	14.00	10	2	5	2.96
			4d	4f	5s	
37 Rubidium	(Rb)	4.17	—	—	1	2.98
38 Strontium	(Sr)	5.69	—	—	2	2.45
39 Yttrium	(Y)	6.5	1	—	2	2.27
40 Zirconium	(Zr)	6.8	2	—	2	2.16
41 Niobium	(Nb)	6.9	4	—	1	2.08
42 Molybdenum	(Mo)	7.1	5	—	1	2.01
43 Technetium	(Tc)	7.3	6	—	1	1.95
44 Ruthenium	(Ru)	7.4	7	—	1	1.89
45 Rhodium	(Rh)	7.5	8	—	1	1.83
46 Palladium	(Pd)	8.3	10	—	—	1.79

**TABLE 1.2** Continued

z	Element	$\varrho_i$ (eV)	Electron Configuration				Atomic radius (Å)	Electro-negativity (Pauling)
			Inner shells	Outer shells				
47	Silver	(Ag)	7.58	↑	—	1	—	1.93
48	Cadmium	(Cd)	8.99	—	2	—	1.71	1.69
49	Indium	(In)	5.79	(Kr)	—	1	2.00	1.78
50	Tin	(Sn)	7.30	—	2	2	1.72	1.96
51	Antimony	(Sb)	8.64	+ 4d <sup>10</sup>	—	2	1.53	2.05
52	Tellurium	(Te)	8.96	—	2	3	1.42	2.10
53	Iodine	(I)	10.44	—	2	4	1.32	2.66
54	Xenon	(Xe)	12.13	→	—	5	1.24	—
					2	6		
				4f	5d	6s		
55	Cesium	(Cs)	3.89	—	—	—	1	0.79
56	Barium	(Ba)	5.21	—	—	—	2	3.34
57	Lanthanum	(La)	5.61	—	1	2	2.78	0.89
58	Cerium	(Ce)	(5.54)	2	—	2	2.74	1.10
59	Praseodymium	(Pr)	(5.46)	3	—	2	2.70	1.12
60	Neodymium	(Nd)	(5.53)	4	—	2	2.67	1.13
61	Promethium	(Pm)	(5.55)	5	—	2	2.64	1.14
62	Samarium	(Sm)	(5.60)	6	—	2	2.62	1.13
63	Europium	(Eu)	5.64	7	—	2	2.59	1.17
64	Gadolinium	(Gd)	6.2	7	1	2	2.56	1.20
65	Terbium	(Tb)	(5.86)	8	1	2	2.54	1.20
66	Dysprosium	(Dy)	(5.94)	9	1	2	2.51	1.2
67	Holmium	(Ho)	6.0	10	1	2	2.49	1.22
68	Erbium	(Er)	6.1	11	1	2	2.47	1.23
69	Thulium	(Tm)	6.2	12	1	2	2.45	1.24
70	Ytterbium	(Yb)	6.2	13	1	2	2.42	1.25
71	Lutetium	(Lu)	5.4	14	1	2	2.40	1.1

			5d	5f	6s	6p	
72	Hafnium	(Hf)	6.65	2	2	—	2.16
73	Tantalum	(Ta)	7.89	3	2	—	2.09
74	Tungsten	(W)	7.94	4	2	—	2.02
75	Rhenium	(Re)	7.87	5	2	—	2.36
76	Osmium	(Os)	8.7	6	2	—	1.97
77	Iridium	(Ir)	9.2	9	0	—	2.2
78	Platinum	(Pt)	8.96	9	1	—	2.20
79	Gold	(Au)	9.23	10	1	—	2.38
80	Mercury	(Hg)	10.44	10	2	—	2.54
81	Thallium	(Tl)	6.12	10	2	—	2.00
82	Lead	(Pb)	7.42	10	2	—	2.04
83	Bismuth	(Bi)	7.29	10	2	—	2.33
84	Polonium	(Po)	8.42	10	2	—	2.02
85	Astatine	(At)	(9.6)	10	2	—	2.0
86	Radon	(Rn)	10.75	10	2	—	2.2
					6	—	—
							—
87	Francium	(Fr)	(4.0)	—	—	—	0.7
88	Radium	(Ra)	5.27	—	—	1	0.9
89	Actinium	(Ac)	5.17	—	—	2	0.9
90	Thorium	(Th)	6.1	1	2	2	1.1
91	Protactinium	(Pa)	5.9	1(—)	1(2)	2	1.3
92	Uranium	(U)	6.05	2(1)	1(2)	2	1.5
93	Neptunium	(Np)	6.2	3	1	2	1.38
94	Plutonium	(Pu)	6.1	5(4)	—(1)	2	1.36
95	Americium	(Am)	6.0	6(5)	—(1)	2	1.28
96	Curium	(Cm)	6.0	7	—	2	1.3
97	Berkelium	(Bk)	6.2	7	1	2	1.3
98	Californium	(Cf)	6.3	9	2	2	1.3
				10	2	2	—
							—

Let us return to our original task concerning the electron structure of an atom having  $z$  electrons. Note that replacing  $e^2$  by  $ze^2$  in Eq. (1.4.1) will not change the results presented in Section 1.4 except that  $e^4$  should be replaced by  $z^2e^4$  in the energy expression of Eq. (1.4.14). The electron motion is again specified by four quantum numbers,  $n$ ,  $l$ ,  $m$ , and  $s_z$ . Therefore, our task now reduces to assigning a different set of four quantum numbers to each electron. For such an assignment, we need to know the energy associated with each atomic level. A modification of Eq. (1.4.14) to account for the difference in nuclear charge and to include relativistic variation of the mass leads to the following energy expression:

$$\mathcal{E} = -\frac{mz^2e^4}{2(4\pi\epsilon_0\hbar)^2} \frac{1}{n^2} \left[ 1 + \frac{\alpha^2 z^2}{n^2} \left( \frac{n}{l + \frac{1}{2}} - \frac{3}{4} \right) \right] \quad (1.6.1)$$

where  $\alpha = e^2/4\pi\epsilon_0\hbar c$  is the fine structure constant, and  $c$  is the velocity of light.

From the dependence of  $\mathcal{E}$  on  $l$  in Eq. (1.6.1), we see that the  $2p$  level should be slightly above the  $2s$  level in energy and that the  $3d$  level should be slightly above the  $3p$  level (Fig. 1.6). Now we redraw part of Fig. 1.6 as Fig. 1.7, and distribute electrons of a selected number of elements among the various available energy states. For helium it is obvious that the configuration of lowest energy has two electrons in the  $1s$  level. Since two is the maximum number possible for the  $1s$  level, the level is full. A *closed shell* is said to have formed if electrons fill completely a given atomic level. Hence the first shell is completed in helium.

After He comes Li. The third electron of Li must go to a higher energy level, that is, the  $2s$  level, as illustrated in Fig. 1.7. In Be, both the levels  $1s$  and  $2s$  are full. The  $2p$  level begins to become occupied in boron, and it is completely occupied in Ne. Because the energy separation between  $2s$  and  $2p$  levels is not very large, we usually consider them together as constituting a single shell and speak of the next shell when both are complete. The second closed shell, therefore, is completed in neon. This definition of a closed shell also applies to  $3s$  and  $3p$  electrons and to  $4s$  and  $4p$  electrons. Thus, after He and Ne, a closed-shell configuration is again reached in argon. Elements having their shells completed are chemically inert, such as He, Ne, Ar, and Kr.

The one-electron scheme (i.e., the scheme considering each electron as moving independently of other electrons) on which Eq. (1.6.1) is based works well qualitatively up to argon in explaining the distribution of electrons among the different atomic levels. But potassium shows a deviation from the normal pattern (Table 1.2). A state of lower energy is achieved by filling the  $4s$  level first instead of the  $3d$  level, which has a smaller principal quantum number. For electrons in an outer orbit,  $4s$  orbit or  $3d$  orbit, for example, the Coulomb field of the nucleus is partly shielded by the charge cloud of the inner-core electrons,  $1s$  and  $2s$  electrons, for example. Therefore, in Eq. (1.6.1), the value of  $ze$  should be the effective nuclear charge whose influence is actually felt by the electron. The value of  $ze$  will be different even in the same atom for electrons in differ-

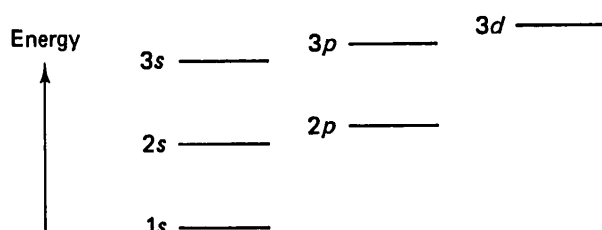


**Figure 1.6** Energy diagram for the few lowest-energy states. The energy separations between the levels are not drawn to scale.

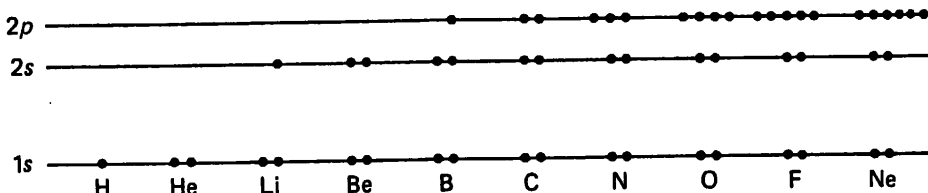


**Figure 1.7** Distribution of electrons among available quantum states in a selected number of chemical elements. Lower-energy states are filled first.

ent atomic orbits because the degree of shielding and hence the value of  $ze$  depend on the depth of penetration of the electron wave function.

For small values of  $n$ , the energy separation between levels with different  $n$  is so large that the effect due to different degrees of shielding is secondary. For large values of  $n$  as in the case of potassium, the  $4s$  wave function penetrates much more deeply than the  $3d$  wave function into the region of low potential energy near the nucleus. The effect on energy caused by the difference in the effective  $ze$  for the  $4s$  and  $3d$  wave functions actually overwhelms that caused by the difference in  $n$  in Eq. (1.6.1). A similar situation occurs in the  $N$  shell (X-ray nomenclature with  $n = 4$ ). Electrons begin to settle in the  $5s$  and  $5p$  levels of the  $O$  shell before they fill up the  $4d$  and  $4f$  levels of the  $N$  shell.

The reader may also be aware of the fact that in Table 1.2 we have assigned to electrons only the values of  $n$  and  $l$ . The existence of different values for the other two quantum numbers  $m$  and  $s_z$  can only be inferred from the maximum number of electrons allowed in Table 1.2 and Fig. 1.7 for a given set of  $n$  and  $l$ . The reason is simple for not mentioning explicitly the values of  $m$  and  $s_z$ . To be able to assign the values of  $m$  and  $s_z$  to the electron, we must consider interactions of second-order importance, such as the electron-electron interaction, in the energy expression.

Let us now discuss how we can use the information derived from the electronic structure of atoms. As mentioned earlier, elements having their shells completed are chemically inert. The same can be said about electrons in an atom. Those electrons that belong to closed shells are core electrons. Because it requires considerable energy to break up a closed shell, the core electrons are inactive in a chemical reaction and are not affected by small external disturbances, for example the application of a small electric field in a conductance measurement. Therefore, in our discussion of material properties, we can ignore the core electrons and speak of only the electrons outside the closed shells. The closed-shell configuration in an atom can easily be identified in Table 1.2 by comparing the given electron configuration with that of a nearest inert gas (He, Ne, Ar, Kr, or Xe).

The alkali metals have a single electron outside closed shells from  $2s$  in Li to  $6s$  in Cs. The halogens, on the other hand, are one electron short of completing the  $s-p$  shell (from the  $2s-2p$  shell in F to the  $6s-6p$  shell in At). The alkali metals and the halogens form salts of the type XY. As discussed in Chapter 2, crystals of alkali halides are electrical insulators. In contrast to alkali halides, the III-V compounds are semiconductors. The electron configurations in elemental semiconductors Ge and Si and those in III-V compound semiconductors are quite similar. By III-V compounds we mean compounds made of group IIIb elements and group Vb elements. The group IIIb elements such as Ga have two  $s$  electrons and one  $p$  electron, whereas the group Vb elements such as As have two  $s$  electrons and three  $p$  electrons. If we suppose that these

electrons are shared equally between the atoms in a compound, we would have a similar electron configuration in III–V compound semiconductors as that in Ge and Si. Therefore, it is not surprising that III–V compounds are also semiconductors having similar electrical properties as Ge and Si. The differences as well as the similarities between the properties of these materials are explored further in subsequent chapters.

## PROBLEMS

- 1.1. According to Rutherford, an atom was thought of as composed of protons and electrons. Neutrons were later found also to be a constituent part of the nucleus. From the Rutherford scattering experiment, what qualitative information can be derived about the relative mass and physical dimension of the proton and the electron? Would the experiment be equally successful if electrons were used instead of  $\alpha$  particles? Which quantity, the atomic number  $z$  or the atomic mass number  $A$ , can be obtained from the experiment? Explain why the two numbers are different.
- 1.2. Consider the motion of an electron in a solid. Apply what we have learned about the Rutherford experiment to the problem and present a qualitative picture of what happens to the electron motion. Does the electron feel the nuclear charge alone or the total charge of an atom? Is the scattering effect stronger in a solid made of neutral atoms such as in Ge than in a solid made of charged ions such as in NaCl?
- 1.3. (a) It was found by Balmer in 1885 that the frequency of a series of emission lines of hydrogen can be fitted in the visible region by

$$\nu = cR \left( \frac{1}{4} - \frac{1}{n^2} \right)$$

where  $R$  is the Rydberg constant and  $c$  is the velocity of light. Find the value of  $R$  (expressed in  $\text{cm}^{-1}$ ).

- (b) One of the emission lines in the series has a wavelength  $\lambda = 6563 \text{ \AA}$  ( $\lambda = c/\nu$ ). Identify the principal quantum numbers of the two states in Eq. (1.2.11).
- 1.4. The first four emission lines of hydrogen in the Balmer series have the following wavelengths:  $\lambda = 6563 \text{ \AA}$ ,  $4861 \text{ \AA}$ ,  $4340 \text{ \AA}$ , and  $4102 \text{ \AA}$ . Show that the observed emission can be accounted for by the old quantum theory.
- 1.5. In the Franck–Hertz experiment, a mercury discharge tube was used, and two important observations were made: the emission of radiation at  $\lambda = 2536 \text{ \AA}$  and a sharp current drop when the applied grid voltage exceeds  $4.9 \text{ V}$ . Determine whether there is any correlation between the two observations and offer a plausible explanation for the current drop. The anode is negatively biased with respect to the grid.
- 1.6. (a) Consider a one-dimensional, mechanical harmonic oscillator that obeys

$$M \frac{d^2x}{dt^2} = -\gamma x$$

where  $\gamma$  is the spring (or force) constant. Show that the energy of the oscillator is

$$\mathcal{E} = \frac{p^2}{2M} + \frac{\gamma x^2}{2}$$

- (b) Applying the Wilson–Sommerfeld quantization rule, show that the energy  $\mathcal{E}$  is quantized and equal to

$$\mathcal{E} = n\hbar\omega$$

where  $\omega = \sqrt{\gamma/M}$  and  $n$  is an integer. (Hint: Let  $x = \sqrt{2\mathcal{E}/\gamma} \sin \theta$  in performing the phase integral.)

- 1.7. (a)** Find the Schrödinger equation for the one-dimensional harmonic oscillator of Problem 1.6 by replacing  $p$  by an appropriate operator.  
**(b)** In the quantum-mechanical treatment, the energy of a harmonic oscillator is

$$\mathcal{E} = \left( n + \frac{1}{2} \right) \hbar \omega$$

Show that the wave function

$$\psi_1 = A_1 x \exp \left( - \frac{M\omega}{2\hbar} x^2 \right)$$

is a solution of the Schrödinger equation for  $n = 1$ .

- 1.8. (a)** Apply the Wilson-Sommerfeld quantization rule to an electron of mass  $m$  which moves with a constant velocity in one dimension between  $x = -a$  and  $x = a$ . The electron undergoes perfectly elastic collisions with rigid walls at  $x = -a$  and  $x = a$ . Show that the energy of the electron is

$$\mathcal{E} = \frac{n^2 \hbar^2}{32ma^2}$$

- (b)** Consider a quantum-mechanical problem in which an electron moves in a one-dimensional potential well (Fig. P1.8). For simplicity, we assume that  $V = 0$  for  $-a < x < a$  and  $V = \infty$  for  $x > a$  and  $x < -a$ . Find the wave function for the electron motion and the quantized energy of the electron.

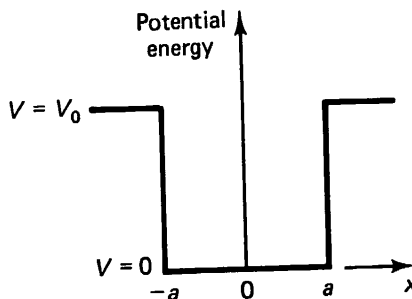


Figure P1.8

- 1.9. (a)** Consider a problem in which an electron faces a one-dimensional potential barrier (Fig. P1.9). The electron energy  $\mathcal{E}$  is such that  $\mathcal{E} < V_0$ . Write down the Schrödinger equation and its solution for the three regions.

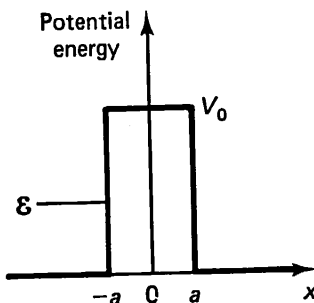


Figure P1.9

- (b) Classically, we know that the electron can never penetrate the barrier for  $\mathcal{E} < V_0$ . Do you reach the same conclusion from the quantum-mechanical treatment? (Hint: Apply the probabilistic interpretation of  $|\psi|^2$  and note that

$$\frac{d^2\psi}{dx^2} = \alpha\psi$$

has an exponential solution if  $\alpha$  is positive and a sinusoidal solution if  $\alpha$  is negative.)

- 1.10.** Show that the average value of  $r$  for the  $1s$  electron in a hydrogen atom is  $\langle r_{1,0,0} \rangle = 1.5a$ , where  $a$  is the Bohr radius.

- 1.11.** The angular-momentum operator  $L_z$  is

$$L_z = \frac{\hbar}{i} \frac{\partial}{\partial\phi}$$

in spherical coordinates. Show that

$$\langle L_z \rangle_{2,1,1} = \hbar, \quad \langle L_z \rangle_{2,1,0} = 0, \quad \langle L_z \rangle_{2,1,-1} = -\hbar$$

for the  $2p$  electrons. [Hint:  $\int_0^\infty v^n \exp(-v) dv = n!$ .]

- 1.12.** Show that  $\Theta_{2,0}$  of Eq. (1.4.20) satisfies Eq. (1.4.7) for  $l = 2$  and  $m = 0$  and that  $R_{2,0}$  of Eq. (1.4.21) satisfies Eq. (1.4.8) for  $n = 2$  and  $l = 0$ . (Hint: Express the terms  $\mathcal{E}$  and  $e^2/4\pi\epsilon_0 r$  in terms of the Bohr radius  $a$ .)
- 1.13.** (a) Use the chemical elements Na, Cl, Ca, and O as examples. Show how these elements can achieve closed-shell configuration by becoming ions.  
 (b) How many distinct orbital wave functions are there for  $d$  electrons? What is the maximum number of electrons for the  $d$  state?

P.01		
6.8	Structure Investigation of Biomolecular Crystals . . . . .	447
6.8.1	Progress in the Methods of X-Ray Macromolecular Crystallography . . . . .	447
6.8.2	Investigation of Protein Structure by the Nuclear Magnetic Resonance (NMR) Method . . . . .	451
6.8.3	Dynamics of Protein Molecules . . . . .	453
6.8.4	Data on the Structure of Large Proteins . . . . .	457
6.8.5	X-Ray Investigation of Ribosomes . . . . .	462
6.8.6	Virus Structures . . . . .	462
6.9	Ordering in Liquid Crystals . . . . .	467
6.9.1	Smectic A Polymorphism in Liquid Crystals (LC) Containing Polar Molecules . . . . .	468
6.9.2	Smectic Lamellar Crystalline Phases and Hexatics . . . . .	470
6.9.3	Freely Suspended Smectic Films . . . . .	472
6.9.4	Cholesteric Blue Phases . . . . .	472
6.9.5	Ohter Liquid Crystalline Phases . . . . .	473
6.10	Langmuir-Blodgett Films . . . . .	475
6.10.1	Principles of Formation . . . . .	475
6.10.2	Chemical Composition, Properties and Applications of LB Films . . . . .	475
6.10.3	Structure of LB Films . . . . .	477
6.10.4	Multicomponent Langmuir-Blodgett Films. Superlattices . . . . .	482
6.11	Photo- and Thermostimulated Phase Transitions in Ferroelectrics . . . . .	485
6.11.1	Photostimulated Phase Transitions in Ferroelectrics . . . . .	485
6.11.2	Thermostimulated Phase Transitions in Ferroelectrics . . . . .	490
References . . . . .		493
Bibliography . . . . .		509
Subject Index . . . . .		515

## 1. Principles of Formation of the Atomic Structure of Crystals

The atoms in crystals are in direct contact, and the interactions of their outer electron shells produce chemical bonding. The condition for the formation of a crystal structure is a sufficiently low temperature, so that the potential energy of attraction between atoms considerably exceeds the kinetic energy of their thermal motion. The diversity of structures of crystals is determined by their composition and by the individual chemical characteristics of their constituent atoms which define the nature of the chemical bond, the electron density distribution, and the geometric arrangement of the atoms within the unit cell. Many important characteristics of crystal structures – interatomic distances, coordination, etc. – can be described on the basis of the geometrical model in which the atoms are represented as rigid spheres of definite radii.

### 1.1 The Structure of Atoms

#### 1.1.1 A Crystal as an Assembly of Atoms

Each atom in a crystal structure is bound to its nearest neighbors at definite distances. It also interacts with the next nearest atoms, both directly and through the first nearest neighbors, then with still further atoms, and so on, i.e., in end effect with the entire structure. The formation of crystals always results from the collective interaction of atoms, although it may sometimes be regarded approximately as the result of pair interactions. The assembly of atoms in the crystal lattice is also united by its intrinsic system of thermal vibrations.

The concepts of the chemical bond, valence, etc., play an important part in crystal chemistry and the theory of crystal structures. They have mainly been developed to explain the structure of molecules, whereas in a crystal the interaction of the whole set of atoms must be taken into consideration. Let us take, for instance, the simplest compound NaCl. If we write down its formula as  $\text{Na}^+\text{Cl}^-$  (in accordance with the valences of these atoms and the concepts of the positive charge of Na and negative of Cl), we obtain “molecules”  $\text{Na}^+\text{Cl}^-$ , of which the crystal seems to be made up. In fact, the structure of NaCl, as well as most of the ionic, covalent, and metallic structures, has no molecules at all: the formula NaCl is realized in the high-symmetry packing of these atoms, each of

which is surrounded by 6 neighbors of a different sort, then, further on, by 12 of the same sort, etc. On the other hand, in a number of crystals the molecules, or some other stable atomic groupings, retain their individuality. In this case the weaker forces binding these groupings into a crystal structure have to be explained. There are also many intermediate cases.

The task of "calculating" the concrete crystal structure is extremely complicated. However, generalization of a huge amount of chemical data on interatomic bonds and valence, quantum-mechanical information on the nature of atomic interactions and on cooperative interactions of particles, and, above all, diffraction and other investigations have made it possible to formulate a number of laws and regularities describing and governing the general principles and peculiarities of various crystal structures. Some of them are rigorously substantiated by theory and have a quantitative expression, while the others are semiempirical or qualitative. Nevertheless, on the whole these theoretical and empirical data, which comprise the subject of the theory of the atomic structure of crystals, or crystal chemistry, ensure reliable orientation in the tremendous diversity of crystal structures, explain many of their peculiarities, and enable one to calculate and predict some of their properties.

This chapter begins by explaining the general principles of the formation of chemical bonds in molecules and crystals. Then it considers the main geometric laws of the construction of crystal structures and some general questions of crystal chemistry. After that we discuss the basic types of crystal structures and classify them according to the nature of their chemical bonds. We also consider the structures of polymers, liquid crystals, and biological substances.

The chemical bond between atoms in molecules and crystals is realized by the electrons of their outer shells. Therefore, although atoms in a crystal always differ, to some extent, from free atoms, this difference actually refers exclusively to their outer shells. The interaction of these shells, the changes in their structure, and the redistribution of electrons from atom to atom or into the common "electron gas" of the crystal – all these actually reflect different aspects or possibilities of approximate description of the state of atoms and electrons assembled in the crystal structure. Even the simplest – ionic – type of bond, when oppositely charged ions attract each other electrostatically, requires, in the first place, an explanation of the reasons why it is "profitable" for one atom to give up an electron and become a cation, and for another to accept it and also become an ion, but with the opposite sign, i.e., an anion. Then problems arise concerning, for example, the equilibrium of the repulsive and attractive forces.

The stability of the inner shells of atoms, the relative stability of the outer shells, and the trend towards the formation of some stable states at the chemical bond in molecules and crystals are the starting points from which chemistry and crystal chemistry begin their analysis of the possible arrangement of atoms. Therefore we must first of all recall some basic information on the structure of atoms.

### 1.1.2 Electrons in an Atom

Electrons in an atom are in the spherically symmetric Coulomb field of the nucleus  $Ze/r$ ; they interact, repelling each other owing to electrostatic forces, and obey the Pauli principle. The stationary states of the electrons in an atom are described by the Schrödinger equation  $H\Psi = E\Psi$ . Wave function  $\Psi(x, y, z)$ , which is the solution to the Schrödinger equation is generally complex, and the square of modulus  $|\Psi|^2 = \Psi\Psi^*$  gives the probability density of finding electrons at point  $x, y, z$ , i.e., the electron density of the atom  $\rho(x, y, z)$ .

Let us consider the hydrogen atom. Here the Schrödinger equation in the spherical coordinates has the form

$$\left( \frac{\hbar^2}{8\pi^2 m} \nabla^2 + \frac{e^2}{r} \right) \psi(r, \theta, \varphi) + E\psi(r, \theta, \varphi) = 0 \quad (1.1)$$

and is solved analytically.

Each of the set of solutions

$$\psi_{nlm}(r, \theta, \varphi) = R_{nl}(r) Y_{lm}(\theta, \varphi) = R_{nl}(r) \Theta_{lm}(\theta) \Phi_m(\varphi) \quad (1.2)$$

is characterized by a definite combination of quantum numbers  $n$  (principal quantum number),  $l$  (orbital quantum number), and  $m$  (magnetic quantum number), and by the eigenvalue of the energy

$$E_n = -\frac{2\pi^2 me^4}{n^2 h^2}. \quad (1.3)$$

The wave functions  $\psi$  of electrons in an atom – of one electron in a hydrogen atom or of each electron in a multielectron atom – which give the distribution of the electrons in an atom, are called atomic orbitals by analogy to Bohr's atomic orbitals AO. With a given principal quantum number  $n$ ,  $n^2$  combinations according to the following scheme are possible:

$$n = 1, 2, \dots; \quad l = 0, 1, \dots, (n-1); \quad m = 0, \pm 1, \pm 2, \dots, \pm l. \quad (1.4)$$

With a given  $n$  the energy of each one of a set of states is the same, i.e., the states are degenerate.

The solution  $\psi(1.2)$  consists of radial,  $R$ , and angular,  $Y$ , components and may have a different symmetry according to the quantum numbers. The symmetry depends on the type of  $Y_{lm}$  and is described by one of the point groups of symmetry or antisymmetry. Figure 1.1 shows the radial components  $R_{nl}$  for the first states of the H atom. Figure 1.2 represents some orbitals of the H atom. In states with  $l = 0$  ( $m$  is then also zero),  $Y_{00} = 1$ ; these states are spherically symmetric and called s states (Fig. 1.2a). For instance, the orbital with the lowest energy (the ground state) has the form

$$\psi_{1s} = \frac{1}{\sqrt{\pi a_0^3}} \exp\left(-\frac{r}{a_0}\right), \quad (1.5)$$

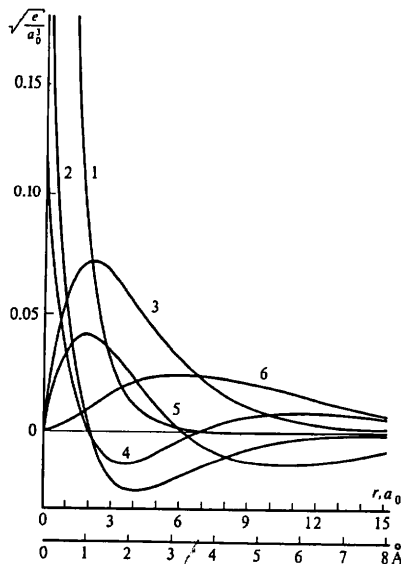


Fig. 1.1. Radial components  $R_{nl}$  of wave functions  $\psi$  of the H atom: (1)  $\psi_{100}$  (ground state 1s), (2)  $\psi_{200}$ , (3)  $\psi_{211}$ , (4)  $\psi_{300}$ , (5)  $\psi_{311}$ , (6)  $\psi_{322}$

where  $a_0 = 0.529 \text{ \AA}$  is the Bohr radius, the atomic unit of length. States with  $l = 1$  are called  $p$  states, with  $l = 2, d$  states, and with  $l = 3, f$  states.

At  $l \geq 1$  the orbitals are no longer spherically symmetric. Thus, at  $l = 1$  three solutions ( $m = 0, \pm 1$ ) of (1.1) are possible. Generally, angular components are complex, but real combinations may be constructed from them. So three real  $p$  orbitals are obtained,

$$\begin{aligned} p_x &= \frac{\sqrt{3}}{2\sqrt{\pi}} R_{n1}(r) \sin \theta \cos \varphi, & p_y &= \frac{\sqrt{3}}{2\sqrt{\pi}} R_{n1}(r) \sin \theta \sin \varphi, \\ p_z &= \frac{\sqrt{3}}{2\sqrt{\pi}} R_{n1}(r) \cos \theta. \end{aligned}$$

These orbitals have a cylindrical symmetry and are elongated either along the  $x$ , or the  $y$ , or the  $z$  axis (Fig. 1.2b). These functions reduce to zero on the plane of antisymmetry  $m'$  (nodal surface) perpendicular to the axis of cylindrical symmetry; their absolute values are mirror equal, but opposite in sign on the both sides of  $m'$ , i.e., they are described by the antisymmetry point group  $\infty/m'$ . The orbitals with  $l = 2$  ( $d$  states) have a more complex configuration (Fig. 1.2c). The orbitals with  $l = 3$  ( $f$  states) are still more complex.

All the orbitals are normalized and orthogonal, i.e., they obey the conditions

$$\int \psi_i \psi_j^* dv = \begin{cases} 1 & \text{for } i = j, \\ 0 & \text{for } i \neq j. \end{cases} \quad (1.6)$$

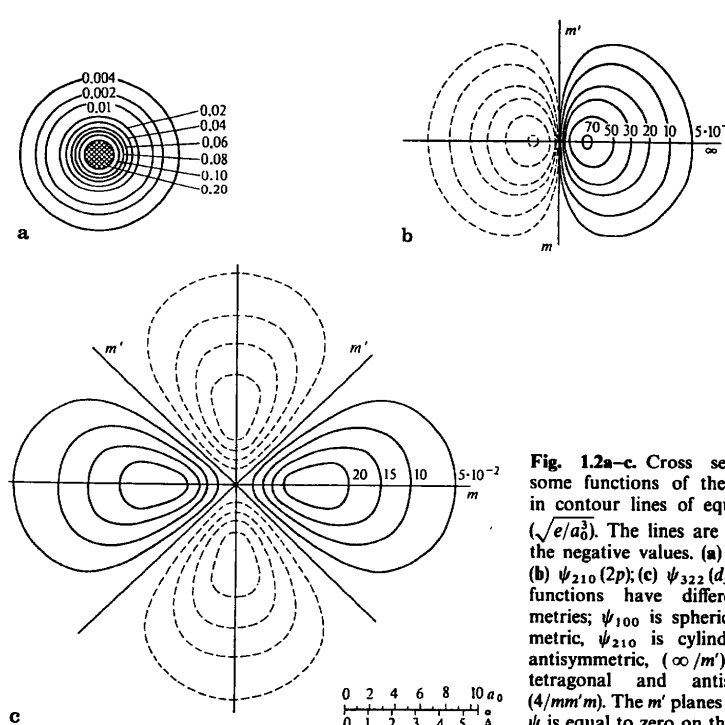


Fig. 1.2a-c. Cross sections of some functions of the H atom in contour lines of equal values ( $\sqrt{e/a_0^3}$ ). The lines are dashed at the negative values. (a)  $\psi_{100}$  (1s); (b)  $\psi_{210}$  (2p); (c)  $\psi_{322}$  ( $d_{x^2-y^2}$ ). The functions have different symmetries;  $\psi_{100}$  is spherically symmetric,  $\psi_{210}$  is cylindrical and antisymmetric ( $\infty/m'$ ),  $\psi_{322}$  is tetragonal and antisymmetric ( $4/mm'm'$ ). The  $m'$  planes are nodal;  $\psi$  is equal to zero on them [1.1]

The first of these relations shows that for each orbital the integral of the probability density  $\psi^2$  of the presence of an electron, taken over the entire volume, is equal to unity, and the second, that for any pair of different orbitals integral (1.6) is equal to zero, which reflects the properties of orbital symmetry. The square of the modulus of the wave function

$$|\psi|^2 = \psi \psi^* = \rho(r) \quad (1.7)$$

is the electron density of an atom in the corresponding state,  $\rho(r)$  being expressed by the number of electrons per unit volume. The models of electron density distribution in a hydrogen atom for the ground (1s) and other states are shown in Fig. 1.3.

Let us consider the function of radial distribution of electrons in the atom  $D(r)$ , which is obtained by integrating  $|\psi|^2$  over the angles. As a result, the dependence on  $Y_{lm}(\theta, \varphi)$  disappears, and the dependence on  $r$  is given by  $R_{nl}(r)$ . Thus, for the hydrogen atom and any multielectron atom the radial distribution of electrons in the  $n, l$  state is described by the function

$$D_{nl}(r) = 4\pi r^2 R_{nl}^2(r) \quad (1.8)$$

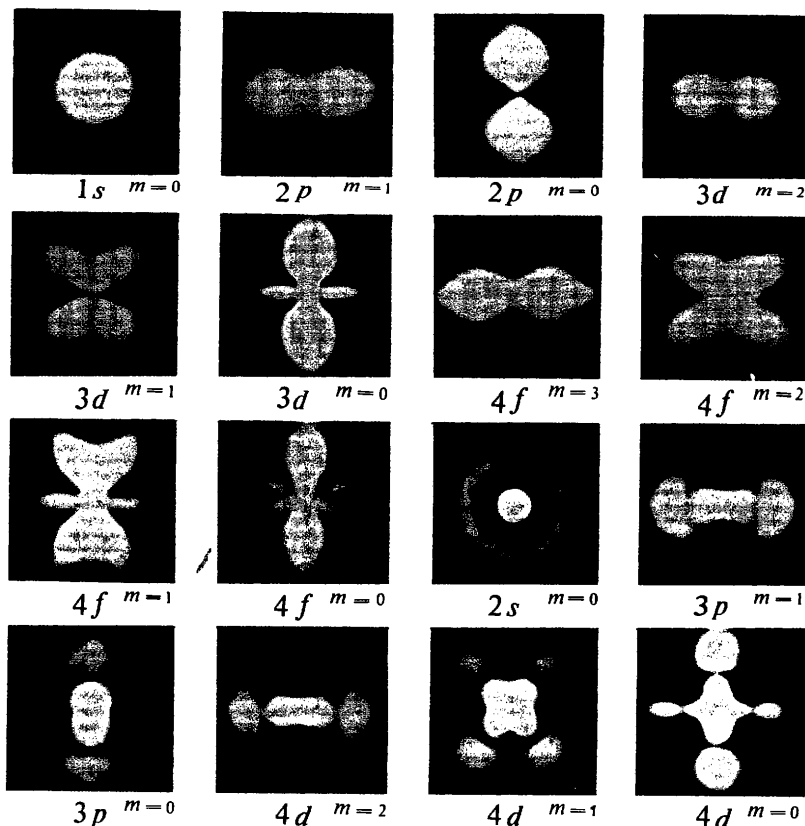


Fig. 1.3. Model of space distribution of the electron cloud in the hydrogen atom in different states [1,2]

so that  $D(r)dr$  gives the total number of these electrons in a spherical layer of radius  $r$  and thickness  $dr$  (Fig. 1.4a)<sup>1</sup>. The hydrogen atom contains one electron while, in general, an atom contains  $Z$  electrons; therefore,

$$\int |\psi|^2 dv = \int \rho(r)dv_r = \int D(r)dr = Z. \quad (1.9)$$

The graphs of radial functions for the hydrogen atom (Fig. 1.4b) clearly show the peculiarities of the radial distribution of the electrons. The maximum of  $D(r)$  for  $n = 1$  – the ground state of hydrogen – lies at  $r = a_0$ , the Bohr radius of the first orbital.

<sup>1</sup> By multiplying  $\rho(r)$  (1.7) and  $D(r)$  (1.8) by  $e$  we can express these functions in terms of the charge.

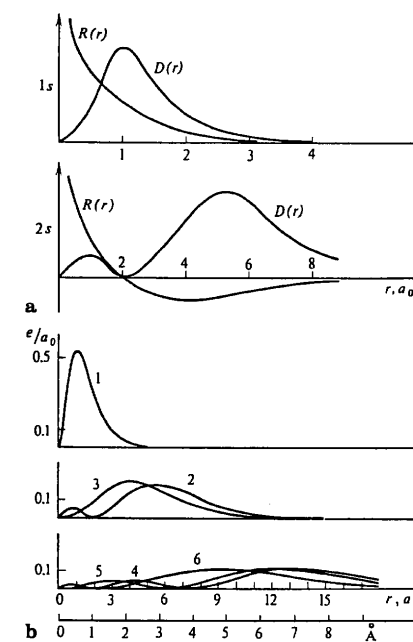
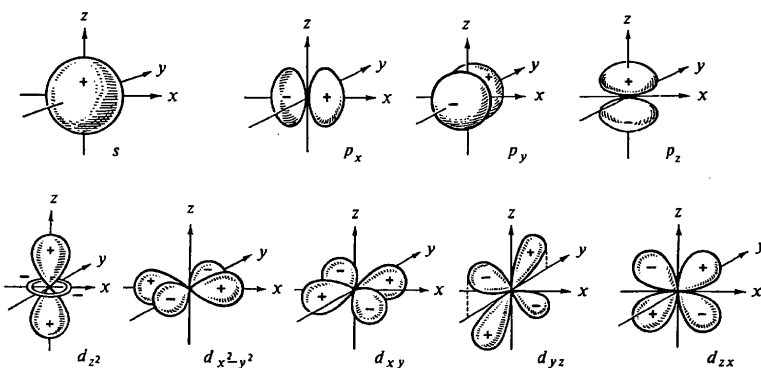


Fig. 1.4a, b. Radial distribution functions of the electron density in the H atom: (a) relationship between the radial component  $R(r)$  of the wave function and the radial distribution  $D(r)$  of functions  $\psi_{1s}$  and  $\psi_{2s}$ ; (b) functions  $D(r)$  for different states  $n, l$ : (1) 1, 0; (2) 2, 0; (3) 2, 1; (4) 3, 0; (5) 3, 1; (6) 3, 2. (cf. Fig. 1.1)

The above laws about the structure of H orbitals hold true for the motion of electrons in any central field and, therefore, can be used for describing the structure of the outer shells of any atom if we assume that the inner electrons, together with the nucleus, form some fixed, spherically symmetric system.

### 1.1.3 Multielectron Atoms and the Periodic System

The task of calculating multielectron wave functions, i.e., of finding the energy levels and the distribution of the electron density of atoms or ions is complicated and cannot be solved analytically, in distinction to the hydrogen atom. The most rigorous method of finding its solution was proposed by D. R. Hartree in 1928 and improved by V. A. Fock in 1930; it is known as the self-consistent field method taking account of the exchange. Each electron of an atom is described by its one-electron wave function, the orbital, and is assumed to be in the potential field of the nucleus and of all the other electrons. It can be assumed with sufficient accuracy that this potential is spherically symmetric, and therefore the types of solutions with respect to the  $s, p, d$ , and  $f$  states are preserved. The orbitals have the same form as for the H atom (Fig. 1.5). One should also take into consideration the electron spin and the Pauli principle; each  $n, l$ , and  $m$  orbit may have not one, but two electrons with opposite spins. Therefore, in

Fig. 1.5. Schematic structure of atomic  $s$ ,  $p$ , and  $d$  orbitals

addition, factor  $m_s = \pm 1/2$ , describing the spin coordinate, is introduced into the formula of the orbital  $\psi(2)$ ; then  $\psi_{nlmm_s}$  is called a spin orbital.

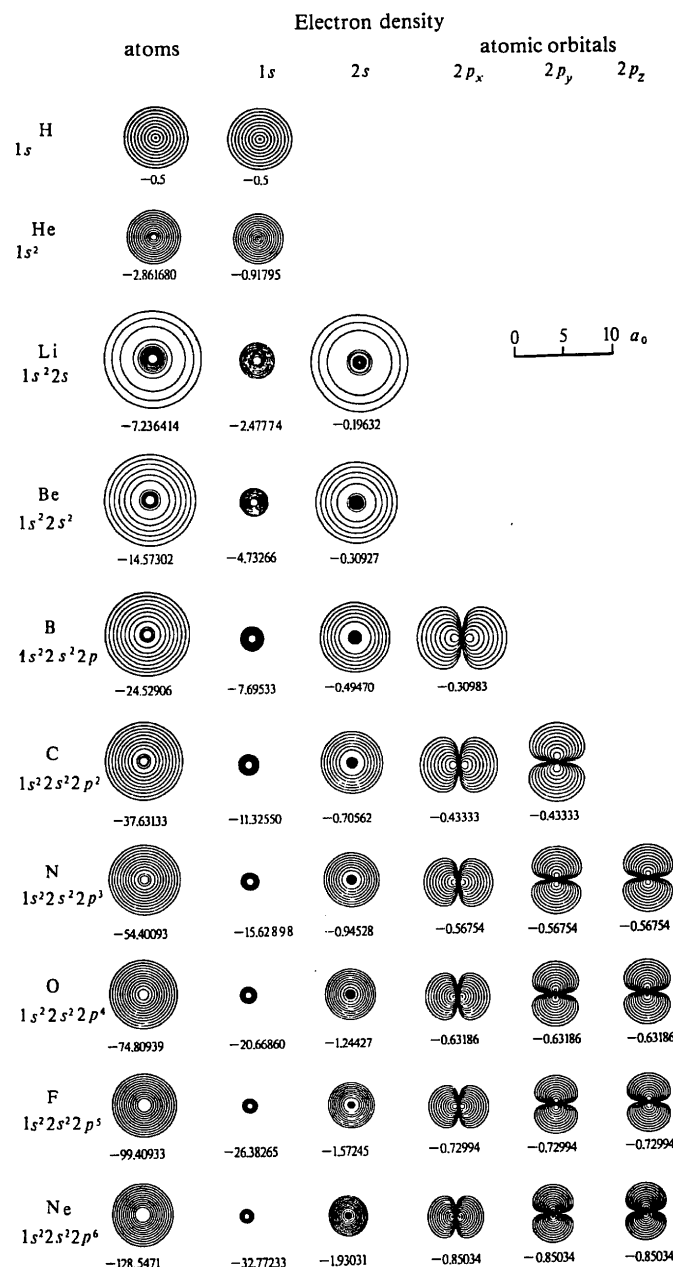
For a system of  $N$  electrons, the full wave function  $\Psi$  can be constructed from  $N$  spin orbitals  $\psi_i(\xi)$ , where  $i$  is the number of the state, and  $j$  is a set of quantum numbers [see below (1.33)]. Functions  $\psi_i(\xi_j)$  are orthonormalized according to (1.6). As a result, we obtain sets of equations whose solution by successive approximations determines both the wave functions and the field correlated with these functions, i.e., the self-consistent field. Beginning with the helium atom, which has two electrons, exchange terms of Coulomb interaction appear in such equations.

By now, computer calculations of wave functions have been carried out for all the atoms and a number of ions (Figs. 1.6, 7). As the number of electrons increases, orbitals with larger quantum numbers are filled. It is seen from Fig. 1.6 that despite the increase in the number of electrons in the shell with increasing  $Z$ , the shells contract within a given period because of the increased Coulomb attraction to the nucleus. For each of the atoms, transitions of electrons from the ground to the excited states, with other quantum numbers and energies<sup>2</sup>, are possible. Therefore calculations for excited states have also been carried out for some atoms.

<sup>2</sup> The chemical-bond theory uses different energy units, electron volt (eV), kilocalories per mole (kcal/mol), kilojoules per mole (kJ/mol); the atomic energy unit, 1 a.e.u. = 27.7 eV; 1 eV = 23.06 kcal/mol = 96.48 kJ/mol, 1 kcal = 4.184 kJ.

Fig. 1.6. Structures of electron shells (squares of wave functions) for the first ten atoms of the periodic system in the ground state, and the electron density of all the constituent orbitals [1.3].

The highest density contour line corresponds to the value  $1e/a_0^3$ , the value of the succeeding contours is decreased by a factor of two. The last line corresponds to  $4.9 \times 10^{-4} e/a_0^3$ . The total and orbital energies are indicated in atomic energy units (1 a.e.u. = 27.7 eV)



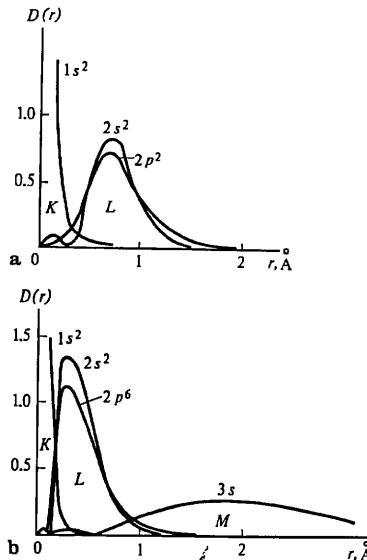


Fig. 1.7a–c. Radial distribution functions  $D(r)$  for the electron shells of the C (a), Na (b), and Cl (c) atoms

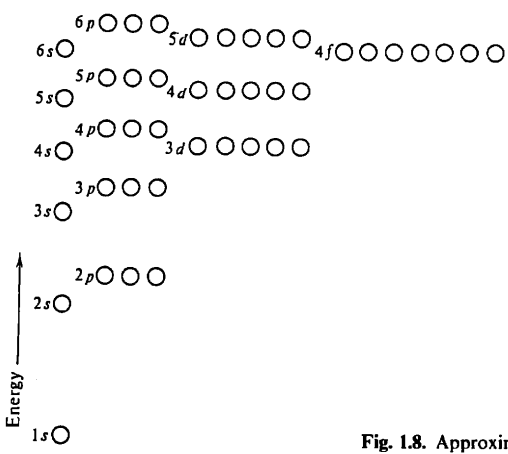


Fig. 1.8. Approximate energy levels of atomic orbitals

Using the formal combinatorics of quantum numbers and knowing the arrangement of the corresponding energy levels of atoms (which predetermines their filling with electrons), it is possible to explain all the basic regularities of Mendeleyev's periodic system. Figure 1.8 gives the sequence of the filling of the levels, and Table 1.1 their systematics. It should be emphasized that while for

Table 1.1. Electron configurations and orbital radii  $r_0$  of elements [1.4]

Z	Element	Electron configuration	Outer shell	$r_0$	Z	Element	Electron configuration	Outer shell	$r_0$
1	H	$1s^1$	$1s$	0.529	51	Sb	$5s^2 5p^3$	$5p$	1.140
2	He	$1s^2$ *	$1s$	0.291	52	Te	$5s^2 5p^4$	$5p$	1.111
3	Li	$2s^1$	$2s$	1.586	53	I	$5s^2 5p^5$	$5p$	1.044
4	Be	$2s^2$	$2s$	1.040	54	Xe	$5s^2 5p^6$ *	$5p$	0.986
5	B	$2s^2 2p^1$	$2p$	0.776	55	Cs	$6s^1$	$6s$	2.518
6	C	$2s^2 2p^2$	$2p$	0.620	56	Ba	$6s^2$	$6s$	2.060
7	N	$2s^2 2p^3$	$2p$	0.521	57	La	$5d^1 6s^2$	$6s$	1.915
8	O	$2s^2 2p^4$	$2p$	0.450	58	Ce	$4f^2 6s^2$	$6s$	1.978
9	F	$2s^2 2p^5$	$2p$	0.396	59	Pr	$4f^3 6s^2$	$6s$	1.942
10	Ne	$2s^2 2p^6$ *	$2p$	0.354	60	Nd	$4f^4 6s^2$	$6s$	1.912
11	Na	$3s^1$	$3s$	1.713	61	Pm	$4f^6 6s^2$	$6s$	1.882
12	Mg	$3s^2$	$3s$	1.279	62	Sm	$4f^6 6s^2$	$6s$	1.854
13	Al	$3s^2 3p^1$	$3p$	1.312	63	Eu	$4f^7 6s^2$	$6s$	1.826
14	Si	$3s^2 3p^2$	$3p$	1.068	64	Gd	$4f^7 5d^1 6s^2$	$6s$	1.713
15	P	$3s^2 3p^3$	$3p$	0.919	65	Tb	$4f^9 6s^2$	$6s$	1.775
16	S	$3s^2 3p^4$	$3p$	0.810	66	Dy	$4f^{10} 6s^2$	$6s$	1.750
17	Cl	$3s^2 3p^5$	$3p$	0.725	67	Ho	$4f^{11} 6s^2$	$6s$	1.727
18	Ar	$3s^2 3p^6$ *	$3p$	0.659	68	Er	$4f^{12} 6s^2$	$6s$	1.703
19	K	$4s^1$	$4s$	2.162	69	Tu	$4f^{13} 6s^2$	$6s$	1.681
20	Ca	$4s^2$	$4s$	1.690	70	Yb	$4f^{14} 6s^2$	$6s$	1.658
21	Sc	$3d^1 4s^2$	$4s$	1.570	71	Lu	$5d^1 6s^2$	$6s$	1.553
22	Ti	$3d^2 4s^2$	$4s$	1.477	72	Hf	$5d^2 6s^2$	$6s$	1.476
23	V	$3d^3 4s^2$	$4s$	1.401	73	Ta	$5d^3 6s^2$	$6s$	1.413
24	Cr	$3d^5 4s^1$	$4s$	1.453	74	W	$5d^6 6s^2$	$6s$	1.360
25	Mn	$3d^5 4s^2$	$4s$	1.278	75	Re	$5d^5 6s^2$	$6s$	1.310
26	Fe	$3d^6 4s^2$	$4s$	1.227	76	Os	$5d^6 6s^2$	$6s$	1.266
27	Co	$3d^7 4s^2$	$4s$	1.181	77	Ir	$5d^7 6s^2$	$6s$	1.227
28	Ni	$3d^8 4s^2$	$4s$	1.139	78	Pt	$5d^9 6s^1$	$6s$	1.221
29	Cu	$3d^{10} 4s^1$	$4s$	1.191	79	Au	$6s^1$	$6s$	1.187
30	Zn	$3d^{10} 4s^2$	$4s$	1.065	80	Hg	$6s^2$	$6s$	1.126
31	Ga	$4s^2 4p^1$	$4p$	1.254	81	Tl	$6s^2 6p^1$	$6p$	1.319
32	Ge	$4s^2 4p^2$	$4p$	1.090	82	Pb	$6s^2 6p^2$	$6p$	1.215
33	As	$4s^2 4p^3$	$4p$	0.982	83	Bi	$6s^2 6p^3$	$6p$	1.130
34	Se	$4s^2 4p^4$	$4p$	0.918	84	Po	$6s^2 6p^4$	$6p$	1.212
35	Br	$4s^2 4p^5$	$4p$	0.851	85	At	$6s^2 6p^5$	$6p$	1.146
36	Kr	$4s^2 4p^6$ *	$4p$	0.795	86	Rn	$6s^2 6p^6$	$6p$	1.090
37	Rb	$5s^1$	$5s$	2.287	87	Fr	$7s^1$	$7s$	2.447
38	Sr	$5s^2$	$5s$	1.836	88	Ra	$7s^2$	$7s$	2.042
39	Y	$4d^1 5s^2$	$5s$	1.693	89	Ac	$6d^1 7s^2$	$7s$	1.895
40	Zr	$4d^2 5s^2$	$5s$	1.593	90	Th	$6d^2 7s^2$	$7s$	1.788
41	Nb	$4d^4 5s^1$	$5s$	1.589	91	Pa	$5f^2 6d^1 7s^2$	$7s$	1.804
42	Mo	$4d^5 5s^1$	$5s$	1.520	92	U	$5f^3 6d^1 7s^2$	$7s$	1.775
43	Tc	$4d^5 5s^2$	$5s$	1.391	93	Np	$5f^4 6d^1 7s^2$	$7s$	1.741
44	Ru	$4d^7 5s^1$	$5s$	1.410	94	Pu	$5f^4 7s^2$	$7s$	1.784
45	Rh	$4d^8 5s^1$	$5s$	1.364	95	Am	$5f^7 7s^2$	$7s$	1.757
46	Pd	$4d^{10}$	$4d$	0.567	96	Cm	$5f^7 6d^1 7s^2$	$7s$	1.657
47	Ag	$5s^1$	$5s$	1.286	97	Bk	$5f^8 6d^1 7s^2$	$7s$	1.626
48	Cd	$5s^2$	$5s$	1.184	98	Cf	$5f^9 6d^1 7s^2$	$7s$	1.598
49	In	$5s^2 5p^1$	$5p$	1.382	99	Es	$5f^{10} 6d^1 7s^2$	$7s$	1.576
50	Sn	$5s^2 5p^2$	$5p$	1.240	100	Fm	$5f^{11} 6d^1 7s^2$	$7s$	1.557
102	No	$5f^{13} 6d^1 7s^2$	$7s$	1.581	101	Md	$5f^{12} 6d^1 7s^2$	$7s$	1.527

\* The atoms below contain this shell

small  $n$  the calculation of the levels, at least with respect to their energy values, is comparatively simple, at large quantum numbers it becomes highly complicated and is carried out with due regard for experimental spectroscopic and other data.

In the helium atom  $\text{He}$  ( $Z = 2$ ) which follows hydrogen, the ground state can accommodate a second electron, but with an opposite spin, on the same  $1s$  orbit, which yields a stable two-electron, the so-called  $K$  shell.

Subsequent filling of energy levels by electrons according to the scheme of Fig. 1.8 is possible at  $n = 2$ , which gives, at  $l = 0$ , the completion of the  $2s$  level of  $\text{Li}$  and  $\text{Be}$  ( $Z = 3, 4$ ), and six more possibilities at  $l = 1$  and  $m = 0, +1, -1$ , which correspond to  $2p$  states of the atoms of  $\text{B}, \text{C}, \text{N}, \text{O}, \text{F}$ , and  $\text{Ne}$  ( $Z = 5-10$ ). At first, the three  $p$  states with parallel spins are filled, those of  $\text{B}, \text{C}$ , and  $\text{N}$ ; then the same states are filled by electrons with antiparallel spins. Thus we obtain the second period of Mendeleev's system, which is completed by a stable eight-electron shell ( $L$  shell) (see Fig. 1.6). The next level,  $3s$ , is spaced far from  $2p$ . Further filling according to the scheme of Fig. 1.8 will lead to the third period ( $n = 3$ ,  $\text{Na-Ar}$ ) of the eight elements with  $Z = 11-18$ ; the corresponding outer shell is called the  $M$  shell (Fig. 1.7b, c). This is followed by two large periods, each of which consists of 18 elements,  $n = 4$ ,  $\text{K-Kr}$ ,  $Z = 19-36$ ;  $n = 5$ ,  $\text{Rb-Xe}$ ,  $Z = 37-54$  (outer  $N$  and  $O$  shells, respectively). The next period contains 32 elements,  $n = 6$ ,  $\text{Cs-Rn}$ ,  $Z = 55-86$ . The last period,  $n = 7$ , begins with  $Z = 87$ . Table 1.1 shows the distribution of the electrons in atoms according to their  $s, p, d$ , and  $f$  levels. The valencies of the transition elements,  $\text{Sc-Ni}$  and  $\text{Y-Pd}$ , rare-earth elements (lanthanides), elements of the platinum group, and transuranic elements, including actinides, are due to the fact that it is energetically advantageous to fill the incomplete inner shells, while the number of electrons on the outermost orbitals may remain constant.

The electron density of the atom as a whole,  $\rho_{\text{at}}$ , is a rapidly decreasing function (Fig. 1.9a). It may be characterized by radial functions (1.8) of the electron density of each shell (Fig. 1.7), while the total radial electron density of the atom is their sum (Fig. 1.9b)

$$D(r) = 4\pi r^2 \sum R_n^2(r). \quad (1.10)$$

The "shell" structure of the atom is clearly seen only in the radial function  $D(r)$  (Fig. 1.9b), which differs from the real electron density  $\rho(r)$  (Fig. 1.9a), by integration over the angles, which yields the resulting factor  $4\pi r^2$ . The maxima of the radial function represent the superposition of the squares of atomic orbitals with similar radii.

The function of the electron density of the atom as a whole, as well as the functions describing the structure of separate shells, extends to infinity. But in practice these functions damp out rather rapidly. The electron distribution in an atom can be characterized by the rms radius of the atom

$$\bar{r}^2 = \int D(r)r^2 dr/Z, \quad \langle r \rangle_{\text{at}} = \sqrt{\bar{r}^2}, \quad (1.11)$$

where  $Z$  is determined by (1.9). When the number  $Z$  of electrons in atom

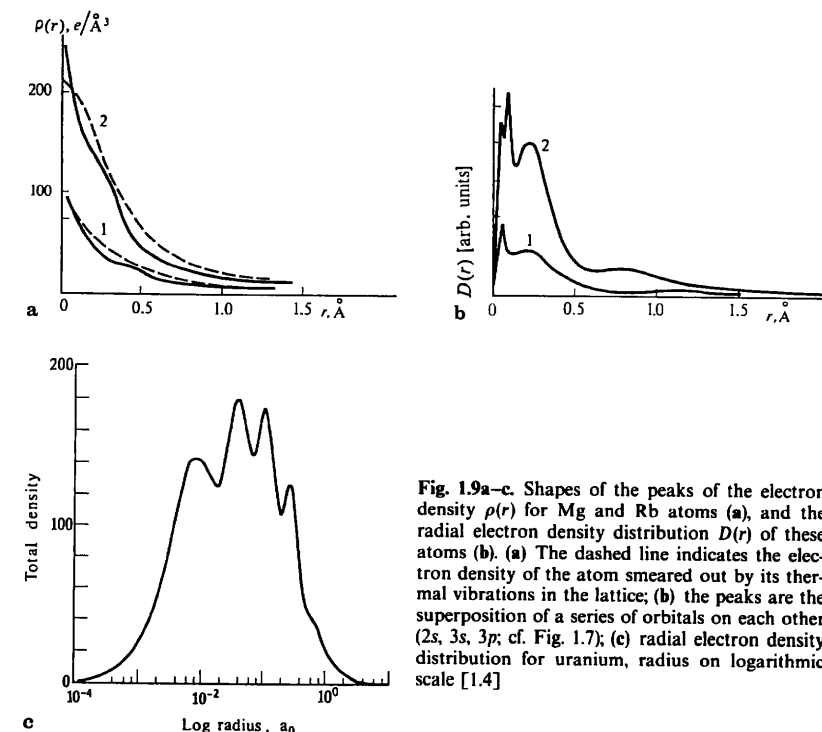


Fig. 1.9a-c. Shapes of the peaks of the electron density  $\rho(r)$  for  $\text{Mg}$  and  $\text{Rb}$  atoms (a), and the radial electron density distribution  $D(r)$  of these atoms (b). (a) The dashed line indicates the electron density of the atom smeared out by its thermal vibrations in the lattice; (b) the peaks are the superposition of a series of orbitals on each other (2s, 3s, 3p; cf. Fig. 1.7); (c) radial electron density distribution for uranium, radius on logarithmic scale [1.4].

increases, so does the charge  $+Ze$  of the nucleus to which they converge. As a result,  $\langle r \rangle_{\text{at}}$  falls off. According to the statistical theory of the atom

$$\langle r \rangle_{\text{at}} \sim Z^{-1/3}. \quad (1.12)$$

This statistical dependence undergoes a number of fluctuations depending on the filling of the shells and the forming of new ones (Fig. 1.10).

Each shell can be characterized by the radius corresponding to the position of the maximum of its radial function, the so-called orbital radius

$$r_{oi} = r \{ \max [R_i^2(r)r^2] \}. \quad (1.13)$$

It would be natural to take the orbital radius  $r_o$  of the outer shell as the characteristic of the size of the atom. Table 1.1 gives the electron configurations of atoms and the orbital radii  $r_o$  of the outer shells after Waber, Cromer [1.4]. Similar results were obtained by Bratsev [1.5].

As mentioned, in spite of the increase in the number of electrons in a given shell its orbital radius diminishes because of the growing Coulomb attraction to the nucleus (Fig. 1.10). When a new shell appears, its  $r_o$  is much larger than that

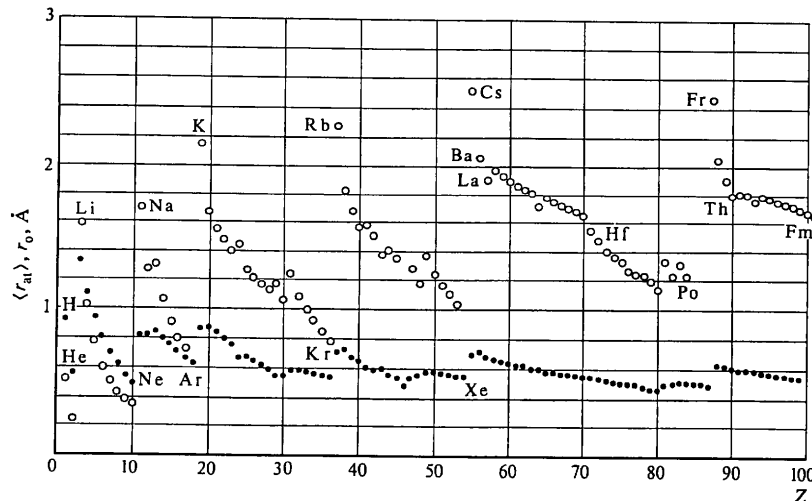


Fig. 1.10. Mean-square atomic radii  $\langle r_{\text{at}} \rangle$  (dark circles) and outer shell orbital radii  $r_o$  (light circles) of neutral atoms vs atomic number  $Z$

of the preceding shell; then, with growing  $Z$  the new shell contracts to the nucleus again. Thus, with an increase in  $Z$  the value of  $r_o$  changes “toothwise”, decreasing inside the periods and rising abruptly as new shells appear, which also affects the variation in  $\langle r \rangle_{\text{at}}$  (1.11). On the average,  $r_o$  increases with atomic number  $Z$ .

A knowledge of the electron structure of atoms is important for many branches of crystallography. Apart from the fact that it supplies information on the geometric characteristics of atoms, it is a starting point for the chemical-bond theory and permits calculating the functions of atomic scattering of X-rays and electrons, etc. In particular, a decrease in  $\langle r \rangle_{\text{at}}$  with increasing  $Z$  means that on the Fourier maps of the electron density of crystals the peaks of  $\rho_{\text{at}}$  of the heavier atoms will always be sharp. The peaks are additionally smeared out by the thermal motion of the atoms (Fig. 1.9a, dashed line; see also [Ref. 1.6, Sect. 4.1.5]), but the thermal motion, too, is less for the heavy atoms than for light ones.

The experimental data obtained by X-ray structure analysis confirm these theoretical predictions. In these investigations the electron density of the crystal obtained by Fourier series summation manifests itself as a set of electron density peaks of separate atoms  $\rho(\mathbf{r}) = \sum \rho_{\text{at},j}(\mathbf{r} - \mathbf{r}_j)$ , and not as a set of their radial functions. The experimental results of investigations into the distribution of  $\rho(\mathbf{r})$  in crystals are in good agreement with the theory. Since, however, the electron density of each atom falls off rapidly and is, additionally, smeared out in the crystal by the thermal motion (Fig. 1.9a), individual atomic shells are not

resolved on ordinary Fourier syntheses of the distribution of  $\rho(\mathbf{r})$ . Nevertheless, it is possible to reveal the outer shells and to investigate the electron redistribution, due to the chemical bond, with the aid of Fourier difference syntheses [Ref. 1.6, Sect. 4.7.10]; this will be discussed in more detail further on.

## 1.2 Chemical Bonding Between Atoms

### 1.2.1 Types of Chemical Bonding

A chemical bond arises when atoms draw closer together and is due to interaction of their outer electron shells. The formation of such a bond (in a molecule or a crystal) means a reduction in the total and, hence, the potential energy of the system. Theory must explain not only the binding of atoms, but all the experimental data on valence; it must explain the directional character of bonds, which occurs in some cases, and their saturation; it must give values of binding energy which agree with experiment; and, finally, it must serve as a basis for calculating the properties of molecules and crystals. The binding of atoms is the result of the electrostatic interaction of the nuclei and all their electrons and can only be explained on the basis of quantum mechanics. The main principles of the theory are verified by consideration and investigation of simple molecules. At the same time, the analysis and calculation of complex multiatomic systems involve considerable mathematical difficulties and require some simplifying assumptions. This entire complex of questions is the subject of quantum chemistry and the quantum theory of the solid state.

According to the traditional terminology, distinction is made between ionic (heteropolar), covalent (homopolar), metallic, and van der Waals types of bonds between atoms, as well as one more special type, the so-called hydrogen bond. The first three types are stronger than the last two. As we shall see further on, this classification into bond types, especially between the first three, is somewhat conventional. All the types of strong chemical bonding are due to the interaction between the outer orbitals of mutually approaching atoms and the formation of common electron states of the new system, i.e., a molecule or a crystal. Although the functions describing the electron distribution in the object are continuous throughout its volume, the distribution has certain features for each type of bond. An increase in the electron concentration in some atoms and a decrease in others result in Coulomb attraction, which is an *ionic* bond. If the shared outer electrons are concentrated predominantly on orbitals spatially fixed relative to the bonded atoms, we speak of a *covalent* bond. If the outer electrons are collective, i.e., distributed throughout the crystal lattice, we have a *metallic* bond.

An isolated atom has a discrete system of energy levels. In a system of  $N$  widely spaced atoms each level is essentially  $N$ -multiply degenerate. The change in the system of these levels as the atoms draw closer together amounts to eliminating the degeneracy due to interaction which leads to the splitting of

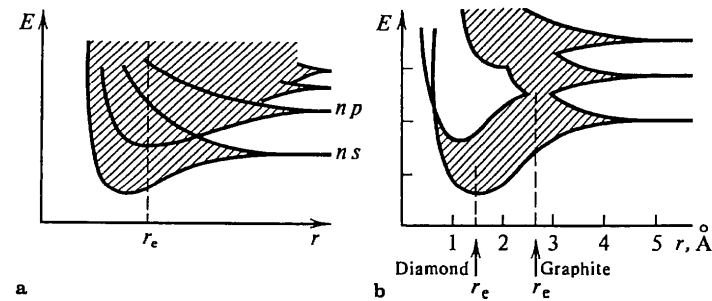


**Fig. 1.11a, b.** Change in the energy spectrum of electrons as the atoms come closer together. (a) In a metallic crystal levels merge into a continuous band as the atoms come together up to the equilibrium distance  $r_e$ ; (b) in a carbon crystal the spectrum depends on the arising polymorphous modification, diamond has a slit between the bands, while graphite does not

the levels. Since there are very many levels, they merge into continuous bands when the atoms form a crystal. The nature of the electron energy spectrum of a crystal depends both on its constituent atoms and on the distances between them (see Chap. 3). Thus, for metals (Fig. 1.11a) the levels merge into a continuous band with vacant levels over the electrons filling the lower part in the bands. With a covalent or ionic bond (Fig. 1.11b) there is a gap in the crystal energy spectrum between the filled lower band and the following ones.

Since the spectrum depends on the interatomic distances, the nature of the bond in certain crystals may change at phase transitions, especially for those due to the pressure. At very high pressures all crystals are metallized.

The simplest qualitative explanation can be given for the ionic bond, which is ascribed to the electrostatic attraction of oppositely charged ions. But all the other bond types, including the ionic, can only be fully understood from the standpoints of quantum-mechanical theory.

It should also be borne in mind that along with those crystals in which the bond can largely be described according to one of the three indicated types, the bond in many other crystals is of an intermediate nature; in this case one can conventionally single out, for example, the ionic and covalent components. There are also a number of special cases, such as complex compounds.

The molecular crystals are somewhat different. The bond between atoms inside the molecules is covalent, and the association of the molecules into a crystal is due to weak van der Waals forces or hydrogen bonds.

Any type of interaction between atoms in a crystal or a molecule can be approximately described (and in many cases accurately enough) by the model of central forces with the aid of a potential interaction energy function  $u(r)$  (Fig. 1.12) found theoretically or empirically. This curve is characterized by the following principal parameters. The condition  $du/dr = 0$  defines the distance  $r_e$  of the minimum from the origin, i.e., the equilibrium interatomic distance, and

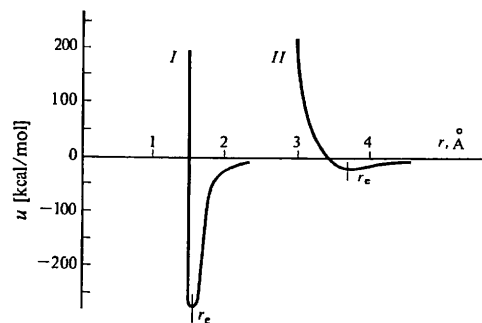


**Fig. 1.12.** Schematic curves of potential energy of atomic interaction for a covalent, ionic, and metallic bond (I) and a van der Waals bond (II)

the energy  $u_e(r_e)$  of a given interatomic bond at absolute zero. This refers to the interaction of a pair of atoms. The equilibrium values of the interatomic distances in a crystal lattice are defined by the condition  $dU/dr = 0$ , where  $U$  is the energy of the lattice as a whole, which can be calculated from the energy of pair interactions  $u(r)$  (see Sect. 1.3.2). The second derivative  $d^2u(r)/dr^2$  of the curve  $u(r)$  at the minimum characterizes the bond “rigidity”. This manifests itself macroscopically in the phonon spectrum of the crystal, its elasticity, so that high frequencies and large elastic constants correspond to more rigid bonds. The steep rise of the curve towards the lesser  $r$  characterizes the mutual “impenetrability” of the atoms. The corresponding macroscopic characteristic of crystals – their compressibility – makes it possible to select empirically an analytical expression for describing the repulsion forces. This steep rise enables one to operate in crystal chemistry with atom models in the form of rigid spheres touching each other in a crystal structure. The asymmetry of the potential well – a flatter shape of the curve  $u(r)$  towards larger  $r$  – increases the amplitude and anharmonism of thermal vibrations with temperature, which augments the interatomic distances, i.e., leads to thermal expansion of the crystal. The vibrational anharmonism also explains various nonlinear effects in the acoustics and optics of crystals. Note that for a covalent bond the central-force approximation, although describing the interaction in the main, is insufficient because the covalent bond forces are directional (Sect. 2.4).

The nature of the chemical bond is expressed in the macroscopic physical properties of crystals. The stronger the bond (the interatomic distances are usually short), the better are the mechanical properties, such as hardness and elasticity, the lower is the coefficient of thermal expansion, and the higher the melting point. The covalent crystals (for instance, diamond) or ion-covalent crystals (for instance, oxides of the type  $MgO$ ,  $Al_2O_3$ ) are the strongest and hardest. Yet even among them a transition to relatively lower strength crystals with a lower melting point (the melting temperature range is  $\sim 2500\text{--}500^\circ C$ ) takes place as the bonding weakens and the interatomic distances increase. A still wider discrepancy of the characteristics of mechanical properties occurs in

P.10  
metals, which include very hard and high-melting as well as low-melting metals, and even those liquid at normal temperatures (mercury). But a specific feature of metals is their high plasticity. The molecular crystals of organic compounds are the weakest and softest, and have the lowest melting point; they also have high coefficients of thermal expansion due to the weakness of the van der Waals bond.

The electrical properties of crystals are determined by the energy spectrum of their electrons (see [Ref. 1.6, Chap. 3]). Ionic crystals are, as a rule, dielectrics; covalent crystals, dielectrics or semiconductors; metals, conductors; and molecular crystals, dielectrics.

The type of the chemical bond is also manifested in the optical properties. A large refractive index is characteristic of ionic and covalent crystals, which are usually transparent in the visible or infrared region, but can also be colored, i.e., absorb light in certain regions of the visible spectrum. For ionic crystals this is due to the cations of the transition or rare-earth elements. Molecular crystals are usually transparent. On the other hand, metals possess a metallic luster, i.e., they are opaque and reflect light well.

We give here the most general characteristics of the manifestation of the chemical bond types in the physical properties of crystals. Further on, in this and subsequent volumes, the question will be treated in more detail. As we have already said, many properties of crystals certainly depend not only on the ideal atomic structure and the type of chemical bond in it, but also on the defects in its real structure. Let us now consider the basic types of chemical bonding. As mentioned above, the quantum-mechanical approach makes it possible to explain and accurately calculate all the types of bonds. At the same time an ionic bond is basically characterized by simple Coulomb interaction; we, therefore, begin our consideration of it from the classical standpoint, followed by the fundamentals of quantum-mechanical treatment.

## 1.2.2 Ionic Bond

When, during interaction of the outer electrons of neighboring atoms, the electron distribution shifts from one to the other, charged ions appear which are attracted electrostatically. This bond is called ionic and is usually found in relatively simple structures consisting of atoms of typical metals and nonmetals.

If a diatomic molecule with a bond of an ionic nature is formed, it naturally has a dipole moment

$$M = rZ', \quad (1.14)$$

where  $Z'$  is the ion charge, and  $r$  is the distance between the ion centers. In a crystal, an ion residing in a field of oppositely charged ions causes polarization of the electron shell, i.e., its slight deformation corresponding to the symmetry of the surrounding field. Then a net dipole moment of the structure may arise (for instance, in ferroelectrics) or may not (for instance, in structures of the NaCl type).

The possibility of the formation of a chemical bond by an atom and its nature depend to a large extent on the stability of the outer electron shell of the atom. This factor can be characterized by the ionization potential of the atom  $I^+$ , i.e., by the energy required to detach the first valence electron. The lowest ionization potentials  $I^+$  are characteristic of alkali and alkaline-earth metals (4–5 eV), and the highest, of noble gases and halides (12–24 eV). Thus, metal atoms readily give up their outer electrons, and their ionization energy is low; after this a stable inner shell remains. On the other hand, atoms of nonmetals tend to add electrons, especially if this addition leads to the formation of stable electron shells of the noble-gases type. In that case, addition of one lacking (for the filling of the outer shell) electron causes a release of energy, the affinity energy  $I^-$ . This is most prominently manifested for halogens:  $I^-$  is 3.5 eV for F, 3.7 eV for Cl, and 3.7 eV for Br. Oxygen readily captures one electron,  $I^- = 3.4$  eV, but the addition of a second electron causes a predominance of electrostatic energy of repulsion and is energetically unprofitable.

Consider the formation of an ionic bond on the example of  $\text{Na}^+$  and  $\text{Cl}^-$ . The ionization energy of Na is 5.1 eV, and the electron affinity of Cl is 3.7 eV. Hence, the formation of a pair of such ions requires an energy of 1.4 eV. The distance between these ions in the molecule is about 2.5 Å, and the electrostatic energy of attraction  $\sim 10$  eV. This value greatly exceeds 1.4 eV, which explains the bond between  $\text{Na}^+$  and  $\text{Cl}^-$ . The same is true for a crystal, although the calculation of the electrostatic energy is then more complicated. Thus, in general, the energy of a system built up of ions attracted to each other is on the whole lower than the sum of the initial energies of the neutral atoms, although the ionization energy of metallic atoms has the opposite sign in the overall balance.

The interaction of the two ions is Coulombic, but when they touch one another the forces of repulsion between the electron shells come into play. The repulsive potential is described by a dependence of the type  $br^{-n}$ , where  $n = 6–9$  and parameters  $b$  and  $n$  can be found from the compressibility of the crystals. Thus,

$$u_{\text{ion}}(r) = -Z'_1 Z'_2 e^2 r^{-1} + br^{-n}, \quad (1.15)$$

where  $Z'_1$  and  $Z'_2$  are the effective charges of the ions. In a more general form, this relation can be rewritten

$$u(r) = -ar^{-m} + br^{-n} \quad (n > m); \quad (1.16)$$

then it can also be used for describing other types of bonds, naturally with different values of the constants. The condition of the minimum of  $du/dr = 0$  gives equilibrium values of  $r_e$  and  $u_e = u(r_e)$

$$r_e = \sqrt[n-m]{\frac{nb}{ma}}, \quad u_e = \frac{u - a}{r_e^m} \left(1 - \frac{m}{n}\right). \quad (1.17)$$

Now we can express  $a$  and  $b$  and, hence,  $u(r)$  in terms of  $r_e$  and  $u_e$ ,

$$u(r) = u_e \frac{nm}{n-m} \left[ -\frac{1}{m} \left( \frac{r_e}{r} \right)^m + \frac{1}{n} \left( \frac{r_e}{r} \right)^n \right]. \quad (1.18)$$

Here, for the ionic bond  $m = 1$ . The exponential dependence  $\exp(-\alpha r)$  proves to be more accurate than the power dependence for describing the repulsive potential in ionic crystals [see (1.35)], the value of  $\alpha^{-1}$  being about  $0.35 \text{ \AA}$ . The interaction in ionic crystals according to (1.15) must be supplemented by the van der Waals forces operating between the ions and the polarization of the ions in each other's field.

The curve of the potential energy of interaction for the ionic bond is shown in Fig. 1.12. The ionic bond energy usually equals about  $100 \text{ kcal/mol}$ , being, for instance,  $137 \text{ kcal/mol}$  for gaseous  $\text{LiF}$ , and  $88 \text{ kcal/mol}$  for  $\text{NaBr}$ .

As discussed above, when atoms join together into a molecule or a crystal mainly owing to the ionic bond, covalent interaction, caused by the joining of the outer electrons, also invariably takes place. Even in crystals of the most prominent representatives of ionic bonding, such as halides of alkali metals, a certain (although very small) fraction of the binding energy is due to covalent interaction.

Chemists and crystal chemists have always been interested in how to describe the tendency of atoms to form an ionic bond and, if the bond is not purely ionic, but ionic covalent, how to estimate the ionic fraction of the bond. The concept of electronegativity (EN) of elements is used for this purpose. L. Pauling

**Table 1.2. Electronegativities EN, ionization potentials  $I^+$ , and the affinity  $I^-$  of certain atoms to an electron\***

Element	EN	Orbital	$I^+$ [eV]	$I^-$ [eV]	Element	EN	Orbital	$I^+$ [eV]	$I^-$ [eV]
H	2.2	<i>s</i>	13.60	0.75	Cl	3.2	<i>p</i>	15.03	3.82
Li	1.0	<i>s</i>	5.39	0.82	K	0.8	<i>s</i>	4.34	1.46
Be	1.6	$\sigma$	9.92	3.18	Ca	1.1	<i>s</i>	7.09	2.26
B	2.0	<i>s</i>	14.91	5.70	Sc	1.3	$\sigma$	7.21	4.03
C	2.6	tetr	14.61	1.34	Cr	1.6	—	—	—
N	3.0	<i>p</i>	13.94	0.84	Fe	1.8	—	—	—
O	3.1	<i>p</i>	17.28	1.46	Zn	1.6	—	—	—
F	4.0	<i>p</i>	20.86	3.50	Br	3.0	<i>p</i>	13.10	3.54
Na	0.9	<i>s</i>	5.14	0.47	Rb	0.8	<i>s</i>	4.18	0
Mg	1.2	$\sigma$	7.10	1.08	Sn	1.8	<i>p</i>	6.94	0.87
Al	1.6	<i>p</i>	6.47	1.37	Te	2.3	<i>p</i>	11.04	2.58
Si	1.9	tetr	11.82	2.78	I	2.6	<i>p</i>	12.67	3.23
P	2.2	$\sigma$	10.73	1.42	Cs	0.7	—	—	—
S	2.6	<i>p</i>	12.39	2.38	Ba	0.9	—	—	—

\* Only some values of  $I^+$  and  $I^-$ , corresponding to the most frequently encountered states of a given atom, are listed. For other types of atomic orbitals (and also depending on hybridization) these values are different, for instance,  $I^+ = 21.01$  and  $I^- = 8.01$  for the *s* state of carbon

has given a semiempirical scale of EN on the basis of thermochemical data (see Table 1.2).

When two atoms combine, the outer electrons shift towards the one whose EN is higher. Naturally, EN is higher for anions than for cations; its values decrease when descending along the groups of the periodic system. The difference between the electronegativities of the combining atoms,  $\Delta_{\text{EN}}$ , roughly characterizes the fraction and energy of the ionic component. According to Pauling, at  $\Delta_{\text{EN}} \approx 3.0$  the bond is almost completely (by ~90%) ionic, and at  $\Delta_{\text{EN}} < 1$  the ionic component is less than 20%. The energy of the ionic component is approximately  $30 \cdot \Delta_{\text{EN}}^2 \text{ kcal/mol}$ .

The concept of electronegativity for atoms can be determined more rigorously in terms of their ionization potentials  $I^+$  and the electron attractive energy  $I^-$  for the corresponding valence state (examples of these values for some atoms in one of their states together with the corrected Pauling's EN values are given in Table 1.2) (see, for instance [1.8, 9]). In this approach the electronegativity  $\chi$  is expressed as one-half of the sum of the ionization potential and the attractive energy

$$\chi = (I^+ + I^-)/2. \quad (1.19)$$

Pauling's EN and  $\chi$  (1.19) can be correlated by a certain normalization. The ionicity of bond  $\varepsilon$  is defined by the equation

$$\varepsilon = \frac{(I^+ + I^-)_{\text{cat}} - (I^+ + I^-)_{\text{an}}}{(I^+ - I^-)_{\text{cat}} + (I^+ - I^-)_{\text{an}}} = \frac{2(\chi_{\text{cat}} - \chi_{\text{an}})}{(I^+ - I^-)_{\text{cat}} + (I^+ - I^-)_{\text{an}}}, \quad (1.20)$$

which contains the corresponding values for cations and anions. According to

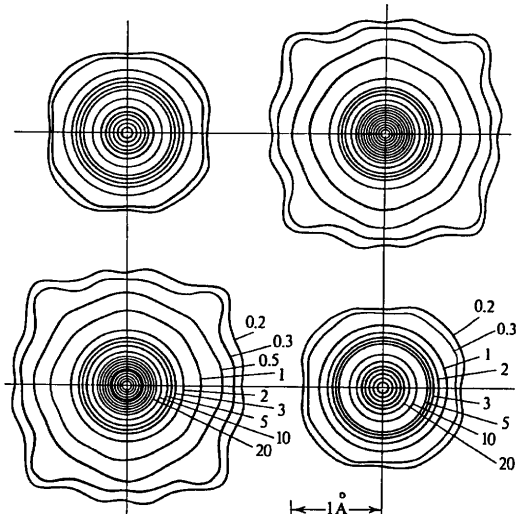


**Fig. 1.13. Electron density of a  $\text{NaCl}$  crystal. Cross section of three-dimensional function  $\rho(x, y, z)$  at  $z = 0$  through the centers of the Na and Cl atoms [1.10]**

(1.20)  $\varepsilon$  is 0.82 for NaCl, 0.83 for LiF, 0.92 for KCl, and 0.94 for RbCl, whereas for HCl it is 0.18.

The physical characteristic describing the ionic contribution to the bond is the effective charge of the ion  $Z'$ .

Let us consider experimental X-ray data on the electron density distribution in a NaCl crystal (Fig. 1.13). These data indicate that the electrons are redistributed from Na to Cl; according to different authors, the number of electrons in  $\text{Na}^+$  is 10.3–10.15 (11 in a neutral atom) and 17.7–17.85 in Cl (as against 17 in neutral atom), i.e., the effective charge is about 0.8 e [1.11]. In a rather large region between the atoms the electron density falls off practically to zero. For LiF these data are 2.1 e for Li and 0.9 for F, i.e., the effective charge is equal to 0.9 e [1.12]. The effective charges in ionic crystals can also be estimated on the basis of X-ray and IR spectra, the dielectric constant, and other methods. Thus, for  $\text{MgF}_2$ ,  $\text{CaCl}$ , and  $\text{MgCl}_2$  estimation of the effective charges of anions leads to values of about 0.7 e, and of cations, 1.2–1.4 e. In silicates, the effective charge of Mg is 1.5–1.0 e; Al, 2.0 e, and Si (according to different estimates), 1.0–2.0 e. The oxygen ion in oxides and silicates has an effective negative charge of 0.9–1.1 e.<sup>3</sup>

The effective charge of the ion  $Z'$  may be related to the formal valence of the atom  $n$  by factor  $\varepsilon$ , which thus determines the degree of ionization of the atom

$$Z' = \varepsilon n. \quad (1.21)$$

The degree of ionization  $\varepsilon$  in (1.21), which is found experimentally, practically coincides with the value of  $\varepsilon$  in (1.20), defined as the ionicity of the bond.

So, for univalent ions the degree of ionization  $\varepsilon$  and effective charges  $Z'$  are close to unity. At the same time, for divalent and, all the more so, trivalent ions, "integral" ionization  $\varepsilon = 1$ , which would lead to values of charge  $Z' = n$ , equal to the valence, takes place very rarely.

Symbols of the type  $\text{O}^{2-}$ ,  $\text{Cr}^{3+}$ ,  $\text{Nb}^{4+}$ , etc., which are often found in the literature, should only be understood as indicating the formal value of the valence, not as the actual value of the charge, which is always smaller and is not integral<sup>3a</sup>. Occasionally encountered symbols of the type  $\text{C}^{4-}$ ,  $\text{Te}^{6+}$ , etc., have no physical meaning.

We shall now treat the electron distribution in ions. The filling of the orbitals in the anions of the crystal does not differ essentially from that in free atoms. For example, quantum-mechanical calculation of electron distribution in  $\text{MgO}$  (such calculations are described in Sect. 1.2.6) showed that in this dielectric crystal, which has four valence zones, one of them is associated with the  $s$  state, and the other three, with three  $p$  states of the oxygen atom (see Fig. 1.28a).

<sup>3</sup> Note that the concept of the effective charge in a partly ionic bond is somewhat conventional, since it depends on the choice of the range of integration of the charge corresponding to each atom and also to the electrons of the bond.

<sup>3a</sup> Exceptions are some rare cases when a metallic ion is surrounded by strong electronegative anions  $\text{F}^-$ , such is the case of  $\text{Cu}^{4+}$  in  $\text{Cs}_2\text{CuF}_6$  [1.12a].

On ionization of a metallic atom to a cation, the filled inner shell becomes the outer shell with a much smaller orbital radius than the initial outer shell, experiencing almost no change upon ionization. Thus,  $r_o(\text{Na}) = 1.713 \text{ \AA}$  and  $r_o(\text{Na}^+) = 0.278 \text{ \AA}$ . On the other hand, the orbital radii of the outer shells of the anions, which have received the electrons needed for their complete filling, coincide almost exactly with the orbital radii of the outer shells of the same neutral atoms. For instance,  $r_o(\text{F}) = 0.396 \text{ \AA}$ ,  $r_o(\text{F}^-) = 0.400 \text{ \AA}$ ,  $r_o(\text{Cl}) = 0.725 \text{ \AA}$ ,  $r_o(\text{Cl}^-) = 0.742 \text{ \AA}$ ,  $r_o(\text{Br}) = 0.851 \text{ \AA}$ , and  $r_o(\text{Br}^-) = 0.869 \text{ \AA}$ . In other words, the electron structure of the anions practically coincides with that of the neutral atom, but their outer electron shell becomes "denser".

Now, using NaCl as an example again, we consider the radial density distribution  $D(r)$  (1.8, 10) for these atoms, taking into account the distance between them in the crystal. To do this, we plot the theoretically calculated radial functions of the outer shells both for neutral atoms and for the ions  $\text{Na}^+$  and  $\text{Cl}^-$ , laying them off towards one another from the ends of a segment equal to the interatomic distance in the crystal (Fig. 1.14a, cf. Fig. 1.7). It should be borne in mind that such a plot is only conventional; it pinpoints fairly well the site where the wave functions overlap, but does not reveal the actual nature of the overlapping because, in fact, it is the wave functions  $\psi$  (which rapidly fall off with increasing  $r$ ) that overlap, and not the radial functions  $D(r)$  (1.8, 10) containing a factor  $r^2$  which causes the maxima to appear. As to the position of the maxima, the situation is as follows. For neutral atoms, the maximum of the radial function for the outer  $3s$  shell of Na coincides in its position with that for the outer  $3p^5$  shell of Cl. For the cation  $\text{Na}^+$ , the outer shell is now  $2p^6$ , whose orbital radius is equal to 0.278  $\text{\AA}$ , and the maximum of the electron density of its former  $3s$  shell was transformed and "incorporated" into the  $3p$  shell of the

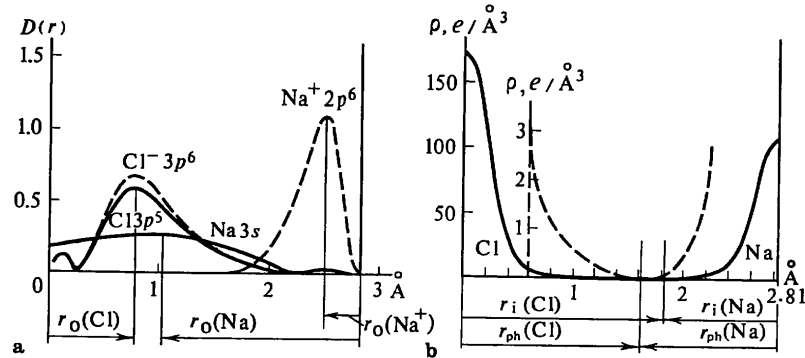


Fig. 1.14a, b. Comparison of (a) the theoretical radial density  $D(r)$  distribution of the outer valence orbitals of  $\text{Na}^+$  and  $\text{Cl}^-$  ions (dashed lines) and neutral Na and Cl atoms (solid lines) with (b) the experimentally obtained distribution of electron density  $\rho(r)$  between these atoms [one-dimensional cross section of  $\rho(x00)$  from Fig. 1.13]. The dashed curve in (b) referring to the atom periphery is scaled up.  $r_o$ : orbital radii,  $r_i$ : effective ionic radii,  $r_{ph}$ : physical ionic radii

anion  $\text{Cl}^-$  after ionization, actually remaining at the same distance from the center of the  $\text{Na}$  atom. Since the resulting maxima of the indicated functions coincide, then, approximately,

$$d(\text{Na}^+\text{Cl}^-) \approx r_o(\text{Na}) + r_o(\text{Cl}). \quad (1.22)$$

i.e., the distance between ions  $\text{Na}^+$  and  $\text{Cl}^-$  is approximately equal to the sum of the orbital radii of the neutral atoms.

If we take the sum  $r_o(\text{Na}^+) + r_o(\text{Cl}^-)$ , it turns out to be much less than the observed distance  $d(A^+/B^-)$  and differs from it by approximately  $\Delta$ , i.e., is the distance between the outer orbital  $r_o$  of the metallic atom and the nearest inner orbital  $r_o$ , which becomes outer on ionization

$$d(A^+/B^-) = r_o(A^+) + r_o(B^-) + \Delta. \quad (1.23)$$

The values of  $\Delta [\text{\AA}]$  for certain metals are:

Li	Be	Na	Mg	Al	K	Ca	Rb	Sr
1.40	0.90	1.43	1.03	1.09	1.57	1.15	1.55	1.14

The physical meaning of  $\Delta$  values is as follows. In accordance with Pauli's principle and the energy levels determined by solving Schrödinger's equation,  $\Delta$  values indicate the shortest distances from the inner cation orbital at which (and not less than at  $\Delta$ ) the next electrons can be positioned, irrespective of whether they form the outer orbital of the neutral metallic atom, or whether they are electrons of the outer orbital of a neighboring anion. Ionization of the metal atom ( $\text{Na}$  in our example) in the crystal actually takes place, since its outer electron has been incorporated in the anion shell. But the distance from this electron to the  $\text{Na}$  nucleus has not actually changed; it is regulated by the value of  $\Delta$ . We emphasize once more that the scheme of superposition of the radial functions (Fig. 1.14) indicates only the site of the overlapping of the orbitals. The picture of ionization and cation-anion contacts is schematized in Fig. 1.15.

On  $\rho(r)$  maps obtained by X-ray analysis (Figs. 1.13, 14), the "border" of the  $\text{Cl}$  atom corresponds to the site of the overlapping of the maxima of the radial functions, while the region of low  $\rho(r)$  lies between the outer shells of the ions  $\text{Na}^+$  and  $\text{Cl}^-$  and is determined by the values of  $\Delta_{\text{Na}}$  (Fig. 1.15).

The foregoing refers to the outer shell of univalent cations, when it is practically fully ionized. In di- and tri-valent cations, not necessarily all the electrons leave the outer orbit; only some of them are incorporated in the anion shells as in the above-discussed case. The schemes of the superposition of radial density functions (Fig. 1.14) and the effect of the quantity  $\Delta$  (Fig. 1.15), which regulate the interatomic distances, remain in force. But the outer orbital of the cation, at a distance corresponding to  $r_o$ , may retain some of the electrons (as shown for  $\text{Na}$  in Fig. 1.15, see also Fig. 1.53). Here, a bond of no longer purely ionic nature corresponds to the real overlapping and rearrangement of the outer orbitals of the cation and anion; a covalent interaction also arises between the ions (we shall discuss it below).

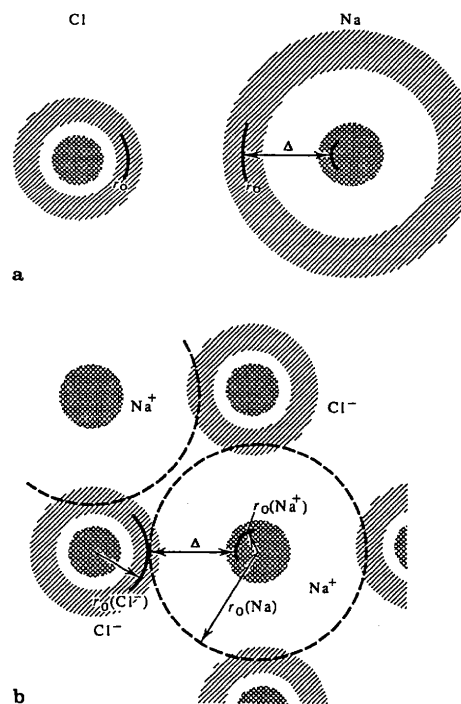
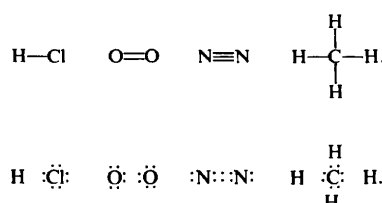


Fig. 1.15a, b. Schematic representation (a) of neutral  $\text{Na}$  and  $\text{Cl}$  atoms and (b) of their ionization in a  $\text{NaCl}$  crystal.  $\Delta$ : distance between the outer ionized 3s orbital of  $\text{Na}$  and its nearest inner 2p orbital. The inner shells are conventionally shown by cross-hatching. The outer shell of the  $\text{Cl}^-$  ion (which has incorporated an electron from  $\text{Na}^+$ ) is at a distance  $\Delta$  from the inner shell of the  $\text{Na}$  atom, which has now become a  $\text{Na}^+$  ion

### 1.2.3 Covalent Bond. Valence-Bond Method

The chemical bond between neutral atoms in molecules and crystals cannot be explained in such a simple, classical way as the ionic bond. At the same time, a covalent bond is typical of most molecules and many crystals.

With the accumulation of a huge amount of experimental data in chemistry and crystal chemistry and the development of the theory of atomic structure it became more and more apparent that the covalent bond is due to the interaction of the outer valence electrons of atoms drawing closer together. The covalent bond is usually defined as a directed chemical bond realized by pairs of electrons. For each chemical valence (denoted by a dash in the scheme) there are



two corresponding electrons (two dots on the scheme). Such a two-electron bond is stable; from the area surrounding the atoms, assuming that their own valence electrons and those of the added atoms are common, one can single out octets of electrons. From the quantum-mechanical standpoint these formal rules are qualitatively interpreted as a trend to form stable orbitals with pairs of electrons having antiparallel spins.

The first quantum-mechanical explanation of the chemical bond was given in 1927 by W. Heitler and F. London, who carried out a quantitative calculation of the molecular ion  $H_2^+$  and the molecule  $H_2$  of hydrogen. The vigorous development of these concepts and their application to the explanation of the structure of molecules and crystals is due to the work of Pauling and many other researchers.

Two (or more) atoms spaced at very large distances can be regarded as isolated stable systems with their intrinsic orbitals and energy levels. If they start to approach each other, then, beginning with a certain distance, interaction between them takes place, and a new common system with characteristics of its own arises. To calculate such a system, certain functions  $\psi$  are chosen as initial. By varying them the solution is improved, the criterion being the attainment and decreasing of the energy minimum. Any functions can, generally speaking, be chosen as the initial ones, but it is natural to use atomic orbitals for this purpose and solve the problem by the methods of perturbation theory.

Heitler and London considered the hydrogen molecule, which consists of protons  $a$  and  $b$  and electrons 1 and 2. The wave functions of the separate atoms are  $\psi_{a1}$  and  $\psi_{b2}$ . When they draw closer together, electron 1 can interact with proton  $b$ , and electron 2, with proton  $a$ . The wave function of the atoms which have drawn together has the form

$$\Psi = c_1 \psi_{a1} \psi_{b2} + c_2 \psi_{a2} \psi_{b1}. \quad (1.24)$$

The electrons interact with both nuclei. The Schrödinger equation for this system has two solutions with energies (supplementary to the initial energy of the hydrogen atoms not drawn together)

$$E = \frac{H_{11} \pm H_{12}}{1 \pm S_{12}}, \quad \text{where} \quad (1.25)$$

$$H_{11} = H_{22} = \iint e^2 \left( \frac{1}{r_{ab}} + \frac{1}{r_{12}} - \frac{1}{r_{a2}} - \frac{1}{r_{b1}} \right) \psi^2(r_{a1}) \psi^2(r_{b2}) dv_1 dv_2, \quad (1.26)$$

$$H_{12} = \iint e^2 \left( \frac{1}{r_{ab}} + \frac{1}{r_{12}} - \frac{1}{r_{a2}} - \frac{1}{r_{b1}} \right) \psi(r_{a1}) \psi(r_{a2}) \psi(r_{b1}) \psi(r_{b2}) dv_1 dv_2, \quad (1.27)$$

$$S_{12} = \iint \psi_{a1} \psi_{a2} \psi_{b1} \psi_{b2} dv_1 dv_2 = \int \psi_{a1} \psi_{b1} dv_1 \int \psi_{a2} \psi_{b2} dv_2 = S_{ab}^2. \quad (1.28)$$

Here, the integrals  $H_{11} = H_{22}$  are simply the electrostatic energy of interaction of the two atoms. Integral  $H_{12}$  also describes the electrostatic interaction of

four particles, but it contains the products  $e\psi(r_{a1})\psi(r_{a2})$  and  $e\psi(r_{b1})\psi(r_{b2})$ , which are the consequence of the fact that electrons 1 and 2 are indistinguishable. This integral cannot be interpreted on the basis of classical concepts. Integral  $H_{12}$  (1.27) is called the exchange integral; it describes the exchange part of the system energy, which basically determines the binding energy of the molecule. Similar exchange terms arise in calculating any multielectron system in the one-electron function approximation, including calculations of atoms by the self-consistent field method, described above. Integral  $S_{12}$  is called the overlapping integral.

The solution to (1.25) with a plus sign is called symmetric with an energy  $E_{\text{symm}}$ , the arrangement of the electron spins for it being antiparallel. The solution to (1.25) with a minus sign is called antisymmetric with an energy  $E_{\text{ant}}$ ; it is antisymmetric in respect to the coordinates, and the arrangement of the spins is parallel. Figure 1.16 shows the curves for the dependence of energies  $E_{\text{symm}}$  and  $E_{\text{ant}}$  on the distance to the nucleus (1.25). It can be seen that  $E_{\text{symm}}$  has a minimum, i.e., it corresponds to the formation of a covalent bond.  $E_{\text{ant}}$  is positive everywhere, i.e., it does not produce any bonds, although it determines a physically possible state at which the atoms repel each other. This calculation of the hydrogen molecule was approximate; later on a number of improvements were introduced into it, which resulted in excellent agreement of theory with the experimental values: bonding energy  $E = 4.747 \text{ eV} = E_{\text{exp}}$ , and distance  $d_{\text{H-H}} = 0.741 \text{ \AA} = d_{\text{exp}}$ .

The above consideration of the  $H_2$  molecule was the prototype of one of the methods [the *valence-bond (VB) method*] for calculating the chemical bond, in which the wave function of the whole system is composed of single-electron wave functions of the separate atoms, as in (1.24), with due consideration for all the permutations of the electrons; the solution of the Schrödinger equation with variation of the coefficients  $c$  helps to find the minimum of the system energy.

Thus, from the standpoint of the VB method, the nature of the covalent bond is explained quantum mechanically. The covalent bond is realized in the hydrogen molecule by a pair of electrons with antiparallel spins and is formed between

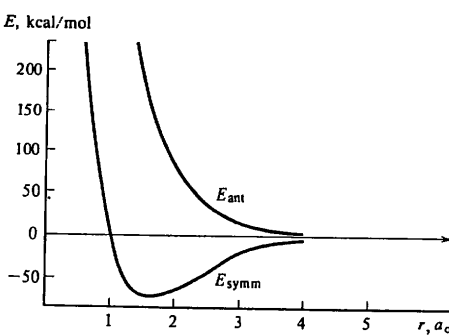


Fig. 1.16. Dependence of the energies  $E_{\text{symm}}$  and  $E_{\text{ant}}$  of two unexcited hydrogen atoms on the distance between nuclei

P.15 multielectron atoms according to the same principles. One of the electrons forming a covalent bond can be contributed to the orbital, as we have seen, by each of the contacting atoms. But there is another possibility for the formation of a two-electron covalent bond, namely, when one of the combining atoms (or groupings) – a donor – has an excess of electrons not involved in any bond, while the other – an acceptor – has a free orbital unoccupied by electrons. Such a covalent bond in which there are ultimately two electrons per each valence is called a donor–acceptor bond.

#### 1.2.4 Hybridization. Conjugation

None of the atomic orbitals, except  $s$ , have a spherical symmetry. Therefore, directional covalent bonds can be explained as a result of their combination with  $s$  orbitals and with each other. The formation of directional bonds in this way is called hybridization. For instance,  $sp$  hybridization, i.e., a combination of  $s$  and  $p$  orbitals, gives a directional  $sp$  orbital;  $sp^2$  hybridization, i.e., a combination of one  $s$  and two  $p$  orbitals, produces trigonal bonds (Fig. 1.17).

The contribution of each AO to the resulting hybridized orbital is determined by its symmetry (antisymmetry) and by the condition of orthonormalization of AO. The direction of the resulting bonds may not coincide with that of the density maximum of the initial AO, as seen from Fig. 1.17. Another example

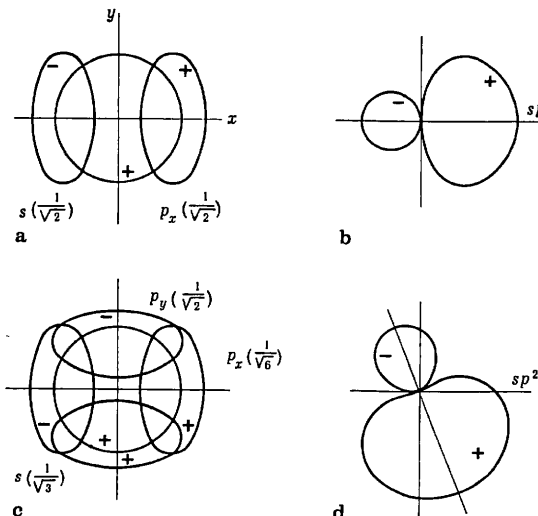


Fig. 1.17a–d. Generation of (a, b) hybridized atomic  $sp$  orbitals and (c, d) one of the  $sp^2$  orbitals forming trigonal bonds of the carbon atom. (a, c) position of the  $s$  and  $p$  AO (the weights of the AO are indicated); (b, d) resultant hybridized orbitals, their positive regions correspond to superposition of the positive regions of the initial AO

is the tetrahedral arrangement of single bonds of the carbon atom, such as in methane  $\text{CH}_4$ , diamond, or hydrocarbons. This bond is attributed to  $sp^3$  hybridization with the formation of four equivalent orbitals of the type

$$\varphi_i = \frac{1}{2} (\psi_s \pm \psi_{px} \pm \psi_{py} \pm \psi_{pz}). \quad (1.29)$$

Here,  $\psi_s$  is spherically symmetric and  $\psi_p$  are elongated along three mutually perpendicular axes  $x, y, z$  (Fig. 1.18). But hybridization imparts tetrahedral direction to the resulting orbital; for instance, all the plus signs in (1.29) give an orbital  $\varphi_{[111]}$  elongated in the direction [111]. Accordingly, the three other cases are  $\varphi_{[1\bar{1}\bar{1}]}$ ,  $\varphi_{[\bar{1}1\bar{1}]}$ , and  $\varphi_{[\bar{1}\bar{1}1]}$ . Tetrahedral bonds, which are quite common, determine the structure of Ge, Si, and many semiconductor compounds.

In addition to directional covalent bonds – linear, trigonal, and tetrahedral – other types of directional bonds are also known. Thus, the tetrahedral bonds of atoms of transition metals which have electrons in the  $s, p$ , and also  $d$  states are ascribed to the hybridization of  $d^3 s$  states. The observed plane square configurations, as in ion  $[\text{PtCl}_4]^{2-}$ , are attributed to  $dsp^2$  hybridization; octahedral, to  $sp^3d^2$  hybridization; etc. (see Sect. 2.5).

The formation of hybrid orbitals is energetically favorable, because pairs of electrons electrostatically repelling one another arrange themselves at a maximum distance from one another.

The number of electron pairs depends on the participation of  $s, p$ , or also  $d$  electrons in the formation of the bond. The maximum spacing leads to their disposition at the vertices of the following configurations: 2 – line, 3 – triangle,

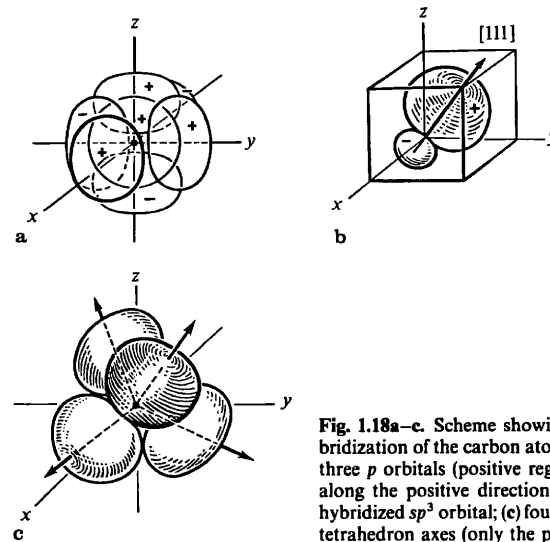


Fig. 1.18a–c. Scheme showing the origin of tetrahedral hybridization of the carbon atom. (a) superposition of one  $s$  and three  $p$  orbitals (positive regions  $p_x, p_y$ , and  $p_z$  are oriented along the positive directions of the  $x, y, z$  axes); (b) arising hybridized  $sp^3$  orbital; (c) four such orbitals directed along the tetrahedron axes (only the positive regions are shown)

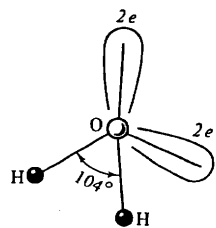


Fig. 1.19. Scheme of the structure of the water molecule; the arrangement of two lone electron pairs is indicated. The molecule has two positively charged projections (protons) and two negative ones, where the lone pairs are concentrated

4 – tetrahedron, 5 – trigonal bipyramidal, 6 – octahedron, 8 – square antiprism, etc., depending on the number of pairs.

Apart from the electron pairs involved in the bond, other electron pairs may remain on the free orbitals. Such pairs are called lone or unshared. For instance,



the water molecule  $\text{H}_2\ddot{\text{O}}$  contains two lone pairs. If we interpret directional bonds from this point of view, the valence angles are deformed because the lone pair electrons repel the shared ones slightly more strongly than the latter repel one another. The “corner” structure of the  $\text{H}_2\text{O}$  molecules is thus ascribed to the directional  $p$  bonds and to the presence of two lone pairs (Fig. 1.19). The structure of the pyramidal molecule  $\text{NH}_3$  is interpreted similarly. Theoretical calculations [1.13] and experimental investigations into the distribution of the electron density by the method of difference deformation syntheses<sup>4</sup> show maxima due to lone pairs of electrons (Fig. 1.20a–d).

If the covalent bond is formed by two or three electron pairs, then multiple (double or triple) bonds arise, which are stronger and shorter than single ones.

Not all the bonds in a number of compounds are of integral order; according to their characteristics, i.e., the energy and distance between the bonded atoms, they have an intermediate character, the bond order being fractional. Nevertheless, the compound formula can be written with classical valence dashes; for instance,  $\text{H}_2\text{C}=\text{CH}-\text{CH}=\text{CH}_2$ . With this alternation of bonds of formally integral order their properties are actually partly or wholly equalized, becoming intermediate between those of “pure” double and single bonds. This is called “conjugation”. Another classical example is benzene, for which it is possible to write two principal Kekulé valence schemes,



<sup>4</sup> As indicated in [Ref. 1.6, Sect. 4.7.10] a map of deformation Fourier synthesis of electron density is the difference between the observed electron density of the crystal structure and the spherically symmetric electron densities of nonbonded atoms, whose centers occupy the same positions as in the crystal, i.e., it reveals precisely the deformation of the electron density caused by the chemical bond. Thermal vibrations of atoms are also taken into account.

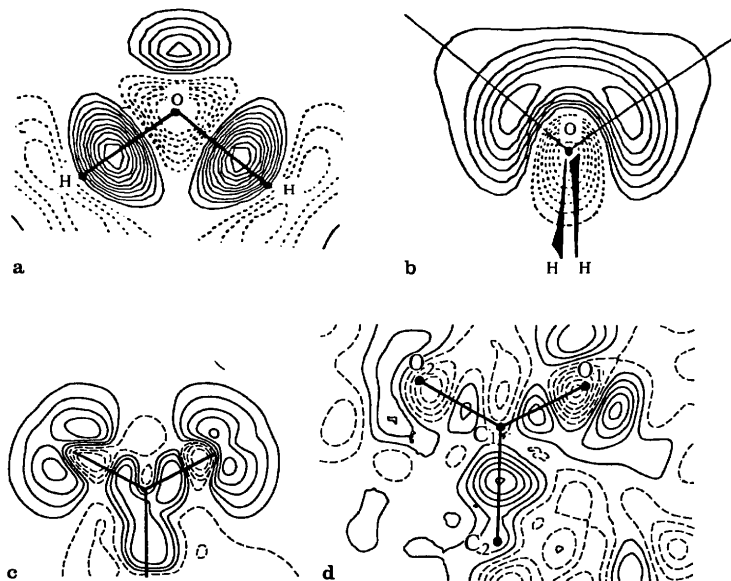


Fig. 1.20a–d. Difference deformation electron density maps of some molecules, showing the charge of lone electron pairs and covalent bond bridges. (a, b) water molecule in  $\text{LiOH} \cdot \text{H}_2\text{O}$ . Contour interval  $0.005 \text{ e } \text{\AA}^{-3}$ ; (a) the plane of  $\text{H}-\text{O}-\text{H}$  atoms; (b) perpendicular plane [1.14]; (c, d) group  $\text{C}-\text{C}=\text{O}$  of the molecule of  $\alpha$ -glycine; (c) theoretical calculation; (d) experimental data contour interval  $0.008 \text{ e } \text{\AA}^{-3}$  [1.15]

with single and double bonds. But in actuality all the bonds in benzene are equivalent, their order being  $1\frac{1}{2}$ . Equivalent bonds of the same nature (order  $1\frac{1}{3}$ ) are inherent in the hexagonal net of carbon atoms in graphite (see Figs. 1.31 and 2.5). The higher the order of the bond, the shorter is the bond. The dependence of the interatomic distance on the bond order in various compounds is given in Fig. 1.46.

The physical significance of the conjugation phenomenon and of the formation of intermediate-order bonds lies in the fact that the electrons are actually not fixed on a definite bond, but belong to the molecule as a whole, and the condition of “multiplicity” of finding an electron pair on a bond is energetically advantageous in many cases, but not necessarily in all.

Interpretation of intermediate-order bonds in complex multiaatomic molecules may involve the writing of classical valence schemes for them. Thus, the equivalence of bonds in benzene can formally be obtained by forming a “superposition” of two formulae (1.30). The structures, which are obtained by superposition of several structures corresponding to possible classical formulae, were

named resonance structure by L. Pauling. The resonance concept helped to supply qualitative and semiquantitative [with calculation similar to (1.26–28)] descriptions of the structure of many molecules. But since the initial structures, between which the resonance occurs, do not exist as such, this concept is purely conventional.

A description of intermediate bonds more consistent with physical reality is given by the molecular-orbital method, which will be considered below.

Thus, the principal type of two-electron bond does not exhaust the whole diversity of covalent interactions between atoms. In addition to the above-mentioned compounds with intermediate bonds, so called electron-excessive and electron-deficient compounds are also known. In the former, the two-electron orbitals are all used up, but there are also electrons residing outside them. The bond in these compounds is comparatively weak. Electron-deficient compounds (typical examples are boranes) do not have a sufficient number of electrons to form two-electron orbitals, but here, too, covalent interaction is still possible.

### 1.2.5 Molecular-Orbital (MO) Method

This is the basic method in modern quantum chemistry. The valence-bond theory considers the bonds between any pair of atoms in terms of the interaction of pairs of electrons whose orbitals belong to mutually approaching atoms, i.e., are single centered. One can, however, proceed from a more general assumption and consider the orbitals of one electron in the field of all the nuclei making up the molecule (or crystal) – *multicenter single-electron functions* – and then take into account the interaction of such orbitals. Here, the Schrödinger equation is solved for fixed nuclei at rest (Born–Oppenheimer's adiabatic approximation).

It is further assumed that when an electron approaches one of the nuclei, its motion must be as if it were assigned by the corresponding AO. Thus, in the case of a diatomic molecule, when considering the motion of each electron in the field of both atoms simultaneously, as the initial approximation the MO are composed of the AO

$$\psi_m = c_a \psi_a \pm c_b \psi_b,$$

and in the general case of multiaatomic molecule

$$\psi_{mi} = \sum_p c_{ip} \psi_p, \quad (1.31)$$

where  $i$  is the number of MO,  $p$  are the number of AO, and  $c_{ip}$  are the coefficients determining the weight of the AO in MO. For instance, for a hydrogen molecule it is possible to use this method for constructing, from  $1s$  orbitals, two MO with electron densities

$$|\psi_m|^2 \sim \psi_a^2 + \psi_b^2 \pm 2\psi_a\psi_b. \quad (1.32)$$

The degree of overlapping of the atomic orbitals is described by the integral of

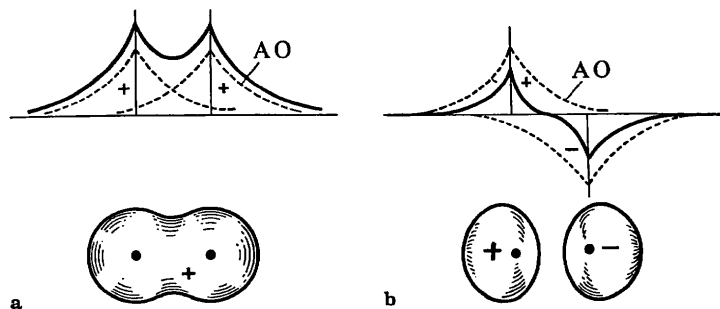


Fig. 1.21a, b. Bonding and antibonding molecular orbitals of the  $H_2$  molecule. (a) origin of bonding MO; (b) origin of antibonding MO

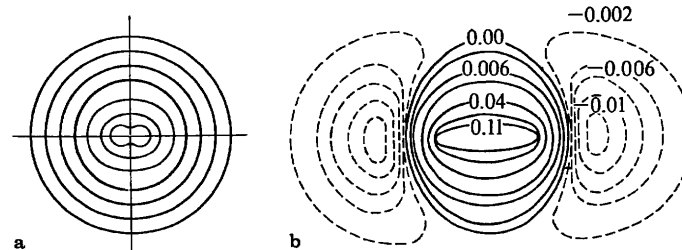


Fig. 1.22. (a) Electron density, (b) difference deformation density of the  $H_2$  molecule

the overlapping

$$S = \int \psi_a \psi_b dv. \quad (1.33)$$

If the integral is positive, the electrons concentrate between the atoms, and a bonding MO<sup>5</sup> may arise, to which the plus sign in (1.32) corresponds. For a bonding MO (Fig. 1.21a), the electrons are between the nuclei of the mutually approaching atoms and thus draw them together. Figure 1.22a shows the electron density of the  $H_2$  molecule calculated theoretically, and Fig. 1.22b gives the picture of the deformation difference density obtained by subtracting the spherically symmetric density of individual  $H$  atoms from the electron density of the molecule (Fig. 1.22a). The maximum between the  $H$  nuclei in Fig. 1.22b and the minima behind the nuclei show the electron redistribution due to the formation of a covalent bond; the maximum corresponds to the positivity of the integral of overlapping (1.33). If the signs of the AO are opposite when MO are

<sup>5</sup> For bonding and antibonding MO the corresponding German terms *gerade* and *ungerade* are also used.

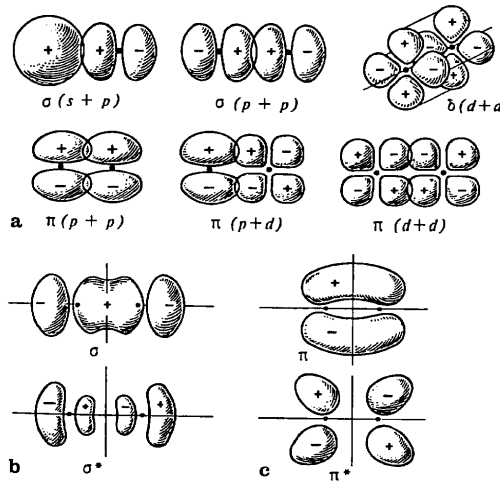


**Fig. 1.23a–c.** Origin of the most important molecular orbitals from atomic orbitals. AO symmetry, its signs, and symmetry of the superposition are essential, (a) AO combinations; (b, c) examples of bonding and antibonding MOs (the latter are marked with an asterisk).  $\sigma$ -MO is obtained from combination  $(p + p)$ -AO using the signs indicated in (a);  $\sigma^*$ -MO is obtained on change of sign of the right  $p$ -AO.  $\pi$ - and  $\pi^*$ -MO are obtained similarly

being formed (Fig. 1.21b), then antibonding MO arise, the probability of finding electrons between nuclei is low, and, being behind both nuclei, the electrons of such orbitals weaken the bond. The lowest energy levels of the molecule are those which are in line with the formation of bonding MOs when the integral of overlapping (1.33) is positive, and which is equal to zero for antibonding MO. It should be emphasized that the positive or zero value of the integral of overlapping is simply determined from the symmetry and antisymmetry of the atomic orbitals (Fig. 1.23). The MO of a molecule with a definite symmetry are described by the irreducible representations of the corresponding point group  $G_0^3$ .

Figure 1.23 shows the most important types of MO formed when AO combine. So-called  $\sigma$  bonds are formed when  $s$  AO combine or when  $s$  AO is combined with  $p$  AO, or also when two  $p$  AO directed along the line of the bond are combined. Another type of bond, namely a  $\pi$  bond, is formed when  $p$  AO combine normal to the line, or  $p-d$  AO or  $d-d$  AO;  $\delta$  bonds arise from “parallel”  $d$  AO. Such MO, for instance, serve to form the electron distribution in the bonds of diatomic, second-period molecules – from  $\text{Li}_2$  to  $\text{F}_2$ . The distribution of the electron density  $\rho(r)$  in molecules such as  $\text{Li}_2$  and  $\text{O}_2$  is shown in Fig. 1.24. Linear combinations of the atoms involved in the bonds are constructed to explain and calculate their multiple (double, triple) bonds from the initial wave functions. Wave functions of different types ( $s$ ,  $p$ ,  $d$ , etc.) can be combined for this purpose. The electrons may be located on both bonding and antibonding MO. Generally, the bond order is defined as the difference between the numbers of electron pairs located on bonding and on antibonding MO.

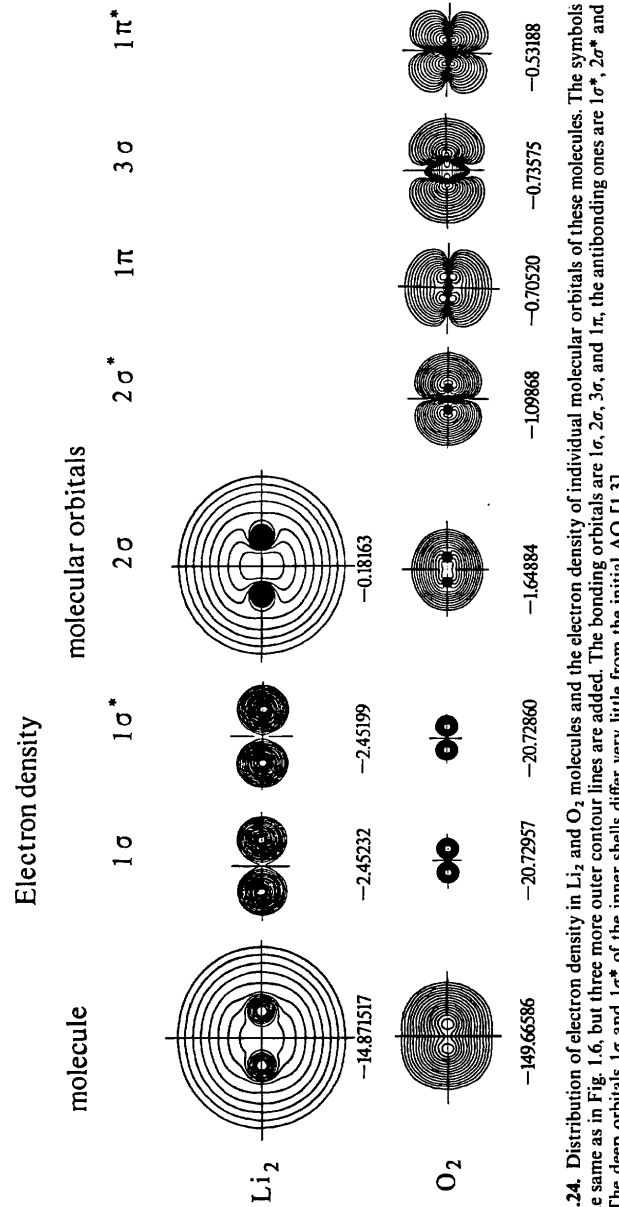


**Fig. 1.24.** Distribution of electron density in  $\text{Li}_2$  and  $\text{O}_2$  molecules and the electron density of individual molecular orbitals of these molecules. The symbols are the same as in Fig. 1.6, but three more outer contour lines are added. The bonding orbitals are  $1\sigma$ ,  $2\sigma$ ,  $3\sigma$ , and  $1\pi$ , the antibonding ones are  $1\sigma^*$ ,  $2\sigma^*$  and  $1\pi^*$ . The deep orbitals  $1\sigma$  and  $1\sigma^*$  of the inner shells differ very little from the initial AO [1.3]

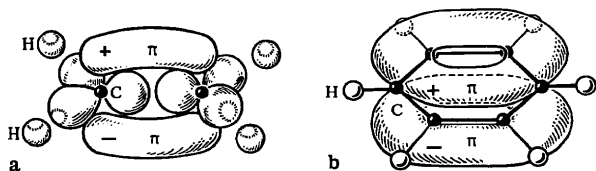


Fig. 1.25a, b. Chemical bond in molecules of ethylene  $C_2H_4$  (a) and benzene  $C_6H_6$  (b). Trigonal hybridized  $sp^2$  AO [shown only in (a)] form ordinary bonds of C atoms among themselves and C–H bonds. The additional bond between the C atoms is due to the  $\pi$  MO. The  $\pi$  orbitals lie above and below the planes of the molecules, forming "bananas" in the case of ethylene and "bagels" in the case of benzene



$sp^2$  hybridization of C atoms on the basis of  $s$ ,  $p_x$ , and  $p_y$  AO and a combination of these orbitals with the  $s$  AO of the H atom results in an MO with H atoms and a  $\sigma$  bond C–C. To the second valence dash corresponds the  $\pi$  MO produced from the  $p_z$  AO. From the standpoint of MO theory the formation of intermediate-order bonds is interpreted as the result of MOs embracing the entire molecule. For instance, in benzene such a solid framework forms  $\pi$  MO (Fig. 1.25b).

Single  $\sigma$  bonds are cylindrically symmetric relative to the bond line. This means that the atomic groupings joined by these bonds can rotate about them to the extent permitted by the steric interaction of the other atoms contained in these groupings (see Fig. 2.61). The other covalent bonds – multiple and intermediate – are constructed from MOs of definite symmetry, which almost always determines the azimuthal arrangement of the groupings bonded by them, i.e., rotation about these bonds is not possible.

Calculations of multiaatomic molecules and, all the more so, of crystals by the MO method are very complicated. The problem is to find the multi-electron wave function of a given system by the self-consistent-field (SCF) method. Because of the complexity of these calculations they were impossible until the advent of modern electronic computers. The principal method used for solving such problems is the method of linear combinations of atomic orbitals (LCAO) and the molecular orbitals composed of them, the SCF-LCAO-MO method. The calculation is based on the choice of the "basis", i.e., a set of initial atomic functions describing the electron states of isolated atoms (or ions). One can also narrow down the basis by assuming the inner shells to be intact and taking into account the wave functions of only the outer shells, which are responsible for the chemical bond. Then, single-electron MO are formed as linear combinations of AO, while the full wave function  $\psi(1, 2, \dots, N)$  of the molecule is determined

from these MO,

$$\Psi = \frac{1}{\sqrt{N!}} \left| \begin{array}{c} \psi_1(1)\psi_1(2) \dots \psi_1(N) \\ \psi_2(1)\psi_2(2) \dots \psi_2(N) \\ \dots \dots \dots \\ \psi_N(1)\psi_N(2) \dots \psi_N(N) \end{array} \right|. \quad (1.34)$$

The numbers in the arguments of orbitals  $\psi_i$  stand for three orbital and one spin coordinates of the electron. The Pauli principle is fulfilled for MO; each of them can carry not more than two electrons with differing spin coordinates. Functions  $\psi_i$  are orthonormalized, one of the results being the appearance of factor  $1/\sqrt{N!}$ . Function  $\Psi$  is antisymmetric. The larger the number  $N$  of the initial AO in the basis, the more accurate is the approximation of the molecular orbitals, but the calculations become much more complicated because the number of single-electron integrals of the type (1.26) is then approximately proportional to  $\sim 1/2N^2$ , and that of two-electron integrals of the type (1.27), to  $\sim N^4$ . Generally speaking, various functions can be chosen as the basis, provided they are close to the functions describing isolated atoms at small distances from nuclei. Of great importance in the choice of the basis is the simplification of the calculations. Use is made of numerical Hartree-Fock atomic orbitals or exponential hydrogenlike Slater orbitals of the type  $r^{n-1} \exp(-\beta r) Y_{lm}$  which are more convenient for calculations, and also Gaussian approximations of  $r^{n-1} \exp(-\alpha r^2) Y_{lm}$ . Carrying out complete, non-empirical, ab initio calculations takes into account all the electrons of the system; positions may be assigned for the nuclei, but, in a more general sense the nuclei are not fixed. These calculations are extremely complicated; therefore, it is customary to make semiempirical calculations only for valence electrons or some of them, fixing the nuclei and the other electrons. In calculations of comparatively simple molecules, such as  $CO_2$ , bases of several tens of Slater or Gaussian functions are usually employed, and the number of integrals is of the order of  $10^5$ – $10^6$ , which is time consuming. To simplify the solution of such problems, various approximations are used.

In recent years various approaches have been developed to the direct solution of the Schrödinger equation for crystals (Sect. 6.3.5).

## 1.2.6 Covalent Bond in Crystals

The problem of calculating the chemical bond in crystals is solved by the universal method: by finding the solution of the Schrödinger equation  $H\Psi = E\Psi$  for a crystal. As the number  $N$  of atoms in crystals is enormous, it may seem impossible to find the solution. However, the most important simplifying factor is the presence of translational periodicity in a crystal. The crystal potential determining Hamiltonian  $H$  is periodic,  $v(\mathbf{r}) = v(\mathbf{r} + \mathbf{t})$ , where  $\mathbf{t}$  is any

lattice translation. On the other hand, for the same reason wave function  $\Psi$  can be represented as a sum of Bloch functions

$$\psi_i = \chi(r) \exp(2\pi i \mathbf{k}r), \quad (1.35)$$

where  $\mathbf{k}$  is the wave vector of the electron in the reciprocal lattice. The solution of the Schrödinger equation is expressed precisely by Bloch functions. This consideration leads to the band theory of electrons in a crystal, which is covered in Chap. 3. The band theory predicts the allowed energies of free electrons in the crystal  $E(\mathbf{k})$ . It is a general approach applicable not only to the covalent, but also to the metallic and ionic bond.

The interaction of electrons with the crystal lattice is due to their wave nature. Similar phenomena arise in electron diffraction by crystals [Ref. 1.6, Sect. 4.8]. Proper free electrons of a crystal are also reflected from the lattice planes, which leads to a fundamental conclusion that not all the values of energies  $E(\mathbf{k}) = \hbar^2 k^2 / 2m$  are possible. The permissible values of vector  $\mathbf{k}$  are limited in the reciprocal space by polyhedra, i.e., Brillouin zones (Fig. 1.26). As we shall see in Chap. 3, inside these zones  $\mathbf{k}$  (and hence  $E$ ) takes on a practically continuous multitude of values (actually, there are  $N$  values, where  $N$  is the number of unit cells in the volume of a crystal). Within a zone the energy is a continuous function of  $\mathbf{k}$ . The mathematical methods used for solving the Schrödinger equation for a crystal strongly depend on the bond in the crystal concerned. If the electron-atom bond is strong, as in ionic and covalent crystals, these methods are closer to the above-discussed methods for analyzing the covalent bond in molecules. On the other hand, in metals where the outer electrons of atoms are collective, it is also possible to apply other approaches (Sect. 1.2.8). In all the cases the lattice potential can be represented as a sum of atomic potentials  $V(\mathbf{r}) = \sum v_a(\mathbf{r} + \mathbf{t})$ , and the mutual overlapping of  $v_a$  ultimately defines the distribution of the coupling electrons among the atoms. Then, the potential is also expanded in a Fourier series  $V(\mathbf{r}) = \sum_H v_H [-\exp(2\pi i H \mathbf{r})]$ ,

which yields the set of equations for functions  $\psi_i$  (1.35), the Fourier coefficients of potential  $v_H$ , and energies  $E(\mathbf{k})$ . The calculation is greatly simplified because the inner shells (atomic cores) remain unaltered and can be excluded from

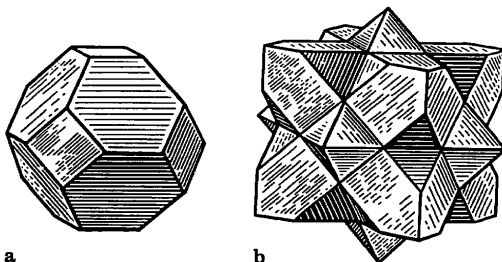


Fig. 1.26. (a) first and (b) second Brillouin zones for the structure of copper

consideration; it suffices, therefore, to take into account the potential on the periphery of the atoms and between them, which changes comparatively slowly.

The band structure and wave functions of the electrons for covalent crystals are calculated according to the above-described schemes. Since the covalent bond is realized by electrons localized on MOs between pairs of neighboring atoms, it can be described very well on the basis of the SCF-LCAO-MO method with expansion of the atomic functions in spherical harmonics of the type (1.2). A set of electrons of  $N$  crystal atoms is regarded as distributed over  $2N$  two-center orbitals of the type (1.31). Indeed, the characteristics of the bond in a single tetrahedral bond C-C in an organic molecule or in diamond are very similar. Analogous tetrahedral bonds arise in crystals of Si and Ge, and in  $A^{III}B^{IV}$  compounds; in the latter, they are already of a donor-acceptor nature. Other methods – those of so-called orthogonalized plane waves and of the pseudopotential (Sect. 1.2.8) – also help to calculate the characteristics of the covalent bond in crystals.

For covalent crystals, the energy-level structure is such that the energy necessary for transferring an electron from a completely filled 1s band (valence band) to the vacant 2s band (conduction band) is high. This energy (the width of the forbidden band) is equal to 5.4 eV for diamond, and  $\sim 1$ –3 eV (cf. Fig. 1.11) for typical semiconductors. Here, certain states of the atoms ( $s$ ,  $p$ , etc.) can be correlated with the corresponding energy bands of the crystal.

As an example, we consider the calculation of the electron density of covalent crystals of the diamond type (Ge, Si, GaAs, ZnSe, etc.) carried out by the pseudopotentials method [1.16]. After solving the Schrödinger equation, one finds the wave functions  $\psi_{n,k}(\mathbf{r})$  of the valence bands  $n$ ; the electron density of each state is proportional to  $|\psi_{n,k}|^2$ , and the total electron density is equal to  $e \sum |\psi_{n,k}|^2$  [see (1.39)]. For  $n = 1$  ( $n = 2$ ) the valence density is similar to the  $s$  states of the free atoms (Fig. 1.27a), and for  $n = 3$  ( $n = 4$ ) (Fig. 1.27b), to the  $p$  states. The summary distribution (Fig. 1.27c) reflects the tetrahedral  $sp^3$  state with an increase in density of the valence electrons between the atoms. For GaAs and, to a greater extent, for ZnSe, the ionic component of the bond is prominent. Thus, for ZnSe the first band – the state with  $n = 1$  (Fig. 1.27d) – clearly describes the ionic component of the bond: the corresponding charge is concentrated around Se. The summary distribution of the valence density of ZnSe also has a covalent “bridge” on the bond, as in Ge.

An example of the application of these methods to the ion structure is the calculation of  $\rho(\mathbf{r})$  for a MgO crystal using the pseudopotentials method [1.17]. To find Bloch functions and distributions of  $\rho_n(\mathbf{r})$  corresponding to the four valence bands, use was made of the pseudopotentials found from the experimental energy dependence of the imaginary part of the dielectric constant. As can be seen from Fig. 1.28a–c, the  $\rho(\mathbf{r})$  of the valence bands are very similar to the charge distribution in the relevant atomic states. According to calculations, the Mg atom is practically fully ionized, and the O states correspond to the  $s$  state and to three  $p$  states (recall that the electron density of the inner filled shell is excluded). The charge of O is 0.9 e.

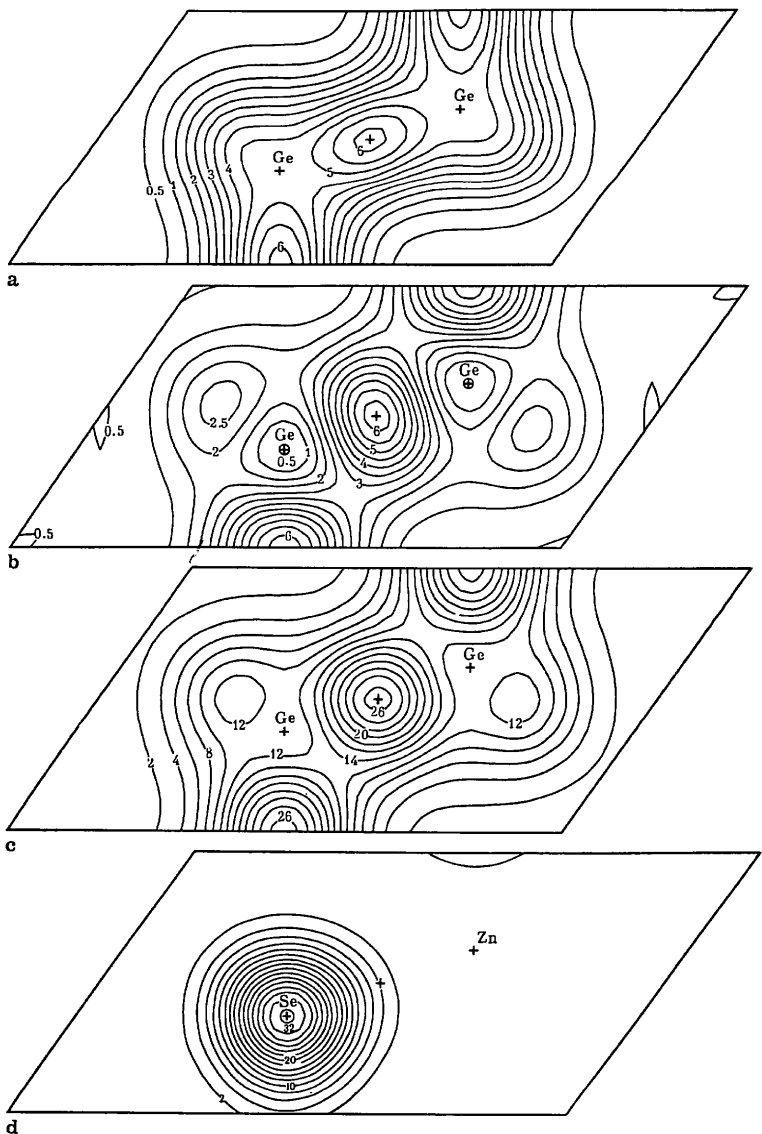


Fig. 1.27a–d. Theoretically calculated valence electron density contour map in the (1-10) planes of Ge (a, b, c) and ZnSe (d) crystals. (a) electron density of the first valence band of  $\rho_1$  (s type) of Ge; (b) electron density of the third band of  $\rho_3$  (p type) of Ge; (c) total electron density ( $sp^3$  type) of Ge; (d) electron density of the first band of ZnSe showing a shift of the charge towards Se (ionic component of the bond) [1.16]

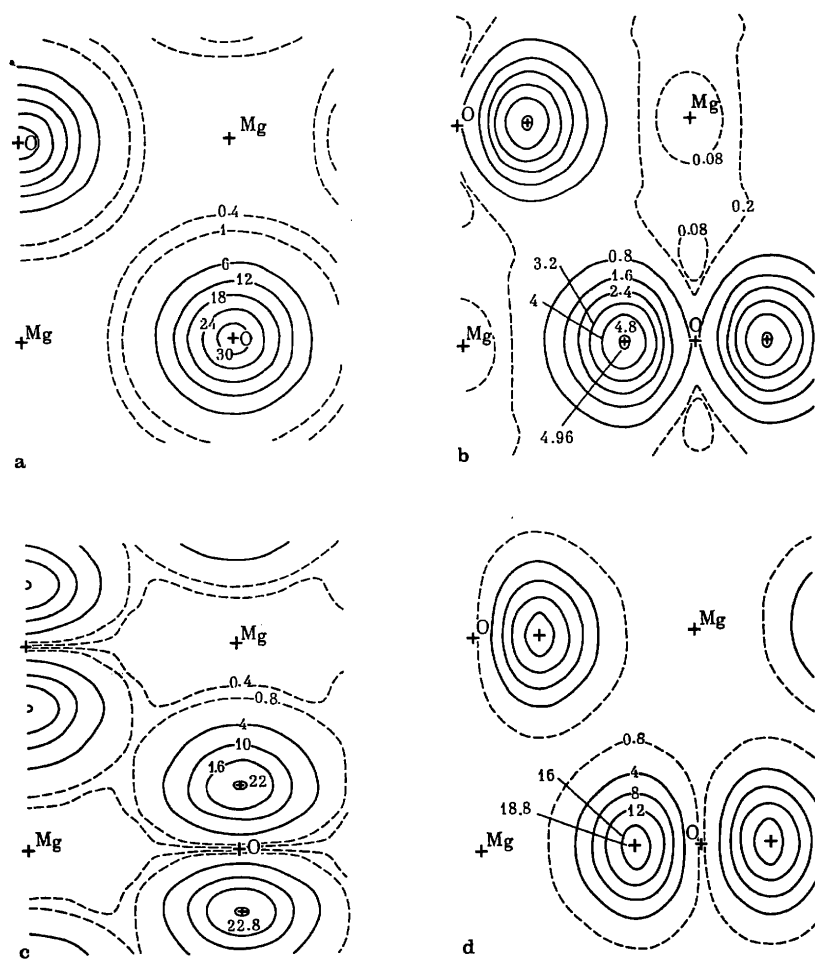


Fig. 1.28a–d. Theoretically calculated band components of the valence electron density in the (100) plane of MgO crystal passing through the centers of the atoms. (a)  $\rho_1$  (s type); (b)  $\rho_2$ ; (c)  $\rho_3$ ; (d)  $\rho_4$  (all p type) [1.17]

In estimating the energy and the force constants of the covalent bonds a sufficiently good approximation is provided by the curves of the potential interaction energy  $u(r)$  of the type shown in Fig. 1.12 obtained semi-empirically or by approximating the exact calculations. A satisfactory description of attraction forces is given by an expression of the type  $ar^{-m}$  ( $m = 4$ ). As  $r$  decreases and a minimum is passed, the short-range repulsive forces increase sharply; they are

P.22  
due to the electrostatic repulsion of nuclei and electron shells of various atoms which exceeds the attraction of the nuclei to the electrons and the exchange energy [see (1.27)]. Repulsion can be approximated by the expression  $br^{-n}$ , and then equations of the type (1.16, 17) ( $m = 4$  and  $n = 6-9$ ) are applicable for covalent forces. Quantum-mechanical calculations of the repulsive potential give the exponential dependence; for the covalent forces

$$u(r) = -ar^{-m} + c \exp(-\alpha r), \quad m = 4. \quad (1.36)$$

From the condition  $du/dr = 0$ , which determines the equilibrium state of  $r_p$  and the energy  $u_p = u(r_p)$ , we find

$$u(r) = \frac{u_p}{m - \alpha r} \left\{ \frac{\alpha r_p^{m+1}}{r^m} + m \exp[\alpha(r - r_p)] \right\}. \quad (1.37)$$

The energy of covalent bonds depends on their order; triple and double bonds have the highest energy of all types of bonds, for instance, 225 kcal/mol in the triple bond in  $N_2$  and 150 kcal/mol in the double bond  $C=C$ . In single bonds (or per unit bond order) it ranges from 60–70 kcal/mol (for the strongest bonds) to 30–40 kcal/mol or less (for instance, 36 kcal/mol for  $F_2$ ). A lower  $r_e$  corresponds to a higher binding energy. The constant  $\alpha$  can be calculated via the second derivative  $d^2u/dr^2$  at the point of minimum. For a covalent bond this derivative is large and the bond is rigid; its characteristics change only slightly (including the value of  $r$ ) on the transition from the molecule to a crystal.

It is noteworthy that there is a certain small component of the covalent bond even in the most typical ionic compounds. Similarly, with the exception of such genuinely covalent crystals as diamond, other covalent compounds composed of different sorts of atoms have the ionic component of the bond. For instance, in borazon BN (a structural analogue of diamond) a charge transfer from boron to nitrogen already takes place; the same is true of another compound with this type of structure ZnS, where the effective charges are estimated at 0.5–0.8 e.

Such a partly ionic (i), and partly covalent (c) bond can be described within the framework of the VB method by the wave function

$$\Psi = a_i \psi_i + a_c \psi_c \quad (1.38)$$

where the degree of ionicity  $\varepsilon = a_i^2/(a_i^2 + a_c^2)$ . The degree of ionicity can also be estimated by the MO-LCAO theory, leading to (1.20).

It is easy to take into account the ionic component by adding to (1.36) the first term  $ar^{-1}$  from (1.15, 16), i.e., electrostatic attraction coefficient  $a$  is determined by the effective charges.

Semiempirical equations of the type (1.36, 37) only permit estimating the energy as a function of the interatomic distance between the bound atoms. At the same time the covalent bond is also directional, with the corresponding energy of deformation of valence angles. Rotations of groupings about a single bond are also possible, which defines the fraction of the so-called torsional energy. These contributions to the energy are covered by the appropriate equations, which will be treated in Sect. 2.6.

### 1.2.7 Electron Density in a Covalent Bond

The electron density of any system – an atom, a molecule, or a crystal – is described by the square of its wave function  $|\Psi|^2$ . While described by orthogonal orbitals  $\psi_i$  of the type (1.7, 34) the electron density has the form

$$\rho(r) = e |\Psi|^2 = \sum_{i=1}^N |\psi_i|^2. \quad (1.39)$$

Each atom is a highly concentrated cloud of electron density; the overwhelming number of its electrons are within a peak of comparatively small radius (Fig. 1.9). The electrons realizing the valence bond are associated with a certain region of the wave function  $\Psi$ , and the relevant increase in the values of the electron density between atoms corresponds to the overlapping integral (1.33).

Let us consider, as an example, the structure of an element, for instance diamond, C. By analogy with the above construction for NaCl in Fig. 1.14, let us plot the radial electron density functions  $D(r)$  [see (1.8)] of the initial atoms towards each other from the ends of the segment connecting the nearest atoms. The maxima of these functions for the outer orbitals of both  $p$  shells will be found at approximately the same place (Fig. 1.29a). Recall again that this construction is conventional; it shows the place where the orbitals overlap, but does not describe the actual electron density  $\rho(r)$ . In the distribution of the electron density of the crystal there is no maximum of  $\rho(r)$  on the bond line. It can only be said that in the case of the formation of a covalent bond the summary electron density along this bond, i.e., on the straight line joining the bound atoms, is higher than that at the same distance from the atom, but in a direction not corresponding to the bond. It is also higher than the practically near-zero electron density between the atoms in the case of a purely ionic bond (Fig. 1.13). At the same time, if we eliminate the electron density of the inner shells by subtraction, such a maximum is observed for the distribution of the valence electrons. This is indicated both by theoretical (Fig. 1.27b, c) and experimental data obtained from precision X-ray investigations with calculation of

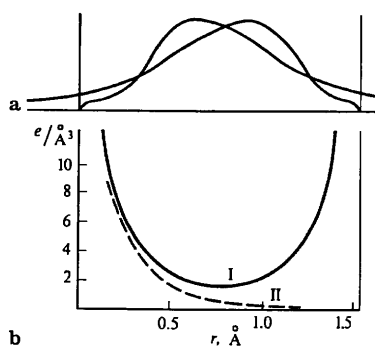


Fig. 1.29a, b. Electron density of a single C-C bond. (a) overlapping of the radial density distribution maxima of the valence orbitals of the C atoms; (b) experimentally found distribution of the electron density along the line of the covalent C-C bond (curve I) and in the direction "between the bonds" (curve II)

$\rho(r)$  by a Fourier synthesis. Figure 1.30a shows the electron density map of diamond (a classic example of a crystal having a covalent bond) on a plane passing through one of the series of atoms forming the structure. The

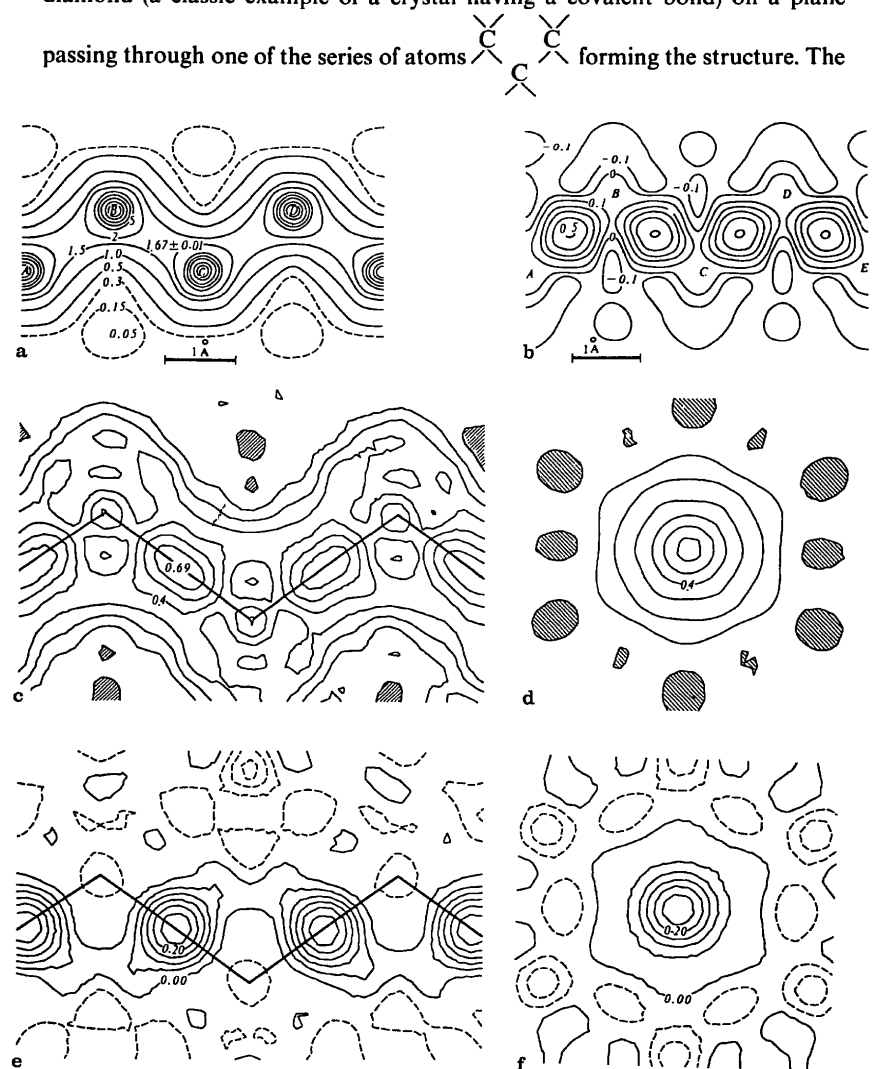


Fig. 1.30a-f. Experimental electron density maps of diamond and silicon. (a) cross section  $\rho(xxz)$  of diamond through the centers of C atoms (peak height  $174 e/\text{\AA}^3$ ); (b) corresponding difference deformation density [1.10]; (c, d) electron density of valence electrons  $\rho_{\text{val}}$  in a Si crystal along the plane of Si-Si bonds (c) and perpendicular to the Si-Si bond in its center (d). The lines are drawn at intervals of  $0.1 e/\text{\AA}^3$ ; (e, f) the same for the deformation difference density  $\rho_{\text{def}}$ , the contours are drawn at intervals of  $0.05 e/\text{\AA}^3$ , negative values are shown by dashed lines [1.18]

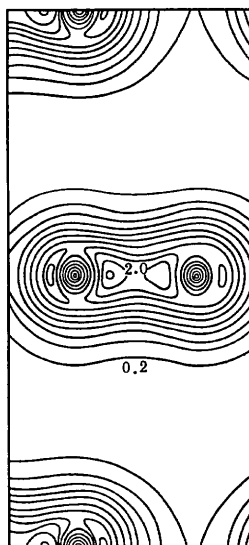


Fig. 1.31. Electron density of valence electrons in the C-C bond in graphite (vertical section of the unit cell) [1.19]

“bridges” of increased density can be seen between the C atoms. An increase in  $\rho$  is determined by the maxima of the difference deformation density (Fig. 1.30b).

Similar, very accurate data for Si have been obtained by measuring X-ray structure factors (not intensities) on the basis of the pendulum solution of dynamic theory [Ref. 1.6, Sect. 4.3]. (The standard deviation of  $\rho$  is  $0.007 e\text{\AA}^{-3}$ ). Figure 1.30c, d gives difference maps of the valence electron density of Si (the inner-shell electron density has been subtracted). The valence density peaks are elongated along the bond line and are approximately cylindrically symmetric relative to it. Their height of  $0.69 e\text{\AA}^{-3}$  is in good agreement with the theoretically calculated value,  $0.65 e\text{\AA}^{-3}$ . Figure 1.30e, f shows the deformation difference density (the total spherically symmetric electron distribution of nonbonded atoms has been subtracted)<sup>6</sup>. According to these data the deformation difference electron density of the Si-Si bond is slightly lower than that of C-C in diamond. According to these and other data the deformation density  $\rho_{\text{def}}$  of a single bond at a maximum is  $0.3-0.4 e\text{\AA}^{-3}$ . According to theoretical data the summary charge of the valence-electron peak on the bond is about  $0.1 e$ .

In the case of multiple bonds the electron density is naturally higher. Figure 1.31 presents the valence density of the bonds between the carbon atoms in graphite (the  $1s^2$  electrons are excluded). These bonds are hybridized, their order being  $1\frac{1}{3}$ .

<sup>6</sup> See footnote 4, p. 30.

Similar information was obtained for the structure of organic molecules in crystals by combining X-ray and neutron-diffraction data (recall that the latter supply accurate positional parameters of the nuclei and the parameters of the anisotropic thermal vibrations). Examples are given in Fig. 1.32 (see also Fig. 1.20). Thus, in investigating cyanuric acid (Fig. 1.32a) the difference deformation synthesis clearly reveals maxima due to the covalent bond, unshared

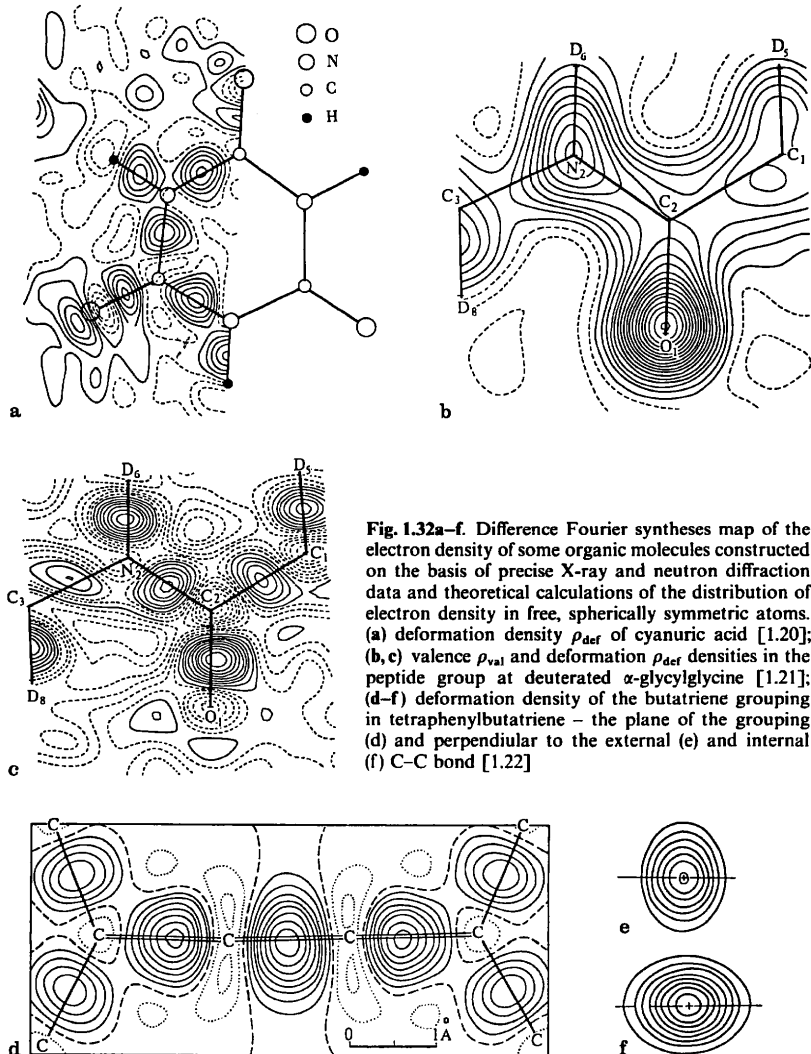


**Fig. 1.32a–f.** Difference Fourier syntheses map of the electron density of some organic molecules constructed on the basis of precise X-ray and neutron diffraction data and theoretical calculations of the distribution of electron density in free, spherically symmetric atoms. (a) deformation density  $\rho_{\text{def}}$  of cyanuric acid [1.20]; (b, c) valence  $\rho_{\text{val}}$  and deformation  $\rho_{\text{def}}$  densities in the peptide group at deuterated  $\alpha$ -glycylglycine [1.21]; (d–f) deformation density of the butatriene grouping in tetraphenylbutatriene – the plane of the grouping (d) and perpendicular to the external (e) and internal (f) C=C bond [1.22]

electrons of the O atoms, and the electron outflow (negative electron density) from the external part of H atoms. The same features are prominent on difference valence (Fig. 1.32b) and deformation (Fig. 1.32c) syntheses of deuterio- $\alpha$ -glycylglycine (a deuterated crystal is more suitable for neutron diffraction studies).

Figure 1.32d, e represents cross sections of difference deformation syntheses of the butatriene grouping for tetraphenylbutatriene, a representative of the cumulenes. The experiment was carried out at 100 K. The characteristics of the double bonds C=C are of interest here. The values of  $\rho_{\text{def}}$  at their peaks are  $0.9 \text{ e } \text{\AA}^{-3}$  for the internal and  $0.75 \text{ e } \text{\AA}^{-3}$  for the external bond, which naturally exceeds the values characteristic of single bonds. The sections perpendicular to the bonds (drawn through the bond midpoint) are elliptical, i.e., these bonds (as distinct from single ones) do not show cylindrical symmetry. The charge in the external C=C bond is elongated along the normal to the butatriene plane, and in the internal bond, in this plane. This agrees with the predictions of the classic theory of  $\pi$  electrons in cumulene systems (cf. Fig. 1.25a, see also Fig. 2.75).

Deformation and valence difference syntheses also enable one to establish the charge at the peak by integrating over the positive or negative electron density peak at the site of the subtracted atom. It turns out that there is almost always some charge redistribution from atom to atom in a molecule. Thus, in the peptide group of the molecule of deuterio- $\alpha$ -glycylglycine  $\text{O}_2\text{CCD}_2\text{NCO-CD}_2\text{ND}_3$  the O atoms have a negative charge of about  $-0.5 \text{ e}$ , and N, about  $-0.4 \text{ e}$ ; atoms of C bound with O have a positive charge of  $+0.3$  to  $+0.4 \text{ e}$ ; and those bound with D, a weak negative charge of  $-0.1 \text{ e}$ ; all the D atoms are charged positively,  $+0.1$  to  $+0.3 \text{ e}$ . The summary charge of the bond electrons can be similarly established by integrating over the corresponding peaks.

Methods for a parametric description of experimentally obtained electron distribution of valence-bound atoms in various systems have also been developed. One such approach consists in expanding  $\rho$  with respect to a set of basis functions  $\varphi$

$$\rho(xyz) = \sum_{\mu} \sum_{\nu} P_{\mu\nu} \varphi_{\mu} \varphi_{\nu}^* \quad (1.40)$$

and finding coefficients  $P_{\mu\nu}$  [1.23]. Slater's or Gaussian orthonormalized orbitals (multipoles) can be chosen as basis functions as in (1.34) [1.24–26]; the anisotropic thermal motion is also taken into account. On the basis of such a description and taking into account the symmetry of the system it is possible to calculate the electron population density  $q(A)$  of atoms and  $q(AB)$  of bonds between atoms, and to compare it with the data obtained with theoretical predictions. It is essential to take into account the quantum properties of the electron distribution – the Pauli principle – in many calculations. The matrix of  $P_{\mu\nu}$  values should then satisfy condition  $P^2 = P$  [1.27].

Most of the results of the calculations of  $q(A)$  and  $q(AB)$  agree with the theoretical predictions, some others diverge, for instance as regards the shape and distribution of the electron density regions corresponding to lone pairs.

### 1.2.8 Metallic Bond

In a covalent bond, superposition and some redistribution of electrons of the outer shells of atoms take place, the orbitals of these electrons being mainly localized between the pairs of neighboring atoms. The discrete energy levels of the atoms change and form a quasicontinuous filled band in the crystal.

The nature of a metallic bond is the same as that of covalent bond, namely, sharing the outer electrons; the localization of these electrons, however, is different. In metallic atoms the outer orbitals are filled with a small number of electrons, and the ionization energy  $I^+$  necessary for the detachment of outer electrons, which can be considered a measure of the stability of the orbital (see Table 1.2), is small. In most cases this is a spherically symmetric  $s$  orbital, which is comparatively wide. When metallic atoms draw close together and form crystals of metals or alloys, these orbitals overlap with a great number of identical neighboring orbitals; for instance, in metals with a face-centered cubic lattice they overlap with 12 orbitals (Fig. 1.33). Therefore the concept of localization of outer electrons near a given atom or between pairs of atoms loses its meaning, and their entire system, described by the wave function,  $\Psi$ , common for the whole crystal, is characterized by its approximately uniform value in the space between the atoms. This also corresponds to the classical concepts of the electron theory about the presence of a "gas" of free electrons in metals.

As mentioned in Sect. 1.2.6, the methods for calculating the metallic bond are based on the band theory. In metals, the electrons can freely shift to vacant levels immediately adjoining the filled levels, which actually explains the metallic properties. Since the band is not filled completely, the surface of vectors  $k$ , corresponding to the maximum energy and called the Fermi surface, does not

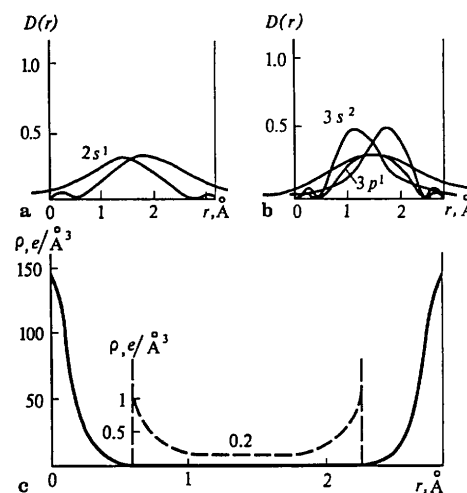


**Fig. 1.33a–c.** Electron density distribution in the structure of metals. Overlapping of the radial distribution functions of outer electrons in Li (a) and Al (b). Experimentally determined electron density in aluminium (c) along the Al-Al line (the dashed curve referring to the atom periphery is scaled up)

touch the faces of the Brillouin zone or forms "channels" in the periodic reciprocal space (see Chap. 3 for details). The methods for calculating the structure of metals use various models. Since only the outer electrons are common for the atoms of metals, the problem can be solved, for instance for alkali metals, by representing the lattice potential as a sum of the potentials of the ionic core with the shell of the noble gas atom in whose field the conduction electrons are moving (one-electron approximation). If we divide the whole volume of the lattice into equal Dirichlet polyhedra (see [Ref. 1.6, Fig. 2.89] surrounding the given atom (such a construction for metals is called a division into Wigner-Zeitz cells, see Sect. 2.8), it can be assumed that within the filled shell of the core the potential is spherically symmetric, and outside the shells it changes only slightly, being practically constant. By fitting the solutions together at the boundaries of shells and polyhedra one can find the general solution.

In the one-electron approximation, the interaction due to Coulomb repulsion between the free electrons is neglected. There are several methods which take into account these effects, and also exchange interaction and spin effects. One can ultimately obtain, in terms of one metallic atom, simplified expressions for the energy of the type

$$u(r) = -\frac{a}{r} + \frac{b_1}{r^2} + \frac{b_2}{r^3} + b_3, \quad (1.41)$$

where the constants are calculated theoretically or semiempirically from the compressibility data, etc. Expression (1.41) with the first two terms can also be obtained from the classical concepts about the interaction of a negatively charged gas with the positive ionic cores. The energy curves for alkali metals, obtained with the aid of quantum-mechanical calculations, are given in Fig. 1.34. It is important to emphasize that, in view of the cooperative nature of the interaction, these curves are only valid for a crystal; they do not describe the interaction between a pair of atoms, for instance in a  $\text{Me}_2$  "molecule". The physical meaning of the attraction forces in the metal structure is that the potential distribution in it enables the outer electrons to occupy lower energy levels than in free atoms.

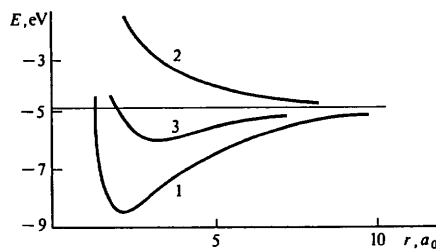


**Fig. 1.34.** Energy curves for the lattice of metallic sodium. (1) interaction energy of a free electron with  $\text{Na}^+$ ; (2) kinetic energy of electrons; (3) total energy

In metals with several electrons in the outer shell the interaction is more complicated because not all these electrons are free, i.e., not all of them shift to the conduction band. Therefore, the covalent interaction also contributes a certain component to the attraction forces. A purely metallic bond is non-directional, i.e., it is spherically symmetric, therefore, many structures, for instance those of the metals Na, K, and many others, are close-packed cubic. At the same time, for many metals the effects of bond orientation become apparent, when, for instance, body-centered cubic or hexagonal structures are formed. The quantum-mechanical calculations have only been performed in several cases. In such calculations, the pseudopotential method is used for multivalent metals. In this method the pseudowave function is calculated, instead of the true wave function; the latter must be orthogonal to all the wave functions of electrons in the inner shells and, therefore, has a complex oscillating form within the ionic cores of the metal. The pseudowave function coincides with the true wave function outside the ionic cores, but remains smooth inside them. The equation defining the pseudowave function is obtained from the conventional Schrödinger equation by replacing the local true potential with the nonlocal pseudopotential. This includes, in addition to the term corresponding to attraction, a term describing the effective repulsion of conduction electrons from the ionic cores. In approximate calculations of the interaction energy and other characteristics of metals, equations of the type (1.41) can also be used.

X-ray investigations positively confirm the presence of a continuously distributed constant electron density in the metal structure and the ionization of the outer atomic shell. The electron density of an ionized metallic atom is spherically symmetric [1.8, 28, 29]. The mean electron density of the interatomic space is constant and equals about  $0.15\text{--}0.20 \text{ e Å}^{-3}$  (Fig. 1.33c, cf. Fig. 1.14b); the obtained values of the number of electrons in atoms for some metals are as follows: 10.4 for Mg, 10.2 for Al, 23.0 for Fe, and 20.0 for Cr, which approximately corresponds to ionization equal to the valency of the metal.

Note that the above-discussed three basic types of "strong" bonds – ionic, covalent, and metallic – are close in energy and characteristic interatomic distances. Below (in Sect. 1.4) we shall revert to the causes of this similarity. We recall once more that in many compounds the bond is intermediate in nature. This refers, for instance, to such an important class of compounds as semiconductors, which are formed by such elements as P, S, Ge, Si, Ga, As, Se, Sb, Te, etc., as well as to some intermetallic compounds. The bond in them cannot be allocated to a single definite type; it has features of both a covalent and a metallic bond, and sometimes of an ionic bond. The ionization of atoms and the existence of a small valence bridge electron density are detected in such compounds by experimental X-ray investigations (cf. Fig. 1.27a–d, see also Sect. 2.4).

It should always be kept in mind that a chemical bond in a compound is a quite definite state of the outer electrons of a given multiatomic system. Its division into certain components is, to a large extent, conventional.

It should also be emphasized that many substances which under normal conditions are insulators or semiconductors experience phase transitions and

acquire metallic properties with an increase in pressure; the bond in them also acquires a metallic character. This is natural because forced mutual approach of atoms under external pressure increases the overlapping of outer shells and, hence, the number of shared outer electrons; the energy spectrum also changes – the bands merge together. Thus, Te becomes a metal at  $\sim 40 \text{ kbar}$ , Ge at  $160 \text{ kbar}$ , and InSb at  $20 \text{ kbar}$ . The problem of metallic hydrogen is of interest. According to theoretical estimates ordinary molecular hydrogen  $\text{H}_2$  can be transformed into metallic hydrogen at a pressure of about 2 megabar. It has been suggested that this phase may be metastable, i.e., it may remain metallic after the pressure is lifted, and will also be superconducting. Some hypotheses assume that depending on the particular structure of the energy spectrum (for instance, for Ni), a pressure increase may, contrariwise, result in a loss of metallic properties.

### 1.2.9 Weak (van der Waals) Bonds

Noble gases, whose atoms have completed shells, crystallize into highly symmetric structures at low temperatures. Organic molecules having a system of strong, completely saturated (covalent) bonds also form crystals. A number of physical characteristics (melting point, mechanical properties, etc.) show that the bonds between the particles in all such crystals are weak. According to X-ray data, the shortest distances between non-valence-bonded atoms, i.e., atoms of "contacting" neighboring molecules or atoms of noble gases, considerably (by 50 or 100%) exceed the "short" distances of strong bonds. The attraction forces operating here are commonly called van der Waals forces, because they explain the correction for molecular attraction in the van der Waals equation for the state of gases.

If molecules possess a constant electric moment  $\mu$ , one of the components of these forces is the classical dipole–dipole interaction. It is reduced by the thermal motion, which disturbs the dipole orientation. The energy of such interaction is defined by

$$u_1(r) = -\frac{2}{3}\mu^2 r^{-6} \frac{1}{kT}. \quad (1.42)$$

This is called the orientation effect. Naturally, its fraction in intermolecular interactions is large only for molecules with a high  $\mu$ , for instance, for  $\text{H}_2\text{O}$  and  $\text{NH}_3$ .

Some contribution to the molecular interaction is also made by another, so-called induction effect, which takes into account the possibility of the polarization of molecules by one another, i.e., the possibility of inducing dipoles. The corresponding energy is also proportional to  $r^{-6}$ ,

$$u_2(r) = -2\alpha\mu^2 r^{-6}, \quad (1.43)$$

where  $\alpha$  is the polarization.

The principal component of the intermolecular forces is the so-called dispersion interaction between neutral atoms or molecules, which completely explains,

in particular, attraction between the atoms of inert elements. This interaction is due to the presence, in the atoms, of instantaneous dipoles induced by the moving electrons of neighboring atoms and can be considered quantum mechanically. According to F. London, while finding it one must take into account both the ground,  $\psi_0$  and  $\varphi_0$ , and excited,  $\psi_n$  and  $\varphi_n$ , states of the mutually approaching atoms. Since the atoms are spaced wide apart and only remote regions of the wave functions overlap, the exchange can be neglected. It is possible to deduce, on the basis of the second approximation of perturbation theory, that

$$u_3(r) = -Kr^{-6}, \quad K = \frac{3h}{2} \frac{v_1 v_2}{v_1 + v_2} \alpha_1 \alpha_2. \quad (1.44)$$

Here,  $K$  is expressed in terms of polarization  $\alpha_1$ ,  $\alpha_2$ , and the characteristic frequencies  $v_1$ ,  $v_2$  of atom excitation are the same as those responsible for the light dispersion. If we take into account not only the dipole, but also the multipole interaction, terms with  $r^{-8}$  and  $r^{-10}$  also appear. The zero energy is taken into consideration as well. The potential of repulsion of molecules or ions is expressed by the exponential function. As a result, the following equation holds true for the description of interaction of the atoms of neighboring molecules:

$$u(r) = u_1 + u_2 + u_3 + c \exp(-\alpha r) = -ar^{-6} + c \exp(-\alpha r). \quad (1.45)$$

This equation is the same as (1.35), but with  $m = 6$  and with different  $a$ ,  $c$ , and  $\alpha$ . For instance, for interactions of C atoms  $a = 358$  kcal/mol,  $c = 4.2 \times 10^4$  kcal/mol, and  $\alpha = 3.58 \text{ \AA}^{-1}$ . The fraction of the three components in the intermolecular bond energy depends on the dipole moment  $\mu$  and the polarization  $\alpha$  of the molecules. For instance, for  $\text{H}_2\text{O}$   $u_1 = 190$ ,  $u_2 = 10.0$ , and  $u_3 = 93.0$  ( $\text{erg} \cdot 10^{-60}$ ); and for CO  $u_1 = 0.003$ ,  $u_2 = 0.05$ , and  $u_3 = 67.5$ . Thus, for molecules with a small or zero dipole moment (these constitute the vast majority of the molecules of organic compounds) the molecular interaction energy is practically entirely due to the dispersion forces. Equation (1.45) can be rewritten in the form (1.37) by introducing the equilibrium distance  $r_e$  and energy  $u_e$ . The characteristic distance  $r_e$  for the van der Waals forces is 3–4 Å. At the same time, the exponential repulsive term in (1.45) produces a sufficiently rapidly increasing left-hand branch of the interaction energy curve (Fig. 1.13, Curve II), so that the mutual approach of non-valence-bound atoms is also sharply limited. This permits introducing the concept of intermolecular radii (see Sect. 1.4).

The van der Waals forces of molecular interaction are much weaker than the forces of the covalent, ionic, and metallic bonds. They may be called forces of weak interaction in contrast to the three types of strong bonds. These forces rapidly diminish with distance; the minimum of (1.45) is shallow and less prominent than for strong interactions (Fig. 1.12). Therefore the distances between non-valence-bounded atoms in crystal structures have (for a given pairs of atoms) a slightly greater spread than for strong bonds (see Fig. 1.50).

### 1.2.10 Hydrogen Bonds

One more variety of binding forces is known, the so-called hydrogen bond. It is formed between H atoms included in the groupings NH or OH and electronegative atoms of N, O, F, Cl, or S, which is denoted schematically as  $\text{AH} \dots \text{B}$ .

The localization of H atoms is sufficiently achieved by all three diffraction methods (Figs. 1.32, 35–37). The maximum of the potential, which corresponds to the position of the nucleus, is recorded by the electron diffraction technique. The value of the potential, which increases with reducing electron density of the shell, points to some positive ionization of the H atom in the H bond (Fig. 1.35). The position of the proton (or deuterium) and its thermal motion are determined by the neutron diffraction method (Fig. 1.36). The position of the electron cloud of H is determined by X-ray diffraction using difference syntheses of electron density. If the peaks of all the atoms, except H, are subtracted (Fig. 1.37, see also Fig. 2.64), it is usually found that the maximum of the electron density  $\rho_H$  does not coincide with the position of the proton but is shifted towards the atom with which H forms a covalent bond. Thus, according to spectroscopic and neutron diffraction data the C–H distance is 1.09 Å and the N–H distance about 1.00 Å, while the maximum of the electron density peak is located 0.1–0.2 Å closer to C or N atom. The shift of the maximum of  $\rho_H$  is attributed to the anisotropy and anharmonicity of thermal motion and the ionization of the H atom, especially when it is involved in the hydrogen bond. The “external” part of the H atom actually has a decreased electron density. The same is revealed by Fourier deformation difference syntheses with subtraction of the spherically symmetric electron density of the H atom (see Figs. 1.20, 33). This is manifested

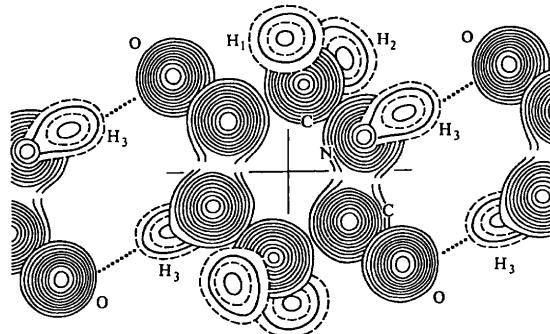


**Fig. 1.35.** Fourier synthesis map of the electrostatic potential of diketopiperazine constructed from electron diffraction data. Chains of molecules linked by hydrogen bonds in the crystal are clearly seen. Solid contours are drawn at 15 V, and dashed ones, at 7.5 V intervals. The potentials of the  $\text{H}_1$  and  $\text{H}_2$  atoms of the  $\text{CH}_2$  group are 32 and 33 V, and that of the  $\text{H}_3$  atom of the NH group involved in the  $\text{NH}-\text{H}$  hydrogen bond is 36 V, which points to its ionization [1.30].

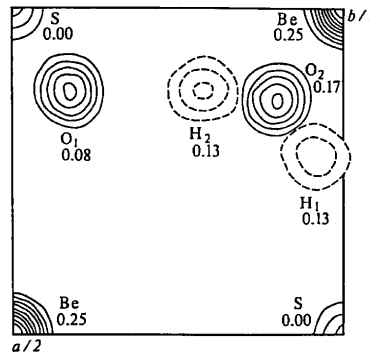


Fig. 1.36. Fourier synthesis of the nuclear density of  $\text{BeSO}_4 \cdot 4\text{H}_2\text{O}$ . The contours are drawn at intervals of  $0.46 \text{ cm} \cdot 10^{-12} \text{ \AA}^{-3}$ , the z coordinates of the nuclei are indicated [1.31]

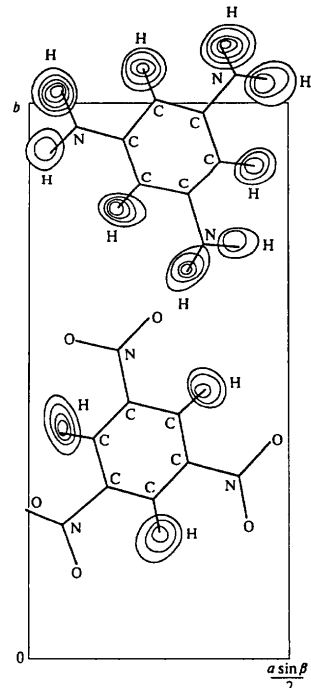


Fig. 1.37. Difference electron density map of the 1:1 complex of s-trinitrobenzene and s-triaminobenzene; the electron density of the hydrogen atom is shown [1.32]

in the deformation synthesis: the outer region has negative values of difference density.

The H bonds of molecules in liquids and gases are often responsible for the formation of dimers and, in crystals, also of chains (Fig. 1.35) or two- and three-dimensional nets; the latter are observed, for instance, in the structure of ice (Fig. 1.38). The hydrogen bond is directional, the atom *B* lies approximately on the continuation of the covalent bond *A*-H and is spaced not more than  $20^\circ$  from this straight line.

The distances in  $\text{NH} \dots \text{N}$  and  $\text{NH} \dots \text{O}$  bonds vary from 2.7 to 3.0 Å. The  $\text{OH} \dots \text{O}$  bonds are divided into short (2.45–2.6 Å) and long ones (up to 2.9 Å). According to X-ray data the O-H distances in hydrates of metal fluorides lie in the range of 0.7–1.0 Å, and the OH-F distance, 2.50–2.90 Å [1.33]. It can be seen that these distances are, as a rule, shorter than in van der Waals interactions between *A* and *B* atoms and are a priori shorter than in van der Waals H and *B* contacts. The energy of hydrogen bonds is slightly higher (i.e., they are stronger) than that of weak molecular interaction; it equals about 5–10 kcal/mol. The principal features of the hydrogen bond *AH*...*B* can be explained by assuming that the H atom in the *AH* grouping is partially ionized; according to various data, including X-ray and electron diffraction, it contains

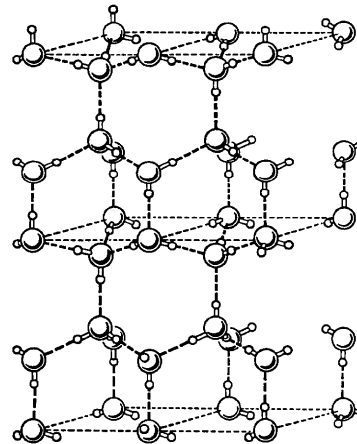


Fig. 1.38. The structure of ice. The hydrogen bonds  $\text{OH} \dots \text{O}$  are tetrahedral, the H atoms of one  $\text{H}_2\text{O}$  molecule are directed towards the lone electron pairs of the O atom of the other  $\text{H}_2\text{O}$  molecules (cf. Fig. 1.19)

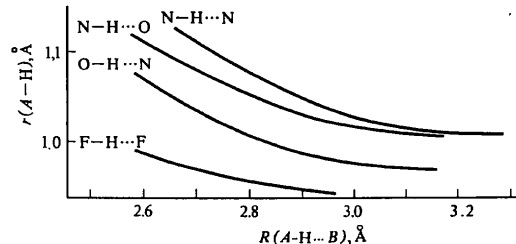


Fig. 1.39. Relationship between the length of the *A*-H bond and that of the hydrogen bond *A*-H...*B*

from 0.5 to 0.85 e. The ionization of the H atom promotes its attraction to electronegative atoms. In the structure of ice as well as in other structures with bonds of the type *AH*...*O* the proton is directed towards the sites of increased concentration of electrons of the O atom, i.e., towards its lone electron pairs. This is directly revealed in deformation difference syntheses of electron density (see Figs. 1.20, 37). At the same time the quantum-mechanical effect of the overlapping of the outer parts of the orbitals of the H and *B* atoms also takes place. The ionic nature of the hydrogen bond is also evident from the fact that its constituent molecules or groupings usually possess a dipole moment. This, among other things, may be responsible for the ferroelectric properties of some compounds with hydrogen bonds.

Accurate neutron diffraction determinations showed that the shorter (stronger) the *A*-H bond, the longer (weaker) is the hydrogen bond *A*-H...*B* (Fig. 1.39). The hydrogen bonds determine the structure and properties of many inorganic compounds, such as water, crystallohydrates, and ammoniates. Thus, the structure of ice (Fig. 1.38) is assigned by the "corner" arrangement of the H atoms in the water molecule at an angle of  $\sim 109^\circ$ , which is close to

tetrahedral. Here, H constantly moves from position OH...O to O...HO and back because they are equivalent, both of them being statistically occupied with a weight of 1/2. A similar effect occurs in the structure of  $\text{KH}_2\text{PO}_4$ ; the two potential wells between the atoms are equivalent, but as the temperature decreases the H atom stays in one of them. In the compound  $\text{KHF}_2$ , a strong hydrogen bond F-H-F with a spacing of 2.26 Å is formed; the two wells then merge together, so that the H atom finds itself between two F atoms, where it produces strong vibrations along the elongated potential well.

Hydrogen bonds are of great importance in many organic compounds. They determine many important features of the structures and functions of molecules of organic nature, such as proteins and nucleic acids (Sect. 2.9).

### 1.2.11 Magnetic Ordering

So far we have been considering the various forces of chemical bonds between atoms which lead to the formation of crystal structures. There is, however, one more type of interaction inherent in atoms possessing a magnetic moment, which results in additional interaction among them. In addition to ordered periodic arrangement of atoms in certain crystal structures, an order of a different kind is observed, namely a regular, consistent orientation of the magnetic moments of the atoms.

The resultant magnetic moment of the electron shell of an atom depends on its structure and the presence of uncompensated electron spins. Such a moment is inherent in atoms of the metals of the iron group, Fe, Co, and Ni with an uncompensated  $3d$  shell, as well as in atoms of rare-earth elements, Gd, Dy, Tb, Ho, and others with an uncompensated  $4f$  shell.

The time-average function of electron density  $\rho(xyz)$  is a scalar function of the coordinates. The magnetic moment of the atom is described by an axial vector or, what is the same, by the equivalent ring elementary current, whose plane is perpendicular to the indicated vector. The symmetry of the axial vector is  $\infty/m$  (Figs. 1.40, 41). Thus, the space distribution of the magnetic moment is a vector function of the coordinates  $j(xyz)$ . The description of the magnetic structure of a crystal thus includes, in addition to the electron density function,

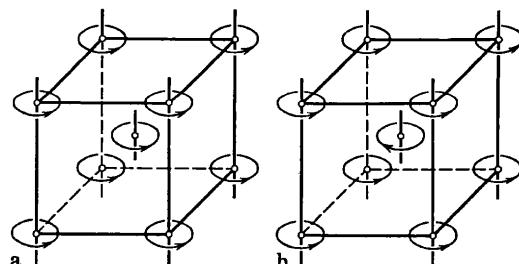


Fig. 1.40a, b. Magnetic ordering. Magnetic moment distribution in a ferromagnetic crystal of iron (a) and in an antiferromagnetic crystal of manganese fluoride (b)

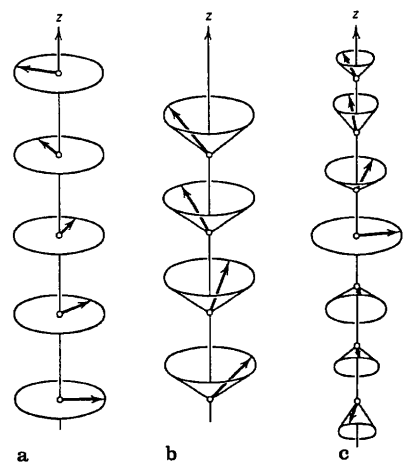


Fig. 1.41a-d. Helicoidal structures, simple spiral (a); ferromagnetic spiral (b); complex spiral (c); and static longitudinal spin wave (d)

the distribution of the magnetic moment of those atoms which have such a moment. It is usually sufficient to indicate the orientation of vectors  $j_i(r)$  with respect to the center of each such atom. Using neutron diffraction analysis, it is possible to find the distribution of the electrons with an uncompensated spin, the so-called spin density [Ref. 1.6, Fig. 4.99].

Spin interactions leading to a consistent orientation of magnetic moments are quantum mechanical in nature. The calculation of the hydrogen molecule (1.26–28) shows, for example, that an essential component defining the binding energy is the exchange integral  $H_{12}$  (1.27); two solutions corresponding to parallel and antiparallel spin orientation are possible.

Similarly, when the lattice contains atoms with an uncompensated spin, an exchange interaction arises and leads to magnetic ordering of the atoms. This ordering is manifested macroscopically in the ferro- or antiferromagnetic properties of the substance. The exchange energy of electrons may be either positive or negative. In the former case, parallel spin orientation corresponds to a decrease in the overall energy minimum (Fig. 1.40a). The summary magnetic moment of the unit cell is not equal to zero (this is a ferromagnetic system). In the latter case the spin arrangement is antiparallel, and the summary magnetic moment of the cell is equal to zero (this is an antiferromagnetic system) (Fig. 1.40b).

Since magnetic interactions are weak and do not affect ordinary chemical interactions in crystals, the magnetic structure of crystals exists within the framework of the ordinary crystal structure, but does not necessarily coincide with it. The periods of the magnetic structure ("the magnetic unit cell") may coincide with those of the ordinary cell (then sometimes called a "crystallochemical" cell), but may also be its small multiples (double, triple, quadruple) in

a certain direction. As we already know (see [Ref. 1.6, Figs. 2.98, 99]), the symmetry of magnetic structures is described by groups of antisymmetry or, more generally, of color symmetry. Point antisymmetry groups give a macroscopic description of magnetic structures (31 groups describe ferromagnetics, and 59 groups, antiferromagnetics). There are 275 space groups of antiferromagnetics out of all the Shubnikov groups, and 629 antiferromagnetic groups [1.34]. Another approach to the description of magnetic structures is based on the theory of the representations of point or space groups [1.35]. As explained in [Ref. 1.6, Chap. 2], the two approaches are essentially equivalent, because the groups of generalized symmetry can be based on representations of groups of ordinary symmetry.

Apart from ferromagnetic and antiferromagnetic ordering, there are other types of magnetic ordering. Ferrimagnetism is an intermediate type. In it the magnetic moments of atoms are antiparallel, but different in magnitude, so that the resultant moment of the magnetic unit cell is nonzero. Along with uniaxial antiferromagnetics one encounters multiaxial ferrimagnetics with a pairwise-antiparallel arrangement of spins in several orientations, as well as "polygonal" structures.

Besides the types of orientation which can be fitted into the theory of generalized crystal symmetry, in which the magnetic cell is a multiple of the ordinary cell, there are types of ordering which are not associated with the periodic arrangement of atoms (incommensurate structures, see Sect. 1.6.5). These are the various helicoidal orderings (Fig. 1.41a-d). They have the following structure. The magnetic moments turn gradually along the axis of a helicoid. They may be perpendicular to this axis (Fig. 1.41a) or inclined to it (Fig. 1.41b) (umbrella structures). The inclination and rotation angles may gradually change (Fig. 1.41c). Otherwise their direction may coincide with the axis varying periodically in their magnitude and direction along and against the axis (Fig. 1.41d). In describing such structures, the one-dimensionally periodic groups  $G_1^3$  can be used.

For complex magnetic structures, the theory of exchange interactions and ordering is no longer restricted to taking into account the direct contact of magnetic atoms (sometimes there is no such contact at all), but gives due consideration to contact with order atoms as well ("indirect exchange"). This helps to explain magnetic "long-range action" and ordering in complex oxides, fluorides, and other metallic compounds from the group of iron and rare-earth elements.

Since the magnetic interaction energy is low, as indicated above, magnetic ordering is destroyed by thermal motion, while the crystal structure proper remains intact. This occurs at definite points of magnetic phase transitions.

By now, over a thousand magnetic structures have been investigated. A more detailed discussion of the relationship between ordering and the domain structure of magnetic materials and the macroscopic magnetic properties of crystals will be given in [1.7].

## 1.3 Energy of the Crystal Lattice

### 1.3.1 Experimental Determination of the Crystal Energy

The free energy  $F$  of a system of atoms forming a crystal structure consists of the potential energy of the chemical bond  $U$  between the atoms (cohesion energy) and the free energy of thermal motion  $F_T$

$$F = U + F_T. \quad (1.46)$$

To decompose a crystal into atoms at the temperature of absolute zero and separate them to an infinite distance from each other requires work equal to the potential energy of the chemical bond taken with the opposite sign —  $U$ . This energy in terms of 1 mole (or gram atom) of the substance is precisely the energy of the crystal (the energy of the complete dissociation of the crystal — i.e., of its "atomization"), which is by tradition called the "lattice energy." For elements, metals and alloys, and covalent structures the crystal energy is equal to the heat of sublimation  $S$  at absolute zero. The heat of sublimation, in turn, is equal to the sum of the heat of evaporation  $E$  and the heat of fusion  $F$ , plus the heat of dissociation of the molecules  $D$ , provided they arise in evaporation or sublimation,

$$-U = S + D = E + F + D. \quad (1.47)$$

For molecular crystals, it is natural to use molecules, rather than atoms, as structural units; accordingly, the energy of breaking the intermolecular bonds should be used for the lattice energy; it is equal to the heat of sublimation  $S$  or to the sum  $E + F$  at absolute zero. Thus, theoretical calculations of the lattice energy can be compared with the experimental data.

Historically, the first calculations were made for ionic crystals; their lattice energies implied the energy  $U_i$  of the dissociation of such a crystal into ions, rather than atoms. It is obvious that  $U_i$  differs from  $U$  (1.47) by the ionization energies of cations  $I^+$  and the affinity  $I^-$  of anions for electrons

$$-U_i = S + D + I^+ - I^-. \quad (1.48)$$

Experimental values of  $U_i$  for ionic crystals can be obtained by means of the so-called Born-Haber circular process, which is shown in Fig. 1.42 for a compound of the type  $MX$ , where  $M$  and  $X$  are single-charged ions (for instance, NaCl). The energy values in all the stages of the process (except  $I^+$  and  $I^-$ ) reflect the change in the heat content in corresponding reactions at 298 K. From the figure it follows that

$$-U_i = Q + S + I^+ + \frac{D}{2} - I^-. \quad (1.49)$$

Molecular crystals have the lowest lattice energies (on decomposition to molecules),  $U \sim 1-5$  kcal/mol. The lattice energy  $U$  of elements ranges from several

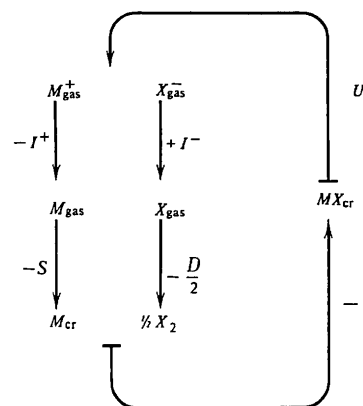


Fig. 1.42. Born-Haber cycle

tens to a hundred kilocalories per gram atom. For instance, it is equal to 130 kcal/g at. for B, 26 for Na, 170 for C, 42 for Ca, 101 for Co, 26 for I, and 160 for Os. The lattice energy of ionic and covalent crystals is of the order of hundreds of kilocalories per mole.

### 1.3.2 Calculation of the Potential Energy

Finding the free energy of a crystal is a key factor in determining all the thermodynamic functions and other characteristics of the crystal structure, in particular, its lattice parameters, various physical constants, etc.

If we vary  $F(1.46)$  for an arbitrary arrangement of atoms, corresponding then to the equilibrium crystal structure, there is the deepest minimum of  $F$ , at which

$$\delta F = \delta U + \delta F_T = 0. \quad (1.50)$$

The principal contribution to (1.46) is made by lattice energy  $U$ ; the condition  $\delta U = 0$  determines the arrangement of atoms in a given lattice at absolute zero. Finding the equilibrium arrangement of atoms in a crystal is a complicated task; in calculating the lattice energy it is usually assumed that the atomic coordinates are known, although it is possible to solve the more complex problems as well. It is also clear that if we neglect the free energy of thermal motion, we cannot solve the problem of phase transitions and polymorphism in solids. We shall elaborate on this in Chap. 4; meanwhile, we shall consider the possibilities of potential energy computations.

Quantum-mechanical calculations of the crystal energy are rather intricate, but calculations of  $U$  become reasonably straightforward if pairwise interactions are assumed and semiempirical expressions for energies of the type (1.16, 40) or their variations are used.

Thus, assuming that the interatomic forces are central and the atom–atom interaction potential energy has the form

$$u_{ik} = u_{ik}(r_{ik}), \quad (1.51)$$

i.e., that they are independent of each other, the potential energy of any atomic association in a crystal can be represented by a sum of such expressions. It is a good approximation for all types of bonds, except the metallic. Therefore, for pairwise interactions (for instance, for electrostatic ones) the total potential energy is the sum of interatomic potentials over all the possible pairs

$$U = \frac{1}{2} \sum_{i,k} u_{ik}(r_{ik}). \quad (1.52)$$

For  $n$  atoms, the sum (1.52) contains  $n(n - 1)/2$  terms, the factor 1/2 arising since each function  $u_{ik}$  refers to a pair of atoms. Functions (1.51) decrease rapidly and make an appreciable contribution only at  $r_{ik}$  not exceeding 10–20 Å, which reduces the number of terms in the sum, nevertheless leaving it rather considerable.

In the case of a covalent bond an atom interacts almost exclusively with its nearest neighbors, and therefore only the terms  $u_{ik}(r_{ik})$  of the interaction between such covalently bound pairs of atoms can be taken into consideration in sum (1.52). For a metallic bond, the pairwise interactions are not considered when the calculations are made in terms of one atom, for instance by (1.41), and the whole lattice is actually taken into account.

Energy calculations are simplest if the compound is homodesmic, i.e., if it has one type of bond, and if its chemical composition is not complicated. Then the number of terms in  $u_{ik}$  (1.51) is not large. As the crystal structure is periodic, summation (1.52) can be performed over the atomic arrangement within a unit cell, and then over the cells. These sums are called lattice sums.

The first, and now classical calculations of the ionic energy of lattices  $U_i$  were carried out by M. Born and his associates. Let us consider such a calculation for a NaCl-type lattice. We find lattice sum (1.52) for the first – electrostatic – term. The environment of any Na or Cl atom is the same. Each of them is surrounded by six neighbors of opposite signs at a distance of  $r = d(AB)$ , then by 12 neighbors of the same sign at a distance of  $r\sqrt{2}$ , then by eight neighbors of opposite signs at a distance of  $r\sqrt{3}$ , and so on (Fig. 1.13). Consequently, the electrostatic energy of interaction of one atom of a NaCl-type structure with the other atoms of the lattice is

$$U = \frac{e^2}{r} \left( 6 - \frac{12}{\sqrt{2}} + \frac{8}{\sqrt{3}} - \frac{6}{\sqrt{4}} + \frac{24}{\sqrt{5}} - \dots \right) = \frac{e^2}{r} M. \quad (1.53)$$

The series in (1.53) converges rapidly; the value  $M$  is called Madelung's constant. Its value in (1.53) for a NaCl-type structure is 1.748; for other structural types, the values of  $M$  are as follows: 1.76 for CsCl, 5.04 for CaF<sub>2</sub>, 1.64 for ZnS, 4.38 for CdI<sub>2</sub>, and 24.24 for Al<sub>2</sub>O<sub>3</sub>. (In the case of non-univalent ions,  $M$  includes, as

a factor, the product of the formal charges of cation and anion.) In addition to the electrostatic energy of attraction and repulsion, which is covered by the sum (1.53), we should take into account the contribution of the repulsive forces between the electron shells – the second term in (1.15) of the type  $r^{-n}$ . Similarly to  $M$  in (1.53), factor  $M'$  will arise, but since the repulsive forces decay rapidly with distance,  $M'$  depends almost only on the nearest neighbors of the given atom. In the final analysis, taking into consideration that in the case under review all the atoms make an identical contribution to the total lattice energy and also assuming that there are  $N$  such atoms in a gram molecule, we get

$$-U_i(r) = N(Me^2r^{-1} - M'br^{-n}). \quad (1.54)$$

The second term in (1.54) is small compared with the first. Thus, Born's equation (1.54) helps to calculate the lattice energy in high-symmetry ionic crystals. A comparison of the calculated values with the experimental data is given in Table 1.3.

In the case of single-charged ions the agreement is good, which supports the theoretical conclusions. When the ion charge increases, the agreement becomes worse, but is still satisfactory. In the light of the available data, however, it cannot be regarded as a confirmation of Born's theory. Indeed, the ion charge in such compounds, for instance, in  $\text{Al}_2\text{O}_3$ , does not coincide with the formal valency and is nonintegral. On the other hand, determination of  $U_i^*$  for such compounds according to the Born–Haber cycle (1.49) is also inconsistent, because it includes the electron “affinity” of a multicharge ion, which in fact does not exist. Besides, for the last compounds given in Table 1.3 there is a considerable fraction of covalent bond.

If we assume that the equation for the potential energy of pairwise interactions has the form (1.16) or (1.41), its parameters can be found from macroscopic measurements of the crystal. Thus, substitution of (1.16) into (1.52) yields

$$U = \frac{a}{2} \sum_{ik} r_{ik}^{-m} + \frac{b}{2} \sum_{ik} r_{ik}^{-n}, \quad (1.55)$$

and the four parameters  $a$ ,  $b$ ,  $m$ , and  $n$  can be found from the experimental values of the lattice energy, the molar volume, the compressibility, and the thermal expansion of the crystal.

The Born equation (1.53) was simplified by A. F. Kapustinsky who used the following considerations. The value of  $M$  for different structures can be replaced by a near-constant coefficient if it is referred to the sum of ions  $\Sigma$  in the formula

**Table 1.3.** Comparison of the experimental and theoretical values of ionic energy of some crystal lattices (in kcal/mol)

$U_i$	LiF	NaCl	RbI	CaF <sub>2</sub>	MgO	PbCl <sub>2</sub>	Al <sub>2</sub> O <sub>3</sub>	ZnS	Cu <sub>2</sub> O	AgI
Experiment $U_i$	242	183	145	625	950	521	3618	852	788	214
Theory $U_i$	244	185	149	617	923	534	3708	818	644	190

unit. Then

$$U = 256 \frac{Z_1 Z_2 \gamma}{d(AB)} [\text{kcal/mol}]. \quad (1.56)$$

This equation deviates from expression (1.54) by about 1%–3%. The energy of interaction of a definite ion with the lattice as a whole, which can be calculated by (1.56) in the simplest cases, should not depend strongly on the particular structure. Therefore A. E. Fersman suggested that this energy should be regarded approximately as a constant increment of a given ion, and named that increment the “energy constant” (EC). The values of EC for some ions are as follows:

K <sup>+</sup>	Na <sup>+</sup>	Li <sup>+</sup>	Cu <sup>+</sup>	Ba <sup>2+</sup>	Fe <sup>2+</sup>	Mg <sup>2+</sup>	Al <sup>3+</sup>	F <sup>-</sup>	Cl <sup>-</sup>	Br <sup>-</sup>	O <sup>2-</sup>	S <sup>2-</sup>	N <sup>3-</sup>
0.36	0.45	0.55	0.70	1.35	2.12	2.15	4.95	0.37	0.25	0.22	1.55	1.15	3.60

In this approximation the lattice energy is simply equal to  $U = 256 \Sigma \text{EC}$ . This equation, as well as (1.56) or its slightly more complicated versions, is approximate because it is based on the concept of a pure ionic bond in all cases and overstates the share of energy contributed by multicharge ions. Yet it enables one to estimate the energy of complicated structures, for instance, minerals, which is essential to geochemistry.

In the years following the development of M. Born's classic theory, calculations of the crystal lattice energy were carried out for many crystals on the basis of more accurate approximations of the interaction potentials, mainly for the repulsive term, and also on the basis of quantum-mechanical considerations. In these calculations the repulsive potential has a more accurate form,  $\exp(-\alpha r)$  (1.36), due consideration being given to van der Waals, dipole–dipole (1.44), and multipole interactions, to the zero vibrations of the lattice, and, finally, to the so-called many-particle interactions, i.e., the overlapping of remote regions of the wave functions of atoms not only with the nearest, but also with the next nearest neighbors.

Thus, for NaCl the electrostatic term (1.53) is 205.6 kcal/mole, van der Waals attraction, 5.7, repulsion energy, 24.9, zero energy, 1.4, and the total ionic energy of the lattice  $U_i = 185.2$  kcal/mole at 298 K, which practically agrees with experiment.

Quantum-mechanical calculations of crystal energy require solving the Schrödinger equation and can be carried out, as mentioned above, for a lattice on the basis of the MO–LCAO method with expansion of Bloch's functions (1.35).

For ionic crystals, the first electrostatic term (1.52) appears, in a further quantum-mechanical consideration, in the same form, while the other components are the energy due to consideration of the extended (as opposed to the pointlike) distribution of the ion charge and the covalent exchange energy corresponding to (1.27). The most comprehensive calculations with an allowance for the various corrections, not only give the values of the lattice energy, but also allow one to calculate the equilibrium interatomic distances  $r$ , i.e.,

ultimately the parameters of the lattice. This can be done by varying the value of  $r$  in the expressions for the energy and finding its minimum. Thus, for LiF it was found that  $d(\text{LiF}) = 2.01 \text{ \AA}$  ( $d_c = 2.00 \text{ \AA}$ ). Since the terms appearing in the ultimate expression are large and have different signs, the theoretical and experimental energy calculations sometimes disagree.

Energies  $U_a$  (atomization) for some crystals (including the ionic ones) are given in Table 1.4. Recall that  $U_a$  is always less than  $U_i$  by  $-I^+ + I^-$  (1.48). For instance,  $U_a^{\text{exp}}$  is equal to 242 kcal/mol for LiF and 950 kcal/mol for MgO (see Table 1.3).

For covalent crystals, exact energy calculations are naturally possible only on the basis of quantum-mechanical considerations. A simplified calculation can be made in the pairwise-interaction approximation (1.52), where the terms corresponding to the nearest neighbors remain, and the summation can be reduced to the interaction of neighbors in a single unit cell. The energies of covalent crystals are high, for instance,  $U = 170 \text{ kcal/g}$  at for diamond.

For metals, quantum-mechanical calculation actually yields the lattice energy per atom. The values of coefficients  $a$ ,  $b_1$ , and  $b_2$  in equation (1.41) are obtained by summation of several terms of equal degrees but with different signs; therefore, they are not reliable enough, and the theoretical and the experimental values of  $U$  do not always agree sufficiently well (Table 1.5).

Using lithium as an example we can illustrate the above-mentioned difference between the interaction energy of a pair of atoms characterized by the potential curve  $u(r)$  and that of identical atoms in the lattice, when the equilibrium distance is determined by condition  $dU/dr = 0$ , rather than by  $du/dr = 0$ . In the  $\text{Li}_2$  molecule, the binding energy is equal to 1.14 eV, and distance  $r_e$  is about 2.7 Å. In a lithium crystal  $U = 1.7 \text{ eV}$ , and the interatomic distance is greater, 3.03 Å. Although the energy of a metal lattice cannot be represented as a sum of pairwise interactions, the formal division of 1.7 eV by 12 yields 0.14 eV

**Table 1.4.** Comparison of experimental and theoretical values of atomization energy for certain crystals (in kcal/mol)

Substance	LiF	NaCl	KI	MgO	CaF <sub>2</sub>	AgI	Al <sub>2</sub> O <sub>3</sub>	SiO <sub>2</sub>
Experiment $U_a$	199	150	122	239	374	108	730	445
Theory $U_a$	202	152	125	262	428	116	695	416

**Table 1.5.** Comparison of experimental and theoretical values of lattice energy for certain metals (in kcal/mol)

Substance	Li	Na	K	Cu	Be
Experiment	39	26	23	81	75
Theory	36	24	16	33	36–53

(each Li atom has 12 neighbors), and thus helps to estimate the weakening of “individual” bonds, with an ultimate gain in the crystal lattice energy compared with the molecule. A similar effect of an increase in interatomic distances and energy gain compared with molecules is also observed for ionic crystals. At the same time rigid covalent bonds only slightly change their characteristics in molecules and crystals.

### 1.3.3 Organic Structures

For the simplest crystals with van der Waals bonds the calculation of the lattice energy by (1.45–52) gives satisfactory agreement with experiment (Table 1.6).

Since the van der Waals forces rapidly decrease with distance, it is sufficient to sum (1.52) over the atomic pairs within a sphere of radius 10–15 Å.

For complicated molecules, a good approximation of the potential of the forces acting between atoms of different molecules is (1.45), the “6 exp” potential. Thus, to compute hydrocarbon structures it will suffice to find the constants in (1.45) for three types of interaction, C and C, C and H, and H and H, proceeding from the experimental data for several typical structures. Then, assuming these potentials to be universal, it is possible to use them for analyzing all the known or new structures of this type. If the molecules have a dipole or quadrupole moment, one can also compute the corresponding electrostatic interaction; the hydrogen bonds can also be accounted for with the aid of an potential curve.

With this approach [1.36], a sufficiently good physical model of an organic crystal can be obtained and its structure and properties described. The simplest problem is to calculate the potential energy, i.e., the heat of sublimation for a given structure. Here, we obtain satisfactory agreement with experiment, for instance, for benzene  $U_{\text{exp}} = 11.0 \text{ kcal/mol}$ , and  $U_{\text{theor}} = 11.7 \text{ kcal/mol}$ . In general, when the structure’s energy is described by (1.52) on the basis of atom–atom potentials of the type (1.45),  $U$  is found to be a multidimensional function of the periods  $a$ ,  $b$ ,  $c$  and angles  $\alpha$ ,  $\beta$ ,  $\gamma$  of the unit cell, the coordinates of the centers of gravity of the molecules in the cell  $x_i$ ,  $y_i$ ,  $z_i$ , and the Eulerian angles  $\theta$ ,  $\varphi$ , and  $\psi$ , which assign the orientation of the molecules,

$$U = U(a, b, c, \alpha, \beta, \gamma, x_1, y_1, z_1, \theta_1, \varphi_1, \psi_1, x_2, y_2, z_2, \theta_2, \varphi_2, \psi_2, \dots). \quad (1.57)$$

The structure at absolute zero corresponds to the minimum of this multidimensional function. It is difficult to solve the problem in the general form, and one can investigate the shape and minima of the energy surface only by changing

**Table 1.6.** Comparison of experimental and theoretical values of lattice energy for some substances (in kcal/mol)

$U$	Ne	Ar	O <sub>2</sub>	CH <sub>4</sub>	Cl <sub>2</sub>
Experiment	0.52	1.77	0.74	2.40	6.00
Theory	0.47	1.48	1.48	2.70	7.18

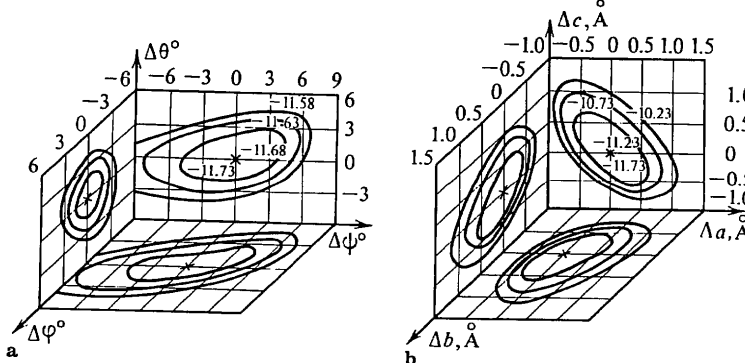


Fig. 1.43a, b. Cross sections of  $u(\theta, \varphi, \psi)$  (a) and  $u(x, y, z)$  (b) at the minimum of the energetic surface of benzene. The energy values are indicated in kcal/mol [1.36]

some variables and assuming the others to be fixed. For instance, knowing the unit cell and the space group of a crystal, one can seek the orientation of the molecules. Thus, for benzene the minimum actually gives agreement between the calculated and observed orientation with an accuracy to  $1^\circ$ – $3^\circ$ . It is also possible to find the parameters of the unit cell with a given orientation of the molecules (Fig. 1.43) or both the unit cell and the orientation with a given space group and the number of molecules in the cell, and thus one can assign in (1.57)  $x, y, z, \theta, \varphi, \psi$  of only one molecule, while for the others the same values depend on the symmetry elements.

Proceeding from an analysis of the shape of the minimum we can compute the physical characteristics of a crystal, for instance,  $\partial^2 U / \partial x_i^2$  defines the elasticity coefficients and the shape of the surfaces of compression along different directions. It is possible to identify the characteristics of the spectrum of intermolecular vibrations, and so on. By stating the problem as in (1.57) the existence of the crystal structure is postulated beforehand by introducing the unit cell parameters. In principle, one can try to simulate the very origin of three-dimensional periodicity, i.e., of the crystal, so that the cell and symmetry are obtained automatically, by calculating  $U$  with assigned interaction of a sufficiently large number of atoms or molecules.

Recall that the minimum of  $U$  corresponds to the structure at the temperature of absolute zero. The structure of a given phase may remain unaltered (experiencing only thermal expansion) up to the melting point. In other cases, a change in structure – a phase transition – may take place. This is due to the contribution of the free energy of the thermal motion of atoms or molecules to the general expression (1.46) (for more details see Sect. 4.3).

## 1.4 Crystallochemical Radii Systems

### 1.4.1 Interatomic Distances

Entering into a chemical bond and forming a crystal, atoms arrange themselves at definite distances from each other. The experimental data on crystal structures prove that interatomic distance  $d(AB)$  between a given pair of atoms  $A$  and  $B$  in one type of a chemical bond remains constant with an accuracy to about  $0.05$ – $0.1$  Å in all structures, i.e., it is practically independent of the given structure. This distance corresponds to the minimum of the curve for the potential interaction energy (Fig. 1.12) of a given pair of atoms in the crystal.

Each atom has its own spatial distribution of electrons, which, even for outer electrons, changes comparatively little with the formation of a strong chemical bond, to say nothing of the weak van der Waals bond. Therefore it is possible, as a first approximation, to assign certain “sizes”, i.e., certain constant “radii” to atoms, depending on the type of bond, so that the distances between different pairs of atoms are sums of these values. This is called the additivity of the crystallochemical radii. Once established, crystallochemical radii are well maintained in newly discovered structures, i.e., they possess the power of prediction. Thus, the huge amount of experimental data on interatomic distances accumulated in structural investigations is generalized in the radii systems. At the same time, as we shall see below, the very concept and the concrete values of crystallochemical radii are, in a sense, conventional.

The concept of crystallochemical radii has been developed by many crystallographers and geochemists; the trail was blazed by Bragg, who proposed the first system of radii in 1920 [1.37]. A considerable contribution to this area was made by Goldschmidt [1.38] and later by other researchers, who compiled various tables of radii. New improvements in radii systems have been introduced in recent years.

### 1.4.2 Atomic Radii

By considering the interatomic distances in the structures of elements it is easy to construct a system of the atomic radii of the elements  $r_{\text{at}}$ . This quantity is equal to half the shortest interatomic distance (Fig. 1.44)  $r_{\text{at}} = 1/2 d(AA)$ . In the structures of elements (Sect. 2.1) the atoms are bound by a metallic or covalent bond; therefore, the set of atomic radii can be subdivided into  $r_m$  and  $r_c$  according to the type of bond. Experiments confirm the additivity of such radii also for the structures of compounds with the corresponding type of bond. For instance, the C–C distance in diamond is equal to 1.54 Å, i.e., the covalent radius (of a single bond) of carbon is 0.77 Å. The Si–Si distance in silicon is equal to 2.34 Å, whence the corresponding radius is 1.17 Å. The observed Si–C distance in silicon carbide, 1.89 Å, is in good agreement with the sum  $r(C) + r(Si) = 1.94$  Å. Thousands of such examples can be quoted. The same is

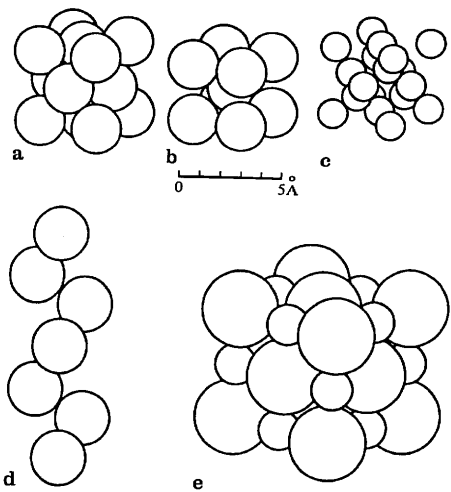


**Fig. 1.44a–e.** Simplest structures depicted as contacting spheres. (a) Cu; (b)  $\alpha$ -Fe; (c) diamond; (d)  $\alpha$ -Se; (e) NaCl. In the structures of elements the sphere radius  $r_{\text{at}}$  is defined as half the interatomic distance. The radii of spheres in structures of different atoms (NaCl) are determined on the basis of the additivity principle in series of structures and other data

true for metallic radii. For instance,  $r(\text{Nb}) = 1.45 \text{ \AA}$ ,  $r(\text{Pt}) = 1.38 \text{ \AA}$ ,  $\Sigma r = 2.83 \text{ \AA}$ , and the distance between these atoms in the compound is  $2.85 \text{ \AA}$ . When constructing the system of metallic radii, the data on the distances between different metallic atoms in intermetallic compounds are also taken into consideration. Thus,

$$d(AB) \approx r_{\text{at}}(A) + r_{\text{at}}(B). \quad (1.58)$$

The system of atomic radii is presented in Table 1.7 and Fig. 1.45. Interatomic distances with a given type of bond vary to some extent, depending on the coordination. They decrease with decreasing coordination number (c.n.), each bond becoming stronger and, hence, shorter. For metals, the  $r$  values in Table 1.7 are given for c.n. 12; the decrease in distance for other c.n. is as follows: c.n. 8 by 2%, c.n. 6 by 4%, and c.n. 4 by 12%.

The covalent bond is directional. The lengths of these bonds and the relevant resulting coordinations depend on the bond multiplicities. For C, N, O, and S the shortening of  $r_c$ , as compared with the single bond, equals 12%–14% for a double bond, and 20%–22% for a triple bond. The dependence of the length of the C–C bond on order (including intermediate-order bonds) is presented in Fig. 1.46. Tetrahedral single covalent bonds are very common. The corresponding system of radii is given in Table 1.13.

As has already been mentioned, the equilibrium interatomic distance for a covalent and metallic bond corresponds to a strong overlapping of the outer shells, which is illustrated by the scheme of overlapping radial density functions in Fig. 1.29 and 1.33. Therefore the atomic radii (1.58) are approximately equal to the orbital radii (1.13) of the outer shells

$$r_{\text{at}} \approx r_o, \quad d(AB) \approx r_o(A) + r_o(B). \quad (1.59)$$

Period	Subgroup																
	Ia	IIa	IIIa	IVa	Va	VIIa	VIIIa	1b	IIb	IIIb	IVb	Vb	VIIb	VIIIb			
1													H 0.46	He 1.22			
2	Li 1.55	Be 1.13											B 0.91	C 0.77	N 0.71	O 1.60	
3	Na 1.89	Mg 1.60											Al 1.43	Si 1.34	P 1.3	S 1.6	Cl 1.92
4	K 2.36	Ca 1.97	Sc 1.64	Ti 1.46	V 1.34	Cr 1.27	Mn 1.30	Fe 1.26	Co 1.25	Ni 1.24	Cu 1.28	Zn 1.39	Ga 1.39	Ge 1.48	As 1.6	Se 1.98	
5	Rb 2.48	Sr 2.15	Y 1.81	Zr 1.60	Nb 1.45	Mo 1.39	Tc 1.36	Ru 1.34	Tc 1.34	Ru 1.37	Pd 1.44	Os 1.56	In 1.66	Sn 1.58	Te 1.61	Br 1.7	Kr 2.18
6	Cs 2.68	Ba 2.21	La 1.87	Hf 1.59	Ta 1.46	W 1.40	Re 1.37	Os 1.35	Ir 1.35	Pt 1.38	Au 1.44	Hg 1.60	Tl 1.71	Pb 1.75	Bi 1.82	Po 1	Xe 1
7	Er 2.80	Ra 2.35	Ac 2.03														Rn 1.74
Lanthanides			Ce 1.83	Pr 1.82	Nd 1.82	Pm 1.81	Sm 1.81	Eu 2.02	Gd 1.79	Tb 1.77	Dy 1.76	Ho 1.75	Er 1.74	Tu 1.93	Yb 1.74	Lu 1.74	
Actinides			Th 1.80	Pa 1.62	U 1.53	Np 1.50	Pu 1.62	Am 1.62	Cm 1.62	Bk 1.62	Cf 1.62	Fm 1.62	Md 1.62	(No) 1.62	Lr 1.62		

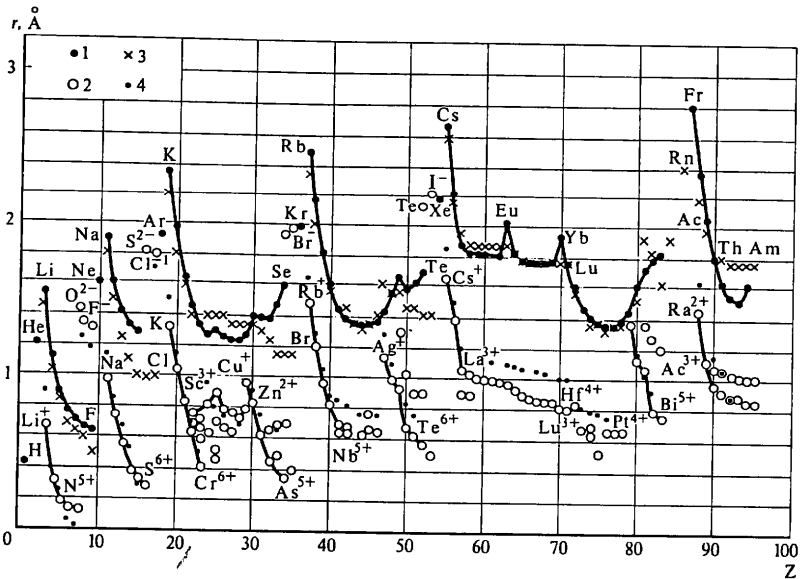


Fig. 1.45. Systems of crystallochemical radii. (1) atomic radii  $r_{at}$ ; (2) ionic radii  $r_i$ ; (3) atomic-ionic radii  $r_a$ ; (4) physical ionic radii  $r_{ph}$  (in the graph they are given for the maximum valence and c.n. 6 or for the maximum c.n. for the given element if it is less than 6)

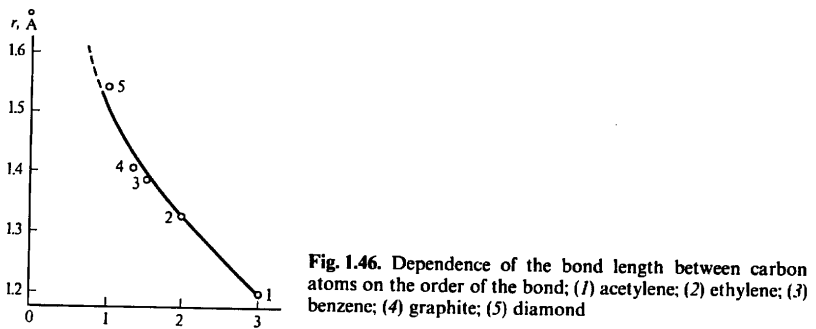


Fig. 1.46. Dependence of the bond length between carbon atoms on the order of the bond; (1) acetylene; (2) ethylene; (3) benzene; (4) graphite; (5) diamond

The curves of the atomic radii versus the atomic number are defined by the structure of the electron shells of the atom, and the graph of Fig. 1.45 is close to that of the orbital radii in Fig. 1.10. Both graphs reflect the rules for the filling of electron shells. The appearance of a new shell (the beginning of a period) increases  $r_{at}$ ; then, with increasing  $Z$  inside the period,  $r_{at}$  is reduced because the Coulomb forces of attraction of the electrons to the nucleus become stronger.

Towards the end of the large periods the increase in the number of electrons nonetheless gradually increases  $r_{at}$ . The filling of the inner shells either slightly affects  $r_{at}$  or, in lanthanides and actinides, reduces them.

As the orbital radii  $r_o$  (1.12) characterize the free atoms, and the overlapping of the outer shells of nonexcited atoms is only an approximation for calculating the equilibrium interatomic distance, from which  $r_{at}$  is found, the agreement between the graphs of  $r_{at}$  in Fig. 1.45 and  $r_o$  in Fig. 1.10 is not complete. A comparison of Tables 1.1 and 1.7 and of Figs. 1.10 and 1.45 shows that the orbital radii  $r_o$  approximately coincide with the atomic radii  $r_{at}$  for the beginning and the middle of the periods, respectively. At the end of each period,  $r_o$  continues to fall off with increasing  $Z$ , while the atomic radii  $r_{at}$  of period III decrease slower than the  $r_o$ , and the  $r_{at}$  in the larger periods IV, V, and VI even begin to increase. For some elements (for instance, Ag, Sb, Te, Hg, Ta, Pb, Bi) the divergences may reach several tenths of an Angstrom. This can evidently be explained by the insufficiency of the pure AO model for these elements; thus it is necessary to take into account the interactions of their electron shells in crystals, and the corresponding changes in energy levels.

#### 1.4.3 Ionic Radii

By analogy with the system of atomic radii, it is possible to construct a system of ionic radii  $r_i$  for ionic compounds. The procedure of establishing them from the interatomic distances is, however, ambiguous. To find  $r_i$ , use is made of the cation-anion distances in a series of isomorphous (i.e., identically built) structures. Classical series of this kind are those of cubic structures of halides of alkali metals and also of some oxides. Figure 1.44 depicts the structure of NaCl, and Fig. 1.47, a series of face-centered structures isomorphous to it (three structures – CsCl, CsBr, and CsI – are built differently; the anion atom centers the cube, not its face). From the observed cation-anion ( $A-B$ ) distances

$$d(A_1B) = r_i(A_1) + r_i(B), \quad d(A_{II}B) = r_i(A_{II}) + r_i(B)$$

one finds the differences in cation sizes

$$r_i(A_1) - r_i(A_{II}) = d(A_1B) - d(A_{II}B) \quad (1.60)$$

and, similarly, from  $d(AB_1)$  and  $d(AB_{II})$ , those of the anions

$$r_i(B_1) - r_i(B_{II}) = d(AB_1) - d(AB_{II}). \quad (1.61)$$

It is clear that in order to establish a definite system one must either have  $r_i$  of some atoms as a "reference" or employ some other data. Indeed, if a certain system of  $r_i$  helps to calculate the interatomic distances

$$d(AB) = r_{cat} + r_{an}, \quad (1.62)$$

then the system of radii

$$r'_{cat} = r_{cat} \pm \delta, \quad r'_{an} = r_{an} \mp \delta, \quad (1.63)$$

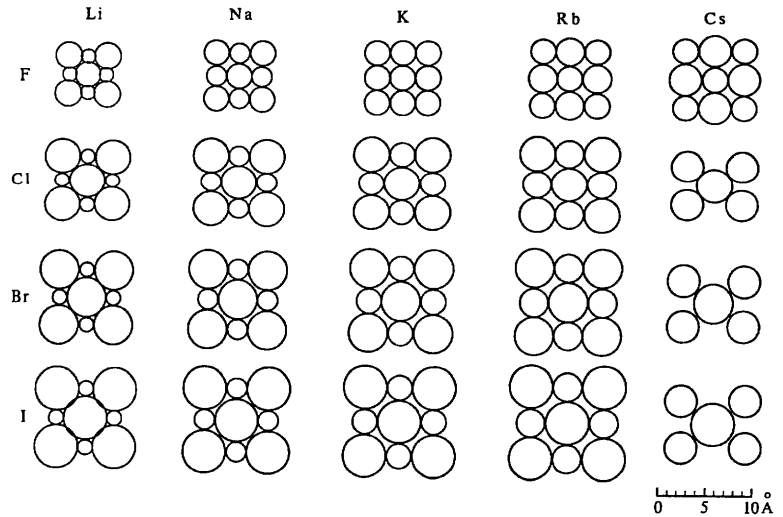


**Fig. 1.47.** Arrangement of ions with radii  $r_i$  in the (100) face of the cubic unit cell of the alkali-halide structures. For the structures of CsCl, CsBr, and CsI, the arrangement of the ions in the diagonal (100) plane is shown

would give the same distances

$$d(AB) = r'_{\text{cat}} + r'_{\text{an}}. \quad (1.64)$$

Proceeding from the data on molar refraction, Goldschmidt [1.38] assumed that the ionic radius of the fluoride anion  $r(F^-) = 1.33 \text{ \AA}$  and that of oxygen  $r(O^{2-}) = 1.32 \text{ \AA}$ . Pauling [1.39, 40] adopted crystals of NaF, KCl, RbBr, and CsI as standards, assuming the ratio  $r_{\text{cat}}/r_{\text{an}}$  in them to be about 0.75, and established a somewhat different system, in which  $r_i(F^-) = 1.36 \text{ \AA}$ ,  $r_i(O^{2-}) = 1.40 \text{ \AA}$ . One more criterion helping to eliminate the uncertainty in the choice of  $\delta$  (1.63) consists in using the distances in structures with large anions and assuming that these (identical) anions are in contact [1.41]. In the isomorphous series of alkali halides (Fig. 1.43) LiCl and LiBr are such structures, and the “touching” of anions is also observed in a number of other structures. In such a case

$$d(BB) \approx 2r_{\text{an}}. \quad (1.65)$$

The “classical” systems of effective ionic radii are built so that  $r_{\text{an}}$  sufficiently describes both the cation-anion (1.62) and anion-anion (1.65) distances in the case of “contacting” anions, although some deviations are observed for large anions. For instance,  $r_i(I^-) = 2.20 \text{ \AA}$ ,  $2r_i(I^-) = 4.40 \text{ \AA}$ , and the  $I-I$  distance in LiI is  $4.26 \text{ \AA}$ .

**Table 1.8a. Ionic radii**

Period	Subgroup																	
	Ia	IIa	IIIa	IVa	Va	VIIa	VIIa	Ib	IIb	IIIb	IVb	Vb	VIb	VIIb	VIIIb	H	He	
1																		
2	Li 1 + 0.68	Be 2 + 0.34																
3	Na 1 + 0.98	Mg 2 + 0.74																
4	K 1 + 1.33	Ca 2 + 1.04	Sc 3 + 0.83	Ti 2 + 0.78	V 2 + 0.72	Cr 3 + 0.69	Mn 3 + 0.64	Fe 3 + 0.70	Co 3 + 0.67	Ni 3 + 0.64	Cu 2 + 0.74	Zn 2 + 0.78	Ga 2 + 0.83	Ge 3 + 0.62	As 3 + 0.69	Se 2 - 1.93	Br 1 - 1.96	Kr
5	Rb 1 + 1.49	Sr 2 + 1.20	Y 3 + 0.97	Zr 4 + 0.82	Nb 4 + 0.68	Mo 5 + 0.66	Tc 6 + 0.65	Ru 4 + 0.62	Rh 4 + 0.65	Pd 4 + 0.64	Ag 1 + 1.13	Pt 1 + 0.99	In 1 + 1.30	Sn 2 + 1.02	Te 3 + 0.90	J 2 - 2.11	I 1 - 2.20	Xe
6	Cs 1 + 1.65	Ba 2 + 1.38	La 3 + 0.82	Hf 4 + 0.82	Ta 5 + 0.66	W 6 + 0.65	Re 6 + 0.65	Os 6 + 0.65	Ir 6 + 0.65	Pt 4 + 0.64	Au 1 + 1.37	Hg 1 + 1.12	Tl 1 + 1.21	Pb 2 + 1.26	Bi 3 + 1.20	Po 4 + 0.76	At 5 + 0.74	Rn
7	Fr 2 + 1.44	Ra 3 + 1.11	Ac 4 + 1.11															
Lanthanides	Ce 3 + 1.02	Pr 3 + 1.00	Nd 3 + 0.99	Pm 3 + 0.98	Sm 3 + 0.97	Eu 3 + 0.97	Gd 3 + 0.94	Tb 3 + 0.89	Dy 3 + 0.88	Ho 3 + 0.86	Er 3 + 0.85	Tu 3 + 0.85	Yb 3 + 0.81	Lu 3 + 0.80				
Actinides	Th 3 + 1.08	Pa 3 + 1.06	U 3 + 1.04	Np 4 + 0.99	Pa 3 + 1.02	U 3 + 1.01	Cm 3 + 1.00	Bk 3 + 1.00	Cf 4 + 0.86	Es 4 + 0.86	Fm 4 + 0.86				No 3 + 0.81	Lr 3 + 0.80		

Table 1.8b. Ionic radii

Ion	ec	c.n.	sp	$r_{ph}$	$\bar{r}_i$	Ion	ec	c.n.	sp	$r_{ph}$	$\bar{r}_i$	Ion	ec	c.n.	sp	$r_{ph}$	$\bar{r}_i$
$\text{Al}^{3+}$	$6p^6$	6	$4d^{10}$	2	1.26	1.12	$\text{Be}^{2+}$	$1s^2$	4	0.41	0.27	$\text{Cr}^{4+}$	$5f^8$	8	1.06	0.92	
$\text{Al}^{3+}$	$6p^6$	4	$4d^{10}$	4	1.14	1.00	$\text{Bi}^{3+}$	$6s^2$	6	0.59	0.45	$\text{Cl}^{1-}$	$3p^6$	6	1.67	1.81	
$\text{Ag}^{+}$	$4s^2$	5			1.16	1.02	$\text{Bi}^{5+}$	$5d^{10}$	6	1.10	0.96	$\text{Cl}^{1-}$	$3s^2$	3	0.26	0.12	
		6			1.23	1.09	$\text{Br}^{3+}$	$5s^2$	5	1.17	1.03	$\text{Cl}^{1-}$	$2p^6$	4	0.22	0.08	
		7			1.29	1.15	$\text{Br}^{5+}$	$5d^{10}$	8	1.31	1.17	$\text{Cm}^{3+}$	$5f^7$	6	0.41	0.27	
$\text{Ag}^{2+}$	$4d^9$	8			1.36	1.22	$\text{Br}^{3+}$	$5s^2$	6	1.10	0.96	$\text{Cm}^{4+}$	$5f^6$	6	1.11	0.97	
		9			1.42	1.28	$\text{Br}^{4+}$	$5s^2$	6	0.97	0.83	$\text{Cm}^{4+}$	$5f^6$	6	0.99	0.85	
$\text{Ag}^{2+}$	$4d^8$	6			0.93	0.79	$\text{Br}^{1-}$	$4p^6$	8	1.07	0.93	$\text{Co}^{2+}$	$3d^7$	8	1.09	0.95	
		7			0.88	0.94	$\text{Br}^{1-}$	$4p^6$	6	1.82	1.96				0.72	0.58	
$\text{Ag}^{3+}$	$4d^8$	6			0.81	0.67	$\text{Br}^{3+}$	$4p^2$	4	0.73	0.59				0.81	0.67	
		8			0.89	0.75	$\text{Br}^{5+}$	$4s^2$	3	0.45	0.31				0.79	0.65	
$\text{Al}^{3+}$	$2p^6$	4			0.53	0.39	$\text{Br}^{+}$	$3d^{10}$	4	0.39	0.25				0.885	0.745	
		5			0.62	0.48									1.04	0.90	
$\text{Am}^{2+}$	$5f^7$	6			0.675	0.535	$\text{C}^{+}$	$1s^2$	3	0.06	-0.08	$\text{Co}^{3+}$	$3d^6$	8	0.685	0.545	
		7			1.35	1.35	$\text{C}^{+}$	$1s^2$	4	0.29	0.15	$\text{Co}^{4+}$	$3d^5$	4	0.54	0.40	
$\text{Am}^{3+}$	$5f^6$	9			1.40	1.26	$\text{Ca}^{2+}$	$3p^6$	6	0.30	0.16	$\text{Cr}^{2+}$	$3d^4$	6	0.67	0.53	
		10			1.15	0.975	$\text{Ca}^{2+}$	$3p^6$	7	1.14	1.00	$\text{Cr}^{2+}$	$3d^4$	6	0.87	0.73	
$\text{Am}^{4+}$	$5f^5$	8			1.23	1.09				1.20	1.06	$\text{Cr}^{6+}$	$3p^6$	4	0.71	0.57	
		11			1.51	1.37	$\text{Cd}^{2+}$	$4s^2$	6	1.26	1.12	$\text{Cr}^{3+}$	$3d^3$	6	0.40	0.26	
$\text{As}^{3+}$	$4s^2$	8			0.99	0.85	$\text{Cd}^{2+}$	$4s^2$	8	1.32	1.18	$\text{Cr}^{4+}$	$3d^2$	4	0.55	0.44	
		12			1.09	0.95	$\text{Ce}^{4+}$	$4d^{10}$	10	1.45	1.31	$\text{Cs}^{1+}$	$3d^4$	8	0.69	0.55	
$\text{As}^{3+}$	$3d^{10}$	4			0.72	0.58	$\text{Ce}^{4+}$	$4d^{10}$	12	1.48	1.34	$\text{Cs}^{5+}$	$3d^4$	4	0.485	0.345	
		13			0.60	0.46	$\text{Ce}^{4+}$	$4d^{10}$	5	0.92	0.78				0.63	0.49	
$\text{Al}^{7+}$	$5d^{10}$	6			0.76	0.62	$\text{Ce}^{4+}$	$4d^{10}$	6	1.01	0.87				1.92	1.78	
		14			1.51	1.37	$\text{Ce}^{4+}$	$4d^{10}$	7	1.21	1.07				1.95	1.81	
$\text{Au}^{1+}$	$5d^{10}$	6			0.82	0.68	$\text{Ce}^{4+}$	$4d^{10}$	8	1.17	1.03				1.99	1.85	
		15			0.41	0.27	$\text{Ce}^{4+}$	$4d^{10}$	9	1.336	1.196				2.02	1.88	
$\text{Au}^{5+}$	$5d^6$	6			1.49	1.35	$\text{Ce}^{4+}$	$4d^{10}$	10	1.39	1.25	$\text{Cu}^{1+}$	$3d^{10}$	12	0.60	0.46	
		16			1.52	1.38	$\text{Ce}^{4+}$	$4d^{10}$	12	1.48	1.34	$\text{Cu}^{1+}$	$3d^4$	4	0.74	0.60	
$\text{B}_{\alpha}^{2+}$	$5p^6$	6			1.56	1.42	$\text{Ce}^{4+}$	$5p^6$	6	1.01	0.87	$\text{Cu}^{2+}$	$3d^9$	6	0.91	0.77	
		17			1.61	1.47	$\text{Ce}^{4+}$	$5p^6$	8	1.11	0.97	$\text{Cu}^{2+}$	$3d^9$	5	0.71	0.57	
$\text{Ba}^{2+}$	$5p^6$	6			0.25	0.11	$\text{Ce}^{4+}$	$5p^6$	10	1.21	1.07	$\text{Cs}^{+}$	$4s^2$	12	0.79	0.65	
		18			1.66	1.52	$\text{Ce}^{4+}$	$5p^6$	12	1.28	1.14	$\text{Cs}^{+}$	$4s^2$	5	0.79	0.65	
$\text{Be}^{2+}$	$1s^2$	12			1.75	1.61	$\text{Cr}^{3+}$	$6d^1$	6	1.09	0.95	$\text{Cu}^{3+}$	$3d^8$	6	0.73	0.54	
		13			0.30	0.16	$\text{Cr}^{3+}$	$5f^8$	6	0.961	0.821	$\text{Cu}^{3+}$	$3d^8$	6	0.68	0.54	

$\text{D}^{1+}$	$1s^0$	2			0.04	-0.10	$\text{Gd}^{3+}$	$4f^7$	8	1.193	1.053	$\text{La}^{3+}$	$4d^{10}$	12	1.50	1.36
	$4f^{10}$	6			1.21	1.07	$\text{Ge}^{2+}$	$4s^2$	9	1.247	1.107	$\text{Li}^{1+}$	$1s^2$	4	0.730	0.590
$\text{Dy}^{3+}$	$4f^9$	8			1.27	1.13	$\text{Ge}^{2+}$	$4s^2$	6	0.87	0.73	$\text{Lu}^{3+}$	$4f^{14}$	8	0.90	0.76
	$4f^9$	6			1.33	1.19	$\text{Ge}^{4+}$	$3d^{10}$	4	0.530	0.390	$\text{Lu}^{3+}$	$4f^{14}$	6	1.06	0.92
$\text{E}^{3+}$	$4f^{11}$	7			1.30	1.052	$\text{H}^{1+}$	$1s^0$	1	0.670	-0.530	$\text{Mg}^{2+}$	$2p^6$	6	1.001	0.861
	$4f^{11}$	9			1.67	1.023	$\text{Hf}^{4+}$	$4f^{14}$	2	-0.04	-0.18	$\text{Mn}^{2+}$	$2p^6$	4	1.177	1.032
$\text{Eu}^{3+}$	$4f^7$	8			1.223	1.083	$\text{Hf}^{4+}$	$4f^{14}$	4	0.772	-0.18	$\text{Mn}^{2+}$	$2p^6$	5	0.71	0.57
	$4f^7$	10			1.030	0.890	$\text{Hg}^{2+}$	$5d^{10}$	6	0.85	0.71	$\text{Mn}^{5+}$	$3d^2$	6	0.80	0.66
$\text{Eu}^{2+}$	$4f^7$	9			1.34	1.223	$\text{Hg}^{2+}$	$5d^{10}$	8	0.97	0.83	$\text{Mn}^{2+}$	$3d^5$	8	1.03	0.89
	$4f^7$	11			1.39	1.25	$\text{Hg}^{2+}$	$5d^{10}$	4	1.33	1.19	$\text{Mn}^{2+}$	$3d^5$	5	0.80	0.66
$\text{Eu}^{3+}$	$4f^6$	8			1.44	1.30	$\text{Ho}^{3+}$	$4f^{10}$	6	1.10	0.96	$\text{Mn}^{2+}$	$3d^4$	6	0.89	0.75
	$4f^6$	10			1.49	1.35	$\text{Ho}^{3+}$	$4f^{10}$	8	1.16	1.02	$\text{Mn}^{5+}$	$3d^2$	6	0.81	0.67
$\text{Fe}^{3+}$	$3d^5$	6			1.07	0.87	$\text{Ho}^{3+}$	$4f^{10}$	6	1.28	1.14	$\text{Mn}^{2+}$	$3d^4$	7	0.970	0.830
	$3d^5$	7			1.206	1.066	$\text{Ir}^{3+}$	$4d^{10}$	9	1.155	1.015	$\text{Mn}^{7+}$	$3p^6$	4	1.04	0.96
$\text{F}^{1-}$	$2p^6$	9			1.145	1.120	$\text{Ir}^{3+}$	$4d^{10}$	10	1.212	1.072	$\text{Mn}^{4+}$	$3d^3$	4	0.53	0.39
	$2p^6$	3			1.285	1.205	$\text{Ir}^{3+}$	$4d^{10}$	6	2.06	1.12	$\text{Mn}^{3+}$	$2p^6$	6	0.670	0.530
$\text{F}^{1+}$	$1s^2$	6			1.16	1.30	$\text{Ir}^{3+}$	$4d^{10}$	4	0.38	0.44	$\text{Mn}^{5+}$	$3d^1$	4	0.47	0.33
	$1s^2$	7			1.17	1.31	$\text{Ir}^{3+}$	$4d^{10}$	6	1.09	0.95	$\text{Mn}^{6+}$	$3d^1$	4	0.395	0.255
$\text{Fe}^{4+}$	$3d^4$	8			1.06	0.92	$\text{Ir}^{3+}$	$5d^5$	6	0.56	0.42	$\text{Mn}^{7+}$	$3p^6$	4	0.39	0.25
	$3d^4$	9			0.63	0.49	$\text{Ir}^{3+}$	$5d^4$	6	0.71	0.57	$\text{Mn}^{6+}$	$4p^6$	5	0.64	0.50
$\text{Fe}^{6+}$	$3d^2$	4			0.39	0.25	$\text{K}^{1+}$	$3p^6$	6	1.51	1.37	$\text{N}^{3-}$	$2p^6$	6	0.73	0.59
	$3d^2$	5			1.94	1.80	$\text{K}^{1+}$	$3p^6$	6	1.52	1.38	$\text{N}^{3-}$	$2p^6$	5	0.87	0.73
$\text{Fe}^{3+}$	$3d^4$	8			0.78	0.64	$\text{La}^{3+}$	$4d^{10}$	6	1.60	1.46	$\text{N}^{3-}$	$2p^6$	7	1.32	1.46
	$3d^4$	9			0.61	0.47	$\text{La}^{3+}$	$4d^{10}$	7	1.24	1.04	$\text{Na}^{1+}$	$2p^6$	6	1.14	1.00
$\text{Fe}^{3+}$	$3d^5$	6			0.69	0.55	$\text{La}^{3+}$	$4d^{10}$	8	1.300	1.160	$\text{N}^{3+}$	$2p^6$	7	1.16	1.02
	$3d^5$	7			0.75	0.60	$\text{La}^{3+}$	$4d^{10}$	9	1.356	1.216	$\text{N}^{3+}$	$2p^6$	8	1.32	1.18
$\text{Fe}^{3+}$	$3d^4$	8			0.92	0.78	$\text{La}^{3+}$	$4d^{10}$	10	1.41	1.27	$\text{N}^{3+}$	$2p^6$	9	1.38	1.24
	$3d^4$	7			0.72	0.55										

Table 1.8b. (continued)

Ion	ec	c.n.	sp	$r_{ph}$	$\eta$	Ion	ec	c.n.	sp	$r_{ph}$	$\eta$	Ion	ec	c.n.	sp	$r_{ph}$	$\eta$
Na <sup>+</sup>	$2p^6$	12		1.53	1.39	O <sup>5+</sup>	$5d^2$	6		0.685	0.545	P <sup>2+</sup>	$5d^8$	4s <sub>2</sub>		0.74	0.60
Nb <sup>3+</sup>	$4d^2$	6	0.86	0.72	0.82	O <sup>5+</sup>	$5d^1$	6	0.665	0.525	P <sup>4+</sup>	$5d^6$	6	0.94	0.80		
Nb <sup>4+</sup>	$4d^1$	6	0.82	0.68	O <sup>5+</sup>	$5p^6$	4	0.53	0.39	P <sup>5+</sup>	$5d^5$	6	0.765	0.625			
Nb <sup>5+</sup>	$4p^6$	4	0.93	0.79	P <sup>3+</sup>	$3s^2$	6	0.58	0.44	P <sup>6+</sup>	$5p^3$	6	0.71	0.57			
Nb <sup>6+</sup>		6	0.62	0.48	P <sup>5+</sup>	$2p^6$	4	0.31	0.17	P <sup>8+</sup>	$5p^2$	6	1.14	1.00			
Nb <sup>7+</sup>		7	0.78	0.64	P <sup>6+</sup>		5	0.43	0.29	P <sup>9+</sup>	$5p^1$	6	1.00	0.86			
Nd <sup>2+</sup>	$4f^4$	8	0.83	0.69	P <sup>1+</sup>	$5p^2$	6	0.38	0.28	P <sup>5+</sup>	$5s^3$	8	1.10	0.96			
Nd <sup>3+</sup>	$4f^3$	6	1.123	0.983	P <sup>4+</sup>	$6d^1$	6	1.18	1.04	P <sup>6+</sup>	$5s^2$	6	0.88	0.74			
Nd <sup>4+</sup>	$3d^6$	6	1.20	0.99	P <sup>5+</sup>	$6p^6$	6	1.04	0.90	P <sup>8+</sup>	$5s^1$	6	0.85	0.71			
Nd <sup>5+</sup>	$5f^{14}$	6	1.49	1.35	P <sup>6+</sup>		6	1.15	1.01	R <sup>2+</sup>	$6p^6$	8	1.62	1.48			
Nd <sup>6+</sup>	$5f^5$	6	1.24	1.1	P <sup>7+</sup>		7	1.37	1.23	R <sup>4+</sup>	$6p^6$	12	1.84	1.70			
Ni <sup>3+</sup>	$3d^7$	6	0.830	0.690	P <sup>8+</sup>		8	1.43	1.29	R <sup>6+</sup>	$6p^6$	14	1.86	1.72			
Ni <sup>4+</sup>	$3d^6$	6	0.70	0.36	P <sup>9+</sup>		10	1.54	1.40	R <sup>8+</sup>	$5d^3$	6	0.77	0.63			
Ni <sup>5+</sup>	$5f^4$	6	0.74	0.60	P <sup>10+</sup>		11	1.59	1.45	R <sup>10+</sup>	$5d^2$	6	0.72	0.58			
Ni <sup>6+</sup>	$5f^3$	6	1.01	0.87	P <sup>11+</sup>		12	1.63	1.49	R <sup>12+</sup>	$5d^1$	6	0.69	0.55			
Ni <sup>7+</sup>	$5f^2$	8	1.12	0.98	P <sup>12+</sup>	$4d^9$	8	1.08	0.94	R <sup>14+</sup>	$5p^6$	4	0.52	0.38			
Ni <sup>8+</sup>	$5f^1$	6	0.89	0.75	P <sup>13+</sup>	$4d^8$	6	0.73	0.59	R <sup>16+</sup>	$4d^6$	6	0.67	0.53			
Ni <sup>9+</sup>	$5p^6$	2	0.86	0.72	P <sup>14+</sup>	$4d^7$	6	0.78	0.64	R <sup>18+</sup>	$4d^5$	6	0.74	0.60			
Ni <sup>10+</sup>	$2p^6$	3	1.21	1.35	P <sup>15+</sup>	$4d^6$	6	1.00	0.86	R <sup>20+</sup>	$4d^4$	6	0.69	0.55			
Ni <sup>11+</sup>		4	1.24	1.38	P <sup>16+</sup>	$4f^4$	6	0.90	0.76	R <sup>22+</sup>	$4d^3$	6	0.82	0.68			
Ni <sup>12+</sup>		6	1.26	1.40	P <sup>17+</sup>	$4f^2$	8	1.23	1.09	R <sup>24+</sup>	$4d^1$	4	0.52	0.36			
OH <sup>1-</sup>		8	1.28	1.42	P <sup>18+</sup>	$6s^2$	6	1.08	0.94	S <sup>2-</sup>	$3p^6$	6	1.70	1.84			
OH <sup>2-</sup>		3	1.18	1.32	P <sup>19+</sup>	$5d^10$	6	1.22	1.08	S <sup>4-</sup>	$3s^2$	6	0.51	0.37			
OH <sup>3-</sup>		4	1.20	1.34	P <sup>20+</sup>	$5p^6$	6	0.81	0.67	S <sup>6-</sup>	$2p^6$	4	0.26	0.12			
Os <sup>4+</sup>	$5d^4$	6	1.21	1.35	P <sup>21+</sup>	$4f^3$	6	1.13	1.09	S <sup>8-</sup>	$2p^6$	6	0.43	0.29			
Os <sup>5+</sup>	$5d^3$	6	1.23	1.37	P <sup>22+</sup>	$4f^2$	8	1.26	1.126	S <sup>10-</sup>	$4p^6$	5	0.90	0.76			
Os <sup>6+</sup>	$5d^2$	5	0.770	0.630	P <sup>23+</sup>	$4f^1$	6	0.99	0.85	S <sup>12+</sup>	$4d^{10}$	6	0.94	0.80			
Os <sup>7+</sup>		6	0.715	0.575	P <sup>24+</sup>	$4f^1$	6	1.10	0.96	S <sup>14+</sup>	$3p^6$	6	0.74	0.60			
Os <sup>8+</sup>		6	0.63	0.49						S <sup>16+</sup>	$3s^3$	6	0.85	0.745			

Sc <sup>3+</sup>	$3p^6$	8	1.010	0.870	T <sup>2-</sup>	$5p^6$	6	0.70	0.56							0.87	0.73
Sc <sup>2+</sup>	$4p^6$	6	1.84	1.98	T <sup>4+</sup>	$5s^2$	3	2.07	2.21							0.95	0.81
Sc <sup>4+</sup>	$4s^2$	6	0.64	0.50	T <sup>6+</sup>		6	0.66	0.52							1.00	0.86
Sc <sup>5+</sup>	$3d^{10}$	4	0.42	0.28	T <sup>8+</sup>		4	0.80	0.66	V <sup>2+</sup>	$3d^3$	8	0.93	0.79		0.780	0.640
Si <sup>4+</sup>	$2p^6$	6	0.56	0.42	T <sup>10+</sup>		6	1.11	0.97	V <sup>3+</sup>	$3d^2$	6	0.73	0.67		0.67	0.53
Sm <sup>2+</sup>	$4f^6$	8	1.36	1.22	T <sup>12+</sup>	$4d^{10}$	4	0.57	0.43	V <sup>4+</sup>	$3d^1$	5	0.72	0.58		0.86	0.72
Sm <sup>3+</sup>	$4f^5$	9	1.41	1.27	T <sup>14+</sup>	$6p^6$	6	1.08	0.94	V <sup>5+</sup>	$3p^6$	4	0.495	0.355		0.51	0.35
Sm <sup>4+</sup>	$4f^4$	9	1.46	1.32	T <sup>16+</sup>		9	1.23	1.09	V <sup>6+</sup>	$3s^2$	6	0.60	0.46		0.74	0.60
Sm <sup>5+</sup>	$4f^3$	9	1.098	0.938	T <sup>18+</sup>		10	1.27	1.13	Xe <sup>8+</sup>	$4d^{10}$	4	0.68	0.54		0.54	0.40
Sm <sup>6+</sup>	$4f^2$	8	1.219	1.079	T <sup>20+</sup>	$3d^2$	12	1.35	1.21	W <sup>4+</sup>	$5d^2$	6	0.80	0.66		0.62	0.50
Sm <sup>7+</sup>	$4f^1$	7	0.89	0.75	T <sup>22+</sup>	$3d^1$	6	1.00	0.86	W <sup>5+</sup>	$5p^6$	4	0.56	0.42		0.56	0.42
Sm <sup>8+</sup>	$4d^{10}$	4	1.38	1.24	T <sup>24+</sup>	$3p^6$	4	1.19	1.05	V <sup>7+</sup>	$3p^6$	5	0.65	0.51		0.74	0.60
Sm <sup>9+</sup>	$5f^5$	5	0.69	0.55	T <sup>26+</sup>	$4d^{10}$	5	0.56	0.42	V <sup>8+</sup>	$3d^2$	6	0.74	0.60		0.54	0.40
Sm <sup>10+</sup>	$5f^4$	6	0.76	0.62	T <sup>28+</sup>	$6s^2$	6	0.65	0.51	Xe <sup>8+</sup>	$4d^{10}$	4	0.62	0.48		0.62	0.48
Sr <sup>2+</sup>	$4p^6$	8	0.95	0.81	T <sup>30+</sup>	$4f^3$	6	0.88	0.74	Y <sup>3+</sup>	$4p^6$	6	1.040	0.900		1.10	0.96
Sn <sup>4+</sup>	$5d^2$	7	1.32	1.18	T <sup>32+</sup>	$4f^2$	7	1.73	1.59	Y <sup>5+</sup>	$4f^{13}$	6	1.159	1.019		1.215	1.075
Sn <sup>5+</sup>	$5p^6$	6	1.35	1.21	T <sup>34+</sup>	$5d^{10}$	12	1.84	1.70	Y <sup>7+</sup>	$4f^{14}$	6	1.16	1.02		1.182	1.042
Sn <sup>6+</sup>	$5p^5$	8	1.40	1.26	T <sup>36+</sup>	$5d^10$	4	0.89	0.75	Zn <sup>2+</sup>	$3d^{10}$	4	0.74	0.60		0.82	0.68
Ta <sup>3+</sup>	$5d^2$	12	1.58	1.44	Tm <sup>2+</sup>	$4f^{13}$	6	1.17	1.03	Yb <sup>3+</sup>	$4f^{13}$	6	1.008	0.868		0.880	0.740
Ta <sup>4+</sup>	$5d^1$	6	0.86	0.72	Tm <sup>3+</sup>	$4f^{12}$	7	1.23	1.09	Zr <sup>4+</sup>	$4p^6$	4	1.04	0.90		1.056	0.925
Ta <sup>5+</sup>	$5p^6$	7	0.82	0.68	Tm <sup>4+</sup>		6	1.020	0.880				1.125	0.985			
Ta <sup>6+</sup>		8	0.78	0.64	Tm <sup>5+</sup>		8	1.14	0.994				1.182	1.042			
Tb <sup>4+</sup>	$4f^7$	6	0.90	0.76	T <sup>35+</sup>	$10s^2$	9	1.19	1.05	Zn <sup>2+</sup>	$3d^{10}$	4	0.74	0.60		0.82	0.68
Tb <sup>5+</sup>	$4f^6$	8	1.02	0.88	T <sup>37+</sup>	$5f^1$	7	1.31	1.17	Y <sup>9+</sup>	$4f^{13}$	6	1.28	1.14		1.28	1.14
Tb <sup>6+</sup>	$4d^3$	6	0.785	0.645	T <sup>39+</sup>	$6p^6$	7	0.98	0.84	Y <sup>13+</sup>	$4f^{13}$	6	1.008	0.868		0.880	0.740
Tb <sup>7+</sup>	$4d^2$	6	0.74	0.60	T <sup>41+</sup>	$6p^6$	4	0.59	0.45	Y <sup>17+</sup>	$4f^{13}$	9	1.04	0.90		1.04	0.90
Tb <sup>8+</sup>	$4p^6$	4	0.51	0.37	T <sup>43+</sup>					Y <sup>21+</sup>	$4f^{13}$	9	1.04	0.90		1.04	0.90

(Ion) symbol and formal charge of an element; (ec) electron configuration; (c.n.) coordination number; (sp) spin; ( $r_{ph}$ ) physical radius; ( $r$ ) effective radius

The ionic radii corresponding to Goldschmidt's system, as corrected by *Belov and Boky* [1.42], who assumed  $r_i(O^{2-}) = 1.36 \text{ \AA}$ , are given in Fig. 1.45 and Table 1.8a. In this table, the anion radii of each period of Mendeleev's table are larger than the cation radii in the same period. For instance,  $r(Li^+) = 0.68 \text{ \AA}$  and  $r(F^-) = 1.33 \text{ \AA}$ ; both types of radii increase when going down the subgroup  $r(Na^+) = 0.98 \text{ \AA}$  and  $r(Cl^-) = 1.81 \text{ \AA}$ , etc. According to the system of  $r_i$ , cations never touch each other.

The distances between ions observed in simple structures usually agree with the sum of the corresponding radii with an accuracy up to about 1%–3%. In complicated structures with asymmetric coordination and also in structures with large anions the deviations from additivity may reach a few per cent. The coordination can be taken into account by a corresponding correction. The tabulated  $r_i$  refer to a cation coordination number equal to 6. On transition to a larger coordination number the radii  $r_i$  somewhat increase; for instance, for a c.n. 8 they increase by 3% and for 12, by 12%. The deviations from additivity observed in structures with large ions were attributed to the comparative softness and "polarizability" of their electron shell. For instance, in AgBr,  $\Sigma r_i = 3.09 \text{ \AA}$ , and  $d(AgBr) = 2.88 \text{ \AA}$ .

The above-considered ionic radii are called effective, because their system corresponds fairly well to the purpose of describing and predicting inter-atomic distances. Many regularities in crystal chemistry, including the coordination of atoms in a number of compounds, phenomena of isomorphous substitutions, etc., were interpreted on the basis of the "classical" system, but some inconsistencies arose in its practical use.

At the time of the introduction of the system, the knowledge of the electron distribution in atoms and crystals was very vague, and the values of ionic radii did not correlate with it. If we refer, for example, to Fig. 1.14 and draw the boundary corresponding to the effective ionic radii, its course will not be related to any real characteristic of the electron distribution in atoms or to the parameters of the interaction curve.

The present-day chemical bond theory and experimental X-ray data on the electron density distribution in crystals provide physical substantiation for the concepts of crystallochemical radii, in general, and ionic radii, in particular.

In the case of a pure ionic bond the electron density peaks of cations and ions in crystals are isolated, and a reasonable criterion for determining the ionic radii would be the distance from the peaks to the electron density minimum along the straight line joining their centers [1.43–45]. The minimum for NaCl is shown in Fig. 1.14. Such ionic radii found on the basis of experimental X-ray data on the electron density distribution in the structures of alkali–metal halides, which may be called "X-ray" or "physical" ( $r_{ph}$ ) radii, have the following values [ $\text{\AA}$ ]:

$Li^+$	$Na^+$	$K^+$	$Rb^+$	$Cs^+$	$F^-$	$Cl^-$	$Br^-$	$I^-$
0.94	1.17	1.49	1.63	1.86	1.16	1.64	1.80	2.05

This minimum of electron density lies in the zone of the decrease of clashing

"tails" of the orbitals of the ionized metallic atom and anion. According to (1.23) this zone has a width  $\Delta$ , and the minimum is found to lie near  $\Delta/2$ , i.e., the cation radius

$$r_{ph}(A^+) = r_o(A^+) + k\Delta, \quad k \approx 0.5. \quad (1.66)$$

It is significant that another criterion – calculation on the basis of refined potentials of interaction in ionic crystals – leads to about the same values of ionic radii as those given by X-ray data on the electron density minimum.

After a computer analysis of interatomic distances in the structures of over 1000 compounds – oxides, fluorides, etc. – *Shannon and Prewitt* [1.46] and *Shannon* [1.47] elaborated a system of ionic radii corresponding to the "physical" values, in which they adopted  $r_{ph}(F^-) = 1.19 \text{ \AA}$  and  $r_{ph}(O^{2-}) = 1.26 \text{ \AA}$  for coordination number 6 (Table 1.8b; calculated values of  $r$  are given for some ions). The additivity scheme of (1.62, 63) naturally holds true here. The physical ionic radii differ from the classical, but not too much; for cations they are about  $\delta = 0.15\text{--}0.2 \text{ \AA}$  larger, and for anions by the same amount smaller than those adopted in the classical systems. Table 1.8b also gives the refined system of effective "classical" radii for which  $r_i(O^{2-}) = 1.40$  and  $r_i(F^-) = 1.33$  for c.n. 6, were accepted as basic values.

In Table 1.8b the values of radii are given for different coordination numbers. It is noteworthy that in this system the dependence of the ionic radii on the coordination number has been found not only for cations, but also for anions. For instance,  $r_{ph}(O^{2-})$  increases with c.n. and the bonds are weakened.

Another interesting feature is the dependence of the ionic radii of transition metals on their spin state. The outer  $d$  shells of these atoms have a spin configuration depending on the splitting of the levels in the crystal field where they are located and which is formed by the surrounding atoms. In a weak field the spins of the  $d$  electrons are parallel and not compensated; this is a high-spin (hs), strongly paramagnetic state. In a strong field the spins are compensated owing to the pairwise antiparallel arrangement. This is the lowspin (ls) state; the electron "packing" in the  $d$  shell becomes closer and its radius decreases<sup>7</sup>. Table 1.8 (column  $r_{ph}$ ) indicates the relevant radii for both states, the difference reaching almost 0.2  $\text{\AA}$  (see Fig. 1.48).

The system of physical ionic radii corresponds to the real characteristic of the electron density distribution, i.e., to its minimum between ions. This system gives a good description of interatomic distances in ionic crystals. Its interpretation of the radii of anions and single-charged cations is particularly clear. For incompletely ionized divalent and (all the more so) multivalent cations, when the bond becomes partly covalent, the physical interpretation of these radii becomes vague; they should be treated more cautiously, as formal characteristics. Naturally, this is generally because the atoms in the crystal are described by the

<sup>7</sup> An interesting example is the decrease in the size of the  $Fe^{2+}$  ion and its entry into the plane of the porphyrine ring while the oxygen atom is being added to the hemoglobin molecule during oxygenation (Sect. 2.9.4).

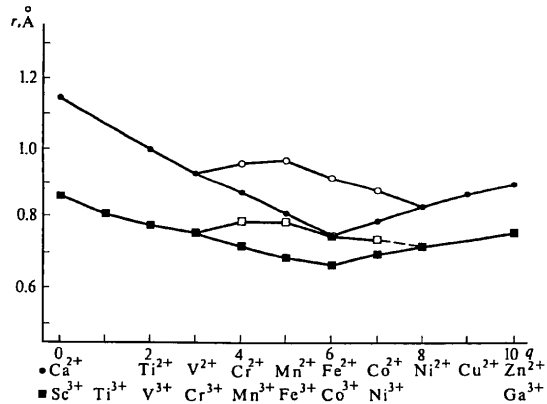


Fig. 1.48. Dependence of the physical ionic radii  $r_{ph}$  on the number of 3d electrons ( $q$  is the number of  $d$  electrons). Dark circles denote divalent metals,  $ls$  state; open circles, divalent metals,  $hs$  state; dark squares, trivalent metals,  $ls$  state; and open squares, trivalent metals,  $hs$  state

conventional, crystal geometrization concept as “spheres” with certain radii, and because the continuous electron density, not necessarily spherical, is divided into definite parts in conformity with some criteria. At the same time, as we shall see below, this is not the only possible physical approach to the description of interatomic distances in ionic crystals.

#### 1.4.4 The System of Atomic–Ionic Radii of a Strong Bond

When considering the three main types of strong bond – ionic, covalent, and metallic – we saw in Sect. 1.2.3 that although each of them has its own specificity, in all cases the chemical bond is realized by overlapping – mutual penetration of outer electron shells of the atoms (experiencing some changes in the process). Then the “radius” may be defined as the distance from the atom center to the site of interpenetration of the electron shells of neighboring atoms; it is approximately equal to the orbital radius of the free atom.

At the same time, it was noted long ago that interatomic distances  $d(AB)$  in ionic and partly ionic structures can also be described fairly well by the sums of the atomic radii. This is not accidental. As discussed in Sect. 1.2, the ionic bond can also be interpreted from the standpoint of the overlapping of outer orbitals. Considering again the example of NaCl, we can lay off the radial functions of the neutral atoms Na and Cl, taking their centers at a distance corresponding to the interatomic distance in the crystal; then we find that the position of the outer orbital of Na coincides with that of the outer orbital of Cl (1.22) (Fig. 1.14). Thus, similar to the case of atomic radii (1.59), we have

$$d(A^+ B^-) \approx r_o(A) + r_o(B), \quad (1.67)$$

i.e., the distance between ions of opposite signs is approximately equal to the sum of the orbital radii of the neutral atoms, although we actually have  $\text{Cl}^-$  and  $\text{Na}^+$  ions in this crystal. The reason is that electrons – either proper ones, belonging to the outer  $3s$  shell of the neutral atom of Na, or foreign ones belonging to the  $3p^6$  shell of the  $\text{Cl}^-$  anion – can only be positioned at the distance  $r_o(\text{Na})$  from the Na nucleus or, what is the same, at a distance  $\Delta$  (1.23) from the inner  $2p^6$  shell of the Na atom. If the cation is incompletely ionized, its outer orbital, depleted in electrons, overlaps with the electron-enriched outer orbital of the anion to form a partly covalent bond. In this case, too, (1.67) holds true

$$d(AB) \approx r_o(A) + r_o(B). \quad (1.68)$$

Thus, as indicated by Slater [1.48, 49], for all types of bonds, including the ionic, the interatomic distance approximately corresponds to the sum (1.59, 67, 68) of orbital radii  $r_o$  and is defined by the coincidence of the positions of the outer orbitals of the neutral atoms during the chemical bond formation (Figs. 1.14, 29, 33).

For a number of structures, the theoretically predicted sum of orbital radii is in good agreement with experiment; for instance, for the Al–O, Si–O, and Si–F distances as well as for many others, the differences lie within 0.01–0.004 Å. In other cases the deviations are greater and may reach 0.2 Å. Deviations for certain atoms are due to the fact that in crystals atoms may transfer to excited states which are close in energy to the ground state, but have slightly different values of  $r_o$ , and also that the difference between low- or high-spin states of atoms with  $d$  electrons is neglected. Having this in mind, J. Slater and other authors proposed an empirical system of unified atomic–ionic radii  $r_{ai}$

$$r_{ai} \approx r_{at} \approx r_o, \quad (1.69)$$

which is also suitable for describing anion–cation contacts in ionic structures (Table 1.9, Fig. 1.45). It is based on data relating to interatomic distances in many compounds and is accurate for  $r_{ai}$  to about 0.05 Å. The sums of  $r_{ai}$  describe the interatomic distances of most structures with an accuracy of about 0.1 Å neglecting any corrections, say, for coordination, etc.

Being unified for all three types of strong bonds, the system of  $r_{ai}$  naturally cannot be as accurate in describing specific structures as the systems of covalent, metallic and ionic radii, which are ramified and include many corrections. Lebedev [1.50] proposed a system of  $r_{ai}$ , which is similar to Slater's system, but differs from it by 0.1–0.15 Å for the atoms of some elements; in particular,  $r_{ai} = 0.50$  Å is accepted for oxygen, 1.60 Å for magnesium, etc.

Figure 1.49 presents the structures of NaCl and LiBr drawn with the help of physical ionic and atomic–ionic radii.

In the system of radii of a strong bond, the cation radii are larger than the anion ones in contrast to the systems of ionic radii  $r_i$ . The reason is that the quantity  $\Delta$  (1.23) divided into approximately equal parts between cations and anions in the system of  $r_{ph}$ , completely belongs to the cations in the  $r_{ai}$  system.

Table 1.9. Atomic-ionic radii [Å] [1.48]

Period	Subgroup																	
	Ia	IIa	IIIa	IVa	Va	VIa	VIIa	VIIIa	Ib	IIb	IIIb	IVb	Vb	VIb	VIIb	VIIIb		
1																		
2	Li 1.45	Be 1.05							B 0.85	C 0.70	N 0.65	O 0.60	F 0.50					
3	Na 1.80	Mg 1.50							Al 1.25	Si 1.10	P 1.00	S 1.00	Cl 1.00	Ar				
4	K 2.20	Ca 1.80	Sc 1.60	Ti 1.40	V 1.35	Cr 1.40	Mn 1.40	Fe 1.40	Co 1.35	Ni 1.35	Cu 1.35	Zn 1.30	Ga 1.25	As 1.15	Se 1.15	Kr		
5	Rb 2.35	Sr 2.00	Y 1.85	Zr 1.55	Nb 1.45	Mo 1.35	Tc 1.35	Ru 1.30	Rh 1.35	Pd 1.40	Ag 1.40	Cd 1.35	In 1.55	Sn 1.45	Te 1.40	I 1.40	Xe	
6	Cs 2.60	Ba 2.15	La 1.95	Hf 1.55	Ta 1.45	W 1.35	Re 1.35	Os 1.30	Ir 1.35	Pt 1.35	Au 1.35	Hg 1.30	Tl 1.90	Pb 1.80	Bi 1.60	Po 1.90	At 1.90	Rn
7	Fr	Ra	2.15	Ac	1.95													

Lanthanides	Ce 1.85	Pr 1.85	Nd 1.85	Pm 1.85	Sm 1.85	Eu 1.85	Gd 1.80	Tb 1.75	Dy 1.75	Ho 1.75	Er 1.75	Tu 1.75	Yb 1.75	Lu 1.75
Actinides	Th 1.80	Pa 1.80	U 1.75	Np 1.75	Pu 1.75	Am 1.75	Cm 1.75	Bk 1.75	Cf 1.75	Es 1.75	Fm 1.75	Md 1.75	(No) 1.75	Lr 1.75

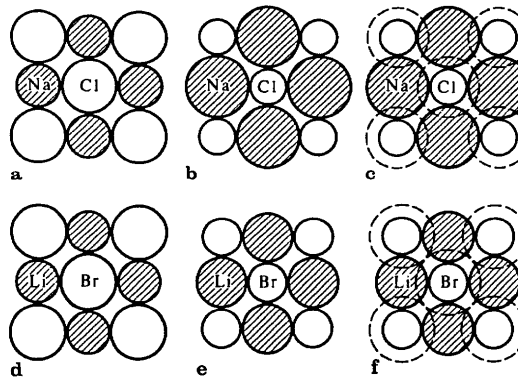


Fig. 1.49a–f. NaCl and LiBr structures, (100) section of cubic unit cell; (a, d) structures are depicted using physical ionic radii, (b, e) atomic–ionic radii, (c, f) atomic–ionic (strong-bond) radii (solid lines) and weak-bond radii of anions (dashed lines)

Using additive constant  $\delta$  in (1.63), one finds that on transition from the physical ionic to atomic–ionic radii  $\delta \approx 0.65 \text{ \AA}$ , i.e.,

$$r_{ai}(\text{an}) \approx r_i(\text{an}) - 0.65 \text{ \AA}, \quad r_{ai}(\text{cat}) \approx r_i(\text{cat}) + 0.65 \text{ \AA}. \quad (1.70)$$

For transition from the classical ionic to the atomic–ionic radii, this constant is  $\delta \approx 0.85 \text{ \AA}$ .

There is no contradiction in the fact that the two systems of  $r_{ph}$  and  $r_{ai}$  for the ionic bond, based on physical interpretation, are different, since they describe entirely different characteristics of electron density distribution between bound atoms. Additivity (1.63) ensures the possibility of computing the interatomic distances (1.62) as in the system of effective ionic radii.

#### 1.4.5 System of Intermolecular Radii

In molecular crystals, the interaction between molecules is determined by weak van der Waals forces or hydrogen bonds. The distances between the nearest atoms of neighboring molecules in this case of the van der Waals bond are comparatively large; their interaction is due to the overlapping of the farthest, unfilled outer orbitals of atoms, whose strong (covalent) bonds are already completely saturated. By analyzing these distances in organic and other crystals where such bonds exist, it is possible to construct, by the familiar method, a sufficiently consistent system of the van der Waals (or, as they are also called, intermolecular) radii, so that the following additivity condition holds for the nearest atoms of neighboring molecules:

$$r_m = \frac{1}{2} d(AA), \quad d(AB) \approx r_m(A) + r_m(B). \quad (1.71)$$

These radii are presented in Table 1.10. Recently, proceeding from the statistical

Table 1.10. Intermolecular (van der Waals) radii

		H	He
		1.17	1.40
C	N	O	F
1.70	1.58	1.52	1.47
Si	P	S	Cl
2.10	1.80	1.80	1.78
As	Se	Br	Kr
1.85	1.90	1.85	2.02
Te	I		Xe
		2.06	2.16

treatment of distances in a large number of organic structures, values of  $r_m$  for some atoms were found, differing slightly from those given in Table 1.10, namely for N 1.50; O 1.29; S 1.84; Cl 1.90; Br 1.95; I 2.10 Å. Intermolecular radii  $r_m$  are always larger than strong-bond radii. As the potential function for weak bonds has a very gradual slope (Curve II in Fig. 1.12), the additivity condition (1.71) permits deviations up to tenths of Å units. Figure 1.50 shows a histogram of deviations of van der Waals contact distances, found experimentally, from standard ones [1.51]. (Recently it has been found that some molecular structures have bonds somewhat shorter than conventional ones (Sect. 6.7.2).) According to the system of  $r_m$  a molecule formed by covalently bound atoms should be represented, with respect to the intermolecular contacts in the crystal, as if it were wrapped in a "coat" with the shape of spheres of indicated radii (Fig. 1.51).

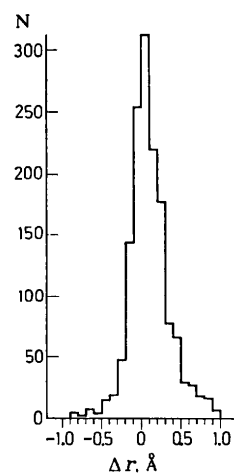


Fig. 1.50. Histogram of the distribution of deviations of interatomic distances at van der Waals contacts from standard values

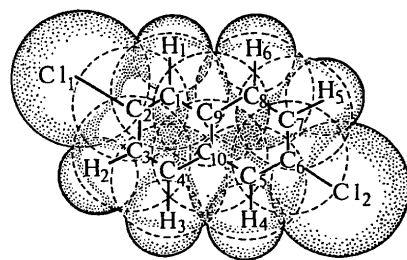


Fig. 1.51. Molecule as a geometric body framed in a "coat" of van der Waals radii

#### 1.4.6 Weak- and Strong-Bond Radii

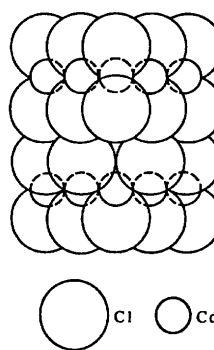
In molecular and noble gas crystals the equilibrium distances between non-covalently bound atoms are defined by the repulsive branch of the weak interaction curve (Fig. 1.12); the system of intermolecular radii serves as a geometric model of this repulsion.

As we have already said, a similar interaction takes place between anions in ionic crystals. Vivid examples are layer lattices, which are flat packets of anions with cations inside (Fig. 1.52). The packets contact each other only by means of anions. These crystals exhibit cleavage due to weak bonds between layers. As in intermolecular contacts, the strong bonds inside some of the structures are saturated, while the contacting anions have the filled shell of noble gas atoms. The distances between them are nearly the same as in molecular crystals; for instance, the Cl-Cl distance in CdCl<sub>2</sub> is 3.76 Å. The tabulated values of the effective ionic radius of Cl<sup>-</sup> and the van der Waals radius of Cl practically coincide,  $r_i(Cl) = 1.81$  Å and  $r_m(Cl) = 1.78$  Å. Another important example is the distance between oxygen atoms. The distance between non-valence-bound anions O<sup>2-</sup> in ionic structures – oxides, silicates, and inorganic salts – ranges from 2.5 to 3.2 Å, which corresponds to the effective ionic radius of oxygen, taken to be  $r_i(O^{2-}) = 1.38$  Å. The tabulated values of the intermolecular radius  $r_m(O)$  are 1.36–1.52 Å, i.e., it is the same value.

Anions in ionic structures do not attract each other (if we neglect the weak van der Waals forces); they experience Coulomb repulsion, but are united in crystal structures owing to their interaction (attraction) with cations. The distances between the anions correspond to the equilibrium of all these forces. Thus, the similarity between the effective ionic radii of anions and the intermolecular radii of the corresponding atoms

$$r_{an} \approx r_i \quad (1.72)$$

is not accidental – it reflects the identical physical nature of the interaction between atoms whose strong chemical bonds are already saturated. These radii

Fig. 1.52. Layer structure of CdCl<sub>2</sub>. Contact of sheets having formula CdCl<sub>2</sub> is due to weak Cl-Cl bonds

may be called weak-bond radii. They can be interpreted physically as quantities determining the minimum distance of "touching" of non-valence-bound atoms (Figs. 1.49f, 50, 51). The physical model corresponding to a strong bond (covalent, metallic, or anion–cation) is the interpenetration of the outer orbitals of the contacting atoms, although it acquires a specific form for each of the main types of bond (Fig. 1.53). Thus, the interpenetration is most pronounced in the covalent bond; the cation electrons are fully or partly incorporated in an anion shell in the case of ionic bond; the valence electrons are collective in metals. From this standpoint, ionic structures, as well as molecular ones, can be described by two systems of radii, namely by the radii of the strong cation–anion bond, and (if there are anion–anion contacts) by weak-bond radii (Fig. 1.49c, f).

In conclusion we reiterate the most essential elements in the construction of the various systems of crystallochemical radii. The covalent, metallic, and "atomic–ionic" radii are approximately equal to the orbital radii of the outer atomic electrons, which are responsible for the formation of a strong chemical bond. The radii of weak bonds describe the geometric picture of the contacts in weak van der Waals atomic interactions. The system of physical ionic radii gives the distances to the minimum of the electron density at cation–ion contacts. The formal scheme of effective ionic radii also describes the interatomic distances, since the additivity conditions are also fulfilled.

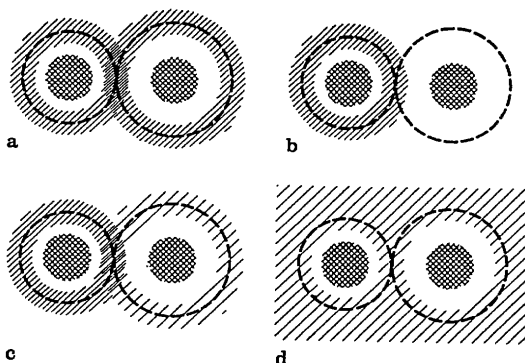


**Fig. 1.53a–d.** Schematic illustration of various types of chemical bonds. Only two bound atoms are shown conventionally. (*Hatching*) outer orbitals; (*cross-hatching*) inner atomic shells; (*dotted circles*) orbital radius.

- (a) Covalent bond. At the site of the superposition of valence orbitals the electron density is increased; it exceeds the sum of the electron densities of the valence orbitals of isolated atoms.
- (b) Ionic bond. The cation (on the right) has lost an electron from the valence orbital, which was incorporated into the anion shell. The anion is so positioned, however, that its shell is at the same distance from the inner cation shell at which the now-ionized electron of the cation was located.
- (c) Covalent bond with a fraction of ionicity – a case intermediate between (a) and (b). The cation shell is depleted and the anion shell enriched in electrons; at the site of the overlapping the electron density exceeds the sum of the electron densities of the valence orbitals of the isolated atoms.
- (d) Metallic bond. The electrons of the valence orbitals are now distributed uniformly throughout the crystal lattice space (except in the core shells); the interatomic electron density is relatively low

## 1.5 Geometric Regularities in the Atomic Structure of Crystals

### 1.5.1 The Physical and the Geometric Model of a Crystal

The theory of crystal structure, i.e., the theory of its formation from an assembly of interacting atoms, is based on the general principles of thermodynamics, solid-state physics, and quantum mechanics. At the same time, the result of this interaction is geometrically amazingly simple; in the unit cell of a three-dimensionally periodic structure the atoms occupy fixed positions at definite distances from each other.

The very consideration of this geometry, irrespective of its physical causes, using certain relatively simple physical or chemical data which are also geometrized, promotes the understanding of many regularities in the atomic structure of crystals.

In the geometric model of a crystal, the arrangements of the crystal's structural units, i.e., atoms or molecules, the distances between them as well as their coordination are considered. Proceeding from the systems of crystallochemical radii, atoms can be modeled as hard spheres, and molecules as solids of more complicated shape. Then packings of such spheres or bodies can be analyzed. The formally geometric consideration is supplemented by taking into account the nature of the chemical bond between the atoms; stable groupings of atoms – coordination polyhedra, complexes, molecules, etc. – are studied, as are their shapes and symmetries and their relationship with the space symmetry of the crystal.

The geometric model of a crystal is the most simplified version of its physical model. The geometric approach was the starting point for the development of concepts of the atomic structure of crystals. It is naturally limited and cannot claim to explain crystal structures in all their details. It does help, however, to formulate and describe a number of regularities in the structure of crystals in a simple and pictorial form.

### 1.5.2 Structural Units of a Crystal

The very expression "the atomic structure of a crystal" shows that the ultimate structural units with respect to which the structure of a crystal is considered (at any rate, at the geometric level) are the atoms. In many cases, however, even before the formation of a crystal or in the course of its formation, the atoms, owing to their chemical nature, draw together into certain stable groupings which are preserved in the crystal as an entity and can conveniently and legitimately be regarded as structural units of crystals. The isolation of structural units according to their crystallochemical features makes possible their definite geometric and symmetric description.

In dividing the crystals into structural units according to the types of association of the atoms, one should consider whether the chemical bond forces acting between all the atoms are the same or different. In the former case the

crystals are *homodesmic*. Since all their interatomic bonds are the same type, the interatomic distances differ but little. Examples of homodesmic structures are those of metals and alloys; covalent structures, as well as many ionic ones, are also homodesmic. The structural units of such crystals are the atoms themselves, which form a three-dimensional network of approximately equivalent bonds; at the same time, definite structural groupings can sometimes be singled out among them.

Stable, isolated, finite groupings or complexes of atoms in a crystal can form if the types of bonds are different. Such crystals are called *heterodesmic*. More often than not, the bonds inside such a structural grouping are fully or partly covalent. A typical example are organic molecules; strong covalent bonds act within the atoms, but weak van der Waals bonds operate between unit molecules in the crystal. Examples of structural groupings in inorganic crystals are the complex anions  $\text{CO}_3^{2-}$ ,  $\text{SO}_4^{2-}$ ,  $\text{NO}_2^-$ , water molecules  $\text{H}_2\text{O}$ , the complexes  $[\text{PtCl}_4]^{2-}$  and  $[\text{Co}(\text{NH}_3)_6]^{3+}$ , intermetallic complexes  $\text{MoAl}_{12}$  (Fig. 1.54), etc. These groupings are finite in all three dimensions; sometimes they are called "insular" groupings. But there may also be one- or two-dimensionally extended structural groupings, chains and layers, which will be discussed below.

### 1.5.3 Maximum-Filling Principle

In considering the formation of a crystal out of structural units from the geometric standpoint, one should take into account their own shape and symmetry, and the nature of interaction among them.

If we first refer to crystals whose structural units are atoms, they can be divided into two subtypes as regards the intrinsic symmetry of atoms. If the

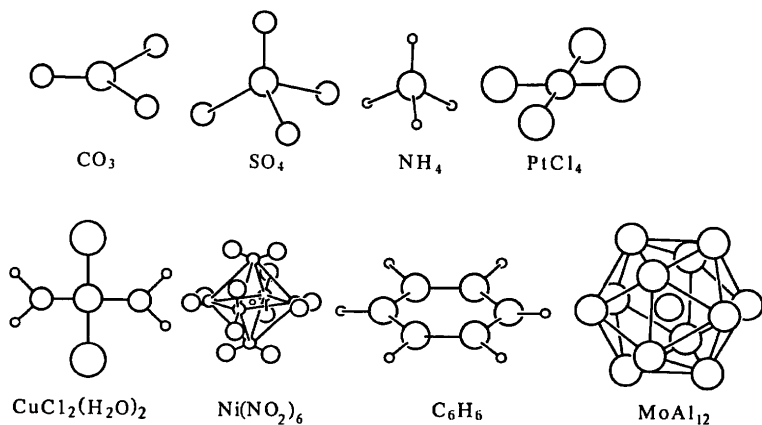


Fig. 1.54. Examples of structural units of crystals: molecules, inorganic anions, complexes, the intermetallic complex  $\text{MoAl}_{12}$

forces acting among atoms are central or approximately so, as in metallic and ionic crystals as well as in crystals of solidified noble gases, one can speak of an intrinsic, spherical or approximately spherical point symmetry of atoms  $\infty/\infty m$ . The other subtype is given by the covalent crystals. The atoms in them have directed bonds and can be regarded as having a definite and nonspherical point symmetry. We shall treat them later. If a crystal has limited or any other kind of structural groupings, the interaction between them can also be reduced to the central interactions among the atoms of neighboring groups despite the great diversity in their forms and symmetry.

The principal contribution to the free energy of a crystal  $F$  (1.46) is made by the potential energy of interaction  $U$ , i.e., the lattice energy. All expressions for the energy of the central interaction forces are dependent on the interatomic distance (1.51); the energy minimum is attained at the equilibrium interatomic distances which are typical of given atoms and of the type of bond between them. These distances can be expressed as the sums of the corresponding crystallochemical radii. The more atoms approaching equilibrium interatomic distances, i.e., the more terms in (1.52) having  $r_{ik}$  corresponding to the largest  $u(r_{ik})$ , the larger is  $U$  (1.52). However, the repulsive branch of the interaction curve, which can be interpreted geometrically as the finite size of atoms (Fig. 1.12), limits the number of atoms reaching the equilibrium interatomic distances. All these circumstances can be expressed as the geometric principle of *maximum filling*. It consists of the following: that, subject to the action of central or near-central forces of attraction, the atoms or more complex structural units of a crystal always tend to approach each other so that the number of permissible shortest contacts is maximal. This can also be expressed as a tendency towards a maximum number  $n$  of atoms (or structural units) per unit volume  $\Omega$  at distances  $r_{ij}$ , not less than the standard permissible distances  $r_{st}$ ,

$$\frac{n}{v_{(r_{ij} \geq r_{st})}} \rightarrow \max. \quad (1.73)$$

The most appropriate formulation is based on the concept of crystallochemical radii  $r$ . If there is a "radius", then naturally a crystal model consists of atoms – balls having these radii and volumes  $V_{at} = 4/3\pi r^3$  are in contact with each other (Figs. 1.44a, b; 47). If we introduce the ratio of the sum of volumes occupied by atoms to the volume of the cell  $\Omega$ , i.e., the so-called packing coefficient,

$$\Sigma V_{at}/\Omega = q \rightarrow \max \quad (1.74)$$

then the maximum filling principle can be described as that of the packing coefficient maximum. It is most clearly expressed in structures built according to the method of the closest packing of identical balls ( $q = 74.05\%$ ). But it is also used when considering the geometric interpretation of structures made up of different atoms as the packing of balls of different radii. The closest packings will be specially considered below. In general, however, according to this principle a structure should not have any vacant sites where atoms (balls) of the largest

radii could be accommodated, and there must be as few sites as possible which are not occupied by other atoms (balls) having smaller radii.

Similarly, if we assign some volume  $V_i$  to multiaatomic structural groupings or molecules, wrapping them in a "coat" of weak-bond radii (as shown in Figs. 1.49, 50), then the maximum-filling principle will be expressed analogously (1.74)

$$\sum V_i / \Omega = q \rightarrow \max. \quad (1.75)$$

Being the geometrization of the concepts of the crystal structure, the maximum-filling principle, or the same idea expressed as the closest-packing principle, is naturally qualitative, because it explains the main tendency in the formation of structures consisting of mutually attracted particles, but not the individual features of the specific structures. Yet owing to its simplicity and generality it plays an important part in crystal chemistry and sometimes aids in drawing quantitative conclusions, for instance in considering the structure of some ionic and molecular crystals (Sect. 2.3.6).

#### 1.5.4 Relationship Between the Symmetry of Structural Units and Crystal Symmetry

As has already been noted, the atoms in a structure – when they are its structural units – can be regarded either as spherically symmetric or as having a different point symmetry corresponding to the orientation of the covalent bonds (cf. Fig. 1.18c). Multiaatomic finite structural groupings also have a definite point symmetry, most often crystallographic (Fig. 1.54), but there may be groupings with a noncrystallographic symmetry as well. The force field around such groupings, i.e., the field of the potential interaction energy, is anisotropic and corresponds to the symmetry of the grouping itself, which presupposes, to some extent, the possibility of its contacts with other atoms or with similar or different groupings. But this anisotropy is not very large, and for geometric consideration it is often possible to assume that the forces of interaction between charged groupings are near central. For instance, the structure of  $\text{Na}_2\text{SO}_4$  can be considered as built up of mutually attracted structural units of  $\text{Na}^+$  and  $\text{SO}_4^{2-}$  (Fig. 1.55).

Inorganic and organic molecules are the most diversified as regards their structure and symmetry. They include asymmetric (symmetry  $I$ ), centrosymmetric ( $\bar{I}$ ), and higher symmetry molecules (see Fig. 2.72) up to giant virus molecules with an icosahedral pseudospherical symmetry (see Figs. 2.169, 174).

Let us now see whether the space symmetry  $\Phi$  of the structure arising from the given structural units is related (and if so, then how) to the point symmetry  $G_0^3$  of these units. When forming a crystal, atoms or more complex structural units occupy definite positions in the unit cell, and arranging themselves in accordance with one or several regular point systems of the general (with symmetry  $I$ ) or particular (with symmetry  $K$ ) position of group  $\Phi$ . Consider whether there is any connection between the intrinsic symmetry  $G_0^3$  of the structural unit and the symmetry  $K$  of its position in the crystal.

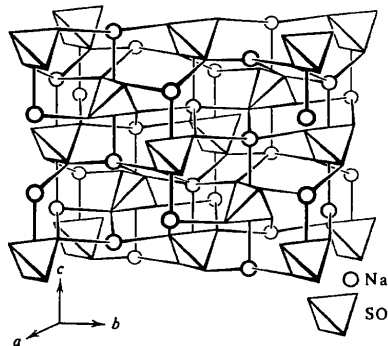


Fig. 1.55.  $\text{Na}_2\text{SO}_4$  structure

On the one hand, many examples of such a relationship are known. For instance, the spherically symmetric atoms in the structures of metal elements occupy all positions with the maximum symmetry  $m\bar{3}m$  in the cubic, high-symmetry space group  $Fm\bar{3}m$ ; the same symmetry is observed for Na and Cl atoms, with central forces acting between them in the structure of  $\text{NaCl}$ . The tetrahedral carbon atom in the diamond structure occupies a position with a tetrahedral symmetry  $\bar{4}3m$ , or, more precisely, predetermines the symmetry of this position. The trigonal complex anion  $\text{CO}_3^{2-}$  "imposes" the rhombohedral symmetry on the calcite structure (see Fig. 2.19), etc. In such cases it can be said that the symmetry of position  $K$ , being a subgroup of the symmetry of structural unit  $G_0^3$ , is maximally close to, or coincides with it:  $G_0^3 \supseteq K$ . This corresponds to the fulfilment of the so-called Curie principle of interaction of symmetries [1.7]. The field of all the particles of the structure, surrounding a given particle with the symmetry  $G_0^3$ , interacts with its own field. This interaction ultimately determines the symmetry  $K$ .

On the other hand, in many structures symmetric atoms or molecules occupy positions  $K$ , which are less symmetric than their proper symmetry. In this case, too, the Curie principle holds, i.e., the point group of positions is a subgroup  $K \subset G_0^3$  of the point group of the structural unit, but the anti-symmetrization may be quite strong so that sometimes the positions may even be asymmetric,  $K = 1$ . For instance, benzene molecules with a high symmetry  $6/m\bar{m}$  are packed in an orthorhombic structure, and the symmetry of the positions of the molecule center is  $\bar{1}$ . The tetrahedral grouping  $\text{SiO}_4$  in different crystals occupies both the positions corresponding to this symmetry (cristobalite) and those whose symmetry is lower, i.e.,  $2, m$ , or  $1$  in many silicates.

The answer to our question is simple. The determining principle of the formation of a structure is the principle of energy minimum, which for undirected interaction forces is expressed geometrically as the maximum-filling principle. If the symmetry of a structural unit during the formation of a crystal is consistent with or helpful in attaining this minimum, then a structure is formed with such a space group  $\Phi$  and such positioning of the structural units within it

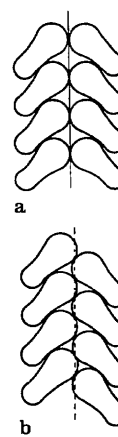
which are closest to their proper symmetry. But if the minimum is attained when the structural units occupy low-symmetry positions, their proper symmetry either does not play any role or is used only partly, i.e., it does not completely coincide with the symmetry of positions.

When speaking of the relationship between the symmetry of positions  $K$  and that of structural unit  $G_0^3$ , one may distinguish two cases. In one, the symmetry  $G_0^3$  of an isolated structural unit in the crystal taken by itself is preserved  $G_0^3 = G_{0(cr)}^3$ . In the other, the effect of the field of the surrounding particles (the lattice field) is such that the structure of a molecule changes and its symmetry is reduced,  $G_0^3 \supset G_{0(cr)}^3 \supsetneq K$ .

It is worth mentioning one more circumstance, which is associated with the simplicity or complexity of the chemical formula of a given substance. The number of most symmetric positions in any space group  $\Phi$  is limited. For structures with a simple formula this may not be meaningful. For instance, in ionic structures having simple formulae of the type  $AX$ ,  $AX_2$ , etc., central forces operate between the atoms which can occupy high-symmetry positions, and the structures usually show a high symmetry. But if there are many sorts of atoms, the number of such positions is simply insufficient, and the symmetry of the structure is reduced. Therefore, usually the more complex the chemical formula of an inorganic compound, the lower is the symmetry of its crystal structure.

If speaking of the relationship between the point symmetry of a structural unit and its position in the crystal, one must also mention those cases where the latter is higher than the former. This is naturally impossible for molecules "at rest", but it can be achieved statistically, either by averaging over all the unit cells of the crystal or by thermal reorientation of the molecules or of their rotation,  $K = G_{0(statist.)}^3 \supset G_0^3$ . Thus, cases are known where asymmetric (with symmetry 1) molecules, which are, however, approximately centrosymmetric in shape, form a centrosymmetric crystal, in which they statistically occupy a position with symmetry 1. Owing to thermal reorientations the grouping  $\text{NH}_4$  with a proper symmetry  $\bar{4}3m$  occupies positions with the symmetry  $m\bar{3}m$  in some crystals, while in certain compounds it is in the state of complete spherical rotation.

We have considered the relationship between the point symmetry of structural units (with nondirectional binding forces between them) and the point symmetry of their positions in the crystal structure. What is more important, however, the space symmetry  $\Phi$  also regulates the mutual arrangement of the structural units, not only by means of point symmetry operations, but also by translations and symmetry operations with a translational component. Let us take a look at Fig. 1.56, which illustrates the role of symmetry operations when particles of arbitrary shape contact each other. It is seen that, from the standpoint of the principle of maximum mutual approach of neighboring particles, point symmetry operations (Fig. 1.56a) are actually inappropriate since they impose the condition of pairwise arrangement of the centers of the atoms along lines (or in planes) perpendicular to the corresponding symmetry elements, and this precludes the most economical utilization of space. On the contrary,



a



b

**Fig. 1.56a, b.** Packing of structural units in a crystal. Point symmetry operations (in this case mirror plane  $m$ ) are not appropriate because the projections of the structural units confront each other (a). Close packing is promoted by symmetry operations which a translational component (b)

symmetry elements with a translational component (Fig. 1.56b) let some particles enter the spaces between others; more precisely, these elements are virtually formed with such packing. Therefore, the important consequences of the maximum-filling principle are, the rules concerning, firstly, the utilization of symmetry elements having a translational component, and, secondly, the implications of the appearance of point symmetry elements between neighboring atoms; if such elements exist, the atoms or structural units should be arranged on them.

If the binding forces are directional, as in covalent crystals, the close-packing principle contradicts the physical model picturing the attainment of the potential energy minimum. Then, representing the structure by means of contacting balls also is not adequate any more. The energy minimum is attained precisely upon saturation of the directional covalent bonds; in this case the principle of a proper point symmetry of atoms is always in the foreground. Therefore, the covalent structures in which atoms have relatively few neighbors (1.3, 4, 7) in accordance with their symmetry, are "lacier" than the maximum-filling structures. Examples are diamond (Fig. 1.44c) and other tetrahedral structures, octahedral structures of the NiAs type (Fig. 1.57). The symmetry of these structures is defined by the symmetry of the constituent atoms. Although covalent structures are "lacier", the volumes per atom in structures with distinct types of bonds differ only slightly, on the average, since the covalent bonds are usually slightly shorter than the ionic or metallic.

Concerning the relationship of the point symmetry of structural units  $G_0^3$ , their positions in the crystal  $K$ , and the space symmetry of structure  $G_3^3$ , one must also mention the so-called local, noncrystallographic symmetry. In some molecular (Sect. 2.6.2) and biological (Sect. 2.9.4) structures such packing of the structural units is observed when they are related symmetrically, for instance, by axes 2; these symmetry elements do not belong to group  $G_0^3$  (they are said to be

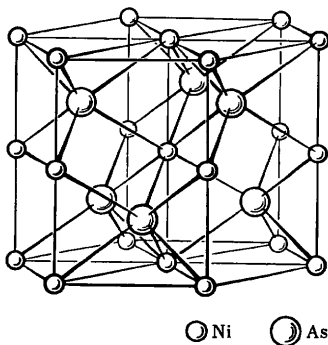


Fig. 1.57. The structure of NiAs with octahedral Ni bonds

noncrystallographic), but act locally, say, between definite (not all) pairs of particles (Fig. 2.150). The so-called noncrystallographic screw axes, which link chains of particles running along different directions in the crystal, are also known (see Fig. 2.75). Later (Sect. 2.6) we shall see how all these phenomena can be explained from the standpoint of the packing energy minimum principle and from the structural features of the units packed.

### 1.5.5 Statistics of the Occurrence of Space Groups

The above considerations are confirmed by the statistics of the distribution of the investigated structures among the space groups. Such data were obtained by processing the results for 5,600 inorganic and 3,200 organic structures (there are 8,800 structures in all) [1.52, 53]. They are listed in Table 1.11, the groups being arranged in the order of increasing symmetry.

Thus, 40% of the inorganic structures belong to only nine groups, 60% of the organic structures to six groups, and half of all the structures to the 12 groups  $\Phi$  listed in Table 1.11.

The occurrence of the listed groups is due to the above consideration concerning the advantage of the presence of "packing" symmetry elements with a translational component, which is typical of practically all the groups of Table 1.11 and is most clearly manifested in inorganic structures having complicated formula, as well as in organic structures. If a structure has a relatively simple formula, its atoms can arrange themselves on point symmetry elements. This mainly explains the lower part of the table; all the groups listed in it belong to the structures of elements and simple inorganic compounds.

Only 40 groups  $\Phi$  (including the just listed 12) are relatively widespread. Representatives of 197 groups  $\Phi$  (out of 219) have been found. An analysis of the frequency of occurrence of group  $\Phi$  shows, however, that, with the increase of the number of investigated crystals the representatives of groups not yet observed may be found.

Table 1.11. Distribution of crystal structures among space groups  $\Phi$  [%]

$\Phi$	Inorganic structures	Organic structures	All structures
$C_1^1 - P\bar{1}$	1	5	3
$C_2^2 - P2_1$	—	8	3
$C_{2h}^5 - P2_1/c$	5	26	13
$C_{2h}^6 - C2/c$	4	7	5
$D_2^4 - P2_1,2_1$	—	13	5
$D_{2h}^{15} - Pbca$	—	3	1
$D_{2h}^{16} - Pnma$	7	—	5
$D_{3d}^3 - R\bar{3}m$	4	—	2
$D_{6h}^4 - P6_3/mmc$	4	—	3
$O_h^1 - Pm\bar{3}m$	4	—	3
$O_h^5 - Fm\bar{3}m$	9	—	6
$O_h^7 - Fd\bar{3}m$	5	—	3

The center of symmetry 1 is present in most of the structures investigated – in 82% of the inorganic and 60% of organic, or altogether in 74% of the substances<sup>8</sup>.

### 1.5.6 Coordination

In analyzing the crystal structure it is important to investigate the environment of an atom (or molecule): the number of its neighbors, their characteristics, and the distances to them. These features are all described by a single concept of "coordination". Consider the coordination of atoms in the simplest structures of metals and ionic compounds and in some other structures; the neighbors surrounding the given atom are positioned symmetrically in relation to it and are located at equal distances from it. The number of such nearest neighbors, or their number in the first coordination sphere, is called the coordination number (c.n.). The next-nearest neighbors form the second coordination sphere, and so on. In more complicated, low-symmetry structures the distances to the nearest neighbors may differ slightly, but the coordination concept can still be used, provided there is a gap between this set of distances (i.e., to the nearest neighbors) and the set of distances to the atoms of the next-nearest coordination sphere. If the distances to the atoms of the first and second spheres do not clearly differ, both c.n. are sometimes indicated, for instance, 8 + 6. The value of the c.n. is associated with the type of chemical bond and the proper symmetry of the atoms. For central forces, the c.n. is usually large 12, 6 + 8, 8 + 6, etc., and for covalent forces, it is small, 3, 4, or 6.

<sup>8</sup> In recent years, due to the development of the structure analysis technique, the percentage of investigated noncentrosymmetric structures has increased.

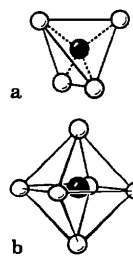


Fig. 1.58a, b. Construction of a coordination polyhedron as exemplified by a tetrahedron (a) and an octahedron (b)

The concept of coordination is also used in molecular structures. The arrangement of the centers and the number of neighboring molecules are considered with respect to the center of a given molecule.

If we join the center of adjacent atoms of the first coordination sphere by straight lines, we obtain a convex polyhedron, i.e., a coordination polyhedron with a number of vertices equal to c.n. The distances from the vertices to the central atom are the interatomic distances in this sphere, and the polyhedron edges are the distances between the nearest neighbors (Fig. 1.58). The various types of coordination polyhedra are shown in Fig. 1.59. The coordination polyhedra for a given c.n. may be different, i.e., have a particular point symmetry. One case is plane configurations. When some coordination polyhedra are singled out in such a structure, they may be either isolated, or linked with other polyhedra via common vertices, edges, or faces.

The concept of polyhedra is not only a method for describing crystal structures. It also has a physical and chemical meaning when the polyhedra are either the structural units discussed above, for instance, tetrahedra  $\text{SiO}_4$ , complex groupings, say  $\text{PtCl}_4$ , or combinations of a central atom with surrounding atoms, which are common in ionic compounds such as octahedra  $\text{MeX}_6$  ( $\text{X}$  anion).

### 1.5.7 Classification of Structures According to the Dimensionality of Structural Groupings

All the structures can be classified by the presence or absence of structural groupings – atoms or their complexes – in which the bonds are stronger (and hence shorter) than those between the groupings, as well as by the dimensionality of these groupings, i.e., by the number of dimensions of space  $k$  within which they are finite. Since the groupings are in a three-dimensionally periodic lattice, the quantity  $m = 3 - k$  indicates the number of dimensions in which the groupings are infinite and periodic.

The values  $k = 0, m = 3$  corresponds to homodesmic structures, their structural units being atoms between which there is a three-dimensional net of approximately equivalent bonds. Such a crystal taken as a whole can be regarded as a giant structural grouping with symmetry  $G_3^3$ .

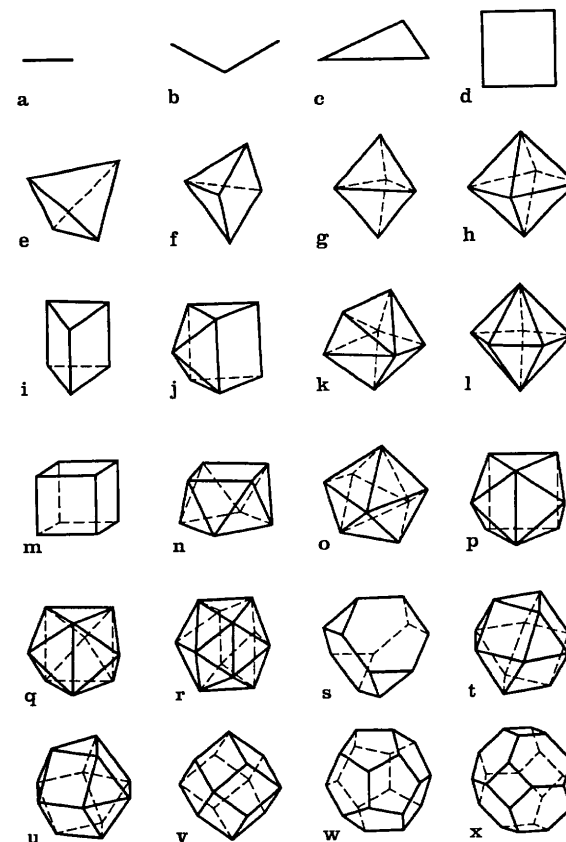


Fig. 1.59a–x. Various types of coordination polyhedra. (a) dumb-bell, c.n. 1; (b) corner, c.n. 2; (c) triangle, c.n. 3; (d) square, c.n. 4; (e) tetrahedron, c.n. 4; (f) tetragonal pyramid, c.n. 5; (g) trigonal bipyramid, c.n. 5; (h) octahedron, c.n. 6; (i) trigonal prism, c.n. 6; (j) one-cap trigonal prism, c.n. 7; (k) seven-vertex polyhedron, c.n. 7; (l) pentagonal bipyramid, c.n. 7; (m) cube, c.n. 8; (n) square antiprism (cube), c.n. 8; (o) trigonal dodecahedron, c.n. 8; (p) two-cap prism, c.n. 8; (q) three-cap trigonal prism, c.n. 9; (r) icosahedron, c.n. 12; (s) truncated tetrahedron c.n. 12; (t) cubooctahedron, c.n. 12; (u) hexagonal cubooctahedron, c.n. 12; (v) rhombododecahedron, c.n. 14; (w) pentagon-dodecahedron, c.n. 20; (x) truncated octahedron, c.n. 24

Further, as  $k$  increases and  $m$  declines, we obtain

- $k = 0, m = 3$ : three-dimensional structures with symmetry  $G_3^3$ ;
- $k = 1, m = 2$ : layer structures, layer symmetry  $G_2^3$ ;
- $k = 2, m = 1$ : chain structures, chain symmetry  $G_1^3$ ;
- $k = 3, m = 0$ : structures with finite groupings of symmetry  $G_0^3$ .

Structures of the first type are, as a rule, homodesmic; the others are heterodesmic. Along with structures which can definitely be allocated to one of the indicated types, there are intermediate structures, i.e., structural groupings, which are not very clearly defined, and also structures with groupings belonging to different types. Let us now consider the basic features of all these structures.

### 1.5.8 Coordination Structures

This name is usually given to structures of the first type, with  $k = 0$  and  $m = 3$ , because the coordinations of atoms in them are approximately equal in all directions. This term is not quite appropriate, since some amount of coordination is inherent in any atom or any structure, thus it would be more correct to call these structures coordination equal.

Coordination-equal structures form most of the inorganic compounds; these include practically all the metals and alloys and most of the ionic and covalent compounds. Their coordination numbers are usually large (12, 6 + 8, 8 + 6) except for the covalent structures. The coordination structures are also found in the crystals of inert elements; they have a large c.n. of 12 (closest packings). These structures are isodesmic, all the bonds in them being identical – not strong, but weak van der Waals bonds.

Among the coordination-equal structures one can single out coordination polyhedra of the same or different types, but they always form some kind of a space array (see Fig. 2.17). Sometimes the stable frameworks of interlaced structural groupings (for instance, silicon–oxygen tetrahedra and  $\text{MeO}_6$ –octahedra) form a lacy space structure, which has rather large holes, isolated or channel-shaped, passing through the entire structure (see Fig. 2.37). These are called skeleton structures.

### 1.5.9 Relationship Between Coordination and Atomic Sizes

Ionic structures can be represented by and described with the aid of coordination polyhedra with cations at the center and anions at the vertices. *Magnus* [1.54] and *Goldschmidt* [1.38] introduced a geometric criterion, the ratio of effective ionic radii,

$$r_{\text{cat}}/r_{\text{an}} = g', \quad (1.76)$$

which determines the coordination number  $n$  and the type of the coordination polyhedron (Fig. 1.60). Since the effective ionic radii of cations are purely conventional values, as noted above, one can use for the geometric criterion the following quantity independent of the choice of  $r_{\text{cat}}$ :

$$g = d(\text{AB})/r_{\text{an}}, \quad (1.77)$$

where  $d(\text{AB})$  is the distance from the polyhedron center to its vertex (i.e., the cation–anion distance), and  $2r_{\text{an}}$  is the polyhedron edge (i.e., the distance

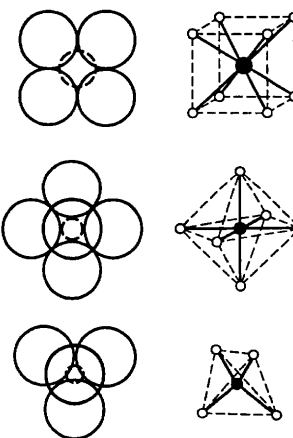


Fig. 1.60. Illustration of the Magnus rule for coordination numbers 4, 6, 8

Table 1.12. Relationship between coordination  $n$  and values of  $g$  and  $g'$

Coordination	$n$	$g$	$g'$
Tetrahedron	4	1.225	0.225
Octahedron	6	1.414	0.414
Thomson (wringed) cube	7	1.592	0.592
Cube	8	1.645	0.645
Cubo-octahedron	8	1.732	0.732
	12	2.000	1.000

between anions). Here,  $g' = g^{-1}$ . Table 1.12 lists the values of  $g$  and  $g'$  permitting coordination  $n$  (or any one below  $n$ ).

If  $g$  is intermediate between the “nodal” values, for instance,  $1.225 \leq g < 1.414$ , then only four anions can settle around the cation (not necessarily contacting each other) at a given  $d(\text{AB})$ . As  $g$  increases, a transition to larger coordination numbers and to the corresponding polyhedra may (and must, from the standpoint of close packing) take place. If, on the contrary, there is contact of all the outer spheres, then on realization of coordination  $n$  and at  $g$  less than the corresponding nodal value (e.g., for the octahedron  $n = 6$  and  $g < 1.414$ ), the cation will “dangle” among the surrounding anions. Such a configuration is unstable from the geometric standpoint. Thus, at a given  $g$ , the geometrically most probable coordination is realized when  $g$  is less than the nearest nodal value, but lower coordinations are also possible. Thus, although at  $g = 1.645$  the formation of a Thomson cube with  $n = 8$  is already possible, at these and higher values a stable grouping is often an octahedron with  $n = 6$  (this is true, for example, of  $\text{KF}$  and  $\text{RbCl}$ ). The Magnus rules hold for a number of ionic

crystals. So, for many halides of alkali metals (see Fig. 1.47) the values of  $g$  correspond to the observed octahedral coordination. The structures of CsCl, CsBr, and CsI have a cubic coordination in conformity with the values of  $g$  (1.75, 1.84, and 1.91). At the same time, these rules are not fulfilled in many cases. Thus, the structures of LiCl, LiBr, and LiF have  $g < 1.415$ , i.e., they would be expected to be tetrahedral (the octahedron is “impossible” for them), but in fact they crystallize as NaCl, with an octahedral coordination. This is due to the conventional nature of the geometric model.

### 1.5.10 Closest Packings

A number of the structures of elements, alloys, and ionic crystals are built on the close-packing principle. Consider the geometry and symmetry of the closest packings of spheres and some related questions.

One two-dimensional close-packed layer of identical spheres is depicted in Fig. 1.61 together with its intrinsic symmetry elements. Axes 6 pass through the centers of the spheres, and axes 3, through the interstices (holes) between spheres. There are twice as many interstices as spheres. The next, identical layer will be packed most closely if its spheres are placed over the voids, between the spheres of the lower layer (Fig. 1.62). The common elements for two, or any number of layers superimposed in this manner will be the axes 3 and planes  $m$ , as before. Hence, the space groups of the closest packings are all the groups which have subgroup  $P3m1$ ; these are (besides the foregoing)  $R3m$ ,  $P\bar{3}m1$ ,  $R\bar{3}m$ ,  $P\bar{6}m2$ ,  $P6_3mc$ ,  $P6_3/mmc$ , and  $Fm\bar{3}m$ ; in all, there are eight such groups [1.55].

If we denote (as in Fig. 1.62) the initial layer of spheres by  $A$ , the possible ways of placing the next layer, either  $B$  or  $C$ , over it are  $b$  and  $c$ . The symbol is irrelevant until the third layer is determined (in Fig. 1.62 it is  $B$ ) which may be placed over the interstices of layer  $B$ . Thus, any combinations of arrangements of new layers can be described by a sequence of letters  $A$ ,  $B$ , and  $C$ , and no identical letters can stand side by side, since that would mean placing one sphere over another. The packing coefficient for any closest packing is 74.05%. The

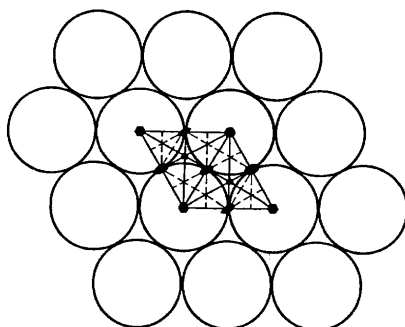


Fig. 1.61. Close-packed layer of spheres and its symmetry

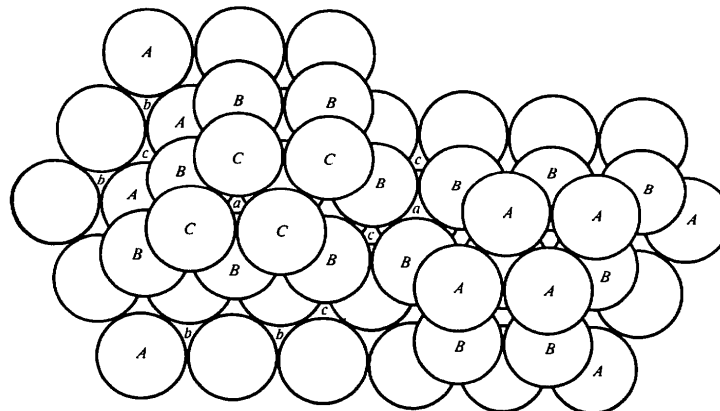


Fig. 1.62. Two principal variants of the formation of three-dimensional closest packing of spheres made up of the layers  $A$ ,  $B$ ,  $C$  stacked over the interstices in the lower layer  $a$ ,  $b$ ,  $c$ ;  $ABC$  (left) and  $ABAB$  (right)

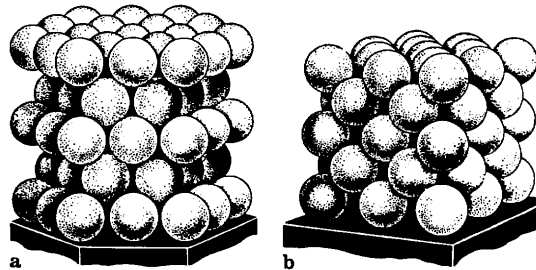


Fig. 1.63a, b. Hexagonal (a) and cubic (b) closest packing. In the cubic packing the closest-packed layers can be singled out in four planes perpendicular to the body diagonals of the cube

two-layer packing  $\dots ABAB \dots$  (right-hand side of Fig. 1.62 and Fig. 1.63a) is called the closest hexagonal and has the symmetry  $P6_3/mmc$ . A remarkable arrangement is the three-layer packing  $\dots ABCABC \dots$  (left-hand side of Fig. 1.62, and Fig. 1.63b). The stacking of the initial three close-packed two-dimensional layers produces an arrangement such that precisely identical layers in it (and only in it) can be singled out along three other directions, as seen from Fig. 1.63b. This packing is cubic face centered, its symmetry being  $Fm\bar{3}m$ .

Further, we can consider the stacking of layers with a periodicity  $n$ , greater than for three layers. Before we do that, we should note that the obvious three-letter notation is redundant. This follows even from the fact that the sequences  $\dots ABAB \dots$ ,  $ACAC \dots$ , and  $BCBC \dots$  denote one and the

same hexagonal packing. It would suffice to label a given layer according to the way the two nearest layers adjoin it from below and from above, namely by the hexagonal (*h*) or cubic (*c*) law. Then the two principal packings will be written as follows (the symmetry is also indicated):

$$n = 2 \begin{array}{l} ABAB \\ h\ h\ h\end{array} D_{6h}^4 = P6_3/mmc, \quad n = 3 \begin{array}{l} ABCABC \\ c\ c\ c\end{array} O_h^5 = Fm\bar{3}m, \quad (1.78)$$

where *n* is the number of layers in the packing. Figure 1.64 shows the coordination polyhedra of spheres of type *h* and *c*, i.e., cubooctahedra, in packing *c*, a regular, and in *h*, a “wrung” one (hexagonal, an analog of the cubooctahedron). Packings with *n* = 4, 5 are as follows:

$$n = 4 \begin{array}{l} ABAC \\ c\ h\ c\ h\end{array} D_{6h}^4 = P6_3/mmc, \quad n = 5 \begin{array}{l} ABCAB \\ h\ c\ c\ h\end{array} D_{3d}^3 = P\bar{3}m1.$$

There are two packings with *n* = 6,

$$n = 6 \begin{array}{l} ABCACB \\ h\ c\ c\ h\ c\end{array} D_{6h}^4 = P6_3/mmc, \quad \begin{array}{l} ABABAC \\ c\ h\ h\ h\ c\ h\end{array} D_{3h}^1 = P6m2.$$

Figure 1.65 shows some packings with different numbers of layers.

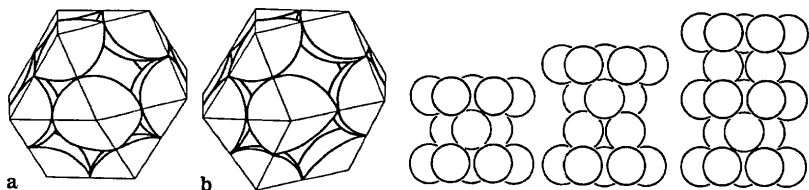


Fig. 1.64a, b. Coordination polyhedra, cubooctahedron *c* (a) and its hexagonal analog *h* (b)

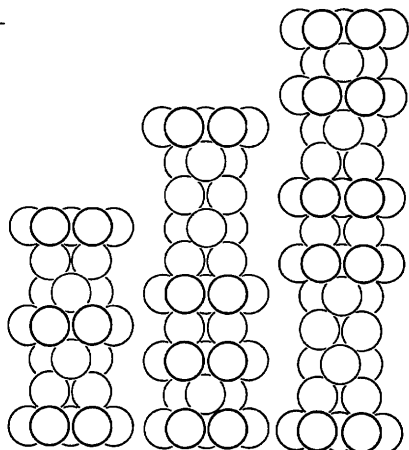


Fig. 1.65. Closest packings with different periodicity number of layers: 2, 3, 4, 6, 9, 12

A complete system of the closest packings of spheres was proposed by *Belov* [1.55]. With a fixed *n*, the number of different packings is naturally limited, but it increases with *n*,

number of layers	2	3	4	5	6	7	8	9	10	11	12	...
number of packings	1	1	1	1	2	3	6	7	16	21	43	...

An example of 8-layer packing is *hccchcc*, and of 12-layer, *hhcchhcchhcc*. It is significant that while at small *n* all the spheres are symmetrically equal, i.e., they occupy a single regular point system, an increase in *n* renders this impossible. This reflects the above-described competition of the principles of closest packing and preservation of proper symmetry of particles in the lattice, which arises when the number of particles in the unit cell is large.

The structures of many elements – metals [Na, Al, Cu, Fe, Au, etc. (*c*), Mg, Be,  $\alpha$ Ni, Cd, Zn, etc. (*h*)] and solid inert elements – are built according to the principle of cubic face-centered (fcc) and hexagonal closest packing (hcp). In some cases the structure deviates from the ideal, examples being the rhombohedral or tetragonal distortion of cubic packing, and deviation from the “ideal” value of  $c/a = 1.633$  in hexagonal packing (Fig. 1.66).

Closest packings are also realized in structures made up of different atoms, provided these structures are homodesmic and the atomic radii are approximately equal. A good example is the structure of alloys, such as Cu<sub>3</sub>Au (see Fig. 2.9b) and semiconductor alloys containing Bi, Sb, S, Te, Ge, and Ag with coordination 12, all of whose atoms have radii of 1.6–1.8 Å. These alloys form multilayer packings, sometimes with a statistical population of more than one position; an example of such a compound is presented in Fig. 1.67.

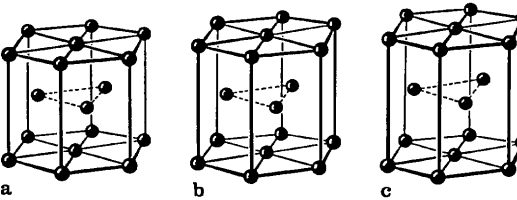


Fig. 1.66a–c. Deviation from the ideal ratio  $c/a = 1.633$  in the structure of some metals.  
(a) Be,  $c/a = 1.57$ ; (b) ideal lattice; (c) Cd,  $c/a = 1.89$

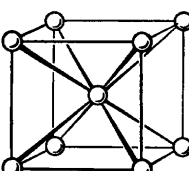


Fig. 1.67. Structure of AgBiTe<sub>2</sub>

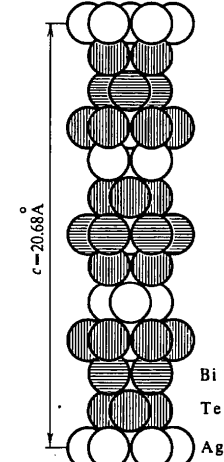


Fig. 1.68. Cubic body-centered structure

Body-centered cubic packing (bcc) is common in the structures of elements and a number of compounds (Fig. 1.68). If we regard it formally as a packing of equal spheres, the packing factor will be equal to 68.01%; it is less than the factor of 74.05% for closest packings, but is still large. Transitions between such two types of cubic structures (for instance,  $\alpha$ - $\gamma$ - $\delta$ -Fe: bcc-fcc-bcc) are very interesting. From the geometric standpoint one can say that the stability of bcc structures is due to the fact that the principle of high symmetry of the atoms is well maintained, and that their coordination (8 + 6) is very high. But a comprehensive explanation of this type of structure can be achieved only by taking into account all the features of atomic interaction and lattice dynamics.

### 1.5.11 Structures of Compounds Based on Close Packing of Spheres

Between closest-packed spheres there are interstices, or holes of two types. Having covered the structure of the densest layer with the next one (Fig. 1.62), we shall now see that holes of the lower layer which are covered by spheres of the upper are surrounded by four spheres, the centers of which form a tetrahedron (the hole  $a$  is covered by a sphere  $A$ , or  $b$  is covered by  $B$ , and  $c$ , by  $C$ ). They are called tetrahedral holes (Fig. 1.69a). There are three spheres above and below

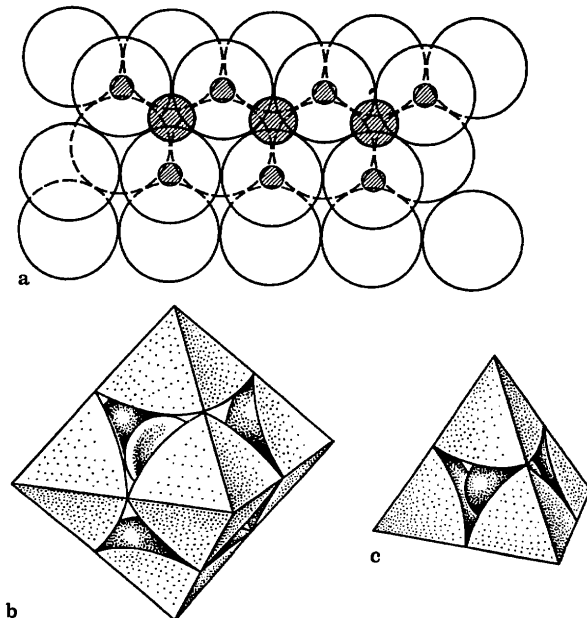


Fig. 1.69a–c. Octahedral and tetrahedral holes between two layers of closest packing with small spheres inserted in them (a); polyhedra around octahedral (b) and tetrahedral (c) holes

holes of the second type; they are octahedral [ $a$  has nonmatching spheres  $B$  and  $C$  above and below, and so on (Fig. 1.69a)]. In any three-dimensional closest packing the number of tetrahedral holes is twice that of the spheres, while the number of octahedral holes is equal to that of the spheres.

The holes could be filled with smaller spheres contacting the principal spheres of radius  $R$ . The radius of such a small sphere for a tetrahedral hole is equal to  $0.225 R$ , and for an octahedral hole  $0.415 R$  (Fig. 1.69b, c). Using the ionic radii systems we can consider the geometric possibilities of "populating" the holes in an anion packing with cations. These possibilities depend on the formal values of  $g$  or  $g'$  according to Table 1.12, which correspond to octahedral and tetrahedral coordinations.

However, in the vast majority of crystals built according to this scheme the "close-packed" spheres of anions no longer contact each other, since the cations "spread out" the packing irrespective of the fact whether we regard it from the standpoint of the system of effective or physical ionic radii or, all the more so, from the standpoint of the atomic-ionic radii of strong bonds. It nevertheless turns out that a number of structures can be described with the aid of such models. It can, therefore, be said that the system of anion-cation bonds, the presence of covalent interactions directed along a tetrahedron or an octahedron, and the mutual repulsion of like-charged ions result in an arrangement where the centers of atoms, in particular those of anions, occupy positions corresponding to the closest packing of spheres (but of a larger diameter). In other words, the positions corresponding to a close packing are energetically favorable. This can no longer be explained from the standpoint of the geometric theory of closest packings, because the main condition, i.e., the mutual contact of the principal spheres, is violated. On the other hand, the principles of maximum filling and symmetry are nearly always maintained.

Proceeding from the versions of closest packings of anions and from the different possibilities of populating voids of one type or another with cations, we can describe, following *Belov* [1.55], various structures. Such a description is equivalent to representing these structures as combinations of vacant or filled octahedra and tetrahedra connected in various ways.

For instance, populating all the octahedral holes in the closest cubic packing produces the structural type NaCl, and populating all of them in hexagonal packing, the NiAs type (Fig. 1.70, cf. Fig. 1.57). Note that the centers of the atoms residing in octahedral holes are arranged according to the close-packing law, and that the entire structure can just as well be regarded as one having the holes populated by anions in a cation packing. The centers of both sorts of atoms form identical lattices, but are shifted relative to one another.

If half of the octahedral holes in a hexagonal packing are occupied, we obtain type CdI<sub>2</sub> (Fig. 1.71); the filling of two-thirds of the holes according to the corundum motif results in Al<sub>2</sub>O<sub>3</sub> type (Fig. 1.72). The filling of all the tetrahedral holes in the closest cubic packing yields the Li<sub>2</sub>O type of structure (Fig. 1.73a).

As indicated above, by using the formal scheme for the accommodation of atoms and holes in close packing the structures can be described by directional,

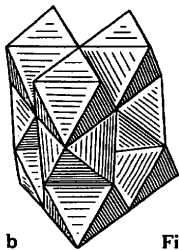
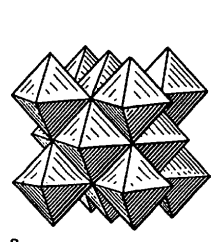


Fig. 1.70a, b

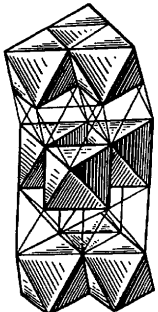


Fig. 1.71

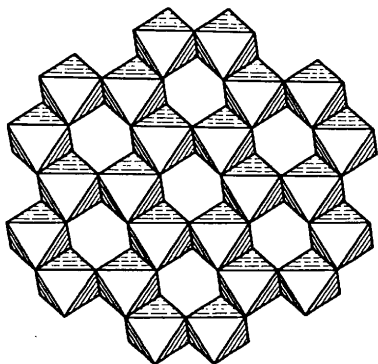


Fig. 1.70a, b. Structure of NaCl (a) and NiAs (b) in polyhedra

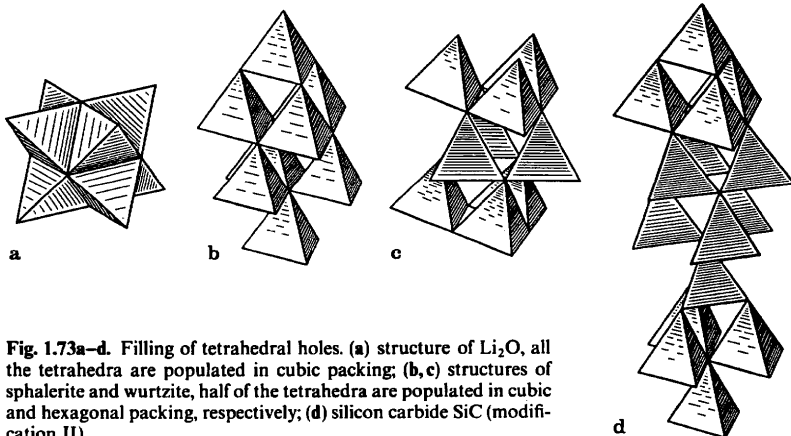
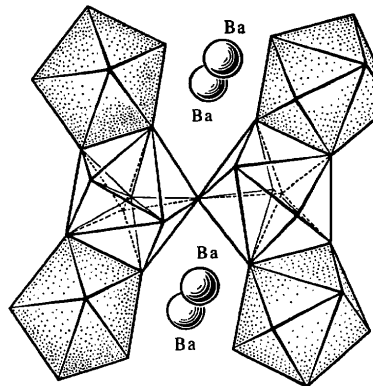
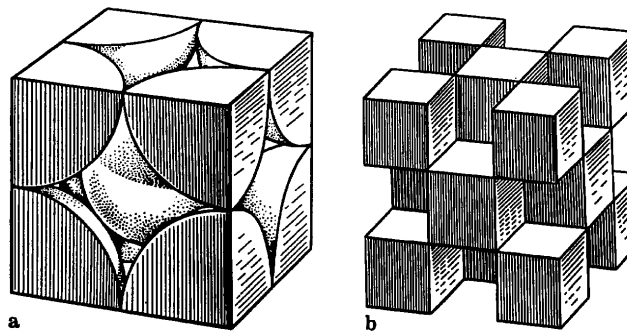
Fig. 1.71. Structure of CdI<sub>2</sub> in polyhedra△ Fig. 1.72. One layer of Al<sub>2</sub>O<sub>3</sub> structure

tetrahedral or octahedral, covalent bonds. Thus, filling half of the tetrahedral holes in cubic packing we obtain the structure of sphalerite, ZnS (Fig. 1.73b), and in a hexagonal, wurtzite (Fig. 1.73c). Various multilayer modifications of SiC, in which tetrahedral nets alternate in different sequences of *h* and *c*, are built similarly (Fig. 1.73d).

If the  $d(AB)/r_{\text{an}}$  ratio increases, then, according to Table 1.12, the coordination number must also increase, and the structures cannot be fitted into the close-packing scheme. High coordination numbers 7, 8, and 11 are indeed observed for the large cations of Ca, Sr, Ba, etc. The coordination polyhedra may be very complex for them (Fig. 1.74). Classical examples of regular polyhedra – cubes – are represented by the structures CsCl and CaF<sub>2</sub> (Fig. 1.75a, b); in the latter, half of the cubes are vacant.

### 1.5.12 Insular, Chain and Layer Structures

If the bonds between the atoms in a structure are of distinct types (heterodesmic structures), such structures are coordination unequal, and it is possible to single out groupings of atoms with  $m = 0, 1, 2$ , which are bound together by short (strong) bonds. The atoms of such distinct groupings are bound by weak (long)

Fig. 1.73a–d. Filling of tetrahedral holes. (a) structure of Li<sub>2</sub>O, all the tetrahedra are populated in cubic packing; (b, c) structures of sphalerite and wurtzite, half of the tetrahedra are populated in cubic and hexagonal packing, respectively; (d) silicon carbide SiC (modification II)△ Fig. 1.74. Eight-vertex polyhedra around Lu atoms in the structure of BaLu<sub>2</sub>F<sub>8</sub>. Ba is surrounded by 11 or 12 atoms of FFig. 1.75a, b. Structures with the cube as a coordination polyhedron. (a) cube in CsCl; (b) packing of cubes in CaF<sub>2</sub>. Structure of CsCl – solid packing of cubes, and of CaF<sub>2</sub> – chess-like packing

bonds. The configurations of the atoms within a grouping depend on the mutual arrangement of the groupings as a whole, i.e., the groupings are stable units of the structure. Since strong bonds are saturated within the groupings, the mutual packing of groupings as stable units is largely defined by weak forces.

The insular structures ( $k = 0$ ) with finite "zero-dimensional" groupings of atoms "islands", include all the molecular compounds except high polymers (Fig. 1.76), structures containing finite complexes of metals with inorganic or organic ligands (Fig. 1.77), and some others. These structures will be considered in detail in Sect. 2.5, 6.

Sometimes it is difficult to draw a clear-cut boundary between zero-dimensional and equal-coordination structures. For instance, such stable groupings as  $\text{NH}_4$  and  $\text{SO}_4$  are finite, but they are not separated from the other surrounding atoms by large distances.

Structures with one-dimensional groupings ( $k = 1$ ) are called chain structures. Typical examples are crystalline polymers built up of infinitely long molecules, and the inorganic structures such as selenium (Fig. 1.44d), semiconductor-ferroelectric  $\text{SbSI}$  (Fig. 1.78), the complex compound  $\text{PdCl}_2$  (Fig. 1.79), and chain silicates of the asbestos type.

The chain itself is described by one of the symmetry groups  $G_1^3$ . In a crystal this symmetry can only decrease, according to the same principles as for insular structures. An example is the structure of paraffins  $\text{C}_n\text{H}_{2n+2}$  (Fig. 1.80). The symmetry of the chains themselves is  $mmc$ , but when they are packed in a lattice, only the "horizontal" planes  $m$  and axes 2 remain, and "packing" symmetry elements  $n$  and  $a$  arise; the space group of the structure is  $Pnam$ . Such a rigid chain retains its configuration in the crystal. Another version is also possible, where the bonds between some rigid chain units, or links, allow different mutual orientations of these elements with the preservation of chain continuity. In this case the conformation of the chains when packed in a crystal structure is, to a large extent, due to the weak bonds between the chains, which are arranged parallel to each other in chain structures.

Layer structures ( $k = 2$ ) have groupings of atoms bounded by strong bonds; these groupings extend infinitely in two dimensions. Good representatives of such structures are graphite (Fig. 2.5), layer structures of the  $\text{CdI}_2$  type (Fig. 1.71), and layer silicates (Fig. 1.81), which can also be regarded as a two-dimensional system of coupled stable coordination polyhedra. Structures which are composed of thick "multistory" layers are sometimes called packets. The stacking of layers according to the close-contact principle can sometimes be done in ways, which differ very little energewise, and therefore various modifications of such structures often arise. For instance,  $\text{CdI}_2$  has many modifications, and there are numerous modifications of various clay minerals, differing in the stacking of the packets or in some features of the structure of the packets themselves.

Concluding this section we emphasize once again that the allocation of some structure to the coordination-equal, the chain, or the layer type sometimes

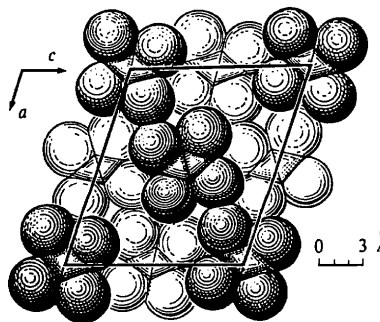


Fig. 1.76

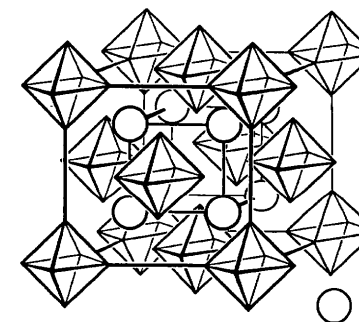


Fig. 1.77

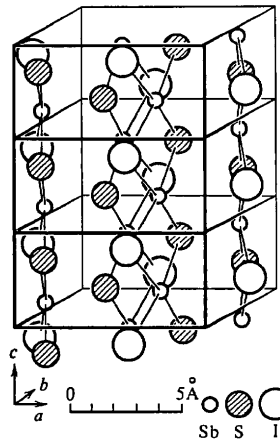


Fig. 1.78

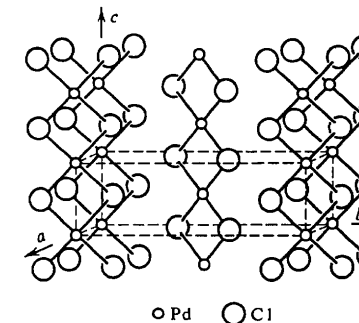


Fig. 1.79

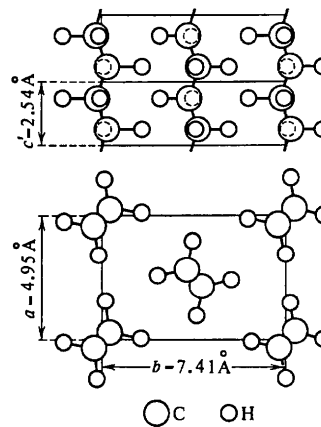


Fig. 1.76. Example of zero-dimensional (insular) structure: tetraiodoethylene

Fig. 1.77. Structure of  $\text{K}_2\text{PtCl}_6$ Fig. 1.78. Structure of  $\text{SbSI}$  [1.56]Fig. 1.79. Structure of  $\text{PdCl}_2$ Fig. 1.80. Structure of paraffin  $\text{C}_n\text{H}_{2n+2}$  in two projections

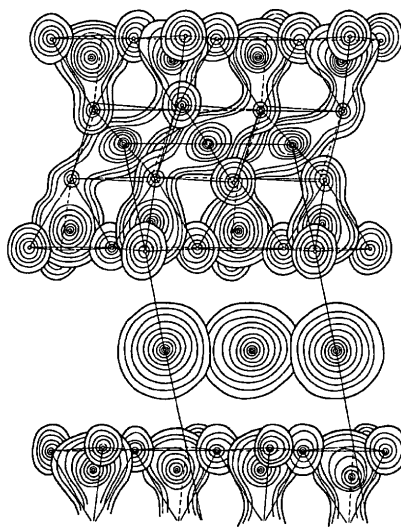


Fig. 1.81. One layer of the mica structure; three-dimensional Fourier synthesis of the lattice potential [1.57]

cannot be made rigorously enough. In coordination-equal structures it is often possible to single out chains or layers which explicitly play an independent structural role, but are in close contact with other atoms of the structure, etc. Some structures are made up of units of two types, for instance, finite complexes and layers or chains, and so on.

## 1.6 Solid Solutions and Isomorphism

### 1.6.1 Isostructural Crystals

Many crystals have an identical atomic structure, i.e., are isostructural. This means that their space groups are identical and the atoms are located over the same regular point systems (RPS); for instance, atoms *A* of one structure and atoms *A'* of another occupy the same RPS, *B* and *B'* occupy another, and so on. It is obvious that isostructural substances are also "isoformular", i.e., their formulae are identical as regards the number of the corresponding atoms. Isostructural crystals may be of different complexity, beginning with simple substances and ending with complicated compounds. For instance, face-centered cubic metals and crystals of inert elements are isostructural. Alkali–halide compounds of the type NaCl (Fig. 1.46), a number of oxides such as MgO, and many alloys such as TiN may serve as other examples. There are large series of isostructural compounds with formulae  $AB_2$ ,  $AB_3$ ,  $ABX_2$ , etc. Each isostructural series is named after one of its most common (or first-

discovered) representatives, for instance, the structural types  $\alpha$ -Fe, NaCl, CsCl,  $K_2PtCl_4$ , etc.

The concept of isostructural crystals is formally geometric. The same structural type may cover crystals with different types of bonds, for instance, ionic and metallic. Yet geometric similarity indicates that the symmetry of the binding forces must be the same; for example, these forces, referring to corresponding atoms, must be, for instance, spherically symmetric or identically oriented.

### 1.6.2 Isomorphism

If crystals are isostructural and have the same type of bond, they are called isomorphous. The parameters of the unit cells of such crystals are close. Their similarity is also manifested macroscopically: owing to the above reasons their external forms are very similar (hence the term isomorphism). This is exactly how isomorphism was discovered at the macroscopic level by E. Mitcherlich in 1819 when observing crystals of  $KH_2PO_4$ ,  $KH_2AsO_4$ , and  $NH_4H_2PO_4$ . Goniometric measurements showed that these tetragonal crystals have identical simple forms, and that the angles between the corresponding faces are similar. Another classical isomorphous group is rhombohedral carbonates  $MCO_3$ ,  $M = Ca, Cd, Mg, Zn, Fe, or Mn$ , for which the vertex angles of the rhombohedrons differ by not more than  $1^\circ - 2^\circ$ . The physical properties of isomorphous substances are similar as well. The present-day investigations of isomorphism are mainly based on X-ray and other diffraction data, which have made it possible to elaborate and extend the initial concepts of isomorphism.

### 1.6.3 Substitutional Solid Solutions

X-ray studies have revealed a close relationship between isomorphism and solubility in the solid state – the phenomena referring to the formation of so-called solid solutions. Isomorphism of crystals is often associated with the possibility of the formation of a series of homogeneous solid solutions of isomorphous substances with a phase diagram of the type shown in Fig. 1.82a.

The most common type of solid solution is a substitutional solution, in which atoms of one component substitute for atoms of another in a given regular point system (Fig. 1.83). The probability of finding a substituting atom

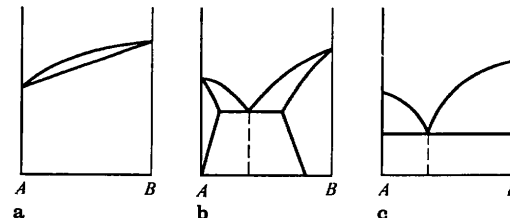


Fig. 1.82a–c. Various types of phase diagrams. (a) The components form continuous solid solutions; (b) limited solubility case; (c) the components do not form solid solutions

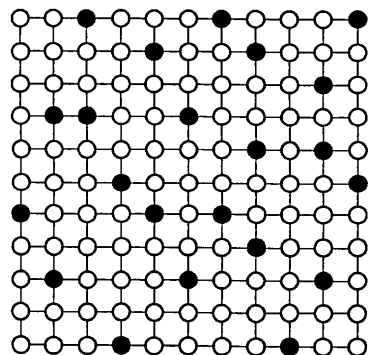


Fig. 1.83. Structure of a substitutional solid solution. Only one regular point system according to which substitution occurs is shown conventionally, there may be other regular point systems according to which no substitution occurs

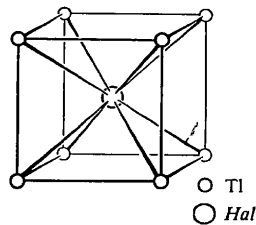


Fig. 1.84. Unit cell of a solid solution  $TlHal'_xHal''_{1-x}$ . At the center of the cell the halogen atoms may replace each other statistically in any concentration

at these points is a constant value depending on the composition of the solid solution. If, for instance, atoms of sort  $A$  in phase  $AB$  can be replaced by atoms of sort  $A'$ , whose atomic fraction is equal to  $x$ , then such a solid solution will be described by the formula  $A_{1-x}A'_xB$ . In this case the probability of detecting the atom  $A$  at a point belonging to a given RPS (or in a given sublattice, as it is sometimes called) is equal to  $1 - x$  and that of detecting the atom  $A'$ ,  $x$ .

Consequently crystals with a formula  $A_{1-x}A'_xB$  ( $0 < x < 1$ ) for any  $x$  are isostructural to each other and with the extreme terms of the series, i.e., compounds  $AB$  and  $A'B$  (Figs. 1.84, and 2.9a).

Thus, the term "isomorphism" is actually used to denote two similar but not quite identical concepts. The first implies similarity of the structure and the shape of crystals of different (but related) chemical compositions, and the second, mutual substitution of atoms or other structural units in crystalline phases of variable composition.

Investigations into the atomic structure of isomorphous substances and their solid solutions have helped to establish not only the geometric similarity of their structures, but also the geometric restrictions on the sizes of the atoms, which can replace one another. For instance, KBr and LiCl are isostructural and have an identical type of bond, but they do not form a series of homogeneous solid solutions. This is due to the significant difference in the size of their ions. An analysis carried out by V. M. Goldschmidt and corroborated by numerous

subsequent investigations showed that in ionic compounds the radii of ions substituting for each other usually do not differ by more than 10%–15%; about the same range of difference between atomic radii exists in the isomorphous structures of covalent and metallic compounds. Therefore, the sizes of the unit cells of isomorphous substances, the interatomic distances in them, the coordinates of generally situated atoms differ but slightly.

The dimensions of the unit cells of solid solutions of isomorphous substances are approximately linearly dependent on the concentration; this is Vegard's law (Fig. 1.85). Often deviations from this law are observed. The curve of the concentration dependence of the periods may slightly buckle upwards or downwards, or have an S shape. Since the atoms of the solute and the solvent generally differ in size, the introduction of impurity atoms into the solvent lattice results in two effects: a macroscopically uniform strain of the crystal lattice of the solvent and local displacements due to each impurity atom.

Thus, the unit cell parameters of solid solutions, observed by X-ray diffraction, and the interatomic distances are averaged over all the cells of the crystal. Uniform strain results in a concentration dependence of the periods of the lattice of a solid solution, which is observed by the X-ray method. Because of the local displacements produced by solute atoms, each cell is distorted to some extent; its size and shape vary depending on the substituting atoms and the neighboring cells (Fig. 1.86). The local displacements are responsible for the weakening of the intensity of the X-ray reflections and the appearance of diffuse scattering concentrated near them. On the average, however, the long-range order is preserved despite local distortions; all the atoms deviate statistically from certain mean positions, which correspond to the ideal three-dimensional periodicity with averaged-out periods. Thus, the periodicity is also statistical, but on

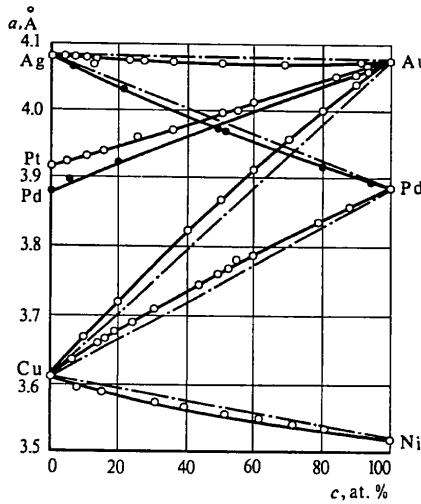


Fig. 1.85. Vegard's law: the periods of unit cells  $a$  of solid solutions of isomorphous substances are linearly dependent on the concentration  $c$

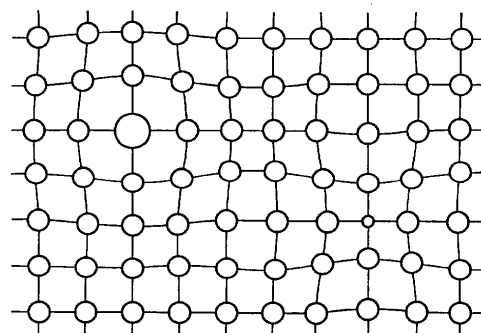


Fig. 1.86. Local deformation of the lattice around impurity atoms of larger or smaller radius

the average it is accurately maintained. Naturally, deviations of atoms from the ideal positions must be proportional to the difference  $\Delta r$  between the radii of the atoms substituting for each other and must depend on their concentration. When the radii differ by 5%–10%,  $\Delta r$  are equal to 0.1–0.2 Å. The X-ray determinations of the r.m.s. displacement of atoms from averaged-out ideal positions  $\sqrt{u^2}$  are of the order of 0.1 Å. Larger values of  $\Delta r$  and  $\sqrt{u^2}$  evidently themselves lead to lattice instability and prevent the formation of a homogeneous solid solution; a separation of components occurs, which results in new phase formation.

It should be mentioned that the similarity of atomic sizes (with the same type of bond) does not always ensure isomorphism by itself. Moreover, a pair of atoms which substitute for each other isomorphously in one structural type, may not do so in another. This is not surprising because isomorphism is a property of structures as a whole, and not of the individual atoms themselves. If the structure has a complicated chemical formula and a large cell, the requirements regarding the differences in sizes of the atoms substituting for each other are slightly milder, since there are greater opportunities for preserving the same equilibrium of interatomic forces by small shifts of other atoms of the cell. Atoms replacing each other isomorphously must also be similar in the type of the bonds they form, which can be characterized by the ionicity fraction  $\varepsilon$  (1.20) [1.58, 59]. The stability of an isomorphous mixture with respect to decomposition is determined by the value of the interchange energy  $u_{\text{int}}$ ; the higher this energy, the higher is the decomposition temperature, and the smaller the substitution limits at a given temperature. In turn,  $u_{\text{int}}$  depends on the squares of the differences in interatomic distances, i.e., the differences in the radii of the ions replacing each other,  $\Delta r$ , and the differences in the degrees of ionicity of the bond of the components,  $\Delta \varepsilon$ ,  $u_{\text{int}} \sim a(\Delta r)^2 + b(\Delta \varepsilon)^2$ . Because of the large difference  $\Delta \varepsilon$ , pairs of elements such as Na and Cu<sup>1</sup>, and Ca and Hg do not replace one another in practice, despite the similarity of their ionic radii.

The phenomenon of substitution of some atoms for others in the structure of crystals is not necessarily associated with the fact that both components, when

mixed, are isostructural and produce a continuous series of homogeneous solid solutions. Limited solubility, when the components are nonisomorphous or nonisostructural, is still more common. The relevant phase diagram is presented in Fig. 1.82b. Here, too, the statistical replacement of atoms of one component by those of another is called isomorphous substitution (although, as indicated above, the components mixed are themselves no longer necessarily truly isomorphous); it proceeds according to the same scheme as for true isomorphism (Fig. 1.9), except that the variable-composition compound, for instance,  $A_{n-x}A'_x B_m$ , exists at limited, rather than at any arbitrary  $x$ , so that  $V_{\max} < n$ . Naturally,  $x_{\max}$  depends on the thermodynamic parameters, i.e., the temperature and pressure. If the components are mutually insoluble, we obtain a phase diagram of the type shown in Fig. 1.82c. The requirements concerning the possibility of the isomorphous replacement of atoms which are not structure isomorphous are less stringent, although the limitation  $\Delta r < 15\%$  remains.

Different versions of isomorphism and isomorphous substitutions are possible according to the number of components and the complexity of the chemical formulae of the phases forming a given phase diagram (or diagram section). Isomorphous substitutions or complete isomorphism occur for one, two, or several sorts of similar atoms, i.e., occupancy of one RPS by similar atoms of  $A$  and  $A'$ , of another by  $B$  and  $B'$ , of a third by  $C$  and  $C'$ , etc. On the other hand, atoms not of two, but of three or more elements  $A, A', A'' \dots$  may be arranged in a single RPS.

Atoms replacing each other often have an identical valency; this is isovalent isomorphism. Heterovalent isomorphism is also possible, when the solute atoms replacing the solvent ones have a different valence. It is then necessary that the lattice as a whole be neutral, i.e., that the valence (charge) be compensated. For instance, divalent ions of  $A$  can be replaced by a set of a univalent  $A'$  and a trivalent  $A''$  ion, provided, of course, that the condition of allowance for the radii and a similar nature of the bond is preserved. Vacancies may also play the role of charge compensators; then, for instance, a univalent ion can be replaced by a divalent or a trivalent one with charge compensation by the corresponding number of vacancies. In covalent semiconductor structures of Ge and Si, which belong to group IV of Mendeleyev's system, host atoms can be replaced by corresponding numbers of atoms of groups III and V; on the other hand, if we introduce atoms only of group III or only of group V, electrons or holes will become compensators, which will yield  $n$  or  $p$  types of semiconductor crystals.

Compensation may occur not only with respect to atoms occupying the same regular point system, but also with respect to different systems. For instance,  $\text{Fe}^{2+}(\text{CO}_3)^{2-}$  and  $\text{Sc}^{3+}(\text{BO}_3)^{3-}$  are isomorphous.

The required approximate equality of the radii restricts the possibilities of isovalent substitution of atoms along the columns (groups) of Mendeleyev's system. This requirement is better fulfilled by diagonal shift, which explains the geochemically and mineralogically important heterovalent isomorphism along Fersman's diagonal rows: Be-Al-Ti-Nb, Li-Mg-Sc, Na-Ca-Y (P3), and Th (Zr).

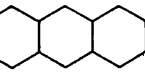
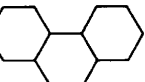
Isomorphous substitutions are very significant in natural and synthetic crystalline substances. Many elements are contained in mineral ores precisely as isomorphous impurities – for instance, rare-earth elements – in silicates, where they replace Ca; Co or Ni often replace Fe in iron-containing minerals. There are many such examples.

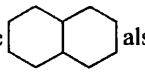
The principle concerning the introduction of certain atoms in a lattice (matrix) and thus changing its properties is essential to the production of many technically important crystals and materials, beginning with high-strength alloys and ending with crystals for quantum electronics and semiconductor technology. Thus, in laser crystals a small part of host cations is replaced by an active ion; for instance, ruby consists of  $\text{Al}_2\text{O}_3$ , in which 0.05% of Al atoms are replaced by Cr; in yttrium-aluminium garnet,  $\text{Y}_3\text{Al}_5\text{O}_{12}$ , up to 1.5% of Y is replaced by the rare-earth element Nd. In fact, practically all crystals contain some dissolved atoms (although in small amounts).

As a specific variant of substitutional solid solutions one can consider *subtractional solid solutions*, where an atom of one of the components does not fill the possible positions completely. An example is  $A_{1-x}A'_yB$ , where  $y < x$  or  $y = 0$ . Here the solution has a formula  $A_{1-x}B$ . The unoccupied positions can be regarded as "vacancy-populated"  $A^*$ , and the formula of the compound can be written as  $A_{1-x}A'_yA^*_{x-y}B$ .

Elements are mixtures of isotopes. Taking this feature of atoms into consideration, the crystals of almost all substances can be regarded as isotopic substitutional solid solutions. Whenever it is possible to single out monoisotopic isomorphous crystals, one can detect slight differences between them. The lattice parameters of hydrides and deuterides (and also of ordinary and heavy ice) differ but slightly, by hundredths of an angstrom. When hydrogen bonds are present, their lengths, thermal vibration parameters, etc., change slightly.

Substitutional solid solutions are also observed in organic crystals, in which the molecule, rather than the atom, must be regarded as the structural unit of the crystal. The requirement regarding the approximate equality of the size and shape of the substituted molecules should be fulfilled in this case, too.

For example, the structure of anthracene  exhibits limited solubility of some of its chloroderivatives or of phenanthrene .

The molecules of naphthalene 

also replace those of anthracene in its lattice, and the part of space which accommodated the third benzene ring remains unoccupied. One large impurity molecule sometimes can replace two matrix molecules under suitable geometric conditions.

#### 1.6.4 Interstitial Solid Solutions

Isomorphous substitution within the structure of a solid solution is due to the possibility of complete or partial statistical replacement of atoms  $A$  by atoms  $A'$

within a given regular point system (Fig. 1.83). Another basic type of solid solution is an interstitial solid solution. Its phase diagram is the same as for substitutional solutions with limited solubility (Fig. 1.82b), but the "dissolving" atoms enter the interstices between the host atoms, statistically populating a new, previously unoccupied regular point system of the space group describing the matrix crystals (Fig. 1.87). The set of RPS occupied by atoms of the host lattice is often called crystal lattice points; it is then said that the atoms entering the space between them enter the interstices. Sometimes transition to another space group, a subgroup of the first, is also possible. Then we can no longer speak of a new compound as being isostructural with the initial one, although the point symmetry group and the simple forms of the single crystal (if it is obtained) may be preserved. Interstitial-type solubility is usually low, being normally just a few per cent and only rarely reaching 10%. Classical examples of interstitial solid solutions are austenite (a solid solution of carbon in  $\gamma$ -iron), where C atoms settle statistically in the octahedral voids of the cubic face-centered structure of the  $\gamma$ -Fe (Fig. 1.88), and the structures of many carbides, nitrides, borides, hydrides of metal, etc., which are called interstitial phases. Since the atoms of a solute enter the spaces between the matrix atoms (often octahedral or tetrahedral holes of closest packings), their sizes should obviously be close to those of the interstices, and not of the host atoms, as in the case

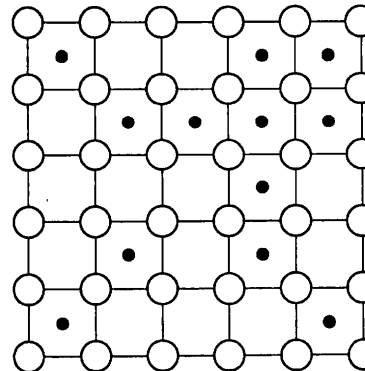


Fig. 1.87. Idealized scheme of the structure of interstitial solid solutions

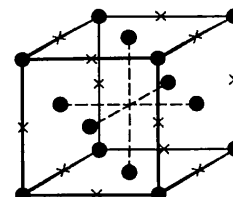


Fig. 1.88. Austenite structure. Crosses represent the positions of the C atoms being incorporated into the  $\gamma$ -Fe lattice

isomorphous substitutions, i.e., they must be smaller than the host atoms. It is therefore easy to understand why interstitial solid solutions are often formed by such atoms as H, B, N, and C, which have small radii. If the size of the interstitial atom does not correspond to that of the interstices, the region of the matrix lattice around them may be greatly distorted. Indications have been found that H molecules enter lattice interstitials in metals, such as Zr and W.

It should be noted, that owing to the metallic nature of the bond in alloys and many interstitial phases, charge redistribution occurs cooperatively throughout the volume of the crystal. The interstices may be filled, not only in accordance with a phase diagram with limited solubility (Fig. 1.82b), but also through attaining the stoichiometric composition, when all the holes of this type are filled. Then a new structure with a definite formula is formed; for instance  $AB_x$ , at  $x = n$ , where  $n$  is an integer (Fig. 1.89). Thus the structure  $AB_x$ , at  $x < n$ , can be interpreted in two ways: either as an interstitial solution of the atoms of B in structure A, or as a defect structure  $AB_n$ , in which some of the possible positions of the atoms of B( $n - x$ ) are vacant (a subtraction solution).

It is also known that, within significant concentration ranges, series of homogeneous solid solutions exist between substances with different formulae (with charge compensation, if the atoms contained in the lattice have different valence). A classic example is the system  $\text{CaF}_2\text{-YF}_3$  (Fig. 1.90), with  $\text{YF}_3$  solubility up to 40%. In the general case such systems with the fluorite-tissonite structures (Fig. 1.90) can be written as  $M_1^{2+} \text{--}_x R_x^{3+} F_{2+x}^{1-}$ , where R is a rare earth element. In the substitution of  $\text{Me}^{2+}$  – by  $\text{Re}^{3+}$  – cations the charge is compensated by additional  $\text{F}^{1-}$  anions entering the structure. At the same time some  $\text{F}^{1-}$  ions leave the main fluorine position of the fluorite phase. Thus formed voids incorporate clusters containing more fluorine than the position

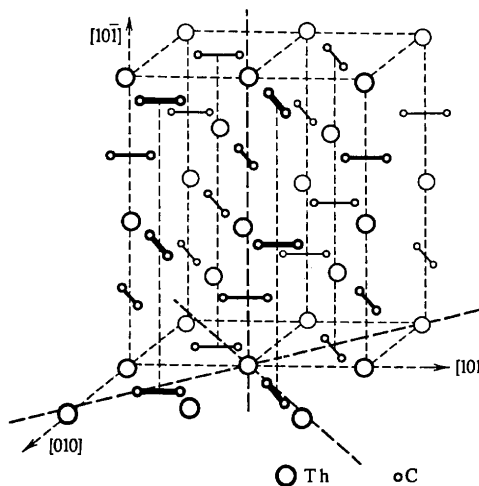


Fig. 1.89. Structure of  $\text{ThC}_2$

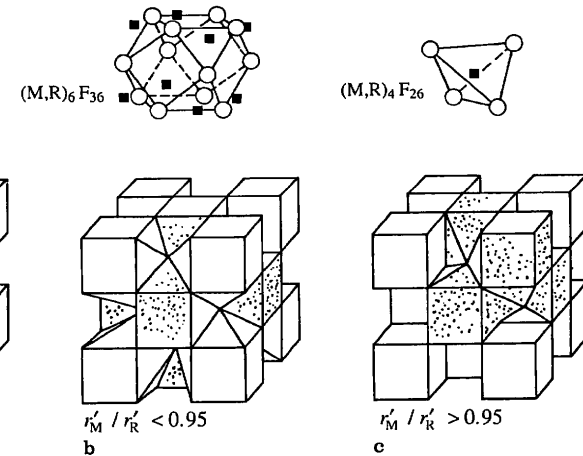


Fig. 1.90a–c. The structures of fluorite (a) and a fluorite-based solid solution  $\text{Ba}_{0.73}\text{Pr}_{0.27}\text{F}_{2.27}$  with additional fluorine atoms on the two-fold axis (b);  $\text{Sr}_{0.69}\text{La}_{0.31}\text{F}_{2.31}$  with additional fluorine atoms on the three-fold axis (c). Above figures (b) and (c) the  $\text{M}_6\text{F}_{32}$  and  $\text{M}_4\text{F}_{26}$  clusters are shown

initially had. Earlier it was assumed that  $\text{F}^{1-}$  ions are randomly distributed in their sites on the two- and three-fold axes. But then it was established that, depending on the ionic radii ratio of the substituted and substituting cations, two types of structures can be formed – with additional fluorine atoms on two-fold axes (Fig. 1.90b) and with additional fluorine atoms on three-fold axes (Fig. 1.90c). The geometries of clusters in this case turned out to be different as well (Fig. 1.90) [1.60].

Specific features of the atomic arrangement in such solid solutions lead to different physical properties of nonstoichiometric fluorides used as the matrices for lasers, ionic conductors and other applications.

Thus, there are many different ways in which impurity atoms can enter the crystal lattice, beginning with isomorphous substitutions in a series of homogeneous solid solutions and ending with incorporation of atoms into new positions with a change in the structure as a whole. Accordingly, the space symmetry of the crystal structure may be retained or changed (reduced in most cases); the decrease in symmetry may also extend to the point group, and transitions to the lower syngonies are also possible.

It is noteworthy that the process of the formation of substitutional or interstitial solid solutions requires a description of not only an ideal crystal structure but also of a real one, with an indication of the distortions in the ideal lattice, the way the atoms enter it, etc.

The atomic interaction in solid solutions excludes a completely random distribution of atoms of sorts A and A' in the substitutional "sublattice" [1.61]. If atoms of sorts A and A' attract each other, then there is an "atmosphere"

around each atom of sort  $A$  due to the preferential distribution of atoms of sort  $A'$ . This phenomenon is called the *short-range order*. In the opposite case, when the atoms of sorts  $A$  and  $A'$  repel each other, an atmosphere of the same kind of atoms is formed around the atoms of sort  $A$ . This phenomenon is usually called *short-range decomposition*. But in both cases we deal with a correlation in the mutual arrangement of atoms  $A$  and  $A'$ . The formation of such linear, two- or three-dimensional associations of related atoms ("block isomorphism") is also possible; they can interact with other lattice defects, such as vacancies and dislocations.

### 1.6.5 Modulated and Incommensurate Structures

In two-phase systems arising with the decomposition of metallic or other solid solutions, the segregations of the new phase are sometimes arranged regularly, rather than randomly with a certain periodicity, as is evidenced by electron-microscopy, X-ray, and electron diffraction data. The shape, orientation, and periodicity of these segregations depend on the initial structure and its orientation relationships with new phase. Such periodic distributions of inclusions are called modulated structures. The periodicity can be observed along one, two, or all three directions. Modulated structures (Fig. 1.91) are observed, for instance, in Au-Pt, Al-Ni, Cu-Ni-Fe, and many other alloys.

The consistent periodic arrangement of the precipitations of the new phase is ascribed to the fact that a substantial energy contribution to such a system is the strain-induced energy due to the mismatch of the crystal lattice of the two phases. The total energy minimum just corresponds to the modulated structure, whose formation results in the disappearance of the long-range fields of elastic stresses.



Fig. 1.91. Electron-microscopic image of the two-dimensional modulated structure of a ticonal-type alloy, (001) plane,  $\times 32,000$  [1.62]

The most general case is the so-called incommensurate structures in which the distribution of some structural parameter, say, charge, magnetic moment, or deformation, is periodic, (in one, two, or three dimensions), but the period  $A_i$  is not multiple to the integral number of crystal lattice periods  $a_i$ , i.e.,  $A_i \neq ka_i$ . In particular, such structures are observed in ferroelectrics and ferroelastics. The periods  $A_i$  depend on temperature and other external conditions. At a certain temperature a transition to the commensurate structure ( $A_i = ka_i$ ) can take place.

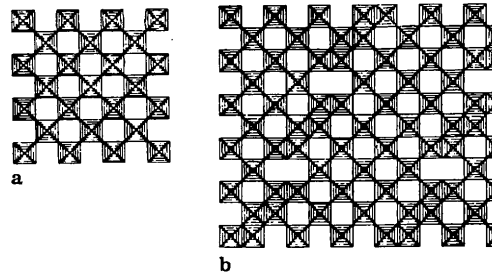


Fig. 1.92a, b. Ideal structure of the  $\text{WO}_3$  type made up of octahedra (a) and a structure with CS along the  $\{103\}$  plane (b)

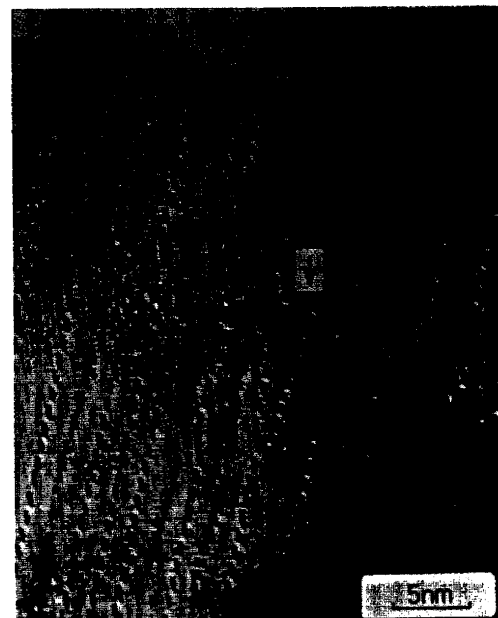


Fig. 1.93. Electron micrograph of a crystal of overall composition  $\text{Ti}_{0.03}\text{WO}_3$  containing mostly  $[103]$  CS planes. Short segment of  $[102]$  GS plane is arrowed [1.65]

### 1.6.6 Composite Ultrastructures

In recent years it has been found, due to the use of high-resolution electron microscopy (see Sect. 4.9.3 in [1.6]), that many structures with a macroscopically nonstoichiometric formula are actually a combination of parts of related structures having stoichiometric formula. A classic example are the oxides of transition metals  $M_nO_{3n-m}$  (tungsten, molybdenum, niobium, etc.) and the intermediate structures resulting from their oxidation or reduction [1.63–65]. The stable elements of these structures are columns of  $MO_6$  octahedra which share the vertices in the ideal case of  $MO_3$ . Contact by the edges produces the so-called crystallographic shear (CS) (Fig. 1.92). CS along  $\{102\}$  yields the structures  $M_nO_{3n-1}$ , and along  $\{103\}$   $M_nO_{3n-2}$ , etc. Thus, the co-existence of these structures in the same crystal results in a macroscopically nonstoichiometric formula of the type  $M_nO_{3n-x}$  (Fig. 1.93. Figure 4.106 in [1.6] may serve as another example.) Coexistence of blocks of different composition in a crystal is known for silicates (Fig. 1.94) and for many other compounds. In all these cases one observes a continuous crystal structure, but one can no longer speak of the same lattice throughout the entire volume of the crystal; there are

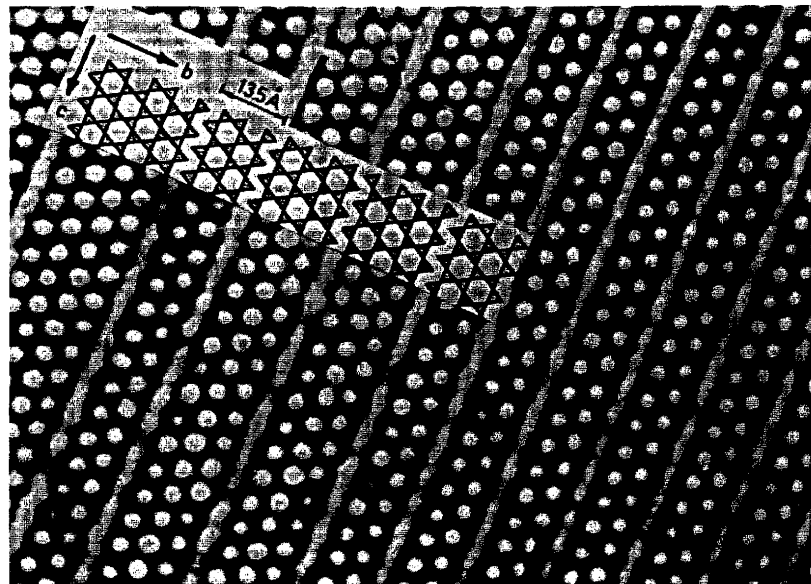


Fig. 1.94. Electron micrograph of three-row Na-Co silicate [theoretical formula  $Co_4Na_2 \cdot Si_6O_{16}(OH)_2$ ]. Besides the regular structure consisting of 3 silicon-oxygen chains, one can see insertions consisting of 4 or 5 chains. On the schematic representation of the structure the  $SiO_4^{2-}$  tetrahedra are denoted by triangles [1.66]

different, although related, lattices alternating at the microlevel and forming a macroscopically unified crystalline aggregate. If this alternation is uniform and regular throughout the whole volume, one can speak of a superlattice. If it is irregular, there is no long-range order in the whole volume; it exists only in individual blocks. Ultrastructures may naturally show various structural defects (Chap. 4).